Symmetry methods for turbulence modeling

Doctoral Thesis by

Silke Guenther
born February 6th, 1977 in Düsseldorf

approved by

Fachbereich Bauingenieurwesen und Geodäsie

Fachgebiet für Strömungsmechanik und Hydraulik

Technische Universität Darmstadt

Referees: Prof. Dr.-Ing. habil. M.Oberlack
Prof. Dr.-Ing. I. David
PD Dr.-Ing. habil. S. Jakirlic

D 17
Darmstadt, October 2005

To Nik

One should model the physics, not the equations.

(P.G. Saffman)

Zusammenfassung

Die vorliegende Arbeit baut auf der in den letzten Jahren entwickelte Turbulenztheorie auf der Basis der Lie-Gruppen-Theorie auf. Mit dem neuen Ansatz sind eine Reihe klassischer semi-empirischer Ansätze, wie z.B. das logarithmische Wandgesetz, bestätigt und eine Vielzahl neuer Turbulenzgesetze hergeleitet worden, die sich ausschließlich aus "first principle" ergaben.

Im Speziellen werden in der vorliegenden Arbeit drei Strömungsfälle untersucht: der Strömungsfall der turbulenten Diffusion, die turbulente Grenzschichtströmung ohne Druckgradient und die voll ausgebildete, turbulente, rotierende Rohrströmung. Mit Hilfe von Symmetriemethoden werden für diese Stömungsfälle lineare und nichtlineare Wirbelviskositäts-modelle, sowie Reynolds-Spannungsmodelle analysiert. Dabei wird überprüft, ob die Modellgleichungen die gleichen Symmetrieeigenschaften wie die Zwei-Punkt-Korrelations Gleichungen haben und zusätzlich in der Lage sind, die turbulenten Skalengesetze für die gegebenen Strömungsfälle zu beschreiben. Basierend auf diesen Untersuchungen werden dann zum Teil Bedingungen für die Modellkonstanten, sowie die Struktur der Modellgleichungen hergeleitet.

Im Folgenden werden die Hauptergebnisse kurz zusammengefaßt:
Beim Strömungsfall der turbulenten Diffusion wird Turbulenz durch die Vibration eines Gitters erzeugt, die dann in das angrenzende Strömungsgebiet senkrecht zum Gitter in das ruhende Fluid hineindiffundiert. Für diesen Strömungsfall wurden mittels der Lie-Gruppen sechs neue stationäre und instationäre Lösungen entwickelt. Dies sind 1.) Turbulente Diffusion mit räumlich anwachsendem integralen Längenmaß, 2.) Turbulente Diffusion mit konstantem integralen Längenmaß, 3.) Turbulente Diffusion in einer konstant rotierenden Umgebung.
Für den ersten Fall ergibt sich eine klassische Diffusionslösung vergleichbar mit der der Wärmeleitungsgleichung. Die turbulent-kinetische Energie nimmt dabei nach einem algebraischen Gesetz ab.
Beim zweiten Fall handelt es sich bei der Lösung um eine Diffusionswellen-Lösung. Für den stationären Fall ergibt sich ein exponentielles Abklingverhalten der turbulenten kinetischen Energie.
Für Fall 3. ergibt sich ein quadratisches Abklingverhalten. Die turbulente Diffusion scheint also nur ein begrenztes Gebiet zu beeinflussen. Die turbulent-kinetische Energie sinkt dabei bis auf Null ab und kann dann nicht wieder zunehmen, da keinerlei Turbulenzquellen vorhanden sind.
Bezüglich der Modellierung des gegebenen Strömungsfalls wurden nun klassische Zweigleichungs- und Reynolds-Spannungsmodelle daraufhin untersucht, ob sie mit diesen invarianten Lösungen konsistent sind. Dazu wurden die invarianten Lösungen in das K-ϵ Modell und das LRR Second-Moment Closure Modell eingesetzt. Für den ersten Fall erhält

man somit Gleichungen aus denen sich der Exponent, der das räumliche Abklingverhalten der turbulent kinetischen Energie und Dissipation beschreibt, berechnen lässt. Für den zweiten Fall wurde festgestellt, dass diese Lösung nur zu den Modellgleichungen konsistent ist, wenn die Modellkonstanten modifiziert werden. Weiterhin wurde festgestellt, dass der dritte Strömungsfall der turbulenten Diffusion mit Rotation bisher nur unbefriedigend bzw. gar nicht durch die bereits existierenden Modelle wiedergegeben wird. Um letztendlich eine ganzheitliche Modellierung der turbulenten Diffusion zu ermöglichen, wurde mit Hilfe der Tensor-Invarianten-Theorie ein zusätzlicher Term für das Modell für die Druck-Scher-Korrelation entwickelt.

Für die turbulente Grenzschichtströmung ohne Druckgradient wurde von Oberlack (2001) ein exponentielles Geschwindigkeits-Gesetz mit Hilfe der Lie-Gruppen-Theorie hergeleitet. Dieses Gesetz wurde in letzter Zeit mehrfach mittels experimenteller oder numerischer Daten bestätigt. In der gegebenen Arbeit wurden daher zahlreiche statistische Turbulenzmodelle dahingehend untersucht, ob sie das exponentielle Gesetz wiedergeben. Dazu wurden, wie schon bei den Untersuchungen zur turbulenten Diffusion, die invarianten Lösungen in die Modellgleichungen eingesetzt. Durch Lösen der reduzierten Gleichungen nach den Koeffizienten des exponentiellen Gesetzes unter Verwendung der Standard Modellkonstanten wurde festgestellt, dass keines der untersuchten Modelle das exponentielle Gesetz wiedergibt. Es konnten allerdings Bedingungen für die Modellkonstanten hergeleitet werden, die eine einwandfreie Modellierung dieses Strömungsfalls ermöglichen.

Die Untersuchungen zur voll ausgebildeten, turbulenten, rotierenden Rohrströmung basieren auf von Oberlack (1999) hergeleiteten Skalengesetzen. In der gegebenen Arbeit wurden nun lineare und nichtlineare Wirbelviskositätsmodelle, sowie Reynolds-Spannungs-Modelle untersucht. Ein Untersuchungsschwerpunkt lag dabei auf einer zusätzlichen, unphysikalischen Symmetrie, die das Standard $K-\epsilon$ Modell, sowie andere Zwei-Gleichungsmodelle für den gegebenen Strömungsfall besitzen. Hierbei wurde festgestellt, dass die unphysikalische Symmetrie in nichtlinearen Wirbelviskositätsmodellen, sowie Reynolds-Spannungsmodellen gebrochen wird und die dafür verantwortlichen Tensorinvarianten und skalaren Invarianten wurden identifiziert. Weiterhin konnte für die zuletzt genannten Modellklassen die Abhängigkeit der achsialen Geschwindigkeitskomponente von der Rotationsrate mit Hilfe von Symmetriemethoden hergeleitet werden.

Die vorliegende Arbeit soll also den Nutzen und die Möglichkeiten der Lie-Gruppen-Theorie im Zusammenhang mit der Kalibrierung und Entwicklung statistischer Turbulenzmodelle darstellen.

Abstract

The given thesis is based on the turbulence theory based on Lie group methods, which has been developed in the last couple of years. With this theory at hand it is possible to derive classical semi-empirical approaches, as for example the law of the wall, from first principles.

Here three different flow cases, which are the turbulent diffusion, the zero-pressure gradient turbulent boundary layer flow and the fully developed turbulent rotating pipe flow have been investigated. Using symmetry methods linear and non-linear eddy viscosity models as well as Reynolds stress models have been analyzed. Thereby it has been checked if the model equations have the same symmetry properties as the two-point correlation equations and if they are able to describe the turbulent scaling laws which have been derived for the given flow cases. Based on these investigations conditions for the model constants and the structure of the model equations have been derived.

In the following the main results are summarized:
For the flow case of turbulent diffusion turbulence is generated by a vibrating grid and diffuses away from the grid in the undisturbed flow. For this flow case six new steady and unsteady solutions have been derived using symmetry methods. These are 1.) Turbulent diffusion with spatially growing integral length-scale; 2.) Turbulent diffusion with a constant integral length-scale; 3.) Turbulent diffusion in a rotating frame.
For the first case a typical diffusion type of similarity variable, such as for the heat equation is received. The turbulent kinetic energy decreases algebraically with the distance from the turbulence source.
The second case gives a diffusion-wave solution. The spatial decay behavior changes from an algebraic to an exponential behavior.
For the third case a quadratic decreasing behavior is received. Thus the turbulent diffusion only influences a finite domain. The turbulent kinetic energy decreases to zero and can not increase again, due to the lack of turbulence source.
Concerning the modeling of the given flow cases two-equation models and Reynolds stress models have been investigated if they are in accordance to the invariant solutions derived using symmetry methods. Therefore the invariant solutions have been inserted into the $K-\epsilon$ model and the LRR second-moment-closure model. For the first case equations are received from which one can derive the exponent, giving the decreasing behavior of the turbulent kinetic energy and the dissipation. For the second case it has been found that the solutions are only consistent with the model equations if the model constants are modified. Finally it has been established, that the third case of turbulent diffusion with rotation cannot be modeled satisfactory by the existing turbulence models. To permit a proper modeling of this flow case an additional term for the pressure strain correlation has been developed using invariant theory.

For the zero-pressure gradient turbulent boundary layer flow an exponential velocity law has been derived by Oberlack (2001) using Lie group theory. This law has recently been validated using experimental and numerical data. Thus a couple of statistical turbulence models have been investigated in the given thesis, if they properly capture the exponential law. Therefore the invariant solutions have been - as for the investigations on the turbulent diffusion - introduced into the model equations. Solving the reduced equations for the coefficients in the exponential law, using the standard model constants, it has been found, that none of the tested models is in accordance with the theory. Anyway, conditions for the model constants could be derived, allowing a proper modeling of this flow case.

The investigations for the fully developed turbulent rotating pipe flow are based on the scaling laws derived by Oberlack (1999). In the given thesis linear and non-liner eddy viscosity models as well as Reynolds stress models have been investigated. Emphasis was thereby placed on an additional unphysical symmetry, which is admitted by the standard $K - \epsilon$ model as well as by other two-equation models. Hereby it was found, that this unphysical symmetry is broken by non-linear eddy viscosity models and Reynolds stress models. Additionally the tensor invariants and scalar invariants, which are responsible for this symmetry breaking, have been identified. Based on this findings a new model for the eddy viscosity has been derived and calibrated Furthermore for non-linear eddy viscosity models and Reynolds stress models the dependence of the axial velocity component on the rotation rate could be derived using symmetry methods.

Within the scope of the given thesis it should thus be shown that symmetry methods provide a very usefull tool for the calibration and development of statistical turbulence models.

Preface

The given thesis has been carried out during my time as a research assistant and PhD student at the department of Hydromechanics and Hydraulics at the Technische Universität in Darmstadt.

This thesis is based on and contains the following papers in slightly modified form:

- Frewer, M., Oberlack, M. & Guenther, S., 2005, Symmetry investigations on the incompressible stationary axisymmetric Euler equations with swirl, *submitted to Fluid Dynamics Research*
- Oberlack, M. & Guenther, S., 2003, Shear-free turbulent diffusion - classical and new scaling laws, *Fluid Dynamics Research*, (**33**), 453-476
- Guenther, S., Oberlack, M., Brethouwer, G. & Johansson, A.V., 2004, Lie group analysis, LES and modeling of shear-free turbulent diffusion in a rotating frame, *Advances in Turbulence X, Proc. of the 10th European Turbulence Conference*, Trondheim/Norway
- Guenther, S. & Oberlack, M., 2005, Incompatibility of the exponential scaling law for a zero pressure gradient boundary layer flow with Reynolds averaged turbulence models, *Physics of Fluids*, (**17**), 4
- Guenther, S. & Oberlack, M., 2005, Symmetry methods in modeling rotating, turbulent pipe flow, *submitted to J. Fluid Mech.*

Acknowledgment

During the creation of this thesis I enjoyed a lot of advice, help and encouragements from my supervisors, my colleagues, my friends and my family. So I will take this opportunity to thank all of them:

First of all, I would like to thank my supervisor Professor Martin Oberlack for all his support and inspiration he gave me throughout the years. I admire his vast knowledge, his magical physical insights and mathematical skills. Thank you, for the time you have given me during our spontaneous meetings.
I would also like to thank Professor Arne Johansson and Dr. Geert Brethouwer, who supervised me during my stay in Stockholm. This three month in Stockholm have been very inspiring, motivating and productive. Thank your for giving me the opportunity to visit your department, and making this great experience. In this context I would also like to thank all members of the MEKANIK group, who kindly took me in and made my stay an unforgettable one.

I would like to express my gratitude to my co-referee Dr.-Ing. habil. Suad Jakirlić, who has always been available with hints and suggestions on rotating flows, supplied me with literature and introduced me into the fluid mechanics community. Thank you also for agreeing to review my thesis.
Thanks also to Professor Ioan David, who agreed to review my thesis, although he is getting retired in October and goes back to Romania. Your lecture and elaborated elucidations have been jointly responsible to arise the interest in fluid mechanics in me.

A special thank also to the BMBF for its financial support, making my work at all possible. Here I would also like to thank all the members of the BMBF group "Turbulente Strömungen mit starker Stromlinienkrümmung". I think this has been a quite interesting project. The meetings with the group - although it was usually hard to find a date - have always been inspiring and encouraging.

My colleagues, the colleagues from the ihwb department and especially the various roommates I have had during my stay at the department all contributed to a great working environment. Thank you, and special thanks to Michael, who agreed to proofread my thesis.

For helping me to relax from work I would like to thank my friends and my running group, as well as the people from the fencing and pentathlon club. Special thanks also to the German federation of modern pentathlon, who always found ways for me to start on the international competitions without taking part at the official training camps.

A big thank you to my parents for their support and to my sister Maya who had probably

a hard time, proofreading my thesis and filling in all the commas.

And finally: Thank you Nik, for being there for me and proofreading all my papers and texts! Thanks also for numerous discussions on the subject. I hope by dedicating you this thesis I can express how much I appreciate your help and support.

Contents

Nomenclature

The notation used is given here in the following order: Upper-case Roman, lower-case Roman, upper-case Greek, lower-case Greek. There are some variables, which are multiply defined. This is due to the fact, that different authors used the same variables to describe different quantities. It seemed useful to me not to change these variables, so that things can be looked up in the given references. To identify the exact meaning of the variable the equation number is given, where the variable is defined or where it appears for the first time.

Upper-case Roman

A^+: model constant (Eq. 3.10)
A_0: constant (Eq. 3.134)
A_i: constants (Eq. 3.33)
B_{ijpqkl}: sixth rank tensor to model the M-tensor M_{ipqj} (Eq. 3.56)
B_2: model constant (Eq. 7.44)
C: universal parameter in the exponential velocity law (Eq. 6.5)
C_0^T: constant (Eq. 3.130)
C_1: model constant = Rotta constant (Eq. 3.43)
C_1^0: model constant (Eq. 3.79)
C_1^1: model constant (Eq. 3.79)
C_1^{HM}: model constant (Eq. 5.63)
C_{1k}: constant (Eq. 7.24)
$C_{1\overline{u_i' u_j'}}$: constant (Eq. 7.23)
$C_{1\epsilon}$: constant (Eq. 7.25)
C_2^{HM}: model constant (Eq. 5.63)
C_2: model constant (Eq. 3.34)
C_{2k}: constant (Eq. 7.30)
$C_{2\overline{u_i' u_j'}}$: constant (Eq. 7.29)
$C_{2\epsilon}$: constant (Eq. 7.31)
C_3: constant (Eq. 7.11)
C_4: model constant (Eq. 3.58)
C_8: constant (Eq. 3.58)
C_{b1}: model constant (Eq. 6.7)
C_{b2}: model constant (Eq. 6.7)
C_D: model constant (Eq. 3.13)
C_K: $= 1/\sigma_K$ model constant (Eq. 7.34)

C_R: model constant (Eq. 3.40)
C_s: model constant (Eq. 3.44)
C_{s1}: model constant (Eq. 5.81)
C_{s2}: model constant (Eq. 5.81)
C_{ij}: Coriolis term (Eq. 2.13)
C_{u_z}: constant (Eq. 7.18)
C_{u_ϕ}: constant (Eq. 7.19)
C_{2u_z}: constant (Eq. 7.26)
C_{2u_ϕ}: constant (Eq. 7.27)
C_W: model constant (Eq. 3.39)
C_ε: $1/\sigma_\varepsilon$ = model constant (Eq. 5.79)
$C_{\varepsilon 1}$: model constant (Eq. 3.18)
$C_{\varepsilon 2}$: model constant (Eq. 3.18)
$C_{\varepsilon 3}$: model constant (Eq. 5.64)
$C_{\varepsilon 4}$: model constant (Eq. 5.67)
$C_{\varepsilon\Omega}$: model constant (Eq. 5.61)
C_μ: model constant (Eq. 3.19)
C'_μ: model constant (Eq. 3.11)
C^*_μ: model constant (Eq. 7.48)
C^{**}_μ: model constant (Eq. 7.49)
$C^{\star\star}_\mu$: model constant (Eq. 7.58)
D: universal parameter in the exponential velocity law (Eq. 6.5)
D_{ij}: diffusion term (Eq. 2.13)
E: universal parameter in the exponential velocity law (Eq. 6.6)
$E(\kappa)$: energy (Eq. 3.147)
F: determinant of the normalized Reynolds stress tensor (Eq. 3.101)
$F(\psi)$: free function in ψ (Eq. 4.41)
$G^{(\lambda)}$: terms of the non-linear model for the rapid pressure strain correlation (Eq. 3.35)
G_λ: coefficients in stress-stain relationship (Eq. 3.23)
$G(\psi)$: free function in ψ (Eq. 4.41)
I_λ: scalar invariants (Eq. 3.25)
K: turbulent kinetic energy (Eq. 2.32)
$\mathcal{K}$: constitutive dependent variables in the thermodynamic consistency principle (Eq. 3.121)
K_i: flux vector of the turbulent kinetic energy (Eq. 3.111)
M_{iqpj}: forth rank tensor to model the rapid pressure strain correlation (Eq. 3.31)
N_{ijpq}: forth rank tensor to model B_{ijpqkl} (Eq. 3.58)
P_{ij}: production tensor (Eq. 2.13)
P: production term (Eq. 7.43)
$\mathcal{Q}_i$: turbulent heat flux vector (Eq. 3.111)
R: pipe radius (below Eq. 7.20)
Re_T: turbulent Reynolds number (Eq. 3.6)
Re_κ local Reynolds number (Eq. 3.150)
R_i Richardson number (Eq. 7.2)

$R_{i\{2\}}$: two-point correlation tensor (Eq. 2.21)
$R_{i\{n+1\}}$: multi-point correlation tensor (Eq. 2.15)
S_κ: local strain-rate parameter (Eq. 3.149)
$\boldsymbol{S}$: shear tensor (Eq. 3.21)
$\boldsymbol{S}^*$: nondimensional shear tensor (Eq. 3.21)
T_{ij}: Cauchy stress tensor (Eq. 3.111)
T^λ: tensor basis (Eq. 3.25)
$\mathcal{V}^M, \mathcal{V}^T$: constitutive independent variables in the thermodynamic consistency principle (Eq. 3.122)
$\boldsymbol{W}$: rotation tensor (Eq. 3.22)
$\boldsymbol{W}^*$: nondimensional rotation tensor (Eq. 3.22)
$X^{(p)}$: operator in the scope of symmetry methods (Eq. 4.11)
Y_{pq}: structure tensor = one-point tensors, determined by the energy-containing eddies (see e.g. Kassinos & Reynolds, 1994) (above Eq. 3.33)

Lower-case Roman

a: arbitrary constant (Eq. 4.45)
$\boldsymbol{a}$: Reynolds stress anisotropy tensor (Eq. 5.74)
$\mathbf{a}$: constant rotation matrix (Eq. 4.25)
$\boldsymbol{a}^*$: nondimensional Reynolds stress anisotropy tensor (Eq. 3.20)
a_i: group parameter (Eq. 5.16)
b: constant (Eq. 3.134)
b_1: group parameter (Eq. 7.17)
$\boldsymbol{b}$: half of the Reynolds stress anisotropy tensor = $\boldsymbol{a}/2$ (Eq. 5.79)
e_{ij}: dissipation rate anisotropy (Eq. 3.78)
e_{ikl}: permutation tensor (Eq. 2.2)
e_α: measure of the total strain rates along the principle axes (above Eq. 3.160)
$\bar{f}_i$: source term of momentum (Eq. 3.113)
h: source term of energy (Eq. 3.113)
ℓ: length-scale (Eq. 3.9)
ℓ_m: mixing length (Eq. 3.10)
ℓ_t: integral length-scale (Eq. 5.1)
m: combination of group parameter (Eq. 5.20)
n: decay exponent in grid turbulence (Eq. 3.91)
p: instantaneous pressure (Eq. 2.2)
$\bar{p}$: mean pressure (Eq. 2.6)
p': fluctualiting pressure (Eq. 2.6)
q: root mean square of the turbulent velocity field (above Eq. 3.151)
q_i: scalar functions in the non-linear model by Sjögren & Johansson (2000) (Eq. 3.36)
q_i: heat flux vector (Eq. 3.111)
$\boldsymbol{r}$: correlation length (Eq. 2.27)

s_i^T, s_i^M: constitutive quantities to be determined for thermodynamic consistent modelling (Eq. 3.117)
t_0: combination of group parameter (Eq. 5.19)
$\boldsymbol{u}$: instantaneous velocity (Eq. 2.1)
u_w: bulk velocit (Eq. 7.23)
u_w: wall velocit (Eq. 7.20)
$\bar{\boldsymbol{u}}$: mean velocity (Eq. 2.5)
$\boldsymbol{u}'$: fluctuality velocity (Eq. 2.5)
$\bar{u}_0(x_1)$: characteristic velocity scale (Eq. 3.6)
$\bar{u}_{1_0}$: constant streamwise velocity (Eq. 3.89)
$\bar{u}_c$: centerline velocity (7.20)
$\bar{u}_\tau$: friction velocity (Eq. 3.95)
$\overline{u_i' u_j'}$: Reynolds stress tensor (Eq. 2.12)
x_0: combination of group parameter (Eq. 5.19)

Upper-case Greek

Δ: Clauser-Rotta length-scale (above Eq. 6.4)
Θ: absolute temperature (Eq. 3.109)
Λ: Lagrange parameter (Eq. 3.119)
$\boldsymbol{\Omega}$: rotation rate (Eq. 2.2)

Lower-case Greek

α: constant (Eq. 3.143)
α_2^k: constant (Eq. 3.143)
α_i: constants in the model for the slow pressure strain correlation (Eq. 3.41)
α_i^M, α_p^T: coefficients in the symbolically written thermodynamic inequality (Eq. 3.126)
β: constant (Eq. 4.44)
β, β^M: coefficients in the symbolically written thermodynamic inequality (Eq. 3.126)
γ_1: constant (Eq. 4.44)
γ_2: constant (Eq. 4.44)
δ_*: displacement thickness (Eq. 6.4)
δ_{ij}: Kronecker-symbol (Eq. 3.5)
$\delta(x_1)$: characteristic length-scale (Eq. 3.6)
ϵ_{ij}: dissipation tensor (Eq. 2.13)
ϵ: dissipation term (Eq. 3.12)
ε: arbitary continous parameter in the scope of Lie group methods (Eq. 4.5)
ζ: constant (Eq. 7.22)
η: entropy (Eq. 3.109)
η: infinitesimal in the scope of symmetry methods (Eq. 4.7)

η: normalized wall normal coordinate in the exponential velocity law = x_2/Δ (Eq. 6.4)
η_K: Kolmogorov length-scale (Eq. 5.2)
ϑ^M, ϑ^T: material and turbulent coldness variables = $1/\Theta^M$ resp. $1/\Theta^T$ (Eq. 3.114)
κ: von Karmann constant $\approx 0.38...0.43$ (Eq. 3.10)
κ: heat conductivity (Eq. 3.111)
κ_i: wave vector in sprectral representation (Eq. 3.146)
λ: constant (Eq. 7.28)
λ_i: unit vector (above Eq. 3.66)
μ: viscosity (Eq. 3.111)
ν: kinematic viscosity (Eq. 2.2)
ν_t: eddy viscosity (Eq. 3.1)
ξ: infinitesimal in the scope of symmetry methods (Eq. 4.7)
$\bar{\pi}^{entr}$: entropy production (Eq. 3.112)
ρ: density (Eq. 2.2)
σ: model constants (Eq. 6.7)
σ_K: model constant (Eq. 3.17)
σ_ε: model constant (Eq. 3.18)
σ^{entr}: source term of entropy (Eq. 3.109)
τ: time-scale (Eq. 2.8)
τ_w: wall shear stress (below Eq. 7.20)
ϕ_{ij}: pressure strain correlation (Eq. 2.13)
$\hat{\phi}_{ij}$: spectral tensor (above Eq. 3.161)
φ_i^{entr}: entropy flux (Eq. 3.109)
χ: function of the velocity ratio $\bar{u}_w/u_\tau$ in the axial velocity defect law for the fully developed rotating pipe flow (Eq. 7.20)
ψ: two-dimensional stream function (Eq. 4.22)
ψ: exponent in the algebraic law for the axial and azimuthal velocity components in the rotating pipe flow (Eq. 7.20)
ψ^M, ψ^T: Helmholtz free energy function (Eq. 3.118)
ω: constant (Eq. 7.28)
ω_i: vorticity (Eq. 3.155)

Abbreviations

The following abbreviations are used in the text.

BC:	boundary condition
DNS:	direct numerical simulation
DRSM:	differential Reynolds stress model
EARSM:	explicit algebraic Reynolds stress model
EVM:	eddy viscosity model
KTH:	Kungliga Tekniska Högskolan (Royal Institute of Technology, Stockholm, Sweden)
LaWiKa:	Laminarer Wind Kanal (laminar wind tunnel of the Hermann-Föttinger-Institute, Berlin, Germany)
LES:	large-eddy simulation
LRR:	turbulence model by Launder *et al.* (1975)
MPC:	multi-point correlation
nls term:	non-linear scrambling term
ODE:	ordinary differential equation
PDE:	partial differential equation
PMLM:	Prandtl's mixing-length model
RDT:	rapid distortion theory
RSTM:	Reynolds stress transport model
SSG:	turbulence model by Speziale *et al.* (1991)
TP:	two-point
TPC:	two-point correlation
ZPG:	zero-pressure gradient
2DMFI:	2D material frame indifference

1 Introduction

Many parts of our day-to-day life as for example the weather, many technical applications and functions in our body are significantly characterized by turbulence. The comprehension of turbulence is therefore of fundamental interest from climatological as well as from technical aspects where turbulence is sometimes desirable and sometimes not, depending on the application. Especially flows with rotation and strong streamline curvature represent a cornerstone problem in the field of turbulence research. These flows play an important role in engineering applications as for example turbomachinery or aeronautics and are thus frequently used as test cases for all kinds of turbulence model.

But what is turbulence or better, how is it defined?
There occurs actually no clear-cut separation between laminar and turbulent flows. A very general definition is that the streamlines of laminar flows lie parallel to each other, while the streamlines of turbulent flows cross each other. Turbulent flows are characterized by the following attributes (Rotta, 1972):

- Turbulence is unsteady.
- Turbulence is rotational.
- Turbulence is three-dimensional.
- Turbulence is stochastic, i.e. an instantaneous velocity field may be considered as random realization of flow and cannot be experimentally reproduced.
- Turbulence is diffusive, i.e. has good mixing properties compared to laminar flows.
- Turbulence is dissipative, i.e. the energy of the large-scale velocity fluctuations is transferred to small-scale motion and finally dissipated to heat.

Using a so called direct numerical simulation (DNS) it is in principle possible to integrate the Navier-Stokes equations numerically, which are the governing equations of fluid mechanics. However since the smallest length- and time-scale has to be resolved to do so, the computational effort becomes enormous. Thus a DNS is just viable for very simple geometries and flows with very small Reynolds numbers. On the other hand performing experiments of turbulent flows bears an enormous amount of time and money.
Therefore the calculability of turbulence is based on heuristic assumptions leading to the turbulence model.
Since for most engineering applications only the averaged flow quantities are of interest the turbulence models discussed in this thesis are all based on the Reynolds averaging procedure, meaning that the instantaneous velocity field is decomposed into a mean and

a fluctuating part (see section 2.2).
There are also other approaches as the large eddy simulation (LES) which are not further discussed here.
Introducing the Reynolds decomposition into the Navier-Stokes equations and averaging gives statistical second order moments, the so called Reynolds stresses, which usually dominate over the viscous stresses in turbulent flows. The Reynolds stresses are not known and therefore the received system of equations is not closed anymore. Attempting to close this system by introducing new transport-equations for the unknown terms yields further unknown correlations of the unresolved fluctuations. This procedure has theoretically to be continued ad infinitum. This so called Reynolds closure problem, has been posed by Reynolds (1895). Since then some of the world's most famous scientists including Heisenberg, Kolmogorov, Landau, von Neumann, and von Weizsäcker investigated this problem. More than 100 years later the turbulence problem itself has still remained an unsolved grand challenge problem of classical physics. Although many aspects of turbulence are more or less phenomenologically understood including its origin, its decay and its interaction with walls and laminar flow regions, a general quantitative Reynolds closure approximation has not been proposed so far.

A solution of the closure problem can just be received by truncating the procedure of introducing transport-equations for the unclosed correlations and introducing empirical modeling approaches.
There exist a couple of modeling approaches to model turbulence properly (see chapter 3). For engineering applications the most widely used models are the eddy viscosity models (EVM). These models are based on the Boussinesq hypothesis (Boussinesq, 1877), which implies that the Reynolds stress anisotropy is proportional to the mean strain rate tensor. The factor of proportionality is thereby the so called eddy viscosity which depends on the state of turbulence and must be determined by the turbulence model. EVMs are in equal measure numerically efficient and have a good accuracy of forecast. Shortcomings of these models appear if more complex flows, as flows with separation, rotation or strong streamline curvature are modeled. An improvement for these flows is received if a transport-equation for the Reynolds stresses is introduced. Models incorporating this transport-equation are called Reynolds stress models (RSTM) or differential Reynolds stress models (DRSM). In the Reynolds stress equation the diffusion, dissipation and pressure strain rate tensor are dependent on unknown correlations and thus need to be modeled in terms of the relevant quantities. DRSMs give for complex flows usually more accurate results than EVMs at the cost of computating time. An intermediate level of modeling between EVMs and DRSMs is the explicit algebraic Reynolds stress model (EARSM). In this approach one considers the transport-equation of the Reynolds stress anisotropy a_{ij} and neglects the advection and diffusion of a_{ij} due to the weak equilibrium assumption. The received algebraic equation is then solved explicitly under the assumption that a_{ij} only depends on the mean velocity gradients. In addition to the relation between a_{ij} and the mean velocity gradient the turbulent time-scale and turbulent kinetic energy have to be determined. This is usually done using a standard two-equation EVM. The EARSMs have the advantage of similar low computational costs as EVM but performing better in more complex flows, since they are based on the transport-equation for a_{ij}.

The model constants in the turbulence models are usually calibrated using classical flow cases as for example homogeneous shear-flows, the decay of grid-turbulence or near-wall turbulence (see section 3.5). For these flow cases exact solutions can be derived which are then fitted to experimental and numerical data.

Guidelines for a systematic development of turbulence models are given by formulating modeling principles (see section 3.6). Among these are the realizability principle, the thermodynamic consistency, the rapid distortion theory (RDT) and last but not least the symmetry methods.

Symmetry methods are a well known methodology to derive exact solutions of non-linear differential equations. Although this method has already been developed in the second half of the last century by Sophus Lie, it needed many decades until it was first used to systematically derive solutions of the Navier-Stokes equations. Till now the symmetries of the Navier-Stokes equations are more or less heuristically incorporated into the model equations. The invariance of the model with respect to a rotation of the coordinate system is for example received if the model is formulated tensorially correct. Also the scalings of space and time are admitted by nearly all Reynolds stress models. Though it is desirable to employ symmetry methods more systematically for the development, improvement or calibration of turbulence models.

The given thesis therefore deals with the use of symmetry methods in the scope of turbulence modeling.
First of all the incompressible stationary axisymmetric Euler equations with swirl, for which an equivalent representation, the Bragg-Hawthorne equation can be derived via a scalar stream function has been investigated (see chapter 4). Thereby the symmetry properties of the Bragg-Hawthorne equation have been compared with the symmetry properties of the incompressible stationary axisymmetric Euler equations.
For the analysis of turbulence models three different flow cases have been investigated using symmetry methods. These are the shear-free turbulent diffusion; with and without rotation and with a constant integral length-scale (chapter 5), the zero-pressure gradient (ZPG) turbulent boundary layer flow (chapter 6), and as an example for rotating flows, the fully developed rotating turbulent pipe flow (chapter 7).
The solutions derived from symmetry methods can be used to derive conditions for the model constants under which a proper modeling of the given flow cases is received.
The symmetry properties of the two- and multi-point correlation equations are furthermore compared with the symmetry properties of the investigated turbulence models. Thereby it has been investigated if the model equations admit all symmetries and invariant solutions which are admitted by the two- and multi-point correlation equations. Furthermore it has been checked if there are any unphysical symmetries admitted by the model equations, which are not admitted by the two- and multi-point correlation equations. The course of action is outlined in figure 1.

The thesis is organized as follows:
In chapter 2 the governing equations, which are the Euler and Navier-Stokes equations (section 2.1), the Reynolds averaged Navier-Stokes equations (section 2.2), and the multi- and two-point correlation equation (section 2.3) are given. Chapter 3 gives a short sum-

mary of the most common turbulence modeling concepts as well as an survey of how the modeling constants are usually calibrated (section 3.5). In section 3.6 the four most important modeling principles which are nowadays used for the development, investigation and improvement of turbulence models are described shortly. A brief introduction into symmetry methods is given in chapter 4, followed by a summary of the symmetries of the Euler and Navier-Stokes (section 4.2) and a symmetry analysis of the Bragg-Hawthorne equation (section 4.3). In the chapters 5, 6 and 7 the flow cases shear-free turbulent diffusion, the ZPG turbulent boundary layer flow and the fully developed rotating turbulent pipe flow have been investigated using symmetry methods. The results are finally summarized in chapter 8 and relevant conclusions are drawn.

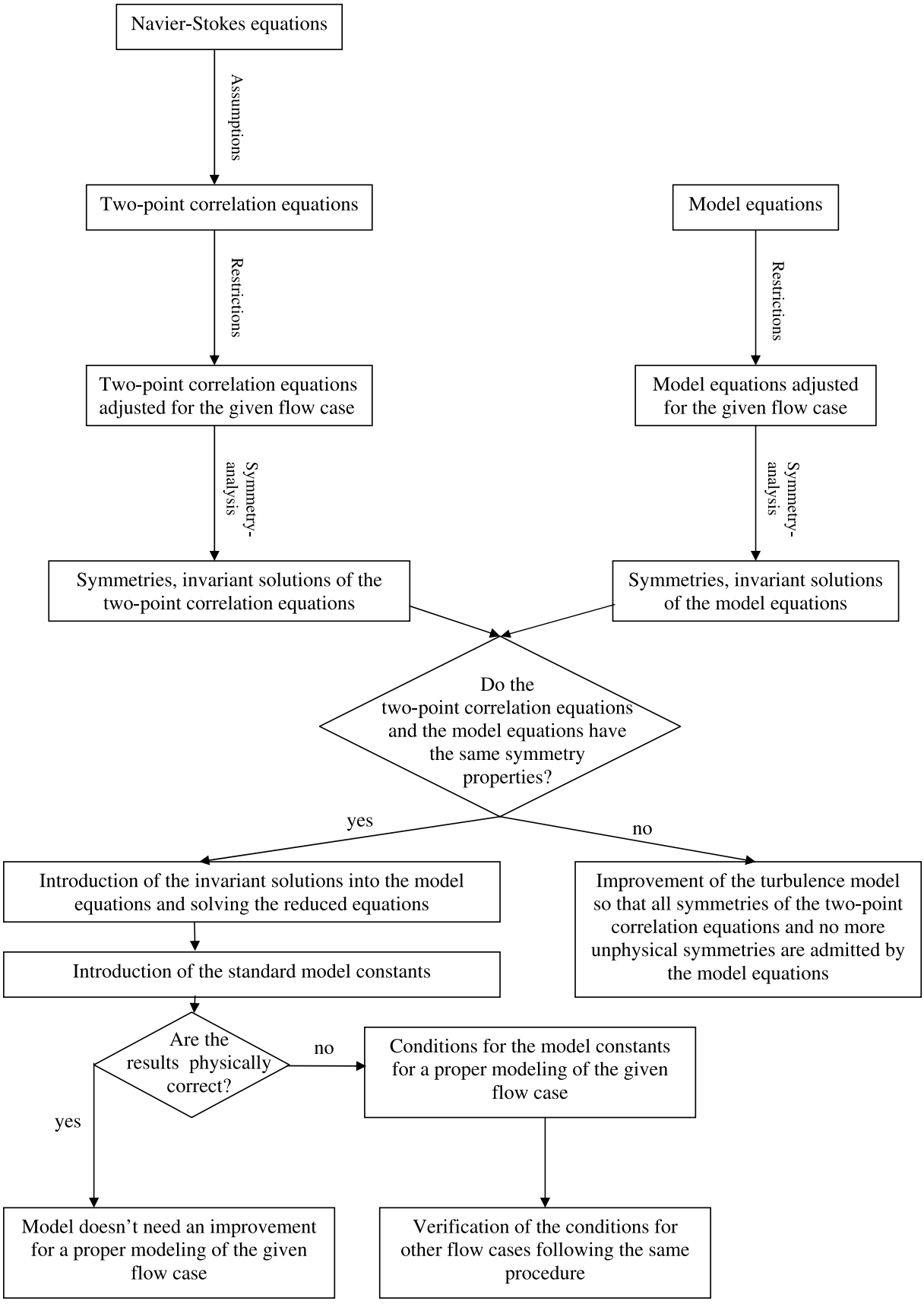

Figure 1.1: Course of action of the use of symmetry methods in the scope of turbulence modeling

2 Governing Equations

2.1 Euler and Navier-Stokes equations

The Navier-Stokes equations are the fundamental partial differential equations describing the flow of incompressible, Newtonsche fluids. The assumption of incompressibility implies that the Mach number is low and the temperature variations negligible. The Navier-Stokes equations correspond to the Euler equations for inviscid flows, that is $\nu = 0$. In cartesian tensor notation the continuity equation reads:

$$\frac{\partial u_k}{\partial x_k} = 0 \tag{2.1}$$

and the momentum equation is

$$\frac{Du_i}{Dt} = -\frac{1}{\rho}\frac{\partial p}{\partial x_i} + \nu\frac{\partial^2 u_i}{\partial x_k \partial x_k} - 2\Omega_k e_{ikl} u_l \tag{2.2}$$

with

$$\frac{D}{Dt} = \frac{\partial}{\partial t} + u_k \frac{\partial}{\partial x_k} \tag{2.3}$$

whereby the Einstein summation convention applies for the double Latin indices. In (2.1) and (2.2) t is the time, $\boldsymbol{x}$ the position vector, $\boldsymbol{u}$ the instantaneous velocity vector, p the pressure, ρ the density and ν the kinematic viscosity. e_{ikl} is an antisymmetric tensor of third rank, which is denoted permutation tensor. The permutation tensor has the following properties:

$$e_{ikl} = \begin{cases} 1 & : \text{ if the arguments are an even permutation,} \\ -1 & : \text{ if the arguments are an odd permutation,} \\ 0 & : \text{ if two or more arguments are equal.} \end{cases} \tag{2.4}$$

When combined with the continuity equation of fluid flow, the Navier-Stokes equations yield four equations in four unknowns (namely the scalar pressure and the three velocity components). Thus the system of equations (2.1) and (2.2) is closed and a plan to attack the turbulence problem can be worked out relying entirely on the application of powerful numerical techniques, provided that the initial conditions are random and the boundary conditions are periodic along the faces of the computational flow domain. However, a specification of the initial and boundary conditions for turbulence can not be considered as definitive, so that the matter has not yet been fully resolved. Therefore, except for degenerate cases in very simple geometries, these equations cannot be solved exactly, so that approximations are commonly made to allow the equations to be solved approximately (see chapter 3).

In chapter 7 of the given thesis the fully developed rotating turbulent pipe flow is investigated. Since rotating flows generally play a very important role in engineering applications, the Navier-Stokes equations in a rotating frame have been written down in appendix A.

2.2 Reynolds averaged Navier-Stokes Equations

For engineering applications as well as for the statistical description of turbulence the instantaneous pressure and velocity field is mostly of minor interest. The attention is more focused on the mean values for the pressure and the velocities. Therefore the instantaneous quantities are split into a mean and a fluctuating part according to the Reynolds decomposition (Reynolds, 1895). The velocity and pressure can therefore be written as:

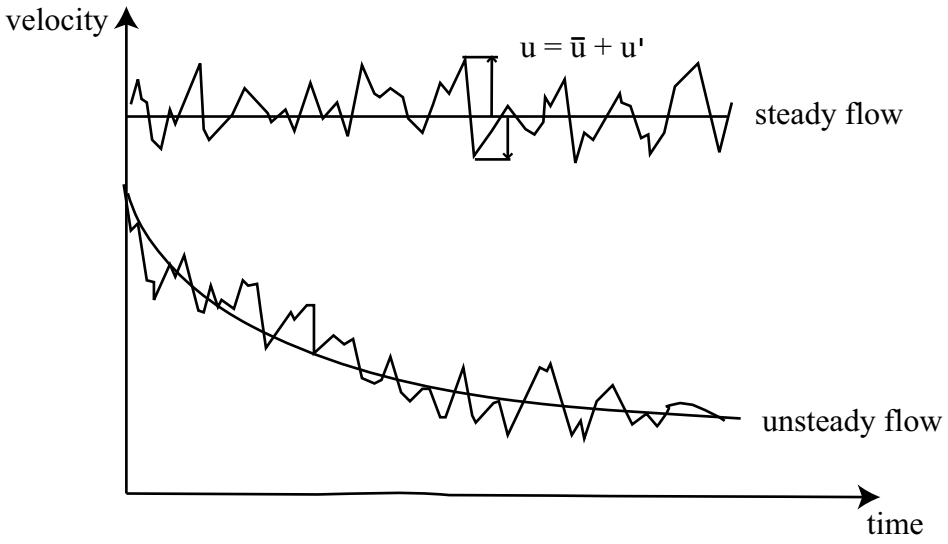

Figure 2.1: Statistic approach of turbulence

$$\boldsymbol{u} = \bar{\boldsymbol{u}} + \boldsymbol{u}', \tag{2.5}$$

$$p = \bar{p} + p'. \tag{2.6}$$

The quantities marked with the bar denote thereby the mean quantities. The average value is generally build by an ensemble averaging:

$$\bar{u} = \lim_{N\to\infty} \left(\frac{1}{N} \sum_{n=1}^{N} u_n \right) \,,\; \bar{p} = \lim_{N\to\infty} \left(\frac{1}{N} \sum_{n=1}^{N} p_n \right). \tag{2.7}$$

For statistically stationary flows it is also possible to use a time average:

$$\bar{u} = \lim_{\tau\to\infty} \frac{1}{\tau} \int_{t-\frac{\tau}{2}}^{t+\frac{\tau}{2}} u\, dt \,,\; \bar{p} = \lim_{\tau\to\infty} \frac{1}{\tau} \int_{t-\frac{\tau}{2}}^{t+\frac{\tau}{2}} p\, dt. \tag{2.8}$$

If the flow is homogeneous in one or more directions, the further possibility exists to average over one of the homogeneous directions.

There are a couple of calculation rules which have to be followed for the derivation of the Reynolds averaged Navier-Stokes equations:

$$\begin{aligned}
\overline{u'} &= 0, \\
\overline{\overline{u}} &= \overline{u}, \\
\overline{u_1 + u_2} &= \overline{u_1} + \overline{u_2}, \\
\overline{\frac{\partial u}{\partial s}} &= \frac{\partial \overline{u}}{\partial s}, \\
\overline{\int u \mathrm{d}s} &= \int \overline{u} \mathrm{d}s, \\
\overline{\overline{u}_{(1)} \overline{u}_{(2)} \dots \overline{u}_{(m)} u'_{(n)}} &= 0, \\
\overline{u'_{(1)} u'_{(2)} \dots u'_{(k)}} &\neq 0.
\end{aligned} \tag{2.9}$$

Introducing the Reynolds decomposition into (2.1) and (2.2) and averaging gives the Reynolds averaged continuity

$$\frac{\partial \bar{u}_k}{\partial x_k} = 0 \tag{2.10}$$

and momentum equation

$$\frac{\bar{\mathrm{D}} \bar{u}_i}{\bar{\mathrm{D}} t} = -\frac{\partial \bar{p}}{\partial x_i} + \nu \frac{\partial^2 \bar{u}_i}{\partial x_k \partial x_k} - \frac{\partial \overline{u'_i u'_k}}{\partial x_k} - 2\Omega_k e_{ikl} \bar{u}_l. \tag{2.11}$$

Due to the averaging of the advection term in the Reynolds averaged momentum equation the symmetrical tensor $\overline{u'_i u'_k}$ appears, which is also called Reynolds stress tensor:

$$\overline{u'_i u'_k} = \begin{pmatrix} \overline{u'_1 u'_1} & \overline{u'_1 u'_2} & \overline{u'_1 u'_3} \\ \overline{u'_1 u'_2} & \overline{u'_2 u'_2} & \overline{u'_2 u'_3} \\ \overline{u'_1 u'_3} & \overline{u'_2 u'_3} & \overline{u'_3 u'_3} \end{pmatrix}. \tag{2.12}$$

The trace of the Reynolds stress tensor is twice the kinetic energy of turbulent motion. This tensor emphasizes turbulent exchange of the momentum due to the fluctuating motion. The six components of the Reynolds stress tensor are not known and therefore the system of equations (2.10) to (2.11) is unclosed. It is then possible to derive an exact equation for the Reynolds stress tensor, which is given by:

$$\begin{aligned}
\frac{\partial \overline{u'_i u'_j}}{\partial t} + \bar{u}_k \frac{\partial \overline{u'_i u'_j}}{\partial x_k} = & \underbrace{-\overline{u'_i u'_k} \frac{\partial \bar{u}_j}{\partial x_k} - \overline{u'_j u'_k} \frac{\partial \bar{u}_i}{\partial x_k}}_{P_{ij}} \underbrace{-2\nu \overline{\frac{\partial u'_i}{\partial x_k} \frac{\partial u'_j}{\partial x_k}}}_{\epsilon_{ij}} + \underbrace{\overline{\frac{p'}{\rho} \left(\frac{\partial u'_i}{\partial x_j} + \frac{\partial u'_j}{\partial x_i} \right)}}_{\phi_{ij}} \\
& + \underbrace{\frac{\partial}{\partial x_k} \left(-\overline{u'_i u'_j u'_k} + \nu \frac{\partial \overline{u'_i u'_j}}{\partial x_k} - \overline{\frac{p'}{\rho} (\delta_{kj} u'_i + \delta_{ki} u'_j)} \right)}_{D_{ij}} \underbrace{- 2\Omega_k [e_{kli} \overline{u'_j u'_l} + e_{klj} \overline{u'_i u'_l}]}_{C_{ij}}.
\end{aligned} \tag{2.13}$$

Thereby P_{ij} designates the rate of energy production. Note, that the negative sign is included in the definition of P_{ij}. This term represents the rate at which energy is transferred from the mean flow to turbulent fluctuations. In most cases turbulent energy is generated from mean shear.

The dissipation term (ϵ_{ij}) has a negative sign and represents dissipation of turbulent kinetic energy by the action of viscosity. One half of the trace of ϵ_{ij} is usually denoted as ϵ, which is the rate of transition of turbulent kinetic energy to heat. The components of ϵ_{ij} permit each component of the Reynolds stress tensor to dissipate at a different rate.

The redistribution term, also called pressure strain correlation term ϕ_{ij} is responsible for the shifting of variance between components of the Reynolds stress tensor $\overline{u_i' u_j'}$ without altering the total energy $K = (1/2)\overline{u_k' u_k'}$. The qualitative effect of redistribution is usually to shift energy from the larger components of the Reynolds stress tensor into the smaller components to make turbulence more isotropic. The redistribution term has no contribution in the equation for the turbulent kinetic energy, since its trace vanishes:

$$\phi_{ii} = \overline{\frac{p'}{\rho}\left(\frac{\partial u_i'}{\partial x_i} + \frac{\partial u_i'}{\partial x_i}\right)} = 0. \tag{2.14}$$

D_{ij} is the diffusion or transport term. This term transports energy, respectively the Reynolds stresses, in space without creating or destroying it. It drives the spatial distribution to uniformity. The diffusion term consists of three terms, the turbulent diffusion, the pressure diffusion and the molecular diffusion. The molecular diffusion can be neglected for high Reynolds numbers.

The Coriolis term C_{ij} appears if the equations are considered in a rotating frame. It contains the rotation rate $\mathbf{\Omega}$, giving the number of rotations per time.

From the given terms the dissipation, pressure strain correlation and turbulent and pressure diffusion term are unknown, leading to an unclosed system of equations. Therefore further equations are essential, which, contain new unknown terms. Herein lies the central obstacle of the entire turbulence theory, known as the closure problem. A solution of the equation is therefore reliant on hypotheses and estimations, based on numerical and experimental data. These equations compose a turbulence model which closes the Reynolds equations approximately.

2.3 Multi- and two-point correlation equations

The motion of any point in a turbulent flow affects the motion at other distant points through the pressure field. Therefore an adequate description cannot be obtained by considering only mean values associated with single fluid particles. For a proper description of a turbulent flow it is essential to consider two or more flow particles at two or more positions. On account of this the multi-point correlation (MPC) equations have been introduced, providing length-scale information on turbulent flows. The multi-point correlation equations can be used for studying the spatial configuration of the flow field.

The MPC is believed to properly model the statistical quantities of turbulence at all scales. In order to write the MPC equations in a compact form we introduce the definition

$$R_{i_{\{n+1\}}} = R_{i_{(0)}i_{(1)}\ldots i_{(n)}} = \overline{u'_{i_{(0)}}(\boldsymbol{x}_{(0)}) \cdot \ldots \cdot u'_{i_{(n)}}(\boldsymbol{x}_{(n)})} \tag{2.15}$$

at $n+1$ points where $u'_{i_{(k)}}$ denotes velocity fluctuation about the mean velocity $\bar{u}_{i_{(k)}}$ at the point $\boldsymbol{x}_{(k)}$.

With this definition at hand it is straight forward to derive the MPC equations from the Navier-Stokes equations (see Oberlack, 2000a)

$$\begin{aligned}\Theta_{i_{\{n+1\}}} = \frac{\partial R_{i_{\{n+1\}}}}{\partial t} + \sum_{l=0}^{n} \Bigg[& \bar{u}_{k_{(l)}}(\boldsymbol{x}_{(l)}) \frac{\partial R_{i_{\{n+1\}}}}{\partial x_{k_{(l)}}} + R_{i_{\{n+1\}}[i_{(l)}\mapsto k_{(l)}]} \frac{\partial \bar{u}_{i_{(l)}}(\boldsymbol{x}_{(l)})}{\partial x_{k_{(l)}}} \\ & + \frac{\partial P_{i_{\{n\}}[l]}}{\partial x_{i_{(l)}}} - \nu \frac{\partial^2 R_{i_{\{n+1\}}}}{\partial x_{k_{(l)}} \partial x_{k_{(l)}}} - R_{i_{\{n\}}[i_{(l)}\mapsto\emptyset]} \frac{\partial \overline{u'_{i_{(l)}} u'_{k_{(l)}}}(\boldsymbol{x}_{(l)})}{\partial x_{k_{(l)}}} \\ & + \frac{\partial R_{i_{\{n+2\}}[i_{(n+1)}\mapsto k_{(l)}][\boldsymbol{x}_{(n+1)} \mapsto \boldsymbol{x}_{(l)}]}}{\partial x_{k_{(l)}}} + 2\Omega_k e_{i_{(l)}km} R_{i_{\{n+1\}}[i_{(l)}\mapsto m]} \Bigg] = 0 \\ \text{for} \quad n = 1, \ldots, \infty \ .\end{aligned} \tag{2.16}$$

by employing the additional definitions

$$\begin{aligned} R_{i_{\{n+1\}}[i_{(l)}\mapsto k_{(l)}]} = & \\ & \overline{u'_{i_{(0)}}(\boldsymbol{x}_{(0)}) \cdot \ldots \cdot u'_{i_{(l-1)}}(\boldsymbol{x}_{(l-1)}) u'_{k_{(l)}}(\boldsymbol{x}_{(l)}) u'_{i_{(l+1)}}(\boldsymbol{x}_{(l+1)}) \cdot \ldots \cdot u'_{i_{(n)}}(\boldsymbol{x}_{(n)})}, \end{aligned} \tag{2.17}$$

$$R_{i_{\{n+2\}}[i_{(n+1)}\mapsto k_{(l)}][\boldsymbol{x}_{(n+1)} \mapsto \boldsymbol{x}_{(l)}]} = \overline{u'_{i_{(0)}}(\boldsymbol{x}_{(0)}) \cdot \ldots \cdot u'_{i_{(n)}}(\boldsymbol{x}_{(n)}) u'_{k_{(l)}}(\boldsymbol{x}_{(l)})}, \tag{2.18}$$

$$R_{i_{\{n\}}[i_{(l)}\mapsto\emptyset]} = \overline{u'_{i_{(0)}}(\boldsymbol{x}_{(0)}) \cdot \ldots \cdot u'_{i_{(l-1)}}(\boldsymbol{x}_{(l-1)}) u'_{i_{(l+1)}}(\boldsymbol{x}_{(l+1)}) \cdot \ldots \cdot u'_{i_{(n)}}(\boldsymbol{x}_{(n)})} \tag{2.19}$$

and

$$P_{i_{\{n\}}[l]} = \overline{u'_{i_{(0)}}(\boldsymbol{x}_{(0)}) \cdot \ldots \cdot u'_{i_{(l-1)}}(\boldsymbol{x}_{(l-1)}) p'(\boldsymbol{x}_{(l)}) u'_{i_{(l+1)}}(\boldsymbol{x}_{(l+1)}) \cdot \ldots \cdot u'_{i_{(n)}}(\boldsymbol{x}_{(n)})}. \tag{2.20}$$

The notation in square brackets denotes the replacement of certain variables or indices with some other quantities standing on the right hand side of the arrow. Each Θ-equation of the tensor order $n+1$ only contains one unclosed term of the order $n+2$. For any of the remaining terms such as $P_{i_{\{n\}}[l]}$ exact equations may be derived from the continuity equation or the Poisson equation for the pressure (see e.g. Oberlack, 2000a).

The two-point correlation tensor admits two additional identities, namely

$$\lim_{x_{(k)}\to x_{(l)}} R_{i_{\{2\}}} = \lim_{x_{(k)}\to x_{(l)}} R_{i_{(0)}i_{(1)}} = \overline{u'_{i_{(0)}} u'_{i_{(1)}}}(\boldsymbol{x}_{(l)}) \quad \text{with} \quad k \neq l \ , \tag{2.21}$$

where $x_{(k)}$ and $x_{(l)}$ may be an arbitrary position vector taken from $x_{(0)}, \ldots, x_{(n)}$ and the null identity

$$R_{i_{\{1\}}[i_{(l)}\mapsto\emptyset]} = 0. \tag{2.22}$$

The latter is derived from the fact that the average of a single fluctuating velocity is zero.

From the continuity equation we also derive the following two sets of equations, which have to be employed as additional kinematic constrains

$$\frac{\partial R_{i_{\{n+1\}}[i_{(l)}\mapsto k_{(l)}]}}{\partial x_{k_{(l)}}} = 0 \quad \text{for} \quad l = 0, \ldots, n \tag{2.23}$$

and

$$\frac{\partial P_{i_{\{n\}}[k][i_{(l)}\mapsto m_{(l)}]}}{\partial x_{m_{(l)}}} = 0 \quad \text{for} \quad k, l = 0, \ldots, n \quad \text{and} \quad k \neq l. \tag{2.24}$$

For simplicity we will proceed with the two-point correlation (TPC) equations which have similar structure as the full set of MPC equations. In particular, they have the same symmetry properties. In order to simplify notation we introduce the short form

$$R_{i_{\{2\}}} = R_{ii_{(1)}} = R_{ij}. \tag{2.25}$$

For the derivation of the TPC equations the transport-equation for the turbulent fluctuating velocities at the point $\boldsymbol{x}$ is multiplied with the fluctuating velocity at the point $\boldsymbol{x}_1$ and vice versa. If the resulting equations are added together we receive (see e.g. Rotta, 1972)

$$\begin{aligned}
\Theta_{i_{\{2\}}} = & \frac{\bar{\mathrm{D}} R_{ij}}{\bar{\mathrm{D}} t} + R_{kj} \frac{\partial \bar{u}_i(\boldsymbol{x}, t)}{\partial x_k} + R_{ik} \left. \frac{\partial \bar{u}_j(\boldsymbol{x}, t)}{\partial x_k} \right|_{\boldsymbol{x}+\boldsymbol{r}} \\
& + \left[\bar{u}_k(\boldsymbol{x}+\boldsymbol{r}, t) - \bar{u}_k(\boldsymbol{x}, t)\right] \frac{\partial R_{ij}}{\partial r_k} + \frac{\partial \overline{p'u'}_j}{\partial x_i} - \frac{\partial \overline{p'u'}_j}{\partial r_i} + \frac{\partial \overline{u'_i p'}}{\partial r_j} \\
& - \nu \left[\frac{\partial^2 R_{ij}}{\partial x_k \partial x_k} - 2 \frac{\partial^2 R_{ij}}{\partial x_k \partial r_k} + 2 \frac{\partial^2 R_{ij}}{\partial r_k \partial r_k} \right] \\
& + \frac{\partial R_{(ik)j}}{\partial x_k} - \frac{\partial}{\partial r_k} \left[R_{(ik)j} - R_{i(jk)} \right] + 2\,\Omega_k \left[e_{kli} R_{lj} + e_{klj} R_{il} \right] = 0,
\end{aligned} \tag{2.26}$$

where the difference between two-points has been introduced according to

$$\boldsymbol{x} = \boldsymbol{x}_{(0)} \ , \qquad \boldsymbol{r} = \boldsymbol{x}_{(1)} - \boldsymbol{x}_{(0)}. \tag{2.27}$$

The vectors $\overline{p'u'}_j$ and $\overline{u'_i p'}$ are special cases of $P_{i_{\{n\}}[k]}$ defined according to

$$\overline{p'u'}_j(\boldsymbol{x}, \boldsymbol{r}, t) = \overline{p'(\boldsymbol{x}_{(0)}, t)\, u'_j(\boldsymbol{x}_{(1)}, t)}, \ \ \overline{u'_i p'}(\boldsymbol{x}, \boldsymbol{r}, t) = \overline{u'_i(\boldsymbol{x}_{(0)}, t)\, p'(\boldsymbol{x}_{(1)}, t)}, \tag{2.28}$$

while $R_{(ik)j}$ and $R_{i(jk)}$ are respectively defined as

$$R_{(ik)j} = \overline{u'_i(x,t) u'_k(x,t) u'_j(x^{(1)}, t)} \ , R_{i(jk)} = \overline{u'_i(x,t) u'_j(x^{(1)}, t) u'_k(x^{(1)}, t)}. \tag{2.29}$$

For the TP case the continuity equations (2.23) and (2.24) simplify to

$$\frac{\partial R_{ij}}{\partial x_i} - \frac{\partial R_{ij}}{\partial r_i} = 0 \ , \quad \frac{\partial R_{ij}}{\partial r_j} = 0, \quad \frac{\partial \overline{p'u'}_i}{\partial r_i} = 0 \ , \quad \frac{\partial \overline{u'_j p'}}{\partial x_j} - \frac{\partial \overline{u'_j p'}}{\partial r_j} = 0. \tag{2.30}$$

The autocorrelation tensor is defined as

$$R_{ii}(\boldsymbol{x}, \boldsymbol{r}, t) = \overline{u_i'(\boldsymbol{x}, t) u_i'(\boldsymbol{x}^{(1)}, t)} \tag{2.31}$$

and the turbulent kinetic energy is simply one half of R_{ii} with zero displacement:

$$K(\boldsymbol{x}, t) = \overline{u_i'(\boldsymbol{x}, t) u_i'(\boldsymbol{x}, t)}. \tag{2.32}$$

Thus the TPC tensor converges to the Reynolds stress tensor for zero displacement. In contradiction to the Reynolds stress tensor the TPC tensor is non-symmetric since

$$R_{ij}(\boldsymbol{x}, \boldsymbol{r}, t) = R_{ji}(\boldsymbol{x} + \boldsymbol{r}, -\boldsymbol{r}, t). \tag{2.33}$$

The TPC equations have, compared to the Reynolds stress equations, less unknown terms (namely only the triple correlation) at the expense of usually three additional dimensions.

Further properties of the TPC tensor are that it obeys the Schwarz's inequality

$$|R_{ij}(\boldsymbol{x}, \boldsymbol{r}, t)| \leqslant \left(\overline{u_i'^2}(\boldsymbol{x}, t) \overline{u_j'^2}(\boldsymbol{x}^{(1)}, t) \right)^{1/2} \tag{2.34}$$

and that the velocities u_i' and u_j' are statistically independent for $\boldsymbol{r} \to \infty$:

$$\lim_{|r| \to \infty} R_{ij}(\boldsymbol{x}, \boldsymbol{r}, t) = 0. \tag{2.35}$$

3 Turbulence models

Turbulence modeling is the often neglected, but a necessary result of all turbulence research. It attempts to make judicious use of various assumptions about the nature of turbulent flows to reduce the intractable Navier-Stokes equations to a simpler, more practical system of equations that can be used to predict the predominantly complex and chaotic fluid behavior. Therefore the closure models may be suitable for one class of flows or flow regions, while less applicable for other classes.

3.1 The eddy viscosity concept

1877 Boussinesq introduced the idea of the eddy viscosity concept, which is used by most common turbulence models. In eddy viscosity models (EVM), the unknown correlations are assumed to be proportional to the spatial gradients of the quantity they are meant to transport. The Reynolds stresses are thus determined from

$$-\overline{u_i' u_j'} = \nu_t \left(\frac{\partial \bar{u}_i}{\partial x_j} + \frac{\partial \bar{u}_j}{\partial x_i} \right). \tag{3.1}$$

The eddy viscosity ν_t is thereby not a fluid property but depends on the state of turbulence and must be determined by the turbulence model. Thus the number of unknowns has been reduced from the six unknown components of the Reynolds stress tensor to one, namely the eddy viscosity.

The approach from Boussinesq has to be extended since the trace of the Reynolds stress tensor has to be

$$R_{ii} = (\overline{u_1' u_1'} + \overline{u_2' u_2'} + \overline{u_3' u_3'}) = 2K \tag{3.2}$$

but is

$$R_{ii} = -\overline{u_i' u_i'} = 2\nu_t \left(\frac{\partial \bar{u}_1}{\partial x_1} + \frac{\partial \bar{u}_2}{\partial x_2} + \frac{\partial \bar{u}_3}{\partial x_3} \right) = 0. \tag{3.3}$$

This request is fulfilled by the extended ansatz

$$-\overline{u_i' u_j'} = \nu_t \left(\frac{\partial \bar{u}_i}{\partial x_j} + \frac{\partial \bar{u}_j}{\partial x_i} \right) - \frac{2}{3} K \delta_{ij}, \tag{3.4}$$

whereby δ_{ij} is the Kronecker-symbol, defined by

$$\delta_{ij} = \begin{pmatrix} 1 & 0 & 0 \\ 0 & 1 & 0 \\ 0 & 0 & 1 \end{pmatrix}. \tag{3.5}$$

The eddy viscosity can then be introduced into the Reynolds averaged Navier-Stokes equations. The challenge of the turbulence model is thus to find appropriate approaches for the eddy viscosity, which is variable in time and space. These models are called closure models of first order, whereby models for the Reynolds stresses are called closure models of second order.

The most simple models describe the eddy viscosity with constants, which are calibrated with numerical or experimental data. These so called algebraic or zero-equation models give only sound results, if the turbulence is homogeneous in time and space. Higher turbulence models of first order put more numerical effort in the determination of the eddy viscosity. These models are distinguished by the number of additional differential equation, having to be solved. They are therefore called zero-equation, one-equation or two-equation models.

3.1.1 Zero-equation models

These models prescribe the eddy viscosity as an algebraic equation. They use no information about the flow but geometry. As a result they cannot predict the dynamic relationships between productive and dissipative areas within the flow. Zero-equation models can be divided into two classes, which are the uniform or constant turbulent viscosity and the mixing-length model.

Constant eddy viscosity

The constant eddy viscosity calculation method is not a proper turbulence model and has little significance for hydrodynamic properties. Therefore it is presented here only very briefly.

In this calculation method a constant eddy viscosity / diffusivity is assumed for the whole flow field whose value is found from experiments either directly, from empirical information, or by trial and error calculations to match the observations of the considered problem. The constant eddy viscosity model is of very little accuracy and can only be applied in the far field where the eddy viscosity varies very little. The assumption of a constant eddy viscosity / diffusivity is sometimes somewhat alleviated and different values are adopted for the horizontal and vertical diffusivities.

In application to a planar two-dimensional free shear-flow, the uniform turbulent viscosity model can be written

$$\nu_t(x_1, x_2) = \frac{\bar{u}_0(x_1)\delta(x_1)}{Re_T}, \tag{3.6}$$

where $\bar{u}_0(x_1)$ and $\delta(x_1)$ are the characteristic velocity and length-scale of the mean flow. Re_T can be interpreted as a turbulent Reynolds number and is therewith a flow dependent constant. The flow varies in the mean flow direction but is constant in the normal direction (x_2-direction). This model can only be applied for very simple flows for which it is possible to define the direction of flow, the characteristic length-scale $\delta(x_1)$ and the characteristic

velocity scale $\bar{u}_0(x_1)$. Furthermore the model is incomplete since Re_T has to be specified, depending upon the nature of the flow and on the definitions chosen for $\bar{u}_0(x_1)$ and $\delta(x_1)$. The constant eddy viscosity concept provides therefore a useful tool for a basic description of the mean velocity profile of very simple flows but is not applicable for more complex flows for which the eddy viscosity is not constant.

Mixing-length model

In Prandtl's (1925) mixing-length model (PMLM), the effective viscosity is taken as being proportional to the square of a quantity having the dimensions of a length that is the so-called mixing-length ℓ_m, multiplied by the absolute value of the local velocity gradient. Thus

$$\nu_t = \ell_m^2 \left| \frac{\partial \bar{u}_1}{\partial x_2} \right| \tag{3.7}$$

and with (3.1)

$$-\overline{u_1' u_2'} = \ell_m^2 \left| \frac{\partial \bar{u}_1}{\partial x_2} \right| \frac{\partial \bar{u}_1}{\partial x_2}, \tag{3.8}$$

with which we can designate the mixing-length ℓ_m from numerical or experimental data. For near wall flows a good approximation for the mixing-length is

$$\ell_m = \kappa x_2, \tag{3.9}$$

which has been extended by van Driest (1956) to

$$\ell_m = \kappa x_2 (1 - e^{(-y^+/A^+)}), \tag{3.10}$$

with A^+ between 25...26. κ is thereby the von Karmann constant lying between 0.38...0.43. The ansatz from van Driest allows a much better fit for the turbulence statistics in a boundary layer.
The mixing-length ℓ_m has to be specified as a function of position. In unbounded flows, ℓ_m is in the order of 0.1 times the layer width. Close to a wall ℓ_m is in the order of 0.4 times the distance from the wall (unless modified in the manner of van Driest (3.10)). In the immediate vicinity of the wall where viscous effects predominate, it diminishes more rapidly.

Calculations based on the PMLM are easy to make, because no additional differential equation must be solved. In unbounded flows (for example jets, wakes, plumes), the variation of the PMLM across the layer width is not large, so that velocity profiles can be fairly well predicted. Although very close to a wall the PMLM is not useful, the processes occurring there can often be handled adequately by use of an empirically-based "wall function". For most boundary layer flows at least the order of magnitude of the mixing-length can be guessed fairly well.
For flows with recirculation or those with non-planar walls, it is impossible to estimate the distribution of mixing-length magnitudes with acceptable accuracy. The PMLM implies that the local level of turbulence depends only on the local generation and dissipation

rates. In reality though, turbulence may be carried or diffused to locations where no turbulence is actually being generated at all. The PMLM cannot represent this. Furthermore this model implies that the turbulent viscosity is always positive (as do one- and two-equation models as well), while in reality it can change sign.

Although its erroneous predictions and non-generality, the mixing-length model has formed the basis for other turbulence models, even recent ones. Modern eddy viscosity models which are based on the mixing-length concept are for example the Cebeci-Smith (Cebeci & Smith, 1974) and the Baldwin-Lomax model (Baldwin & Lomax, 1978). Both models are two-layer models with ν_t given by separate expressions in each layer.
The accurate prediction of these models is however more contributed to the introduced ad hoc (or empirical) functions and constants, rather than any additional physics included in the models. Since the zero-equation models do not have any transport of turbulence, they cannot be expected to accurately predict any flows with non-local mechanisms. Numerical simulations with the zero-equation models are thus usually restricted to attached boundary layer flows, which can be modeled using only local relations.

3.1.2 One-equation models

In order to avoid the local behavior of the mixing-length turbulence models, a transport-equation is needed for some turbulent quantity. Here the turbulent kinetic energy K is a reasonable choice to determine ν_t in the Boussinesq relation (3.4). There are also one-equation models which solve a transport-equation for the eddy viscosity ν_t. These models will be neglected in the following due to minor importance. As the energy K is contained mainly in the large-scale fluctuations, $\sqrt{K}$ is a velocity scale for the large-scale turbulent motion. Using this scale in the eddy viscosity concept, the eddy viscosity can be written

$$\nu_t = C'_\mu \sqrt{K} \ell \tag{3.11}$$

where C'_μ is an empirical constant. The lengt-scale ℓ has to be introduced for dimensional reasons. This equation has been introduced by Kolmogorov (1942) and Prandtl (1945) independently. For the determination of the turbulent kinetic energy a simplified form of its exact transport-equation is used. Contracting the transport-equation for the Reynolds stresses (2.13) by putting $i = j$ and taking the half, gives the equation for the kinetic energy of turbulence

$$\frac{\bar{D}K}{\bar{D}t} = \overline{u'_k u'_l} \frac{\partial \bar{u}_k}{\partial x_l} - \epsilon + \frac{\partial}{\partial x_k} \left[-\frac{\overline{p' u'_k}}{\rho} - \frac{\overline{u'_k u'_l u'_l}}{2} + \nu \frac{\partial K}{\partial x_k} + \nu \frac{\partial \overline{u'_k u'_l}}{\partial x_l} \right]. \tag{3.12}$$

In this equation the pressure strain term is not contained any more, showing the restrictions of models based on equation (3.12). The unclosed K-equation is of no use in a turbulence model because new unknown correlations appear in the diffusion and dissipation terms. Therefore model assumptions have to be introduced for these terms to receive a closed set of equations. Thereby Boussinesq's ansatz (3.4) has been adopted for the production term. The dissipation is usually modeled from dimensional arguments by the

expression

$$\epsilon = C_D \frac{K^{3/2}}{\ell} \tag{3.13}$$

with C_D as an empirical constant. For the diffusion term it is assumed that it depends on the gradient of the turbulent kinetic energy K:

$$\frac{\partial}{\partial x_k}\left[-\frac{\overline{p'u'_k}}{\rho} - \frac{\overline{u'_k u'_l u'_l}}{2} + \nu\frac{\partial K}{\partial x_k} + \nu\frac{\partial \overline{u'_k u'_l}}{\partial x_l}\right] = \frac{\partial}{\partial x_k}\left(\left(\frac{\nu_t}{\sigma_K} + \nu\right)\frac{\partial K}{\partial x_k}\right), \tag{3.14}$$

where σ_K is a further empirical constant.

With these assumptions the K-equation reads

$$\frac{\bar{D}K}{\bar{D}t} = \nu_t\left(\frac{\partial \bar{u}_i}{\partial x_j} + \frac{\partial \bar{u}_j}{\partial x_i}\right)\frac{\partial \bar{u}_i}{\partial x_j} - C_D\frac{K^{3/2}}{\ell} + \frac{\partial}{\partial x_k}\left(\left(\frac{\nu_t}{\sigma_K} + \nu\right)\frac{\partial K}{\partial x_k}\right). \tag{3.15}$$

The empirical constants in equation (3.15) are usually $C'_\mu \approx 0.8$, $C_D \approx 0.8$ and $\sigma_K \approx 1$. The calculations with this model are based on information about the distribution of the length-scale ℓ in the flow field. This information is mostly not available especially for complex flows, leading to a very restricted application range for these models. Equation (3.15) has to be solved simultaneously with the streamwise momentum equation and with equations for other mean-flow variables which may be of interest.
One-equation models do not account for the transport of turbulence length-scale and offer therefore only small advantages over the mixing-length model. Since one-equation models account for convective and diffusive transport of the turbulent velocity scale they are superior to the mixing-length hypothesis when this transport is important. These flows are for example non-equilibrium boundary layers with rapidly changing free-stream conditions, boundary layers with free-stream turbulence and heat transfer across planes with $\partial \bar{u}_1/\partial x_2 = 0$ and recirculating flows.

3.1.3 Two-equation models

Two-equation models have served as the basis for computing turbulent flows during the last two decades. For all two-equation models, the starting point is the Boussinesq approximation (3.1) and the turbulence kinetic energy equation (3.15). In two-equation models a second equation, determining the turbulent length-scale has to be solved in addition to the transport-equation for the turbulent kinetic energy. The length-scale equation not necessarily needs to have the length-scale itself as dependent variable. Any dimensionally correct combination of the turbulent kinetic energy and the length-scale

$$Z = K^m \ell^n \tag{3.16}$$

suffice, because the kinetic energy K is already known from solving the $K-$equation (3.15). For example there are a couple of models which solve an equation for the dissipation rate $\epsilon \sim K^{3/2}/\ell$ (e.g. Chou, 1945; Davidov, 1961; Harlow & Nakayama, 1967; Jones & Launder, 1972) , the frequency $f \sim \sqrt{K}^{1/2}/\ell$ (e.g. Kolmogorov, 1942) or the vorticity

$\omega \sim K/\ell^2$ (e.g. Spalding, 1971; Saffman, 1970). Rotta (1968) and Rodi & Spalding (1970) introduced a transport-equation for $K\ell$ and Rotta (1951) and Spalding (1967) introduced an equation for the length-scale ℓ itself. Some of the equations were derived first in exact form by manipulation of the Navier-Stokes equations and then were turned into a tractable form by model assumptions, while others were conceived heuristically. It is possible to transfer the transport-equations for the different turbulence quantities into each other. Thereby all terms can be transferred exactly into each other besides the diffusion term. Experience with the various equations has shown that this difference is unimportant in free flows. Near walls though the gradient assumption for diffusion with a single constant appears to work better for ϵ than for any other variable. The ϵ-equation does not require a secondary source term while the equations for all other variables require a near-wall correction term. Additionally the ϵ-equation can be derived relatively easily and ϵ appears directly in the K-equation making the ϵ-equation become considerably more popular than the other scale supplying equations.
Therefore in this thesis the discussions on two-equation models are presented in terms of the $K-\epsilon$ model, which is by far the most popular two-equation model. The earliest development efforts based on this model have been done by Chou (1945), Davidov (1961) and Harlow & Nakayama (1968). The best known model is the one developed by Jones & Launder (1972) which is therefore called standard K-ϵ model. In 1974 Launder & Sharma modified the model's closure coefficients. Nowadays most researchers use the coefficients introduced by them.

The equations of the standard K-ϵ model are the one for the turbulent kinetic energy K

$$\frac{\bar{\mathrm{D}}K}{\bar{\mathrm{D}}t} = \nu_t \left(\frac{\partial \bar{u}_j}{\partial x_k} + \frac{\partial \bar{u}_k}{\partial x_j} \right) \frac{\partial \bar{u}_j}{\partial x_k} - \epsilon + \frac{\partial}{\partial x_j} \left[\frac{\nu_t}{\sigma_K} \frac{\partial K}{\partial x_j} \right] \tag{3.17}$$

and the one for the dissipation of the turbulent kinetic energy, ϵ

$$\frac{\bar{\mathrm{D}}\epsilon}{\bar{\mathrm{D}}t} = C_{\varepsilon_1} \frac{\epsilon}{K} \nu_t \left(\frac{\partial \bar{u}_j}{\partial x_k} + \frac{\partial \bar{u}_k}{\partial x_j} \right) \frac{\partial \bar{u}_j}{\partial x_k} - C_{\varepsilon_2} \frac{\epsilon^2}{K} + \frac{\partial}{\partial x_j} \left[\frac{\nu_t}{\sigma_\varepsilon} \frac{\partial \epsilon}{\partial x_j} \right] \quad , \tag{3.18}$$

with

$$\nu_t = C_\mu \frac{K^2}{\epsilon}. \tag{3.19}$$

Model constants are determined from experimental data invoking specific turbulent flows (see section 3.5). For the K-ϵ model constants are given in table 3.1.

C_μ	σ_K	σ_ε	C_{ε_1}	C_{ε_2}
0.09	1.0	1.3	1.44	1.92

Table 3.1: Model constants of the $K-\epsilon$ model.

3.1.4 Non-linear eddy viscosity models

Even though the eddy viscosity models have proven to work well in approximately parallel shear-flows, there are a number of effects that can not be captured by these isotropic eddy viscosity type of model. For example the normal stresses of a purely shearing flow are predicted as equal although this is certainly not observed in experiments . Linear isotropic eddy viscosity models are furthermore not capable to reproduce the flow features appearing in rotating flows or flows with strong streamline curvature. These shortcomings can be removed by a more general constitutive relation containing non-linear terms, as demonstrated by Speziale (1987).

Following the work by Pope (1975) the principles for the derivation of more general effective viscosity relationships between the Reynolds stress tensor and the mean velocity gradient field will be shortly outlined. Non-linear eddy viscosity models are closely related to explicit algebraic Reynolds stress models, which will be described in section 3.4.

The basic assumption behind a non-linear eddy viscosity model is that the Reynolds stresses are uniquely related to the rates of strain, the rates of rotation and local scalar quantities. The two scaling parameters K and ϵ are usually employed to normalize the Reynolds stresses the rates of strain and the rates of rotation as follows:

$$a_{ij} = \frac{\overline{u_i' u_j'}}{K} - \frac{2}{3}\delta_{ij}, \tag{3.20}$$

$$S_{ij}^* = \frac{1}{2}\frac{K}{\epsilon}S_{ij} = \frac{1}{2}\frac{K}{\epsilon}\left(\frac{\partial \bar{u}_i}{\partial x_j} + \frac{\partial \bar{u}_j}{\partial x_i}\right), \tag{3.21}$$

$$W_{ij}^* = \frac{1}{2}\frac{K}{\epsilon}W_{ij} = \frac{1}{2}\frac{K}{\epsilon}\left(\frac{\partial \bar{u}_i}{\partial x_j} - \frac{\partial \bar{u}_j}{\partial x_i} + e_{jik}\Omega_k\right). \tag{3.22}$$

The anisotropy tensor $\boldsymbol{a}$ and the shear tensor $\boldsymbol{S}^*$ are non-dimensional symmetric tensors with zero trace. The rotation tensor $\boldsymbol{W}^*$ is non-dimensional and antisymmetric. Owing to the Cayley-Hamilton theorem, the number of independent invariants and linearly dependent second order tensors that may be formed from the shear and rotation tensor is finite. In general form the stress-strain relationship might be written in the closed tensor polynomial:

$$\boldsymbol{a} = \sum_{\lambda} G_\lambda \boldsymbol{T}^\lambda \tag{3.23}$$

or rewritten to the unnormalized Reynolds stress

$$\overline{u_i' u_j'} = \frac{2}{3}K\delta_{ij} + K\sum_{\lambda} G_\lambda T_{ij}^\lambda. \tag{3.24}$$

Thereby the coefficients G_λ are functions of a finite number of invariants. In the general, three-dimensional case there are ten tensors and five scalar invariants which have been

identified by using the tensor invariant theory (see e.g. Spencer, 1971):

$$\begin{aligned}
\boldsymbol{T}^{*1} &= \boldsymbol{S}^*, \\
\boldsymbol{T}^{*2} &= \boldsymbol{S}^*\boldsymbol{W}^* - \boldsymbol{W}^*\boldsymbol{S}^*, \\
\boldsymbol{T}^{*3} &= \boldsymbol{S}^{*2} - \tfrac{1}{3}\boldsymbol{\delta}\{\boldsymbol{S}^{*2}\}, \\
\boldsymbol{T}^{*4} &= \boldsymbol{W}^{*2} - \tfrac{1}{3}\boldsymbol{\delta}\{\boldsymbol{W}^{*2}\}, \\
\boldsymbol{T}^{*5} &= \boldsymbol{W}^*\boldsymbol{S}^{*2} - \boldsymbol{S}^{*2}\boldsymbol{W}^*, \\
\boldsymbol{T}^{*6} &= \boldsymbol{W}^{*2}\boldsymbol{S}^* + \boldsymbol{S}^*\boldsymbol{W}^{*2} - \tfrac{2}{3}\boldsymbol{\delta}\{\boldsymbol{S}^*\boldsymbol{W}^{*2}\}, \\
\boldsymbol{T}^{*7} &= \boldsymbol{W}^*\boldsymbol{S}^*\boldsymbol{W}^{*2} - \boldsymbol{W}^{*2}\boldsymbol{S}^*\boldsymbol{W}^*, \\
\boldsymbol{T}^{*8} &= \boldsymbol{S}^*\boldsymbol{W}^*\boldsymbol{S}^{*2} - \boldsymbol{S}^{*2}\boldsymbol{W}^*\boldsymbol{S}^*, \\
\boldsymbol{T}^{*9} &= \boldsymbol{W}^{*2}\boldsymbol{S}^{*2} + \boldsymbol{S}^{*2}\boldsymbol{W}^{*2} - \tfrac{2}{3}\boldsymbol{\delta}\{\boldsymbol{S}^{*2}\boldsymbol{W}^{*2}\}, \\
\boldsymbol{T}^{*10} &= \boldsymbol{W}^*\boldsymbol{S}^{*2}\boldsymbol{W}^{*2} - \boldsymbol{W}^{*2}\boldsymbol{S}^{*2}\boldsymbol{W}^*
\end{aligned}$$

and

$$I_1^* = \{\boldsymbol{S}^{*2}\},\ \ I_2^* = \{\boldsymbol{W}^{*2}\},\ \ I_3^* = \{\boldsymbol{S}^{*3}\},\ \ I_4^* = \{\boldsymbol{W}^{*2}\boldsymbol{S}^*\},\ \ I_5^* = \{\boldsymbol{W}^{*2}\boldsymbol{S}^{*2}\}, \tag{3.25}$$

whereby $\{\cdot\}$ is the trace and the following abbreviated notations are used:

$$\begin{aligned}
\boldsymbol{S}^*\boldsymbol{W}^* = S_{ik}^*W_{kj}^*,\ \boldsymbol{S}^*\boldsymbol{W}^*\boldsymbol{S}^*\boldsymbol{W}^* = S_{ik}^*W_{kl}^*S_{lm}^*W_{mj}^*, \text{ etc.} \\
\boldsymbol{S}^{*2} = S_{ik}^*S_{kj}^*,\ \{\boldsymbol{S}^{*2}\} = S_{ik}^*S_{ki}^*, \text{ etc.},\ \boldsymbol{I} = \delta_{ij}.
\end{aligned} \tag{3.26}$$

The linear eddy viscosity model is received using only the first tensor $\boldsymbol{T}^{*1}$.

In order to complete the non-linear effective viscosity hypothesis, the unknown function G_λ appearing in (3.23) have to be determined. This is done by calibrating the coefficients against some chosen set of basic flows. Pope (1975) has determined the coefficients for the two-dimensional case but this will not be outlined in the following since this solution is of minor importance in connection with the given thesis. The equations given by (3.23) has then to be solved together with the equations for the turbulent kinetic energy (3.17) and the dissipation rate (3.18).
Non-linear viscosity models have been proposed by Yoshizawa (1984), Speziale (1987), Rubinstein & Barton (1990), Craft *et al.* (1996) and others.

3.2 Differential Reynolds stress models

The next level of complexity in the hierarchy of turbulence models are models based on the transport-equations of the Reynolds stress tensor (2.13) itself. In these models the Reynolds stress is not coupled directly to the mean velocity gradient. Instead the effect on the evolution of the Reynolds stress tensor in a flow field from the interaction between turbulence and the mean field is modeled. The first model based on the Reynolds stress transport-equation was developed by Rotta (1951) but the development of more advanced models of this class is still ongoing. An advantage of Reynolds stress models

(RSTM) compared to eddy viscosity models is that the anisotropy of the turbulence is preserved. Furthermore RSTMs are, contrary to two-equation models, for most flow cases (one exception will be outlined in chapter (5)) sensitive to rotation due to the inclusion of the Coriolis term in the equation. The six equations for the Reynolds stresses have to be completed by a length-scale determining equation, usually the ϵ-equation.

The explicit form of the production tensor is

$$P_{ij} = -\overline{u_j' u_k'} \frac{\partial \bar{u}_i}{\partial x_k} - \overline{u_i' u_k'} \frac{\partial \bar{u}_j}{\partial x_k}, \tag{3.27}$$

which involves the dependent variable $\overline{u_i' u_j'}$ and the given flow gradients; hence it is a closed term. The half trace of P_{ij} is the production of turbulent kinetic energy. The terms in (2.13) for which model approximations have to be found are the diffusion, dissipation and pressure strain term.

3.2.1 Model approximation for the diffusion term

The quantitative contribution of the diffusion term in the transport-equation (2.13) is usually of minor importance. The turbulent diffusion is composed of two parts. From measurements it is known, that the pressure velocity correlation is small compared to the triple correlation. The most simple model of the diffusion term is the model of Daly & Harlow (1970) given by:

$$\frac{\partial \overline{u_i' u_j' u_k'}}{\partial x_k} - \frac{1}{\rho} \left(\frac{\partial \overline{u_j' p'}}{\partial x_i} + \frac{\partial \overline{u_i' p'}}{\partial x_j} \right) + \nu \frac{\partial^2 \overline{u_i' u_j'}}{\partial x_k^2} = \frac{\partial}{\partial x_k} \left[\left(\nu \delta_{kl} + C_s \frac{K}{\epsilon} \overline{u_k' u_l'} \right) \frac{\partial \overline{u_i' u_j'}}{\partial x_l} \right]. \tag{3.28}$$

C_s is thereby the model constant with the standard value $C_s = 0.25$, whereby Daly & Harlow (1970) suggested 0.22.

3.2.2 Model approximation for the dissipation term

The viscous dissipation is characterized by the small scales for which the assumption of an isotropic distribution is valid in contradiction to the larger scales. The dissipation can thus be modeled by an isotropic ansatz

$$\epsilon_{ij} = 2\nu \overline{\frac{\partial u_i'}{\partial x_k} \frac{\partial u_j'}{\partial x_k}} = \frac{2}{3} \epsilon \delta_{ij}. \tag{3.29}$$

This ansatz is not valid in extreme situations where the Reynolds stress anisotropy is very large and the turbulence is close to a two-component state. It is then favorable to lump the dissipation rate together with the slow part of the pressure strain term.
The trace of the dissipation rate tensor equals twice the dissipation rate of the turbulent kinetic energy.

3.2.3 Model approximation for the pressure strain correlation

The pressure strain term has a purely redistributive effect among the components of the Reynolds stress tensor. It does not appear in the transport-equation for the turbulent kinetic energy, since the pressure strain term has zero trace.
The explicit appearance of the fluctuating pressure can be eliminated by taking the divergence for the fluctuating velocity, thus obtaining the Poisson equation for the pressure

$$-\frac{1}{\rho}\frac{\partial^2 p'}{\partial x_k \partial x_k} = 2\frac{\partial \bar{u}_i}{\partial x_j}\frac{\partial u'_j}{\partial x_i} + \frac{\partial^2 u'_i u'_j}{\partial x_i \partial x_j} - \frac{\partial^2 \overline{u'_i u'_j}}{\partial x_i \partial x_j}. \tag{3.30}$$

Integration of the Poisson equation for the pressure gives the pressure strain correlation, which can be divided into three parts. These are the rapid part, the slow part and the harmonic part. The last part is only of importance in the near wall region and otherwise negligible small compared to the other two parts. The rapid and the slow term of the pressure strain correlation are usually modeled separately.

Rapid part of the pressure strain correlation

The rapid part of the pressure strain correlation describes the interaction between the mean velocity field and the turbulence. It responds directly to changes in the mean flow field. Solving the Poisson equation for the pressure (3.30) for homogeneous flows the rapid pressure strain rate can be written in terms of a forth rank tensor:

$$\phi_{ij}^{rap} = 4K\frac{\partial \bar{u}_q}{\partial x_p}\left(M_{iqpj} + M_{jqpi}\right) \tag{3.31}$$

in which

$$M_{iqpj} = -\frac{1}{8\pi K}\int \frac{\partial^2 R_{ij}}{\partial r_p \partial r_q}\frac{dV}{\mid r \mid}, \tag{3.32}$$

where $R_{ij}(r)$ is the two-point velocity correlation. The problem is now to model the forth rank tensor M_{iqpj}. This tensor has the following properties:

- Modeling assumption: $M_{iqpj} = f\left(\delta_{ij}, a_{ij}\right)$.
- Symmetry condition: $M_{iqpj} = M_{iqjp}$, $M_{iqpj} = M_{qipj}$.
- Continuity condition: $M_{iqij} = 0$.
- Green's condition: $M_{iqpp} = \frac{1}{2}a_{iq} + \frac{1}{3}\delta_{iq}$.
- $M_{iipq} = Y_{pq}$; Y_{pq}= structure tensor (Kassinos & Reynolds, 1994) .
- $M_{iipp} = 2K$.

A natural approach to model the rapid pressure strain correlation is to express M_{iqpj} in terms of the dimensionless Reynolds stress anisotropy tensor. The above given symmetry conditions are satisfied by the linear expansion

$$\begin{aligned} M_{iqpj} =& A_1\delta_{ij}\delta_{pq} + A_2(\delta_{ip}\delta_{jq} + \delta_{iq}\delta_{jp}) + A_3\delta_{ij}a_{pq} + A_4 a_{ij}\delta_{pq} \\ &+ A_5(\delta_{ip}a_{jq} + \delta_{iq}a_{jp} + \delta_{jq}a_{ip} + \delta_{jp}a_{iq}). \end{aligned} \tag{3.33}$$

Insertion of this ansatz into (3.31) and applying the continuity and Green's condition leads to the linear model of Launder *et al.* (1975):

$$\begin{aligned} \phi_{ij}^{rap} =& \frac{4}{5}KS_{ij} + \frac{9C_2+6}{11}K(a_{ik}S_{jk} + a_{jk}S_{ik} - \frac{2}{3}a_{kl}S_{kl}\delta_{ij}) \\ &+ \frac{-7C_2+10}{11}K(a_{ik}W_{jk} + a_{jk}W_{ik}) \end{aligned} \tag{3.34}$$

where different values for the model constant C_2, ranging from 0.4 to 0.56 have been proposed.
A non-linear model for the rapid part of the pressure strain correlation has for example been proposed by Johansson & Hallbäck (1994). Using the Cayley-Hamilton theorem the most general form for the rapid part of the pressure strain correlation contains 15 terms with non-linearity up to forth order, each multiplied by a function of scalar parameters such as the invariants of a_{ij}. Using the symmetry, continuity and Green's condition given above the number of independent functions reduces to nine.
Thus any model for the rapid pressure strain rate can be expressed with the aid of the following eight terms

$$\begin{aligned} G_{ij}^{(1)} &= a_{ij}, \\ G_{ij}^{(2)} &= S_{ij}, \\ G_{ij}^{(3)} &= a_{ik}S_{kj} + S_{ik}a_{kj} - \frac{2}{3}a_{lk}S_{kl}\delta_{ij}, \\ G_{ij}^{(4)} &= a_{ik}W_{kj} - W_{ik}a_{kj}, \\ G_{ij}^{(5)} &= a_{ik}a_{kj} - \frac{1}{3}a_{lk}a_{kl}\delta_{ij}, \\ G_{ij}^{(6)} &= a_{ik}S_{kl}a_{lj} - \frac{1}{3}a_{nk}a_{kl}S_{ln}\delta_{ij}, \\ G_{ij}^{(7)} &= a_{ik}a_{kl}W_{lj} - W_{ik}a_{kl}a_{lj}, \\ G_{ij}^{(8)} &= a_{ik}a_{kl}W_{lm}a_{mj} - a_{ik}W_{kl}a_{lm}a_{mj}. \end{aligned} \tag{3.35}$$

Sjögren & Johansson (2000) found that the nine independent functions appearing in the M tensor expression reduce to six after insertion into the expression for the rapid pressure strain. The most general model for the rapid part of the pressure strain correlation is thus:

$$\begin{aligned} \frac{\phi_{ij}^{rap}}{K} =& (q_1 a_{lk}S_{kl} + q_9 a_{nk}a_{kl}S_{ln})G_{ij}^{(1)} + q_2 G_{ij}^{(2)} + q_3 G_{ij}^{(3)} + q_4 G_{ij}^{(4)} \\ &+ (q_5 a_{lk}S_{kl} + q_{10} a_{nk}a_{kl}S_{ln})G_{ij}^{(5)} + q_6 G_{ij}^{(6)} + q_7 G_{ij}^{(7)} + q_8 G_{ij}^{(8)}, \end{aligned} \tag{3.36}$$

where only six of the scalar functions are independent

$$\begin{aligned} q_2 &= \frac{4}{5} - \frac{1}{10}\left(4q_1 - 3q_7\right) II_a - \frac{2}{5} q_9 III_a, \\ q_3 &= \frac{12}{7} + \frac{9}{7} q_4 - \frac{1}{7}\left(3q_8 + 2q_9\right) II_a - \frac{2}{7} q_{10} III_a, \\ q_5 &= q_9, \\ q_6 &= 6q_1 - 9q_7 - q_{10} II_a, \end{aligned} \tag{3.37}$$

with $II_a = a_{ik}a_{ki}$ and $III_a = a_{il}a_{lk}a_{ki}$.

Sjögren & Johansson (2000) introduced an extension of the rapid part of the pressure strain correlation for an improved prediction of effects of rotation. The new term is quadratic in $\boldsymbol{W}$ scaled with $\sqrt{-II_W} = \sqrt{-W_{ij}W_{ji}}$, so that it is linearly dependent on the magnitude of the rotation

$$N_{ij} = \frac{1}{\sqrt{-II_W}} \left(a_{ik}W_{kl}W_{lj} + W_{ik}W_{kl}a_{lj} - \frac{2}{3} I_{aWW}\delta_{ij} \right). \tag{3.38}$$

The expression for the complete rapid pressure strain correlation is thus

$$\phi_{ij}^{rap} = 4K \frac{\partial \bar{u}_p}{\partial x_q} \left(M_{iqpj} + M_{jqpi} \right) + C_W K N_{ij}, \tag{3.39}$$

whereby the value for the model constant C_W has be chosen as 0.5.

Slow part of the pressure strain correlation

The modeling of the slow part of the pressure strain correlation is based on the return-to-isotropy concept. That means that the slow pressure strain term redistributes energy among velocity components towards isotropy in the absence of external forcing. Rotta (1951) was first to develop a model for the slow part of the pressure strain correlation. Applying dimensional analysis and assuming that the pressure strain rate is proportional to the deviation from isotropy he introduced the model

$$\overline{\frac{p'^{(s)}}{\rho} \left(\frac{\partial u_i'}{\partial x_j} + \frac{\partial u_j'}{\partial x_i} \right)} = -C_R \frac{K^{3/2}}{\ell} \left(\frac{\phi_{ij}^{slow}}{K} - \frac{2}{3}\delta_{ij} \right). \tag{3.40}$$

A general form for the model for the slow part of the pressure strain correlation can be derived by using the Cayley-Hamilton theorem. Thereby it is assumed that the slow part of the pressure strain correlation is a function of the Reynolds stress anisotropy tensor, which has the following properties:

- For isotropic flows: $\phi_{ij}^{slow} = 0 \Rightarrow a_{ij} = 0$.
- Symmetry condition: $\phi_{ij}^{slow} = \phi_{ji}^{slow}$.

- Continuity condition: $\phi_{kk}^{slow} = 0$.

Applying the Cayley-Hamilton theorem the slow term is given by

$$\phi_{ij}^{slow} = \alpha_1 \delta_{ij} + \alpha_2 a_{ij} + \alpha_3 a_{ij}^2. \tag{3.41}$$

(3.41) reduces with the conditions above mentioned to

$$\phi_{ij}^{slow} = \alpha_2 a_{ij} + \alpha_3 \left(a_{ij}^2 - \frac{1}{3} a_{kk}^2 \delta_{ij} \right). \tag{3.42}$$

The most commonly used form for the slow redistribution is the Rotta model

$$\phi_{ij}^{slow} = -C_1 \epsilon a_{ij} \tag{3.43}$$

where C_1 is known as the Rotta constant, usually assigned a value in the range $1.5 - 1.8$.

3.2.4 The Launder-Reece-Rodi model

A well known model, which is based on the transport-equations for the Reynolds stresses is the Launder-Reece-Rodi (LRR) model (Launder *et al.*, 1975). The full equations of the LRR model are

$$\begin{aligned} \frac{\bar{\mathrm{D}}\overline{u_i' u_j'}}{\bar{\mathrm{D}}t} =& - \left[\overline{u_j' u_k'} \frac{\partial \bar{u}_i}{\partial x_k} + \overline{u_i' u_k'} \frac{\partial \bar{u}_j}{\partial x_k} \right] - \frac{2}{3} \delta_{ij} \epsilon \\ & - C_1 \frac{\epsilon}{K} \left(\overline{u_i' u_j'} - \frac{2}{3} \delta_{ij} K \right) + (\phi_{ij} + \phi_{ji})_2 + (\phi_{ij} + \phi_{ji})_w \\ & + C_s \frac{\partial}{\partial x_k} \left[\frac{K}{\epsilon} \left(\overline{u_i' u_l'} \frac{\partial \overline{u_j' u_k'}}{\partial x_l} + \overline{u_j' u_l'} \frac{\partial \overline{u_k' u_i'}}{\partial x_l} + \overline{u_k' u_l'} \frac{\partial \overline{u_i' u_j'}}{\partial x_l} \right) \right], \end{aligned} \tag{3.44}$$

whereby the influence of the mean velocity gradient on the pressure strain correlation may be expressed by

$$\begin{aligned} (\phi_{ij} + \phi_{ji})_2 =& \frac{C_2 + 8}{11} (P_{ij} - \frac{2}{3} P \delta_{ij}) - \frac{30 C_2 - 2}{55} K \left(\frac{\partial \bar{u}_i}{\partial x_j} + \frac{\partial \bar{u}_j}{\partial x_i} \right) \\ & \frac{8 C_2 - 2}{11} \left(D_{ij} - \frac{2}{3} P \delta_{ij} \right), \end{aligned} \tag{3.45}$$

with

$$P_{ij} = - \left(\overline{u_i' u_k'} \frac{\partial \bar{u}_j}{\partial x_k} + \overline{u_j' u_k'} \frac{\partial \bar{u}_i}{\partial x_k} \right), \quad D_{ij} = - \left(\overline{u_i' u_k'} \frac{\partial \bar{u}_k}{\partial x_j} + \overline{u_j' u_k'} \frac{\partial \bar{u}_k}{\partial x_i} \right). \tag{3.46}$$

In the given thesis the near-wall correction to the pressure strain correlation $(\phi_{ij} + \phi_{ji})_w$ is omitted since its contribution is usually negligible.

The transport-equation for ϵ takes the form

$$\frac{\bar{\mathrm{D}}\epsilon}{\bar{\mathrm{D}}t} = -C_{\varepsilon_1} \frac{\epsilon \overline{u_i' u_k'}}{K} \frac{\partial \bar{u}_i}{\partial x_k} - C_{\varepsilon_2} \frac{\epsilon^2}{K} + C_\varepsilon \frac{\partial}{\partial x_k} \left(\frac{K}{\epsilon} \overline{u_k' u_l'} \frac{\partial \varepsilon}{\partial x_l} \right). \tag{3.47}$$

The LRR model constants are given in table 3.2.

C_1	C_2	C_s	C_{ε_1}	C_{ε_2}	C_ε
1.5	0.4	0.11	1.44	1.9	0.15

Table 3.2: Model constants of the LRR model.

3.3 Generalization of the Reynolds stress concept

In today's life several turbulence problems exist, where the effects of strong streamline curvature or system rotation are strong. Reynolds stress transport closures and lower level models seem to have some serious shortcomings concerning the modeling of such flows. Therefore a new model based on the generalization of the Reynolds stress concept, introduced by Johansson (2003) will be presented here. This new model contains more of the turbulence dynamics associated with rotational effects at the cost of algebraic complexity. Due to this complexity the present model seems to be more or less defective for engineering applications. It is therefore the scope of the introduction of this model to illustrate the modeling difficulties and limitations associated with rotational mean flows and the levels of closure where the effects may be appropriately described.

Some difficulties classical Reynolds stress models have with the modeling of rotational flows can be more easily identified if the rapid limit is considered. For this case only the rapid pressure strain term needs to be modeled.

To improve the shortcomings of the classical Reynolds stress closures concerning rotational effects one may take one step up in the hierarchy of modeling. Therefore Johansson (2003) developed a new generalized single-point closure based on transport-equations for the M-tensor. The derivation of this model is restricted to homogeneous, incompressible flows, leaving spatial redistribution and other inhomogeneity effects outside the scope of the present study.
Based on the work of Johansson the derivation and one application of this M-tensor model will be outlined in the following. In a similar manner Oberlack (1995) derived a general form of the model for the pressure strain correlation. Using rapid distortion theory (RDT) he pointed out, that the two-point correlation equation can be solved exactly for homogeneous turbulence with any arbitrary gradient of the mean velocity.

3.3.1 A new generalized single-point closure

Deriving transport-equations for the M-tensor, whereby the Reynolds stresses are left without any need of modeling, a new model that provides physically more realistic prediction of rotational effects has been developed by Johansson (2003).
A general forth rank tensor has 81 elements. To reduce the number of elements the in section (3.2.3) mentioned properties of the M-tensor have been used. With the symmetry conditions the number of elements for the M-tensor decreases to 36. The continuity condition gives nine further equations, leaving 27 independent elements of the M-tensor.

The transport-equation for the M-tensor

The transport-equation for the M-tensor can be written in the following general form:

$$\frac{DM_{ijpq}}{Dt} = P_{ijpq} + \Phi^{(r)}_{ijpq} + \Phi^{(s)}_{ijpq} - \epsilon_{ijpq} + D_{ijpq}\,. \tag{3.48}$$

In this equation all terms on the right hand side besides the production term P_{ijpq} need to be modeled. For P_{ijpq} an exact expression in terms of the M-tensor can be derived.

To derive the exact equation for the M-tensor the rapid homogeneous limit is considered. Further a spectral representation with time-dependent wavenumbers is used. The equations for the velocity fluctuations and the continuity equation then read

$$\frac{d\hat{u'}_i}{dt} = -i\kappa_i\hat{p} - \hat{u'}_j\frac{\partial\bar{u}_i}{\partial x_j} \tag{3.49}$$

$$\kappa_i\hat{u'}_i = 0\,. \tag{3.50}$$

Using

$$\frac{d\kappa_i}{dt} + \frac{\partial\bar{u}_j}{\partial x_i}\kappa_j = 0 \tag{3.51}$$

and the continuity equation (3.50) the pressure can be eliminated and the equation for the fluctuating velocities (3.49) becomes

$$\frac{d\hat{u'}_i}{dt} = \frac{\partial\bar{u}_k}{\partial x_m}\left[\frac{2\kappa_i\kappa_k}{\kappa^2} - \delta_{ik}\right]\hat{u}_m\,. \tag{3.52}$$

Introducing the definition for the spectral tensor

$$\hat{\phi}_{ij} = \langle\hat{u}^*_i\hat{u}_j\rangle\,, \tag{3.53}$$

whereby the asterisk denotes the complex conjugate, its evolution equation can be derived from (3.52):

$$\frac{d\hat{\phi}_{ij}}{dt} = \frac{\partial\bar{u}_k}{\partial x_m}\left(\frac{2\kappa_n\kappa_k}{\kappa^2} - \delta_{nk}\right)\left(\delta_{in}\hat{\phi}_{mj} + \delta_{jn}\hat{\phi}_{im}\right)\,. \tag{3.54}$$

Since the M-tensor may be written in terms of spectral quantities as

$$M_{ijpq} = \int\frac{\kappa_p\kappa_q}{\kappa^2}\hat{\phi}_{ij}d\vec{\kappa}, \tag{3.55}$$

its evolution equation can be received by multiplying (3.54) with $(\kappa_p\kappa_q)/\kappa^2$, making use of (3.51) and integrating over the wavenumber space to

$$\begin{aligned}\frac{dM_{ijpq}}{dt} = \frac{\partial\bar{u}_k}{\partial x_l}(&-\delta_{ql}M_{ijkp} - \delta_{pl}M_{ijkp} - \delta_{ik}M_{ljpq} - \delta_{jk}M_{ilpq}\\ &+2B_{ijpqkl} + 2B_{ljpqki} + 2B_{lipqkj})\,.\end{aligned} \tag{3.56}$$

Thereby the sixth rank B-tensor

$$B_{ijpqkl} = \int \frac{\kappa_p \kappa_q \kappa_k \kappa_l}{\kappa^2} \phi_{ij} d\vec{\kappa} \tag{3.57}$$

needs to be modeled in terms of the M-tensor.
From (3.2.3) we know that the Reynolds stresses are retrieved when the last two indices of the M-tensor are contracted. Therefore the exact Reynolds stress transport-equation can be derived from (3.56) by contraction of the last two indices of the M-tensor. Hence, no modeling is needed for the terms in the Reynolds stress equation.

The second part in (3.56) containing the B-tensor corresponds to the rapid pressure strain correlation. Therefore the model for ϕ^{rap}_{ijpq} in (3.48) is based on an expansion of the B-tensor in terms of the M-tensor. A linear expansion of the B-tensor, that satisfies the right tensor index symmetry properties may be expressed in terms of 16 tensorially independent parts, each multiplied by a numeric model parameter. The ansatz is schematically given by

$$\begin{aligned} B_{ijpqrs} = {} & 2K(C_1 \delta_{ij} N_{pqrs} + C \delta_{i.} N_{j\ldots}) + (C_3 R_{ij} + C_4 Y_{ij}) N_{pqrs} \\ & + C_5(R_{i.} N_{j\ldots} + R_{j.} N_{i\ldots}) + C_6(Y_{i.} N_{j\ldots} + Y_{j.} N_{i\ldots}) + C_7 \delta_{ij} \delta_{..} R_{..} \\ & + C_8 \delta_{ij} \delta_{..} Y_{..} + C_9 R_{..} N_{ij..} + C_{10} Y_{..} N_{ij..} + C_{11} \delta_{ij} M_{....} + C_{12} \delta_{..} M_{ij..} \\ & + C_{13} \delta_{..} M_{..ij} + C_{14} \delta_{..} (M_{i..j} + M_{j..i}) + C_{15}(\delta_{i.} M_{j\ldots} + \delta_{j.} M_{i\ldots}) \\ & + C_{16}(\delta_{i.} M_{\ldots j} + \delta_{j.} M_{\ldots i}) \,. \end{aligned} \tag{3.58}$$

Thereby dots signify permutations of $pqrs$. Y_{ij} is the structure tensor and N_{ijpq} gives the forth rank isotropic tensor, which is defined as

$$N_{ijpq} = \frac{1}{15}(\delta_{ij}\delta_{pq} + \delta_{ip}\delta_{jq} + \delta_{iq}\delta_{jq}) \,. \tag{3.59}$$

The B-tensor is symmetric in the first two and in any pair of the last four indices. Two further constrains are the continuity and the retrieval of the M-tensor upon the contraction of any two of the last four indices:

$$B_{ijpqki} = 0 \,, \tag{3.60}$$

$$B_{ijpqkk} = M_{ijpq} \,, \; B_{ijppkq} = M_{ijkq} \,. \tag{3.61}$$

These constrains reduce the number of model parameters to one (and 15 linearly independent groups of terms). Further details on the model are given in appendix C.

The slow pressure strain term is responsible for the redistribution of energy towards isotropy. The most simple possible approach to model this tendency of isotropization mathematically is to assume that the pressure strain rate is proportional to the deviation from isotropy as was suggested by Rotta (1951). Thus if Φ^{slow}_{ijpq} is modeled according to Rotta's model (see 3.2.3) we receive at the given hierarchy of modeling

$$\Phi^{slow}_{ijpq} = -C_1 \frac{\epsilon}{K} \left(M_{ijpq} - 2K N_{ijpq} \right) \,. \tag{3.62}$$

Herein C_1 is the Rotta constant.

The dissipation rate tensor ϵ_{ij} represents destruction of turbulent kinetic energy due to viscous effects. In the following the attention is focused on high Reynolds numbers and thus local isotropy is assumed. The model for ϵ_{ijpq} can then be written as

$$\epsilon_{ijpq} = 2\epsilon N_{ijpq} \,, \tag{3.63}$$

whereby N_{ijpq} is defined in (3.59).

As model for the diffusion term the model which was introduced by Daly & Harlow (1970) has been chosen. It reads for the given level of modeling

$$D_{ijpq} = C_s \frac{\partial}{\partial x_k} \left(\frac{\overline{u'_k u'_l}}{\epsilon} K \frac{\partial M_{ijpq}}{\partial x_l} \right) . \tag{3.64}$$

As value for the model constant $C_s = 0.25$ corresponds to the one given in section 3.2.1.

3.3.2 Application of the new model to rotational flows

In the following axisymmetric turbulence is considered. Next to isotropic turbulence axisymmetric turbulence is the second most simple form of homogeneous turbulence. All axisymmetric tensors must be expressible in terms of the unit vector λ_i, the Kronecker delta δ_{ij}, the permutation tensor e_{ijk} and a number of scalars depending on the rank of the tensor. The fourth rank M-tensor is then completely described by the five scalars

$$K,\ R_{\lambda\lambda},\ Y_{\lambda\lambda},\ M_{\lambda\lambda\lambda\lambda} \quad \text{and} \quad e_{\lambda ip} M_{i\lambda p\lambda} \,. \tag{3.65}$$

Thereby the shorter notation $R_{\lambda\lambda}$ has been used for $R_{ij}\lambda_i\lambda_j$, etc.
It is interesting to note that the exact expression for the rapid pressure strain rate in axisymmetry can be written

$$\Phi^{rap}_{\lambda\lambda} = 4 \frac{\partial \bar{u}_k}{\partial x_m} M_{m\lambda k\lambda} = 6\sigma M_{\lambda\lambda\lambda\lambda} + 4\Omega e_{\lambda ip} M_{i\lambda p\lambda} \,, \tag{3.66}$$

with Ω as the rotation rate.
In Reynolds stress closures it follows from the assumption that the M-tensor is expandable in terms of the Reynolds stress anisotropy tensor a_{ij} that the quantity $e_{\lambda ip} M_{i\lambda p\lambda}$ is identically zero, and hence that the pressure strain rate will be independent of the rotation rate.

Axial strain with superimposed rotation

To illustrate some of the modeling difficulties for this flow case the Craya formalism (see Craya, 1958) has been used:

$$\phi_{ij}(\vec{\kappa}) = N_1(\kappa,\mu)\beta_i\beta_j + N_2(\kappa,\mu)\gamma_i\gamma_j + S^r(\kappa,\mu)(\beta_i\gamma_j + \beta_j\gamma_i) \,, \tag{3.67}$$

where the three scalars N_1, N_2, and S^r are functions of the scalar wave number κ and $\mu = \vec{\kappa}\vec{\lambda}/\kappa$. The two vectors $\vec{\beta}$ and $\vec{\gamma}$ are unit-vectors orthogonal to $\vec{\kappa}$ defined as

$$\gamma = \frac{\kappa \times \lambda}{|\kappa \times \lambda|} \quad \text{and} \quad \beta = \frac{\kappa \times \gamma}{|\kappa \times \gamma|}\,. \tag{3.68}$$

This equation is the most general expression for axisymmetric turbulence except for an imaginary anti-reflectional part which has been omitted here for brevity. The S^r-part of the spectrum has an anti-reflectional symmetry (with respect to $\vec{\lambda}$) and is closely associated with rotational effects. With I denoting the integrals $\int_0^\infty \cdot \kappa^2 d\kappa$ the five independent elements of the M-tensor and the rapid pressure strain can be expressed as

$$K = \pi \textstyle\int_{-1}^{1}(N_1^I + N_2^I)d\mu\,, \tag{3.69}$$

$$R_{\lambda\lambda} = 2\pi \textstyle\int_{-1}^{1}(1-\mu^2)N_1^I d\mu\,, \tag{3.70}$$

$$Y_{\lambda\lambda} = 2\pi \textstyle\int_{-1}^{1}\mu^2(N_1^I + N_2^I)d\mu\,, \tag{3.71}$$

$$M_{\lambda\lambda\lambda\lambda} = 2\pi \textstyle\int_{-1}^{1}\mu^2(1-\mu^2)N_1^I d\mu\,, \tag{3.72}$$

$$e_{\lambda ip}M_{i\lambda p\lambda} = -2\pi \textstyle\int_{-1}^{1}\mu(1-\mu^2)S^{rI}d\mu\,, \tag{3.73}$$

$$\Phi_{\lambda\lambda}^{rap} = 6\sigma M_{\lambda\lambda\lambda\lambda} + 4\Omega e_{\lambda ip}M_{i\lambda p\lambda}\,. \tag{3.74}$$

Hereby only the fifth element (3.73) of the M-tensor, which becomes non-zero with rotation is associated with S^r. Since this fifth element has no counterpart in Reynolds stress closures the rapid pressure strain becomes independent of rotation for axisymmetric turbulence, whereas the new model keeps the dependence on the rotation rate.

3.4 Explicit algebraic Reynolds stress models

So far, eddy viscosity based two equation models have been dominating in the context of industrial flow computations, but with higher demands on prediction accuracy in increasingly challenging flow situations, the need for more complex models has become more urgent. The level of differential Reynolds stress models includes much more of the flow physics, but the implementation of these models into codes for design work of complex industrial flows is quite difficult. Explicit algebraic Reynolds stress models (EARSM) are a possibility to overcome the deficiencies of two equation models by keeping their numerical robustness. In EARSMs the Reynolds equation (2.13) is left without any explicit modeling. The traditional EARSM idea, which has been introduced by Rodi (1976) is to neglect the advection and the diffusion terms in the exact transport-equation for the Reynolds stress anisotropy tensor. This approach is known as the weak equilibrium assumption. If the weak equilibrium assumption as well as

$$\frac{Da_{ij}}{Dt} = 0\,; D_{ij}^a = 0 \tag{3.75}$$

is used one receives the following symbolicly written equation

$$\frac{\overline{u_i'u_j'}}{K}(\mathcal{P}-\epsilon) = \mathcal{P}_{ij} - \epsilon_{ij} + \phi_{ij} - 2\Omega_m(e_{mkj}\overline{u_i'u_k'} + e_{mki}\overline{u_j'u_k'}), \tag{3.76}$$

where $\mathcal{P}$ and ϵ are the traces of the production respectively diffusion term. The advection term is indeed exactly zero for all stationary parallel mean flows, such as fully developed channel or pipe flow. The weak equilibrium assumption is deficient in curvilinear flows. A weak equilibrium condition for algebraic Reynolds stress models for rotating and curved flow has for example been proposed by Gatski & Wallin (2004).

Rewriting (3.76) in terms of the Reynolds stress anisotropy tensor $\boldsymbol{a}$, the mean strain $\boldsymbol{S}$ and the mean rotation tensor $\boldsymbol{W}$ gives

$$\begin{aligned}(P-\epsilon)a_{ij} =& -\frac{2}{3}KS_{ij} - K(a_{ik}S_{jk} + a_{jk}S_{ik} - \frac{2}{3}a_{mn}S_{mn}\delta_{ij}) \\ & - K[a_{ik}(W_{jk} + 2e_{mkj}\Omega_m) + b_{jk}(W_{ik} + 2e_{mki}\Omega_m)] + \frac{1}{2}\Pi_{ij}.\end{aligned} \tag{3.77}$$

In this equation the dissipation rate tensor and the pressure strain rate tensor need to be modeled.

To model the pressure strain correlation the slow part of the pressure strain rate and the dissipation rate anisotropy, given by

$$e_{ij} = \frac{\epsilon_{ij}}{\epsilon} - \frac{2}{3}\delta_{ij} \tag{3.78}$$

have been lumped together. The general quasilinear model for the pressure strain correlation can be written

$$\begin{aligned}\frac{\Pi}{\epsilon} - \boldsymbol{e} =& -\frac{1}{2}\left(C_1^0 + C_1^1\frac{\mathcal{P}}{\epsilon}\right)\boldsymbol{a} + C_2\boldsymbol{S} + \frac{C_3}{2}\left(\boldsymbol{aS} + \boldsymbol{Sa} - \frac{2}{3}\{\boldsymbol{aS}\}\boldsymbol{I}\right) \\ & - \frac{C_4}{2}(\boldsymbol{aW} - \boldsymbol{Wa}),\end{aligned} \tag{3.79}$$

where $\{\cdot\}$ denotes the trace.

If (3.79) and the dimensionless, rescaled variables:

$$\widehat{\boldsymbol{S}} = g(2 - C_3)\boldsymbol{S}^*, \tag{3.80}$$

$$\widehat{\boldsymbol{W}} = g(2 - C_4)\boldsymbol{W}^*, \tag{3.81}$$

$$\widehat{\boldsymbol{a}} = \left(\frac{2C_3 - 4}{C_2 - \frac{4}{3}}\right)\boldsymbol{a}, \tag{3.82}$$

with

$$g = \left(\frac{1}{2}C_1 + \frac{\mathcal{P}}{\epsilon} - 1\right)^{-1}. \tag{3.83}$$

are introduced one obtains the reduced Reynolds stress transport equation of the form:

$$\widehat{\boldsymbol{a}} = -\widehat{\boldsymbol{S}} - (\widehat{\boldsymbol{a}}\widehat{\boldsymbol{S}} + \widehat{\boldsymbol{S}}\widehat{\boldsymbol{a}} - \tfrac{2}{3}\{\widehat{\boldsymbol{a}}\widehat{\boldsymbol{S}}\}\boldsymbol{I}) + \widehat{\boldsymbol{a}}\widehat{\boldsymbol{W}} - \widehat{\boldsymbol{W}}\widehat{\boldsymbol{a}}, \tag{3.84}$$

where $\{\cdot\}$ denotes the trace and $\boldsymbol{I}$ denotes the unit tensor (for more detail on the derivation of (3.84) see Gatski & Speziale (1993)). (3.84) is a set of linear algebraic equations for the

determination of the components of $\widehat{\boldsymbol{a}}$ in terms of $\widehat{\boldsymbol{S}}$ and $\widehat{\boldsymbol{W}}$; the solution of (3.84) is of the general form

$$\widehat{\boldsymbol{a}} = f(\widehat{\boldsymbol{S}}, \widehat{\boldsymbol{W}}). \tag{3.85}$$

To complete the EARSM formulation the procedure corresponds now to the procedure applied for non-linear eddy viscosity models (see section (3.1.4)). The Reynolds stresses are thus uniquely related to the rates of strain and local scalar quantities. The strategy is then to insert the anisotropy expression (3.23) into equation (3.84). This generates a complex system of equations for the coefficients G_λ:

$$\sum_\lambda G_\lambda \widehat{\boldsymbol{T}}^\lambda = -\sum_\lambda \delta_{1\lambda} \widehat{\boldsymbol{T}}^\lambda - \sum_\lambda G_\lambda \left[\widehat{\boldsymbol{T}}^\lambda \widehat{\boldsymbol{S}} + \widehat{\boldsymbol{S}} \widehat{\boldsymbol{T}}^\lambda - \tfrac{2}{3}\{\widehat{\boldsymbol{T}}^\lambda \widehat{\boldsymbol{S}}\}\boldsymbol{I} - \widehat{\boldsymbol{T}}^\lambda \widehat{\boldsymbol{W}} + \widehat{\boldsymbol{W}} \widehat{\boldsymbol{T}}^\lambda \right], \tag{3.86}$$

where it is made use of the fact that $\widehat{\boldsymbol{T}}^1 = \widehat{\boldsymbol{S}}$. Using the fact that $\widehat{\boldsymbol{T}}^\lambda$ is an integrity basis the solutions for G_λ for the three-dimensional case are given by (see Gatski & Speziale, 1993):

$$\begin{aligned}
G_1 &= \tfrac{1}{2}(6 - 3\widehat{I}_1 - 21\widehat{I}_2 - 2\widehat{I}_3 + 30\widehat{I}_4)/D, & G_6 &= -9/D, \\
G_2 &= -(3 + 3\widehat{I}_1 - 6\widehat{I}_2 + 2\widehat{I}_3 + 6\widehat{I}_4)/D, & G_7 &= 9/D, \\
G_3 &= (6 - 3\widehat{I}_1 - 12\widehat{I}_2 - 2\widehat{I}_3 - 6\widehat{I}_4)/D, & G_8 &= 9/D, \\
G_4 &= -3(3\widehat{I}_1 + 2\widehat{I}_3 + 6\widehat{I}_4)/D, & G_9 &= 18/D, \\
G_5 &= -9/D, & G_{10} &= 0,
\end{aligned} \tag{3.87}$$

where the denominator is

$$D = 3 - \tfrac{7}{2}\widehat{I}_1 + \widehat{I}_1^2 - \tfrac{15}{2}\widehat{I}_2 - 8\widehat{I}_1\widehat{I}_2 + 3\widehat{I}_2^2 - \widehat{I}_3 + \tfrac{2}{3}\widehat{I}_1\widehat{I}_3 - 2\widehat{I}_2\widehat{I}_3 + 21\widehat{I}_4 + 24\widehat{I}_5 + 2\widehat{I}_1\widehat{I}_4 - 6\widehat{I}_2\widehat{I}_4. \tag{3.88}$$

The $\widehat{I}_i$ are the scalar invariants (3.25) given in section (3.1.4). Finally these solutions for the coefficients are put into the anisotropy expression (3.23), which is then solved together with the $K-$ and the $\epsilon-$ equation.
The EARSM approximation is deficient for flow situation with strong streamline curvature since the optimal coordinate system can not be chosen in advance for this kind of flows. Therefore Girimaji (1997) and Sjögren (1997) introduced curvature corrections by imposing the weak equilibrium assumption in a general curvilinear coordinate system. For details on this curvature correction see Girimaji (1997), Sjögren (1997) Wallin & Johansson (2001) and Wallin & Johansson (2002).

3.5 Determination of the empirical constants

The model constants are usually calibrated using classical flow cases as for example homogeneous shear-flows, the decay of grid-turbulence or near-wall turbulence. Although

the constants are determined from experiments in air and water, they should be approximately valid for most other fluids. It should also be remarked, that although the model coefficients are called constants, they are nevertheless variable. They can depend on fluid properties and non-dimensional parameters, such as the Prandtl or Reynolds number. In the following it will be pointed out exemplarily how the coefficients $C_{\varepsilon 2}$, C_1 and $C_{\varepsilon 1}$ are calibrated.

The coefficient $C_{\varepsilon 2}$ is usually determined from the measured rate of decay of the turbulent kinetic energy behind a grid. The experiment for this flow consists of a uniform flow behind a grid with a constant streamwise velocity and the other two velocity-components being zero. In grid-turbulence the diffusion and production terms are zero so that $C_{\varepsilon 2}$ is the only constant, which is appearing in the equations. Thus the modeled $K-$equation reduces to

$$\bar{u}_{1_0} \frac{\partial K}{\partial x_1} = -\epsilon \tag{3.89}$$

with $\bar{u}_{1_0}$ being constant streamwise velocity. The modeled $\epsilon-$equation reduces to

$$\bar{u}_{1_0} \frac{\partial \epsilon}{\partial x_1} = -C_{\varepsilon 2} \frac{\epsilon^2}{K}. \tag{3.90}$$

Solving theses two equations for K and ϵ gives with $K = Ax_1^n$

$$C_{\varepsilon 2} = \frac{n-1}{n}. \tag{3.91}$$

For the decay of turbulent kinetic energy it was found from grid-turbulence experiments, that $n \simeq -1.1... - 1.3$ and therewith $C_{\varepsilon 2} \simeq 1.76...1.9$.

For determining C_1 the anisotropic grid-turbulence is used. Thus the same flow conditions as for the determination of $C_{\varepsilon 2}$ are used but this time with a contraction of the flow area beneath the grid to produce anisotropy. For this flow the exact equation for $\overline{u_1' u_1'}$ becomes

$$\bar{u}_1 \frac{\partial \overline{u_1' u_1'}}{\partial x_1} = -2\nu \overline{\frac{\partial u_1'}{\partial x_l} \frac{\partial u_1'}{\partial x_l}} + \overline{\frac{2p'}{\rho} \frac{\partial u_1'}{\partial x_1}} \tag{3.92}$$

and the modeled equation for $\overline{u_1' u_1'}$ becomes

$$\bar{u}_1 \frac{\partial \overline{u_1' u_1'}}{\partial x_1} = -\frac{2}{3}\epsilon - C_1 \frac{\epsilon}{K} \left(\overline{u_1' u_1'} - \frac{2}{3} K \right). \tag{3.93}$$

Combining the equations (3.92) and (3.93) gives

$$\frac{\overline{\frac{2p'}{\rho} \frac{\partial u_1'}{\partial x_1}}}{2\nu \overline{\frac{\partial u_1'}{\partial x_1} \frac{\partial u_1'}{\partial x_1}}} = -C_1 \left(\frac{3\overline{u_1' u_1'}}{2K} - 1 \right). \tag{3.94}$$

The experimental data from the anisotropic region gives then $C_1 \approx 1...3$, depending on the ratio x/M, with M being the grid spacing.

For the calibration of $C_{\varepsilon 1}$ or σ_ε the near wall region in which the logarithmic velocity profile is valid is considered. The log-layer is a constant-stress-layer with $-\overline{u_1' u_2'} = \bar{u}_\tau^2$ giving for the log-law

$$\frac{\partial \bar{u}_1}{\partial x_2} = \frac{\bar{u}_\tau}{\kappa x_2}. \tag{3.95}$$

$\bar{u}_\tau$ is thereby the friction velocity. The molecular viscosity is small in this layer and the flow is in local equilibrium. Thus the solution for ϵ is

$$P = -\overline{u_1' u_2'} \frac{\partial \bar{u}_1}{\partial x_2} = \frac{\bar{u}_\tau^3}{\kappa x_2} = \epsilon. \tag{3.96}$$

The eddy viscosity is

$$\nu_t = -\overline{u_1' u_2'} \frac{\partial \bar{u}_1}{\partial x_2} = \kappa \bar{u}_\tau x_2, \tag{3.97}$$

and from the $K - \epsilon$ model

$$\nu_t = C_\mu \frac{K^2}{\epsilon}. \tag{3.98}$$

With the solution given for ϵ (3.96) this implies

$$C_\mu = \left(\frac{\overline{u_1' u_2'}}{K} \right)^2. \tag{3.99}$$

Experimentally the stress-intensity ratio $(\overline{u_1' u_2'}/K)^2$ is found to be approximately 0.3 and therefore $C_\mu = 0.09$. Substituting (3.96) and (3.97) into the ϵ-equation (3.18) gives after some algebra

$$\kappa^2 = (C_{\varepsilon 2} - C_{\varepsilon 1}) \sigma_\varepsilon \sqrt{C_\mu}. \tag{3.100}$$

With the von Karmann constant being approximately equal to 0.43 one receives using the other standard constants $\sigma_\varepsilon = 1.3$.

3.6 Modeling principles

By formulating modeling principles guidelines, for a systematic development of turbulence models, are given. The principles can be divided into inviolable and optional ones. Obvious principles are dimensional and tensorial consistency and physical coherence. Dimensional consistency means that all terms in any equation must have the same dimension. This principle is trivial, but still a powerful tool in turbulence modeling. A consistent use of tensor algebra is invoked to ensure that all terms in the equation have the same free subscripts and that matrix multiplication is done correctly. Physical coherence is more a conceptual principle meaning that closure models should be physically plausible substitutions for the real process, e.g. an inviscid effect should not be modeled in terms of viscous parameters. Further principles discussed in this section are

- Realizability.

- Thermodynamic consistency.
- Rapid Distortion Theory (RDT).
- Principles derived from symmetry methods.

These principles make an important contribution to the understanding of turbulence. They lead to new mathematical developments which can give a guideline for the evaluation, improvement and development of turbulence models.
In the given thesis the principles derived from symmetry methods are used to derive constrains which have to be fulfilled by the turbulence models. Anyhow similar to the tensor invariant theory, which is described in the frame work of non-linear eddy viscosity models (section 3.1.4) and explicit algebraic Reynolds stress models (section 3.4) symmetry methods might also be used for the derivation of turbulence models from first principles. The other three principles mentioned above can all be used for the derivation of constrains which have to be fulfilled by the turbulence model. These principles are therefore useful for the calibration of the empirical constants. Furthermore the RDT is a very useful tool for the simplification of differential equations. It can assist at the derivation of turbulence models using for example invariant theory (see section 3.3).

3.6.1 Realizability

One of the basic expectations of a turbulence model is that it yields statistics that are realizable, meaning that the Reynolds stresses have to obey the following statistic fundamental coherences (Schumann, 1977):

- The diagonal components (energies) have to be non negative: $\bar{u}_\alpha^2 \geq 0$.
- The off-diagonal elements have to satisfy the Schwarz inequality: $\left(\overline{u'_\alpha u'_\beta}\right)^2 \leq \overline{u_\alpha^2}\,\overline{u_\beta^2}$.

These expectations give valuable constrains for the development of turbulence models leading to an improved physical accuracy. Realizability is furthermore of practical importance, as realizable models tend to be computationally robust and less stiff (Sjögren & Johansson, 2000). Thus the Schumann realizability constraint has served as the theoretical basis for several turbulence models (e.g. Johansson & Hallbäck, 1994; Ristorcelli *et al.*, 1995; Sjögren & Johansson, 2000).

A convenient measure in the range of realizability is the determinant of the normalized Reynolds stress tensor (Pope, 2000)

$$F \equiv det\left(\frac{\overline{u'_i u'_j}}{\frac{1}{3}\overline{u'_k u'_k}}\right). \tag{3.101}$$

Considering the Lumley triangle (see figure 3.6.1) one can show that the value of F is positive within the Lumley triangle, equal to zero on the two-component line and negative

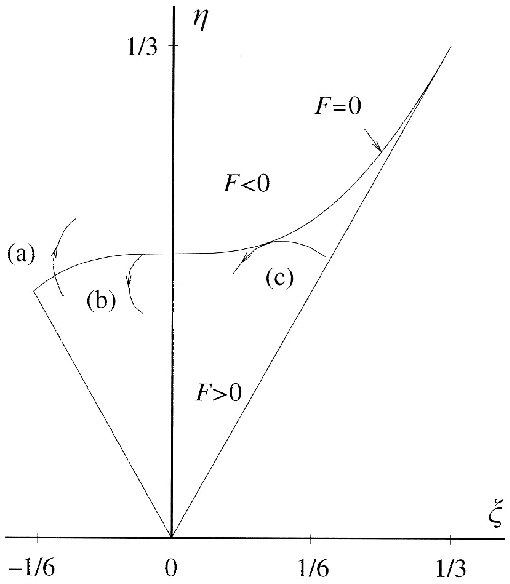

Figure 3.1: The Lumley triangle showing trajectories of three types: (a) violates realizability; (b) satisfies weak realizability; (c) satisfies strong realizability. (Note that other types of trajectories are possible) (Pope, 2000).

in the unrealizable region (across the two-component line) (see Pope, 2000). In the Lumley triangle the variables ξ and η are the two independent invariants of the anisotropy tensor $\boldsymbol{b}$:

$$6\eta^2 = b_{ij}b_{ji} \tag{3.102}$$

and

$$6\xi^3 = b_{ij}b_{jk}b_{ki}. \tag{3.103}$$

In the literature it is distinguished between a weak and a strong form of realizability.
The strong form states that when a principal Reynolds stress component vanishes, its time rate of change must also vanish and its second derivative must be positive (Lumley, 1978). The strong realizability form can be written in terms of F as

$$\left(\frac{d^2F}{dt^2}\right)_{F=0} > 0, \quad \left(\frac{dF}{dt}\right)_{F=0} = 0. \tag{3.104}$$

Rapid pressure strain models based on the strong realizability condition have been developed by Shih & Lumley (1985), Sjögren & Johansson (2000) and Chung & Kim (1995). They claimed that a rapid pressure strain model linear in the Reynolds stresses cannot satisfy the strong realizability constraint and thus developed models which are non-linear in the Reynolds stresses.
The weak form of realizability states that when a principal Reynolds stress component vanishes, its time derivative must be positive, giving the constraint

$$\left(\frac{dF}{dt}\right)_{F=0} > 0. \tag{3.105}$$

Fu *et al.* (1987) and Sarkar & Speziale (1990) developed rapid pressure strain correlation models based on the weak realizability condition. These models are much more simple, than the models based on the strong realizability condition and thus more widely used.

Girimaji (2004) argued that the Schumann proposal is a necessary, but not sufficient condition for comprehensive realizability. Especially the weak realizability approach ignores the realizability of individual moments in the Reynolds stress evolution equation. Girimaji (2004) thus proposed as additional requirement that the closure model for each of the unclosed statistical moments in the Reynolds stress equation has to be individually realizable. Based on this, he derived two realizability constrains on the rapid pressure statistics, namely:

- The rapid pressure gradient variance must be positive which leads to the requirement that the M_{ijkl} tensor must be positive and semi-definite. This gives the realizability constraint on M_{ijkl} for any arbitrary mean flow:

$$\frac{\partial \bar{u}_j}{\partial x_i}\frac{\partial \bar{u}_k}{\partial x_l}M_{iljk} \geq 0. \tag{3.106}$$

  For purely strained flows, the same constraint reduces to

$$S_{ij}\overline{pS_{ij}} \geq 0. \tag{3.107}$$

- The rapid pressure strain correlation closure must satisfy the Schwarz inequality which requires

$$|\overline{u_\alpha \frac{\partial p}{\partial x_\beta}}| \leq \overline{u'_\alpha u'_\alpha}^{1/2}\overline{\frac{\partial p}{\partial x_\beta}\frac{\partial p}{\partial x_\beta}}^{1/2}, \tag{3.108}$$

  whereby repeated Latin indices imply summation, whereas Greek indices do not.

Girimaji (2004) pointed out that an unrealizable closure model is the cause of Reynolds stress realizability violation. Based on Girimaji's finding that the pressure strain correlation constrains (3.108) are violated before the Reynolds stresses become unrealizable, Sambasivam *et al.* (2004) reduced this statement further on the rapid pressure strain correlation. Performing model computations with various second-moment-closure models Sambasivam *et al.* found that a violation of the rapid pressure strain correlation realizability precedes violation of Reynolds stress realizability. They further found, that Reynolds stress realizability based on either weak or strong formulation does not guarantee a realizable rapid pressure strain correlation.

One might object that models which do not guarantee realizability in extreme states, might still be valid in most applications (Schumann, 1977).

3.6.2 Thermodynamic consistency

Since any flow, no matter if turbulent or not, describes an irreversible process it seems to be necessary to include the second law of thermodynamics to the modeling principles. In

Sadiki & Hutter (2000) it is stated, that the realizability constrains, described in section 3.6.1 alone are not able to guarantee conformity with the irreversibility of the turbulent processes.
To define the second law of thermodynamics one has first to understand the first law of thermodynamics. The first law of thermodynamics states that one form of energy, e.g. kinetic, potential, electrical energy, thermal, etc. can be converted into another without loss. The second law states that thermal energy or heat, is special among the types of energies: all forms of energy can be converted into heat, but in a way that is not reversible; it is not possible to convert the heat fully back into its original form. In other words, heat is a form of energy of lower quality. A measure for the amount of energy which is converted irreversible and thus dissipates into heat is the entropy η, which is always positive. The second law of thermodynamics is therefore given by the entropy inequality:

$$\frac{\partial \rho\eta}{\partial t} + \frac{\partial}{\partial x_i}(\eta u_i + \varphi_i^{entr}) - \sigma^{entr} \geq 0, \tag{3.109}$$

whereby ρ is the entropy density, $\varphi_i^{entr} = q_i/\Theta$ is the entropy flux (heat flux vector divided by the temperature) and $\sigma^{entr} = h/\Theta$ the source term of entropy (source term of energy divided by the temperature).
A couple of authors included this thought in their investigations and developments of turbulence models. The first who picked up the idea of irreversibility and investigated turbulence models in respect to their ability to fulfill the second law of thermodynamics was probably Ahmadi (1984). Ahmadi derived the averaged forms of the entropy inequality for incompressible and compressible fluids and studied its consequences for the modeling of turbulence. In Ahmadi (1991*a*) and Chowdhury & Ahmadi (1990) quadratic and cubic eddy viscosity models have been derived and the model constants have been calibrated by means of the second law of thermodynamics. Furthermore Mueller & Wilmanski (1986), Jou *et al.* (1996), Sadiki (1998), Sadiki *et al.* (2000), Sadiki & Hutter (2000) and Sadiki *et al.* (2003) derived consistency conditions in the form of restrictions upon the model constants by using the principle of thermodynamic consistency.

In the following the idea of thermodynamic consistency is schematically outlined along the lines of Sadiki (1998), Sadiki *et al.* (2000) and Sadiki & Hutter (2000). For further details on this subject see Sadiki (1998).

Averaged balance equations and the entropy principle

The averaged equations of continuum thermodynamics, describing the mean local balances of mass density $\bar{\rho}$, specific momentum $\bar{\rho}\bar{u}_i$, internal energy $\bar{\epsilon}$, turbulent kinetic energy K

and the mean local imbalance of entropy in a fully developed turbulent flow are

$$\begin{aligned}
\frac{\partial \bar{u}_i}{\partial x_i} &= 0, \\
\frac{d\bar{u}_i}{dt} &= \frac{1}{\bar{\rho}}\frac{\partial \bar{T}_{ij}}{\partial x_j} + \frac{\partial R_{ij}}{\partial x_j} + \bar{f}_i + (I_{0i} + 2W_{ik}\bar{u}_k), \\
\bar{\rho}\frac{d\bar{\epsilon}}{dt} &= -\frac{\partial \bar{q}_i}{\partial x_i} - \frac{\partial \mathcal{Q}_i}{\partial x_i} + \bar{T}_{ij}\frac{\partial \bar{u}_j}{\partial x_i} + \bar{\rho}\epsilon + \bar{\rho}\bar{h}, \\
\bar{\rho}\frac{dK}{dt} &= R_{ij}\frac{\partial \bar{u}_j}{\partial x_i} + \frac{\partial K_i}{\partial x_i} - \bar{\rho}\epsilon, \\
\bar{\rho}\frac{d\bar{\eta}}{dt} &= \frac{\partial \bar{\varphi}_i^{entr}}{\partial x_i} + \frac{\partial \bar{\varphi}_i^{entr(T)}}{\partial x_i} - \bar{\sigma}^{entr} \geq 0.
\end{aligned} \tag{3.110}$$

In this equation

$$\begin{aligned}
R_{ij} =& -\overline{u_i' u_j'}, \;\; \mathcal{Q}_i = \bar{\rho}\overline{\varepsilon' u_i'}, \;\; \varphi_i^{entr(T)} = -\overline{\rho u_i' \eta'}, \\
K_i =& (\overline{T_{ij}u_j'} - (1/2)\bar{\rho}\overline{u_i' u_j' u_j'}), \;\; \epsilon = \overline{T_{<ij>}u_{j,i}'}/\bar{\rho}, \\
\bar{T}_{ij} =& -\bar{p}\delta_{ij} + 2\mu\bar{S}_{ij}, \;\; \bar{q}_i = -\kappa\Theta_{,i}
\end{aligned} \tag{3.111}$$

define the Reynolds stress tensor, the turbulent heat flux vector, the turbulent entropy flux, the flux vector of the turbulent kinetic energy, the dissipation rate of the turbulent kinetic energy, the Cauchy stress tensor and the heat flux vector. S_{ij} is thereby the symmetric part of the velocity gradient, Θ the absolute temperature, μ the viscosity and κ the heat conductivity. The notation $T_{<ij>}$ means the deviatoric part of the tensor T_{ij}, while $\bar{T}_{ij}$ represents the tensor's averaged value.
The entropy principle is implemented by following the entropy principle introduced by Sadiki & Hutter (2000):

1. In every fluid material, which possesses the potential to form laminar and turbulent motion there exists an quantity, called entropy with non-negative production such that equation $(3.110)_5$ holds.

2. To each field variable in the entropy balance there exists a microscopic (molecular) and mesoscopic (turbulent) contribution which are additive and given by

$$\begin{aligned}
\bar{\eta} = \eta^M + \eta^T, \;\; \varphi_i = \bar{\varphi}_i^{entr} + \varphi_i^{entr(T)} \\
\bar{\sigma}^{entr} = \sigma^M + 0, \;\; \bar{\pi}^{entr} = \pi^M + \pi^T,
\end{aligned} \tag{3.112}$$

   with $(\cdot)^M$ and $(\cdot)^T$ describing the material and turbulent parts, respectively. In (3.112) η^M depends on the molecular fluctuations in the fluid and is a function of the fluid temperature. η^T represents the turbulent fluctuations of the flow and is a function of the state of fluctuation of turbulence. $\bar{\pi}^{entr}$ is the entropy production.

3. The turbulent parts of the quantities in (3.112) vanish when the flow is purely laminar.

4. Entropy supply possesses no turbulent contribution and the material contribution is a linear combination of the momentum and energy supply term:

$$\sigma^M = \Lambda_i^f \bar{f}_i + \Lambda^\epsilon \bar{h}, \tag{3.113}$$

with $\bar{f}_i$ being the source term of momentum and $\bar{h}$ being the source term of energy.

5. There exist two empirical temperatures Θ^M and Θ^T representing measures for the intensity of the molecular and the turbulent fluctuating motions. Associated with these are also the material and turbulent coldness variables ϑ^M and ϑ^T. The coldness is defined as the inverse temperature:

$$\vartheta^M = \frac{1}{\Theta^M}, \quad \vartheta^T = \frac{1}{\Theta^T}. \tag{3.114}$$

6. The entropy production is non-negative for all thermodynamic processes:

$$\bar{\pi}^{entr} = \pi^M + \pi^T \geq 0. \tag{3.115}$$

From item 2 and (3.115) it follows immediately that

$$\pi^M \geq 0 \text{ and } \pi^M + \pi^T \geq 0 \tag{3.116}$$

must hold for all thermodynamic processes, since the entropy principle must also hold for purely laminar flows.
In the mean entropy inequality $(3.110)_5$ $\bar{\varphi}_i^{entr}$ and $\bar{\varphi}_i^{entr(T)}$ may be written as

$$\begin{aligned} &\bar{\varphi}_i^{entr} = \bar{\varphi}_i^{entr(M)} + s_i^M = (\bar{q}_i + \mathcal{Q}_i)\vartheta^M, \quad \text{where } s_i^M = \overline{q_i'\vartheta'} \\ &\text{and } \bar{\varphi}_i^{entr(T)} = \overline{\rho\eta' u_i'} = K_i\vartheta^T + s_i^T \end{aligned} \tag{3.117}$$

for turbulent motions. Thereby s_i^M (through $\mathcal{Q}_i$) and s_i^T are constitutive quantities which have to be determined.
Introducing the Helmholtz free energy function for the mean thermal and turbulent fluctuations according to

$$\psi^M = \bar{\epsilon} - \frac{\eta^M}{\Theta^M}, \quad \psi^T = K - \frac{\eta^T}{\Theta^T}, \tag{3.118}$$

inserting (3.112) into $(3.110)_5$ and taking (3.117) and (3.110 lines 1,3,4) into account gives the inequality

$$\begin{aligned} &\vartheta^M \left\{ -\bar{\rho}\left(\frac{d\psi^M}{dt} - \frac{\eta^M}{(\vartheta^M)^2}\frac{d\vartheta^M}{dt} \right) - \frac{1}{\vartheta^M}\left(q_i + \mathcal{Q}_i\right)\vartheta_{,i}^M + \left(\bar{T}_{ij} + \Lambda^\rho \delta_{ij}\right)\bar{u}_{j,i} + \bar{\rho}\epsilon \right\} \\ &+\vartheta^T \left\{ -\bar{\rho}\left(\frac{d\psi^T}{dt} - \frac{\eta^T}{(\vartheta^T)^2}\frac{d\vartheta^T}{dt} \right) - \frac{1}{\vartheta^T}K_i\vartheta_{,i}^T - \frac{1}{\vartheta^T}s_{i,i}^T + R_{ij}\bar{u}_{j,i} - \bar{\rho}\epsilon \right\} \geq 0, \end{aligned} \tag{3.119}$$

with Λ^P being the Lagrange parameter.
Being the averaged form of the entropy inequality (3.119) gives restricting conditions for the constitutive equations as well as for the turbulent closure assumption. The term $\Lambda^P \bar{u}_{j,i}\delta_{ij}$ takes thereby account of the incompressibility of the fluid in the mass equation.

Constitutive assumptions and equations

The evolution of the dissipation rate is described by the equation

$$\bar{\rho}\frac{d\epsilon}{dt} = \Pi^{\epsilon} + K^{\epsilon}_{i,i}, \tag{3.120}$$

where the single terms have to be in accordance with the entropy inequality. The supply term σ^{ε} vanishes, since the dissipation rate describes an inertial process of the turbulent flow, which does not involve a supply from outside.
The constitutive dependent quantities in (3.110), (3.117) and (3.120) are thus

$$\mathcal{K} = (\psi^M, \eta^M, q_i, \bar{T}_{ij}) \bigcup (\mathcal{Q}_i, K_i, K^{\epsilon}_i, \Pi^{\epsilon}, R_{ij}, \psi^T, \eta^T, s^T_i), \tag{3.121}$$

which have to be written down as functionals of the independent variables, which are required to describe a turbulent flow:

$$\mathcal{V}^M = (\Theta^M, \Theta^M_i, \bar{S}_{ij}), \;\; \mathcal{V}^T = (\Theta^T, \Theta^T_i, \bar{S}_{ij}, \bar{W}_{ij}, \bar{S}^*_{ij}, \epsilon, \epsilon_{,i}) \tag{3.122}$$

where

$$\mathcal{K}^m = \hat{\mathcal{K}}^m(\mathcal{V}^M)\,, \;\; \bar{\mathcal{K}} = \hat{\bar{\mathcal{K}}}(\mathcal{V}^M \bigcup \mathcal{V}^T). \tag{3.123}$$

Lumley (1970) and Sadiki & Hutter (1996) stated that turbulent flows can be considered as laminar flows of non-Newtonian fluids. Using this statement the time derivative of $\bar{u}_{i,j}$ may be replaced by the Jaumann derivative

$$\bar{S}^*_{ij} = \frac{d\bar{S}_{ij}}{dt} + \bar{S}_{ik}W_{kj} + \bar{S}_{jk}W_{ki} \tag{3.124}$$

to account for the viscoelastic effects.
To calculate the constitutive equations for the variables in (3.123), taking account of the entropy inequality $(3.110)_5$ one has to calculate the free energies ψ^M and ψ^T by carrying out all necessary derivatives

$$\begin{aligned}
&\vartheta^M \left\{ -\bar{\rho}\left(\frac{\partial\psi^M}{\partial\vartheta^M} - \frac{\eta^M}{(\vartheta^M)^2}\right)\dot{\vartheta}^M + \frac{\partial\psi^M}{\partial\Delta}\dot{\Delta} + \frac{\partial\psi^M}{\partial\vartheta^M_{,i}\vartheta^M_{,i}}(\vartheta_{,i}\vartheta_{,i})^{\cdot} \right.\\
&\quad \left. + \frac{1}{\vartheta^M}\left(\bar{q}_i + \mathcal{Q}_{,i}\right)\vartheta^M_{,i} + \left(\bar{T}_{ij} + \Lambda^{\rho}\delta_{ij}\right)\bar{u}_{j,i} + \bar{\rho}\epsilon \right\}\\
&\quad + \vartheta^T \left\{ -\bar{\rho}\left(\frac{\partial\psi^T}{\partial\vartheta^T} - \frac{\eta^T}{(\vartheta^T)^2}\right)\dot{\vartheta}^T - 2\bar{\rho}\frac{\partial\psi^T}{\partial\epsilon_{,i}}\left(\epsilon_{,i}\right)^{\cdot} - \bar{\rho}\left(\frac{\partial\psi^T}{\partial\vartheta^M}\dot{\vartheta}^M + \frac{\partial\psi^T}{\partial\Delta^W}\dot{\Delta}^W\right) \right.\\
&\quad -\bar{\rho}\left(\frac{\partial\psi^T}{\partial\Delta^y}\dot{\Delta}^y + \frac{\partial\psi^T}{\partial\Delta^{Sy}}\dot{\Delta}^{Sy} + \frac{\partial\psi^T}{\partial\Delta^{Wy}}\dot{\Delta}^{Wy} + \frac{\partial\psi^T}{\partial S^*_{kk}}\bar{S}^*_{kk}\right)\\
&\quad \left. -\bar{\rho}\frac{\partial\psi^T}{\partial\epsilon}\dot{\epsilon} + \left(R_{ij} - \bar{\rho}\left(\frac{\partial\psi^T}{\partial\Delta}\bar{S}^*_{ij}\right)\right)\bar{S}_{ij} + \frac{1}{\vartheta^T}K_i\vartheta^T_{,i} - \frac{1}{\vartheta^T}s^T_{i,i} - \bar{\rho}\epsilon \right\} \geq 0,
\end{aligned} \tag{3.125}$$

in which

$$\Delta = \frac{1}{2}\bar{S}_{ij}\bar{S}_{ij}, \;\; \Delta^W = \frac{1}{2}W_{ij}W_{ij}, \;\; \Delta^y = \boldsymbol{y}_{,i}\boldsymbol{y}_{,i}, \;\; \Delta^{Sy} = \boldsymbol{y}_i\bar{S}_{ij}\boldsymbol{y}_{,j}, \;\; \text{and} \;\; \Delta^{Wy} = \boldsymbol{y}_i W_{ij}\boldsymbol{y}_{,j},$$

with $\boldsymbol{y} = (\vartheta^M, \vartheta^T, \epsilon)$. Symbolically (3.125) might be written as

$$\vartheta^M(\alpha_i^M \dot{y}_i^M + \beta^M) + \vartheta^T(\alpha_p^T \dot{y}_p + \beta) \geq 0, \;\; i = 1,2,3,\; p = 1,2,\ldots 9 \tag{3.126}$$

where y_i^M and y_p are given by the set of variables $\mathcal{V}^M$ and $(\mathcal{V}^M \bigcup \mathcal{V}^T)$, respectively and α_i, α_p as well as β^M, β are functions of y_i^M and y_p, respectively.
Equation (3.125) is linear in $\dot{y}_i^M$ and $\dot{y}_p$ since they do not appear in the constitutive equations (3.122) and (3.123) and $\alpha_i^M, \beta^M, \alpha_p^T$ and β are independent of $\dot{y}_i$. These variables could assume any value and therefore their factors have to vanish to ensure that the inequality (3.125) holds:

$$\alpha_i^M = 0 \;\text{ and }\; \alpha_p^T = 0 \;\text{ and }\; \vartheta^M \beta^M + \vartheta^T \beta \geq 0 \tag{3.127}$$

giving with (3.125)

$$\begin{aligned}
&\eta^M = (\vartheta^M)^2 \frac{\partial \psi^M}{\partial \vartheta^M}, \;\; \eta^T = (\vartheta^T)^2 \frac{\partial \psi^T}{\partial \vartheta^T}, \\
&\frac{\partial \psi^T}{\partial \vartheta^M} = 0 = \frac{\partial \psi^T}{\partial \Delta^W} = \frac{\partial \psi^T}{\partial y_{1,i} y_{1,i}}, \quad \text{with} \quad y_1 = \left(\vartheta^M, \vartheta^T\right), \\
&\frac{\partial \psi^M}{\partial \Delta} = \frac{\partial \psi^M}{\partial \vartheta_{,i}^M \vartheta_{,i}^M} = 0, \;\; \frac{\partial \psi^T}{\partial \Delta^{Sy}} = \frac{\partial \psi^T}{\partial \Delta^{Wy}} = \frac{\partial \psi^T}{\partial \bar{S}_{kk}^*} = 0.
\end{aligned} \tag{3.128}$$

With (3.128) thermodynamic restrictions on the mean free energy functions are imposed, so that

$$\psi^M = \psi^m(\vartheta^M), \;\; \psi^T = \psi^T(\vartheta^T, \epsilon, (\epsilon_{,i})^2, \Delta). \tag{3.129}$$

The so called residual-inequality remains

$$\begin{aligned}
&\frac{1}{T}\left[-\frac{1}{\bar{T}}\left(q_i + \mathcal{Q}_i\right)\bar{T}_{,i} + \left(\bar{T}_{<ij>} + \left(\Lambda^\rho - \bar{p}\right)\delta_{ij}\right) S_{ji} + \bar{\rho}\epsilon\right] \\
&\quad + \frac{C^T}{K}\left[\left(-\bar{\rho}\frac{\partial \psi^T}{\partial \epsilon} - B_{j,j} + \frac{\bar{\rho}}{K} B_j \left(K_{,j} - \frac{K}{\epsilon}\epsilon_{,j}\right)\right)\left(K_{i,i}^\epsilon + \Pi^\epsilon\right)\right. \\
&\quad \left.\frac{1}{K} K_i \left(K_{,i} - \frac{K}{\epsilon}\epsilon_{,i}\right) + \left(R_{<ij>} - \bar{\rho}\frac{\partial \psi^T}{\partial \Delta}\bar{S}_{ij}^* + B_j \epsilon_{,i}\right)\bar{S}_{ij} - \bar{\rho}\epsilon\right] \geq 0
\end{aligned} \tag{3.130}$$

where (see Ahmadi, 1991*b* and Marshall & Nagdhi, 1988):

$$\frac{1}{\vartheta^M} = \Theta, \;\; \vartheta^T = \frac{C^T}{K}, \;\; C^T = C_0^T \epsilon, \;\; C_0^T = \text{const}$$

At the derivation of (3.130) the terms, in which the time and space differentiations of the dissipation rate and the turbulent extra-entropy flux appear, have been transformed as follows:

$$\begin{aligned}
-\bar{\rho}\frac{\partial \psi^T}{\partial \epsilon_{,i}}(\epsilon_{,i})^{\cdot} - \bar{\rho}\frac{\partial \psi^T}{\partial \epsilon}\dot{\epsilon} - \frac{1}{\vartheta^T} s_{i,i}^T =& \bar{\rho}\mathcal{A}\dot{\epsilon} + \left(\bar{\rho} B_i \dot{\epsilon} - \frac{1}{\vartheta^T} s_i^T\right)_{,i} - \\
& \frac{1}{\left(\vartheta^T\right)^2} s_i^T \vartheta_{,i}^T + B_j \left(\bar{u}_{i,j}\right)\epsilon_{,i}
\end{aligned} \tag{3.131}$$

where

$$\mathcal{A} = -\left(\frac{\partial}{\partial\epsilon} - \nabla_i \frac{\partial}{\partial\epsilon_{,i}}\right)\psi^T, \quad B_i = -\frac{\partial\psi^T}{\partial\epsilon_{,i}}. \tag{3.132}$$

By exploiting the resulting entropy inequality once (3.131) is inserted into (3.125) to obtain (3.130) the second term on the right-hand side of (3.131), which involves the turbulent extra-entropy flux, must vanish. Thus following Maugin (1990) the extra-entropy flux is given by the constitutive relation

$$s_i^T = \bar{\varphi}\bar{\vartheta}^T B_i \dot{\epsilon}. \tag{3.133}$$

Further thermodynamic restrictions are received from (3.130) by introducing explicit expressions for the Helmholtz free energy as well as for the constitutive quantities. The Helmholtz free energy can be written as (see Sadiki, 1998):

$$\psi^T = K\left(\ln\left(\frac{C_0^T\epsilon}{K} + \alpha\epsilon^2\Delta + b(\epsilon_{,i})^2 + A_0\right)\right), \tag{3.134}$$

with α, b, A_0 constant. With (3.134) it follows from (3.128) and (3.131)

$$B_{i,i} = -2bK(\epsilon_{,i})_{,i} - 2bK_{,i}\epsilon_{,i}; \;\; C^T = -\vartheta^T\frac{\partial}{\partial\vartheta^T}\left((\vartheta^T)^2\frac{\partial\psi^T}{\partial\vartheta^T}\right). \tag{3.135}$$

For the remaining constitutive quantities, one could write down complete isotropic function relations, but that would be so complicated to serve no practical purpose. Therefore it is referred to Sadiki *et al.* (2000) for expressions for the anisotropy Reynolds stress tensor, the turbulent heat flux vector, the flux vector of the turbulent kinetic energy and its dissipation rate and the production of the dissipation rate for non-Newtonian fluids

$$\begin{aligned}
a_{ij} =& -\frac{R_{ij}}{K} + \frac{2}{3}\delta_{ij} = -\frac{\mu_t}{K}\bar{S}_{ij} + c_1\frac{\mu_t}{\epsilon}\left(\bar{S}_{ik}\bar{S}_{kj} - \frac{1}{3}\bar{S}_{mm}\bar{S}_{mm}\delta_{ij}\right) \\
&+ \frac{c_8}{K}\left(\epsilon_{,i}\epsilon_{,j} - \frac{1}{3}\left(\epsilon_{,k}\right)^2\delta_{ij}\right) + c_3\frac{\mu_t}{\epsilon}\left(W_{ik}W_{kj} - \frac{1}{3}W_{mn}W_{mn}\delta_{ij}\right) \\
&+ c_2\frac{\mu_t}{\epsilon}\left(\bar{S}_{ik}W_{kj} + W_{ik}\bar{S}_{kj}\right) + c_6\frac{\mu_t K}{\epsilon^2}\left(\bar{S}_{mn}\bar{S}_{mn}\right)\bar{S}_{ij} + c_7\frac{\mu_t K}{\epsilon^2}W_{mn}W_{mn}\bar{S}_{ij} \\
&+ c_4^{'}\frac{\mu_t}{\epsilon}\left(\bar{S}_{ij}^* - \frac{1}{3}\bar{S}_{kk}^*\delta_{ij}\right)
\end{aligned} \tag{3.136}$$

$$\begin{aligned}
\mathcal{Q}_i =& b_1\frac{K^2}{\epsilon}\bar{T}_{,i} + b_2\frac{K^3}{\epsilon^2}\bar{S}_{ij}\bar{T}_{,j} + b_5\frac{K^3}{\epsilon^2}W_{ij}\bar{T}_{,j} \\
&+ b_4\frac{K^4}{\epsilon^3}\bar{S}_{ik}\bar{S}_{kj}\bar{T}_{,j} + b_6\frac{K^4}{\epsilon^3}W_{ik}W_{kj}\bar{T}_{,j} + \left(b_7\frac{K^4}{\epsilon^3}\bar{S}_{ik}W_{kj} + b_8\frac{K^4}{\epsilon^3}W_{ik}\bar{S}_{kj}\right)\bar{T}_{,j} \\
&+ b_2^1\frac{K^5}{\epsilon^4}\left(\bar{S}_{mn}\bar{S}_{mn}\bar{S}_{ij}\right)\bar{T}_{,j} + b_2^2\frac{K^5}{\epsilon^4}\left(W_{mn}\bar{W}_{mn}\bar{S}_{ij}\right)\bar{T}_{,j} \\
&+ b_5^1\frac{K^5}{\epsilon^4}\left(\bar{S}_{mn}\bar{S}_{mn}W_{ij}\right)\bar{T}_{,j} + b_5^{12}\frac{K^5}{\epsilon^4}\left(W_{mn}\bar{W}_{mn}W_{ij}\right)\bar{T}_{,j}
\end{aligned} \tag{3.137}$$

$$
\begin{aligned}
K_i =&\alpha_1^k \left(K_{,i} - \frac{K}{\epsilon}\epsilon_{,i} \right) \\
&+ \left(\alpha_2^k \bar{S}_{ij} + \alpha_3^k \bar{S}_{ik}\bar{S}_{kj} + \alpha_4^k W_{ik}W_{kj} + \alpha_2^{1k}\Delta\bar{S}_{ij} + \alpha_2^{2k} W_{mn}W_{mn}\bar{S}_{ij} \right) \\
&\left(K_{,j} - \frac{K}{\epsilon}\epsilon_{,j} \right)
\end{aligned} \tag{3.138}
$$

$$
\begin{aligned}
K_i^\epsilon =&\alpha_1^\epsilon \epsilon_{,i} \\
&+ \left(\alpha_2^\epsilon \bar{S}_{ij} + \alpha_3^\epsilon \bar{S}_{ik}\bar{S}_{kj} + \alpha_4^\epsilon W_{ik}W_{kj} + \alpha_2^{1\epsilon}\Delta\bar{S}_{ij} + \alpha_2^{2\epsilon} W_{mn}W_{mn}\bar{S}_{ij} \right) \epsilon_{,j}
\end{aligned} \tag{3.139}
$$

$$
\Pi^\epsilon = -\bar{\rho}c_{\epsilon 2}\frac{\epsilon^2}{K} + \gamma_3 \bar{S}_{ij}\bar{S}_{ij} + \gamma_4 W_{ij}W_{ij} + c_{\epsilon 3}\bar{\rho}\frac{\epsilon}{K^2}\left(K_{,i} + \frac{K}{\epsilon}\epsilon_{,i} \right)\left(K_{,i} - \frac{K}{\epsilon}\epsilon_{,i} \right). \tag{3.140}
$$

From the residual inequality (3.130) one can now derive the constitutive equation in the material part

$$
\bar{T}_{ij} = -\bar{p}\delta_{ij} + 2\mu\bar{S}_{ij} \;\text{ with }\; \Lambda^p = \bar{p},\;\; \bar{q}_i = -\kappa\bar{T}_{,i} \tag{3.141}
$$

Thermodynamic compatibility

To guarantee that the equations (3.136) to (3.140) and (3.141) fulfill the residual inequality (3.130) the model coefficients have to be restricted. By substituting (3.136) to (3.140) and (3.141) into (3.130) one receives

$$
\begin{aligned}
&\mu \geq 0, \quad \kappa + \kappa^T \geq 0 \quad \text{with} \quad \kappa \geq 0, \quad b_i = 0, (i \geq 2) \quad \text{and} \quad \kappa^T = -b_1\frac{k^2}{\epsilon}, \\
&\alpha_1^k \geq 0, \quad \alpha_2^k \neq 0, \quad \alpha_3^k = \alpha_4^k = \alpha_2^{1k} = \alpha_2^{2k} = 0, \\
&\alpha_1^\epsilon \neq 0, \quad \alpha_3^\epsilon = \alpha_4^\epsilon = \alpha_2^{1\epsilon} = \alpha_2^{2\epsilon} = 0, \quad \gamma_4 = 0, \\
&c_4' = \bar{\rho}\frac{\partial\psi^T}{\partial\Delta}, \quad \mu_t \geq 0, \quad c_6\Delta \geq -\mu_t, \quad c_3 = 0, \quad c_7 = 0.
\end{aligned} \tag{3.142}
$$

whereby the last line has been identified as the Schwarz-inequality, giving the classical realizability constraint (see section 3.6.1).
The terms $\bar{S}_{ki}W_{kj}$ or $\bar{S}_{kj}W_{ik}$ have a gyroscopic character and therefore give no contribution to the entropy inequality. All coefficients in (3.142) depend only on $\bar{T}$, K, ϵ, $(\epsilon_{,i})^2$ and Δ. In Sadiki (1998) it is furthermore stated that the coefficients in the ϵ-equation cannot be calibrated independently from the coefficients in the K-equation. This can be shown by the relation

$$
-\left(\frac{C_0^T}{\epsilon} + 2K\epsilon\alpha\Delta \right)\frac{\varepsilon}{K^2}C_{\varepsilon 3} + \frac{\alpha_1^k}{K} \geq 0, \;\; C_{\varepsilon 3} \geq 0, \;\text{ and }\; C_8 \propto 2(b - \frac{K}{\epsilon^2}\alpha_2^k) \tag{3.143}
$$

where α_2^k cannot be independently calibrated of C_8.
Furthermore the inequality

$$
\alpha \geq 0 \Rightarrow c_4' = \beta_4' \leq 0, \text{and }\; b \geq 0 \tag{3.144}
$$

must be fulfilled, so that the turbulent free energy is minimal in equilibrium. As further restriction on the model constants Sadiki (1998) gives

$$
c_1 + 2c_4' \neq 0 \quad c_4' \leq 0. \tag{3.145}
$$

Equations (3.142) -(3.145) define the thermodynamic consistent validity domain of the model coefficients. Thus the model coefficients should obey these constrains to be thermodynamically consistent.

3.6.3 Rapid distortion theory

The rapid distortion theory (RDT) uses linearized equations to describe the changes of a given velocity field while subjected to a rapid distortion. This theory is developed of ideas how grid-turbulence behaves as it passes through a wind tunnel contraction. As the flow accelerates through the contraction of the wind tunnel it is strained along the axes of the tunnel. The basic requirement of the theory is thereby that the distortion occurs on a short time-scale compared to the eddy life-time, $\tau = K/\epsilon$. For this case the turbulent time-scale is big in comparison to the distortion, so that the turbulence does not have time to interact with itself. The influence of a mean strain rate field on the evolution of a turbulent field can then be analyzed by studying the linearized dynamic equation for the turbulent field since the non-linear terms can be neglected. Usually a Fourier decomposition with random amplitudes and phases of the given or initial velocity field is introduced to make the treatment of the pressure term and viscous term straightforward.
Rapid distortions have been studied experimentally by sending grid-turbulence through a variable cross section duct (Gence & Mathieu, 1979), or by introducing turbulence into the flow upstream of an impingement plate (Britter *et al.*, 1979). Lee *et al.* (1989) made comparative calculations of a homogeneous shear-flow using direct numerical simulations and RDT-analysis. Analytical studies using RDT-analysis have been conducted by Batchelor & Proudman (1954) of the effect of irrotational distortion, by Townsend (1976) of homogeneous shear and by Mansour *et al.* (1991*b*) and Cambon *et al.* (1992) of pure rotation of a fluid in turbulent motion.

To analyze the linearized Navier-Stokes equations using RDT it is useful to make order of magnitude estimations of the linear and non-linear inertial terms as well as of the viscous terms (see e.g Pearson, 1959). For this purpose it is convenient to study the dynamic equation for the coefficient $\hat{u}_i$ associated with the wavenumber κ_i in a discrete spectral representation

$$\frac{d\hat{u}_i}{dt} = \left[\delta_{in} - 2\frac{\kappa_i\kappa_n}{\kappa^2}\right]\bar{u}_{n,m}\hat{u}_m + i\left[\frac{\kappa_i\kappa_n}{\kappa^2} - \delta_{in}\right]\kappa_m\widehat{u_n u_m} - \nu\kappa^2\hat{u}_i. \tag{3.146}$$

Now a local scaling of the Fourier coefficient based on the energy content in the spectrum around a certain wavenumber is made:

$$\mid \hat{\boldsymbol{u}} \mid \sim \sqrt{E(\kappa)\Delta\kappa} \sim \sqrt{E(\kappa)\kappa}. \tag{3.147}$$

If the analysis is restricted to irrotationally strained turbulence

$$S = \sqrt{S_{ij}S_{ji}/2} \tag{3.148}$$

can be used as a scalar measure for the mean gradient tensor $\bar{\boldsymbol{u}}$. Therewith the linear,

non-linear and viscous term have the following order of magnitude:

$$\begin{aligned} \text{linear} &\sim S\sqrt{\kappa E(\kappa)}, \\ \text{non-linear} &\sim \kappa^2 E(\kappa), \\ \text{viscous} &\sim \nu\kappa^2\sqrt{\kappa E(\kappa)}., \end{aligned}$$

In order to compare the relative magnitude of these terms a local strain-rate parameter S_κ and a local Reynolds number Re_κ have been introduced as the ratio of the linear and non-linear term and the non-linear and viscous term respectively:

$$S_\kappa = \frac{S}{\kappa^{3/2}E^{1/2}}, \tag{3.149}$$

$$Re_\kappa = \frac{E^{1/2}}{\nu\kappa^{1/2}}. \tag{3.150}$$

If now a Kolmogorov inertial range spectrum $\alpha\varepsilon^{2/3}\kappa^{-5/3}$ is assumed and $\kappa_t = \Lambda_T = (q^3/\epsilon)^{-1}$ is chosen as a typical wavenumber of the range of energy containing eddies, where q is the root mean square of the turbulent velocity field, one obtains

$$S_T = \frac{S}{\epsilon/q^2}, \tag{3.151}$$

$$Re_\kappa = \frac{q^4}{\nu\epsilon}, \tag{3.152}$$

where the subscript T denotes a macro scaling. Choosing on the other hand $\kappa_\eta = \eta^{-1} = (\nu^3/\epsilon)^{-1/4}$ as a typical small, dissipative length-scale one obtains:

$$S_\eta = \frac{S}{\omega}, \tag{3.153}$$

$$Re_\eta = 1, \tag{3.154}$$

with $\omega^2 = \epsilon/\nu$ in homogeneous turbulence.
If $S \gg \omega$ then the mean strain is rapid enough to make a linearization of the problem possible and to obtain analytical solutions at least formally (see e.g. Batchelor, 1953). If the mean strain is moderately rapid ($\epsilon/q^2 \leqslant S \sim \omega$) then the linear inertial term is dominated everywhere except in the dissipative range, where all three terms play equally important roles.
If more accurate predictions are desired one can model the non-linear terms by introducing the turbulent viscosity ν_t. For an isotropic ν_t the non-linear term is replaced by $-\nu_t\kappa^2\hat{u}_i$. There ν_t has to be modeled.

For the case of irrotational mean strain the linearized equations become easily solvable. This is done by solving the vorticity equation, which has the form without non-linear terms for the irrotational case

$$\begin{aligned} \frac{d\hat{\omega}_i^n}{dt} &= S_{ij}\hat{\omega}_j^n - \nu(\kappa^2)^n\hat{\omega}_i^n, \\ \frac{\kappa_i^n}{dt} &= -S_{ij}\kappa_j^n. \end{aligned} \tag{3.155}$$

If the coordinate axes are now considered to be parallel, with the principle axes of the strain rate tensor, S_{ij} becomes

$$S_{ij} = \begin{pmatrix} s_1 & 0 & 0 \\ 0 & s_2 & 0 \\ 0 & 0 & s_3 \end{pmatrix}. \tag{3.156}$$

If now the components of S_{ij} are prescribed to be constant in time the equations for the components of the wave number vector become easy to integrate in time.

$$\kappa_1^n = \kappa_{10}^n e^{-s1t}\,,\ \kappa_2^n = \kappa_{20}^n e^{-s2t}\,,\ \kappa_3^n = \kappa_{30}^n e^{-s3t}. \tag{3.157}$$

The equations for the vorticity components become nearly decoupled. The 1-component reads:

$$\frac{\hat{\omega}_1^n}{dt} = s_1 \hat{\omega}_1^n - \nu(\kappa^2)^n \hat{\omega}_1^n, \tag{3.158}$$

which gives after integrating in time:

$$\hat{\omega}_1^n = \hat{\omega}_{10}^n e^{s_1 t} D, \text{ where } D = \exp\left[-\frac{\nu}{2}\sum_{\alpha=1}^{3}\frac{1}{s_\alpha}((\kappa_{\alpha 0}^2)^n - (\kappa_\alpha^2)^n)\right]. \tag{3.159}$$

By introducing the notation $e_\alpha = e^{s_\alpha t}$ as a measure of the total strain ratios along the principal axes one gets for the 1-component of $\hat{u}$:

$$\hat{u}_1 = \left[\frac{1}{e_1}\hat{u}_{10} - \frac{\kappa_{10}}{e_1\kappa^2}\left(\frac{\kappa_{10}}{e_1^2}\hat{u}_{10} + \frac{\kappa_{20}}{e_2^2}\hat{u}_{20} + \frac{\kappa_{30}}{e_3^2}\hat{u}_{30}+\right)\right] D. \tag{3.160}$$

From (3.160) expressions for the evolution of statistical quantities, such as the spectrum tensor $\hat{\phi}_{ij} = (\hat{u}_i^* \hat{u}_j)$ can be derived. If for example the initial state is assumed isotropic:

$$\hat{\phi}_{ij}^0 = \frac{E(\kappa)}{4\pi\kappa^2}(\delta_{ij} - \frac{\kappa_i \kappa_j}{\kappa^2}) \tag{3.161}$$

and the three-dimensional energy spectrum is known or prescribed, then the spectrum tensor is determined completely by the mean strain

$$\hat{\phi}_{11}(\vec{\kappa}) = \frac{E(\kappa)}{4\pi e_1^2 \kappa^4 \kappa_0^2}\left[\kappa_{10}^2\left(\frac{\kappa_{20}^2}{e_2^4} + \frac{\kappa_{30}^2}{e_3^4}\right) + \left(\frac{\kappa_{20}^2}{e_2^4} + \frac{\kappa_{30}^2}{e_3^4}\right)^2\right] D^2. \tag{3.162}$$

From (3.162) second moment one-point measures such as the Reynolds stress tensor and the dissipation tensor can be calculated:

$$< \overline{u_i' u_j'} > \int \hat{\phi}_{ij} d^3\kappa \text{ and } \epsilon_{ij} = 2\nu \int \kappa^2 \hat{\phi}_{ij} d^3\kappa. \tag{3.163}$$

Since the rapid part of the pressure strain correlation, the dissipation and the production term of the dissipation rate are all expressible in terms of the second order correlation spectrum tensor RDT can be used for calibration of the model parameter values of these terms (see e.g. Johansson & Hallbäck, 1994) and (see e.g. Halbäck *et al.*, 1990).

3.6.4 Principles derived from symmetry methods

The principles derived from symmetry methods, which are outlined below are the subject the given thesis. Using symmetry methods three different flow cases have been determined. Further details on this method are thus given in the following chapters.
The necessary symmetry conditions for Reynolds averaged turbulence models have been formulated in Oberlack (2000*b*) as follows:

a.) All symmetries of the two-and multi-point correlation equations have to be admitted by the model equations **(necessary but not sufficient condition!)**.

b.) There should be no additional unphysical symmetries in the model equations also for dimensionally reduced cases such as those admitting rotational symmetry.

c.) The symmetry conditions **(a.)** and **(b.)** have to be admitted by each single model equation and independent of the momentum and continuity equation.

d.) All invariant solutions implied by the symmetries of the two- and multi-point correlation equations also have to be admitted by the model equations.

Condition **(a.)** implies independence of the coordinate system, the Galilean invariance or invariance under a frame rotation since these translations are symmetries of the two- and multi-point correlation. Coordinate system independence means that the model must be independent of its expression by a particular set of components. Galilean invariance implies that the equation should be the same in any two frames of reference that move with a constant relative velocity.
In second-moment-closure modeling this is usually fulfilled by using the substantial derivative (2.3) and by allowing the model to depend on the velocity derivatives but not on the velocity itself. Properly formulated algebraic models should furthermore be invariant under frame rotation, since turbulent motions are most certainly affected by rotation. The Coriolis acceleration should therefore appear in the closure model.

Condition **(b.)** emerged from a symmetry analysis of the $K-\epsilon$ model in plane and axisymmetric parallel shear-flows with rotation. From these test cases Oberlack (2000*b*) found that the $K-\epsilon$ model has too many symmetries which are not contained in the two- and multi-point equations. This obvious shortcoming is further discussed in chapter 7 by investigating the fully developed rotating pipe flow.

From a symmetry analysis of the $K-\epsilon$ model Khor'kova & Verbovetsky (1995) found that condition **(a.)** is usually fulfilled by the most of modern turbulence model equations. Though the $K-\epsilon$ model apparently admits all necessary symmetries, we find that it is still incapable to reproduce all invariant solutions which are derived from the symmetries of the multi-point equations (condition **(d.)**). A first hint towards this problem is given in chapter 5 by investigating shear-free turbulent diffusion. This clear contradiction is further illuminated by the example of the exponential velocity law for the zero-pressure gradient turbulent boundary layer flow in chapter 6.

4 Symmetry methods in fluid mechanics

4.1 Introduction to symmetry methods

In the winter of 1873-1874 the Norwegian mathematician Sophus Lie (figure 4.1) began to develop systematically what became his theory of continuous transformation groups, later called Lie groups. It came to him in the middle of the night. Filled with excitement

Figure 4.1: Sophus Lie 1842 to 1899

he rushed to see his friend Ernst Motzfeldt, woke him up and shouted: "I have found it, it is quite simple!"

In order to understand symmetries of differential equations, it is helpful to consider symmetries of more simple objects. Roughly speaking, a symmetry of a geometrical object is a transformation whose action leaves the object apparently unchanged. For instance, consider the result of rotating a square about its center (see figure 4.2). After a rotation of $\pi/2$ the square looks the same as it did before, so this transformation is a symmetry. Rotations of π, $3\pi/2$ and 2π are also symmetries of the equivalent square. In fact, rotating by 2π maps each point to itself and is a symmetry of every geometrical object. This symmetry is called the trivial symmetry. Furthermore the square can be reflected in the four axes marked in figure 4.2. Thus the square has eight distinct symmetries.

Considering now differential equations gives the following analogy: the geometrical object or, in this case the square, corresponds to the differential equation and the virtual change corresponds to a transformation of variables.

But what are symmetries good for?

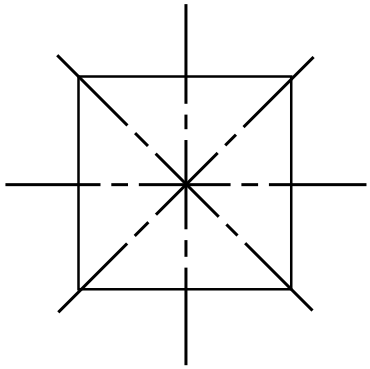

Figure 4.2: A square and its symmetries

There are many ingenious techniques to obtain exact solutions for differential equations, but most of them only work for a very limited class of problems. Symmetry methods provide a very useful tool to analyze and to derive systematically exact solutions of differential equations. They can thus be used for

a.) The reduction of ordinary differential equations (ODE) (complete solution possible, if there are enough symmetries).

b.) The similarity reduction of a partial differential equations (PDE).

c.) The transformation of a non-linear PDE to a linear PDE if special symmetries are admitted by the original PDE.

d.) The mapping of a linear PDE with non constant coefficients to a PDE with constant coefficients.

e.) The constitution of conservation laws.

f.) The derivation of equations from symmetries.

In the following the basic idea of symmetry methods will be explained. For a detailed description of the method see for example Bluman & Kumei (1989), Olver (1986), or Ibragimov (1995*a*, 1995*b* and 1996).

4.1.1 Symmetries of differential equations

For the definition of symmetries some abridging notations have to be introduced.

$\boldsymbol{x}$ and $\boldsymbol{y}$ denote vectors of the length m and n. The derivation of $\boldsymbol{y}$ with respect to $\boldsymbol{x}$ of the order of p can be abbreviated by

$$y_{k,j_1 j_2 \ldots j_p} = \frac{\partial^p y_k}{\partial x_{j_1} \partial x_{j_2} \ldots \partial x_{j_p}}. \tag{4.1}$$

All derivatives of a given order p are combined to new vectors, which are reduced to

$$\underset{1}{\boldsymbol{y}} = \left[y_{k,j_p}\right] \quad , \quad \underset{2}{\boldsymbol{y}} = \left[y_{k,j_p j_q}\right] \quad , \quad \underset{3}{\boldsymbol{y}} = \left[y_{k,j_p j_q j_r}\right] \quad , \quad \cdots$$
$$\text{with } k = 1,\ldots,m \text{ and } j_p, j_q, j_r, \cdots = 1,2,\ldots,n. \quad (4.2)$$

The brackets denote a listing of all possible combinations of k, j_p, j_q and j_r, which delates for higher derivatives.

According to the analogy between geometrical objects and differential equations given in section (4.1) a symmetry is a transformation under which a system of differential equations does not change its functional form. Thus one has to find a transformation

$$\bar{\boldsymbol{x}} = \boldsymbol{\phi}(\boldsymbol{x}, \boldsymbol{y}) \quad \text{and} \quad \bar{\boldsymbol{y}} = \boldsymbol{\psi}(\boldsymbol{x}, \boldsymbol{y}), \quad (4.3)$$

such that the following equivalence holds for (4.3)

$$\boldsymbol{F}\left(\boldsymbol{x}, \boldsymbol{y}, \underset{1}{\boldsymbol{y}}, \underset{2}{\boldsymbol{y}}, \ldots, \underset{p}{\boldsymbol{y}}\right) = 0 \quad \Leftrightarrow \quad \boldsymbol{F}\left(\bar{\boldsymbol{x}}, \bar{\boldsymbol{y}}, \underset{1}{\bar{\boldsymbol{y}}}, \underset{2}{\bar{\boldsymbol{y}}}, \ldots, \underset{p}{\bar{\boldsymbol{y}}}\right) = 0, \quad p = 1,2,\cdots . \quad (4.4)$$

As an immediate result we find that a symmetry maps a solution to a new solution.
In the following we will confine on transformations, which depend on an arbitrary, continuous parameter $\varepsilon \in \mathbb{R}$ of the form

$$\bar{\boldsymbol{x}} = \boldsymbol{\phi}(\boldsymbol{x}, \boldsymbol{y}; \varepsilon) \quad \text{and} \quad \bar{\boldsymbol{y}} = \boldsymbol{\psi}(\boldsymbol{x}, \boldsymbol{y}; \varepsilon). \quad (4.5)$$

These symmetries constitute continuous transformation groups called Lie groups, which allow the construction of analytic solutions. Thus the transformations obey the requirement to have group properties which are:

a.) Any combination of two transformations $T_{\varepsilon_3}\boldsymbol{x} = T_{\varepsilon_2}T_{\varepsilon_1}\boldsymbol{x}$ is a new transformation where $T_{\varepsilon_i} \in G_T$ (closure).

b.) A transformation exists $I \in G_T$, such that $IT_\varepsilon\boldsymbol{x} = T_\varepsilon I\boldsymbol{x} = T_\varepsilon\boldsymbol{x}$ (unitary element).

c.) Any transformation G_T possesses an inverse element, such that $T_\varepsilon^{-1}T_\varepsilon\boldsymbol{x} = T_\varepsilon T_\varepsilon^{-1}\boldsymbol{x} = I\boldsymbol{x} = \boldsymbol{x}$ (inverse element).

d.) Any three transformations $T_{\varepsilon_i} \in G_T, i = 1,2,3$ possess the property $T_{\varepsilon_1}(T_{\varepsilon_2}T_{\varepsilon_3})\boldsymbol{x} = (T_{\varepsilon_1}T_{\varepsilon_2})T_{\varepsilon_3}\boldsymbol{x}$ (associativity).

We do now a Taylor series expansion in ε of the transformation groups (4.5). Assuming that the identity transformation corresponds to $\varepsilon = 0$:

$$\bar{\boldsymbol{x}} = \phi(\boldsymbol{x}, \boldsymbol{y}, \varepsilon = 0) = \boldsymbol{x} \text{ and } \bar{\boldsymbol{y}} = \phi(\boldsymbol{x}, \boldsymbol{y}, \varepsilon = 0) = \boldsymbol{y}, \quad (4.6)$$

and with the introduction of the infinitesimals ξ and η for terms of the order $O(\varepsilon)$ one obtains:

$$\bar{x}_i = x_i + \xi_i(\boldsymbol{x}, \boldsymbol{y})\varepsilon + O(\varepsilon^2) \text{ and } \bar{y}_m = y_m + \eta_m(\boldsymbol{x}, \boldsymbol{y})\varepsilon + O(\varepsilon^2). \quad (4.7)$$

The global form of the transformations (4.5) can be received from the corresponding infinitesimals by integrating the first order system:

$$\frac{d\bar{x}_i}{d\varepsilon} = \xi_i(\bar{\boldsymbol{x}}, \bar{\boldsymbol{y}}) \text{ and } \frac{d\bar{y}_m}{d\varepsilon} = \eta_m(\bar{\boldsymbol{x}}, \bar{\boldsymbol{y}}), \tag{4.8}$$

with the initial conditions:

$$\varepsilon = 0: \quad \bar{x}_i = x_i \quad \text{and} \quad \bar{y}_m = y_m. \tag{4.9}$$

In order to write the symmetry condition (4.4) into infinitesimal form we implement (4.7) into the right hand side of (4.4) and expand with respect to ε to obtain

$$\begin{aligned} \boldsymbol{F}\left(\boldsymbol{x}, \boldsymbol{y}, \underset{1}{\boldsymbol{y}}, \underset{2}{\boldsymbol{y}}, \ldots, \underset{p}{\boldsymbol{y}}\right) + \varepsilon \mathrm{X}^{(p)} \boldsymbol{F}\left(\boldsymbol{x}, \boldsymbol{y}, \underset{1}{\boldsymbol{y}}, \underset{2}{\boldsymbol{y}}, \ldots, \underset{p}{\boldsymbol{y}}\right) \\ + \frac{\varepsilon^2}{2}\left[\mathrm{X}^{(p)}\right] \boldsymbol{F}\left(\boldsymbol{x}, \boldsymbol{y}, \underset{1}{\boldsymbol{y}}, \underset{3}{\boldsymbol{y}}, \ldots, \underset{p}{\boldsymbol{y}}\right) + O(\varepsilon^2) = 0, \end{aligned} \tag{4.10}$$

whereby the operator $X^{(p)}$ is given by

$$\mathrm{X}^{(p)} = \xi_i \frac{\partial}{\partial x_i} + \eta_j \frac{\partial}{\partial y_j} + \zeta_{j;i_1} \frac{\partial}{\partial y_{j,i_1}} + \cdots + \zeta_{j;i_1 i_2 \ldots i_p} \frac{\partial}{\partial y_{j,i_1 i_2 \ldots i_p}}, \tag{4.11}$$

being called prolongation of the generator

$$\mathrm{X} = \xi_i \frac{\partial}{\partial x_i} + \eta_j \frac{\partial}{\partial y_j} \tag{4.12}$$

of order p. In (4.11) $\zeta_{j;i_1 i_2 \ldots i_p}$ is defined according to

$$\begin{aligned} \zeta_{k;i} &= \frac{\mathcal{D}\eta_k}{\mathcal{D}x_i} - y_{k,m} \frac{\mathcal{D}\xi_m}{\mathcal{D}x_i} \text{ and} \\ \zeta_{k;i_1 \ldots i_s} &= \frac{\mathcal{D}\xi_{k;i_1 \ldots i_{s-1}}}{\mathcal{D}x_{i_s}} - y_{k,m i_1 \ldots i:s-1} \frac{\mathcal{D}\xi_m}{\mathcal{D}x_{i_s}}, \quad \text{for } s > 1, \end{aligned} \tag{4.13}$$

with

$$\frac{\mathcal{D}}{\mathcal{D}x_i} = \frac{\partial}{\partial x_i} + y_{k,i} \frac{\partial}{\partial y_k} + y_{k,ij} \frac{\partial}{\partial y_{k,j}} + \cdots. \tag{4.14}$$

Details on the derivation of (4.13) and (4.14) may be taken from Bluman & Kumei (1989). With (4.4) the final symmetry condition may be written in infinitesimal form as

$$[(\mathrm{X})\boldsymbol{F}]\,\big|_{\boldsymbol{F}=0} = 0. \tag{4.15}$$

From this an overdetermined system of linear homogeneous differential equations is received. This is called determining system. The system can then be solved for the infinitesimals $\boldsymbol{\xi}$ and $\boldsymbol{\eta}$. Using Lie's differential equations (4.8) and (4.9) the infinitesimals can be used to derive the global transformations.

It is quite laborious to calculate the determining system by hand. Thus the determining systems, which have been used for the calculations in the given thesis have all been calculated with the Maple package DESOLV_R5 by Carminati & Vu (2000).

4.1.2 Invariant solutions

It is possible to derive invariant solutions from the symmetries of a differential equation. $\boldsymbol{y} = \boldsymbol{\Theta}(\boldsymbol{x})$ is an invariant solution of a differential equation if $(\boldsymbol{y} - \boldsymbol{\Theta}(\boldsymbol{x}))$ is an invariant function with respect to X and if $\boldsymbol{y} = \boldsymbol{\Theta}(\boldsymbol{x})$ is a solution of the differential equation. Therewith we receive

$$[\boldsymbol{y} - \boldsymbol{\Theta}(x)] = 0 \quad \text{with} \quad \boldsymbol{y} = \boldsymbol{\Theta}(x). \tag{4.16}$$

Expanding the derivatives in (4.16) by employing X according to (4.12) we obtain the hyperbolic system

$$\xi_k(\boldsymbol{x}, \boldsymbol{\Theta}) \frac{\partial \theta_l}{\partial x_k} = \eta_l(\boldsymbol{x}, \boldsymbol{\Theta}) \tag{4.17}$$

and the corresponding characteristic equation

$$\frac{dx_1}{\xi_1(\boldsymbol{x}, \boldsymbol{\Theta})} = \frac{dx_2}{\xi_2(\boldsymbol{x}, \boldsymbol{\Theta})} = \cdots = \frac{dx_m}{\xi_m(\boldsymbol{x}, \boldsymbol{\Theta})} = \frac{dy_1}{\eta_1(\boldsymbol{x}, \boldsymbol{\Theta})} = \frac{dy_2}{\eta_2(\boldsymbol{x}, \boldsymbol{\Theta})} = \cdots = \frac{dy_n}{\eta_n(\boldsymbol{x}, \boldsymbol{\Theta})}. \tag{4.18}$$

Solving the characteristic equation one receives the new variables. Therefore it is suggestive to take the $m-1$ solutions of the m equations on the left hand side as new independent variables. Each term of the n terms on the right hand side can be set equal to one of the m terms on the left hand side. The solution of this equation might then be taken as new dependent variable. Due to this procedure the set of independent variables in the original PDE reduces at least by one.

Generating invariant solutions, symmetries are partly broken due to extern conditions. Thus special boundary or initial conditions are given, which are not conform with certain transformations.

4.2 Symmetries of the Navier-Stokes and Euler equations

The Euler equations ($\nu = 0$) in a non-rotating frame admit the ten-parameter symmetry group

$$\begin{aligned}
\mathrm{X}_1 &= \frac{\partial}{\partial t}, \\
\mathrm{X}_2 &= x_i \frac{\partial}{\partial x_i} + u_j \frac{\partial}{\partial u_j} + 2p \frac{\partial}{\partial p}, \\
\mathrm{X}_3 &= t \frac{\partial}{\partial t} - u_i \frac{\partial}{\partial u_i} - 2p \frac{\partial}{\partial p}, \\
\mathrm{X}_4 &= -x_2 \frac{\partial}{\partial x_1} + x_1 \frac{\partial}{\partial x_2} - u_2 \frac{\partial}{\partial u_1} + u_1 \frac{\partial}{\partial u_2} \\
\mathrm{X}_5 &= -x_3 \frac{\partial}{\partial x_2} + x_2 \frac{\partial}{\partial x_3} - u_3 \frac{\partial}{\partial u_2} + u_2 \frac{\partial}{\partial u_3} \\
\mathrm{X}_6 &= -x_3 \frac{\partial}{\partial x_1} + x_1 \frac{\partial}{\partial x_3} - u_3 \frac{\partial}{\partial u_1} + u_1 \frac{\partial}{\partial u_3} \\
\mathrm{X}_7 &= f_1(t) \frac{\partial}{\partial x_1} + \frac{\mathrm{d}f_1(t)}{\mathrm{d}t} \frac{\partial}{\partial u_1} - x_1 \frac{\mathrm{d}^2 f_1(t)}{\mathrm{d}t^2} \frac{\partial}{\partial p}, \\
\mathrm{X}_8 &= f_2(t) \frac{\partial}{\partial x_2} + \frac{\mathrm{d}f_2(t)}{\mathrm{d}t} \frac{\partial}{\partial u_2} - x_2 \frac{\mathrm{d}^2 f_2(t)}{\mathrm{d}t^2} \frac{\partial}{\partial p}, \\
\mathrm{X}_9 &= f_3(t) \frac{\partial}{\partial x_3} + \frac{\mathrm{d}f_3(t)}{\mathrm{d}t} \frac{\partial}{\partial u_3} - x_3 \frac{\mathrm{d}^2 f_3(t)}{\mathrm{d}t^2} \frac{\partial}{\partial p}, \\
\mathrm{X}_{10} &= f_4(t) \frac{\partial}{\partial p},
\end{aligned} \tag{4.19}$$

whereby $f_1(t)$-$f_3(t)$ are at least twice differentiable functions of time. $f_4(t)$ is an arbitrary function of time.

The Euler equations have an additional symmetry if restricted to a two dimensional flow with

$$\boldsymbol{u} = \boldsymbol{u}(x_1, x_2, t) \text{ and } p = p(x_1, x_2, t), \tag{4.20}$$

and the condition

$$\frac{\partial u_1}{\partial x_3} = \frac{\partial u_2}{\partial x_3} = \frac{\partial u_3}{\partial x_3} = \frac{\partial p}{\partial x_3} = 0, \tag{4.21}$$

is introduced. This additional symmetry was sometimes called "2D material frame indifference" (2DMFI) and is in infinitesimal form

$$\begin{aligned}
\mathrm{X}_{2DMFI} = t x_2 \frac{\partial}{\partial x_1} - t x_1 \frac{\partial}{\partial x_2} + (x_2 + u_2 t) \frac{\partial}{\partial u_1} - (x_1 + u_1 t) \frac{\partial}{\partial u_2} + 2\psi \frac{\partial}{\partial p} \\
\text{with} \quad u_1 = \frac{\partial \psi}{\partial x_2} \text{ and } u_2 = -\frac{\partial \psi}{\partial x_1},
\end{aligned} \tag{4.22}$$

whereby ψ is the two-dimensional stream function.
Another extra symmetry of the Euler equations is received due to a restriction to axisymmetric flows. Thus we write the flow equations in a cylindrical coordinate system

with the coordinates r, ϕ and z and the corresponding velocities u_r, u_ϕ and u_z. The flow is axisymmetric if the velocity components and the pressure are independent of ϕ. The equations are then given by

$$\begin{aligned}
\frac{\partial u_r}{\partial t} + u_r\frac{\partial u_r}{\partial r} + u_z\frac{\partial u_r}{\partial z} - \frac{u_\phi^2}{r} + \frac{\partial p}{\partial r} &= 0,\\
\frac{\partial u_\phi}{\partial t} + u_r\frac{\partial u_\phi}{\partial r} + u_z\frac{\partial u_\phi}{\partial z} + \frac{u_r u_\phi}{r} &= 0,\\
\frac{\partial u_z}{\partial t} + u_r\frac{\partial u_z}{\partial r} + u_z\frac{\partial u_z}{\partial z} + \frac{\partial p}{\partial z} &= 0,\\
\frac{\partial u_r}{\partial r} + \frac{u_r}{r} + \frac{\partial u_z}{\partial z} &= 0.
\end{aligned} \tag{4.23}$$

It is interesting to see that these equations admit an additional symmetry of the form

$$\mathrm{X}_{12} = -\frac{1}{r^2 u_\phi}\frac{\partial}{\partial u_\phi} + \frac{1}{r^2}\frac{\partial}{\partial p}. \tag{4.24}$$

With the help of Lie's differential equations the symmetries (4.19), (4.22) and (4.24) may be written in global form

$$\begin{aligned}
T_1 &: \ t^* = t + a_1 \ , \ \boldsymbol{x}^* = \boldsymbol{x} \ , \ \boldsymbol{u}^* = \boldsymbol{u} \ , \ p^* = p,\\
T_2 &: \ t^* = t \ , \ \boldsymbol{x}^* = \mathrm{e}^{a_2}\boldsymbol{x} \ , \ \boldsymbol{u}^* = \mathrm{e}^{a_2}\boldsymbol{u} \ , \ p^* = \mathrm{e}^{2a_2}p,\\
T_3 &: \ t^* = \mathrm{e}^{a_3}t \ , \ \boldsymbol{x}^* = \boldsymbol{x} \ , \ \boldsymbol{u}^* = \mathrm{e}^{-a_3}\boldsymbol{u} \ , \ p^* = \mathrm{e}^{-2a_3}p,\\
T_4 - T_6 &: \ t^* = t \ , \ \boldsymbol{x}^* = \mathbf{a}\cdot\boldsymbol{x} \ , \ \boldsymbol{u}^* = \mathbf{a}\cdot\boldsymbol{u} \ , \ p^* = p,\\
T_7 - T_9 &: \ t^* = t \ , \ \boldsymbol{x}^* = \boldsymbol{x} + \boldsymbol{f}(t) \ , \ \boldsymbol{u}^* = \boldsymbol{u} + \frac{\mathrm{d}\boldsymbol{f}}{\mathrm{d}t} \ , \ p^* = p - \boldsymbol{x}\cdot\frac{\mathrm{d}^2\boldsymbol{f}}{\mathrm{d}t^2},\\
T_{10} &: \ t^* = t \ , \ \boldsymbol{x}^* = \boldsymbol{x} \ , \ \boldsymbol{u}^* = \boldsymbol{u} \ , \ p^* = p + a_7 f_4(t)
\end{aligned} \tag{4.25}$$

and

$$\begin{aligned}
T_{11} &: \ t^* = t, \ \ x_1^* = x_1\cos(a_8 t) - x_2\sin(a_8 t), \ \ x_2^* = x_1\sin(a_8 t) + x_2\cos(a_8 t),\\
&u_1^* = u_1\cos(a_8 t) - u_2\sin(a_8 t) - a_8 x_1\sin(a_8 t) - a_8 x_2\cos(a_8 t),\\
&u_2^* = u_1\sin(a_8 t) + u_2\cos(a_8 t) + a_8 x_1\cos(a_8 t) - a_8 x_2\sin(a_8 t),\\
&p^* = p + 2\,a_8\int_Q (u_2 dx_1 - u_1 dx_2) + \frac{1}{2}a_8^2(x_1^2 + x_2^2),
\end{aligned} \tag{4.26}$$

and

$$\begin{aligned}
T_{12} &: \ t^* = t, \ \ r^* = r, \ \ z^* = z \ , u_r^* = u_r \ , u_\phi^* = \pm(u_\phi^2 - 2ar^{-2})^{\frac{1}{2}} \ ,\\
&u_z^* = u_z, \ \ p^* = p + ar^{-2},
\end{aligned} \tag{4.27}$$

whereby a_1-a_8 are the group parameter, $\mathbf{a}$ is a constant rotation matrix with the properties $\mathbf{a}\cdot\mathbf{a}^\intercal = \mathbf{a}^\intercal\cdot\mathbf{a} = \mathbf{I}$ and $|\mathbf{a}| = 1$ and $\boldsymbol{f}(t) = (a_4 f_1(t), a_5 f_2(t), a_6 f_2(t))^\intercal$, respectively $f_4(t)$ fulfill the properties mentioned in (4.19).
Only the additional two dimensional symmetry of the Euler equations has a pendant in

flows involving friction.
It is much easier to identify the physical meaning of the symmetries from the global form than from the infinitesimal form:
The symmetry T_1 describes a translation in time.
The symmetries T_2 and T_3 are scalings of space and time.
The transformations T_4-T_6 describe the invariance of the equations with respect to a finite rotation of the coordinate system.
The symmetries T_7-T_9 comprise the translation invariance with respect to space for constant f_1-f_3 as well as the classical Galilei invariance, if f_1-f_3 are linear functions of time.
The symmetry T_{10} describes the invariance of the equation with respect to the addition of an arbitrary time dependent function to the pressure.
The global form of the 2DMFI respectively T_{11} reveals that the rotation of a two-dimensional flow does not change the flow if the rotation rate is constant and the rotation is around the axis of independence.
The symmetry T_{12} may be interpreted as a non-linear combination of the potential vortex with a given solution of the system. This may even the trivial solution for u_ϕ which leads to a simple potential vortex for u_ϕ^*.

Considering the Navier-Stokes equations, thus adding the molecular viscosity we receive modified symmetry properties. Thereby two cases corresponding to a constant and a variable molecular viscosity can be distinguished.

First the case

$$\nu = const \tag{4.28}$$

will be described. For this case we have similar symmetries as for the Euler equations. We receive a nine-parameter group of symmetries, which corresponds to the eight symmetries X_1 and X_4-X_{10} of the Euler equations and a ninth symmetry which is a recombination of the two scaling symmetries X_2 and X_3, given by:

$$\mathrm{X}_{23} = 2t\frac{\partial}{\partial t} + x_i\frac{\partial}{\partial x_i} - u_j\frac{\partial}{\partial u_j} + 2p\frac{\partial}{\partial p}. \tag{4.29}$$

The 2DMFI (4.22) maintains its form under the assumption of a constant viscosity and hence also the global form (4.26) is retained. Symmetry (4.29) is in global form

$$T_9: \quad t^* = \mathrm{e}^{2a_6}t \ , \ \boldsymbol{x}^* = \mathrm{e}^{a_6}\boldsymbol{x} \ , \ \boldsymbol{u}^* = \mathrm{e}^{-a_6}\boldsymbol{u} \ , \ p^* = \mathrm{e}^{-2a_6}p. \tag{4.30}$$

A more general approach is received, if the viscosity is considered as further independent variable. Then we receive the symmetries

$$\begin{aligned}
\mathrm{X}_1 &= g_1(\nu)\frac{\partial}{\partial t}, \\
\mathrm{X}_2 &= g_2(\nu)\left[x_i\frac{\partial}{\partial x_i} + u_j\frac{\partial}{\partial u_j} + 2p\frac{\partial}{\partial p} + 2\nu\frac{\partial}{\partial \nu}\right], \\
\mathrm{X}_3 &= g_3(\nu)\left[t\frac{\partial}{\partial t} - u_i\frac{\partial}{\partial u_i} - 2p\frac{\partial}{\partial p} - \nu\frac{\partial}{\partial \nu}\right],
\end{aligned}$$

$$
\begin{aligned}
\mathrm{X}_4 &= g_4(\nu)\left[-x_2\frac{\partial}{\partial x_1}+x_1\frac{\partial}{\partial x_2}-u_2\frac{\partial}{\partial u_1}+u_1\frac{\partial}{\partial u_2}\right],\\
\mathrm{X}_5 &= g_5(\nu)\left[-x_3\frac{\partial}{\partial x_2}+x_2\frac{\partial}{\partial x_3}-u_3\frac{\partial}{\partial u_2}+u_2\frac{\partial}{\partial u_3}\right],\\
\mathrm{X}_6 &= g_6(\nu)\left[-x_3\frac{\partial}{\partial x_1}+x_1\frac{\partial}{\partial x_3}-u_3\frac{\partial}{\partial u_1}+u_1\frac{\partial}{\partial u_3}\right],\\
\mathrm{X}_7 &= g_7(t,\nu)\frac{\partial}{\partial x_1}+\frac{\mathrm{d}g_7(t,\nu)}{\mathrm{d}t}\frac{\partial}{\partial u_1}-x_1\frac{\mathrm{d}^2g_7(t,\nu)}{\mathrm{d}t^2}\frac{\partial}{\partial p},\\
\mathrm{X}_8 &= g_8(t,\nu)\frac{\partial}{\partial x_2}+\frac{\mathrm{d}g_8(t,\nu)}{\mathrm{d}t}\frac{\partial}{\partial u_2}-x_2\frac{\mathrm{d}^2g_8(t,\nu)}{\mathrm{d}t^2}\frac{\partial}{\partial p},\\
\mathrm{X}_9 &= g_9(t,\nu)\frac{\partial}{\partial x_3}+\frac{\mathrm{d}g_9(t,\nu)}{\mathrm{d}t}\frac{\partial}{\partial u_3}-x_3\frac{\mathrm{d}^2g_9(t,\nu)}{\mathrm{d}t^2}\frac{\partial}{\partial p},\\
\mathrm{X}_{10} &= g_{10}(t,\nu)\frac{\partial}{\partial p}.
\end{aligned}
\tag{4.31}
$$

And for the 2DMFI with a variable ν

$$
\mathrm{X}_{2DMFI} = g_{11}(\nu)\left[tx_2\frac{\partial}{\partial x_1}-tx_1\frac{\partial}{\partial x_2}+(x_2+u_2t)\frac{\partial}{\partial u_1}-(x_1+u_1t)\frac{\partial}{\partial u_2}+2\psi\frac{\partial}{\partial p}\right]
$$
$$
\text{with}\quad u_1=\frac{\partial\psi}{\partial x_2}\ \text{ and }\ u_2=-\frac{\partial\psi}{\partial x_1}. \tag{4.32}
$$

From a comparison of the symmetries of the Euler (4.19) and (4.22) and the Navier-Stokes-equations (4.31) and (4.32) one finds that the structure of the symmetries does not change if the viscosity is considered as further independent variable. The global symmetries then correspond to the equations (4.25) and (4.26) with the difference, that the group parameter have to be multiplied by $g_i(\nu)$.

4.3 Symmetries of the Bragg-Hawthorne equation

In the following a symmetry analysis of the Bragg-Hawthorne equation, carried out by Frewer *et al.* (2005) is presented. This analysis should just be an example to illustrate the approach to perform symmetry analysis of differential equations.

We discuss the incompressible stationary axisymmetric Euler equations with swirl, for which we derive via a scalar stream function an equivalent representation, the Bragg-Hawthorne equation (see Bragg & Hawthorne, 1950). Despite of this obvious equivalence, we will show that under a local Lie point symmetry analysis the Bragg-Hawthorne equation exposes itself as not being fully equivalent to the original Euler equations. This is reflected in the way that it possesses more symmetries than its counterpart. In other words, a symmetry of the Bragg-Hawthorne equation is in general not a symmetry of the Euler equations. Not the differential Euler equations but rather a set of integro-differential equations attain full equivalence to the Bragg-Hawthorne equation. For these intermediate Euler equations, it is interesting to note that local symmetries of the Bragg-Hawthorne

equation transform to local as well as to non-local symmetries. On the one hand, this behavior is in accordance with Zawistowski's (2001) result, that it is possible for integro-differential equations to admit local Lie point symmetries. On the other hand, with this transformation process we collect symmetries which can not be obtained when carrying out a usual local Lie point symmetry analysis.

4.3.1 Construction of the Bragg-Hawthorne equation

The Euler equations describing the dynamics of an incompressible stationary axisymmetric flow with swirl are appropriately given in cylindrical coordinates as

$$\begin{aligned} u_r\frac{\partial u_r}{\partial r}+u_z\frac{\partial u_r}{\partial z}-\frac{u_\phi^2}{r}+\frac{\partial p}{\partial r}&=0,\\ u_r\frac{\partial u_\phi}{\partial r}+u_z\frac{\partial u_\phi}{\partial z}+\frac{u_r u_\phi}{r}&=0,\\ u_r\frac{\partial u_z}{\partial r}+u_z\frac{\partial u_z}{\partial z}+\frac{\partial p}{\partial z}&=0,\\ \frac{\partial u_r}{\partial r}+\frac{u_r}{r}+\frac{\partial u_z}{\partial z}&=0. \end{aligned} \tag{4.33}$$

Where the constant density has been absorbed into the pressure variable. This set of equations is a system for the unknown functions (u_r, u_ϕ, u_z, p) depending on the variables (r, z). The maximal symmetry algebra of these Euler equations in the sense of local Lie point transformations is spanned by the following five-dimensional basis

$$\begin{aligned} X_1 &= \frac{\partial}{\partial z},\\ X_2 &= r\frac{\partial}{\partial r}+z\frac{\partial}{\partial z},\\ X_3 &= u_r\frac{\partial}{\partial u_r}+u_\phi\frac{\partial}{\partial u_\phi}+u_z\frac{\partial}{\partial u_z}+2p\frac{\partial}{\partial p},\\ X_4 &= \frac{1}{u_\phi r^2}\frac{\partial}{\partial u_\phi}-\frac{1}{r^2}\frac{\partial}{\partial p},\\ X_5 &= \frac{\partial}{\partial p}. \end{aligned} \tag{4.34}$$

It is to note that through the use of cylindrical coordinates the equations (4.33) show an explicit dependence on r. In other words, relative to this coordinate the equations are not autonomous and therefore can not exhibit a translational invariance in radial direction.
In the following we will focus on an alternative representation for the Euler equations (4.33). Due to the incompressibility and the axisymmetry of the flow, it is possible to introduce a scalar stream function ψ, such that the continuity equation is satisfied identically. The definition is

$$u_r=-\frac{1}{r}\frac{\partial\psi}{\partial z},\quad\text{and}\quad u_z=\frac{1}{r}\frac{\partial\psi}{\partial r}, \tag{4.35}$$

being equivalent to the path-independent line integral

$$\psi - \psi_0 = \int_C r(u_z dr - u_r dz), \tag{4.36}$$

where C denotes an arbitrary curve in the (r,z)-plane connecting two-points (r_0, z_0) and (r, z). Further, by claiming the unknown function u_ϕ to be an arbitrary function of ψ as

$$r u_\phi = C(\psi), \tag{4.37}$$

it is easily verified that the third equation in (4.33) is satisfied identically as well. Finally we connect p with the stream function ψ. For this we rewrite the first equation of (4.33) in terms of the Bernoulli energy function

$$\frac{\partial}{\partial r}\left[p + \frac{1}{2}(u_r^2 + u_\phi^2 + u_z^2)\right] = \frac{u_\phi}{r}\frac{\partial}{\partial r}(r u_\phi) + u_z \frac{\partial}{\partial r} u_z - u_z \frac{\partial}{\partial z} u_r, \tag{4.38}$$

and likewise for the third equation

$$\frac{\partial}{\partial z}\left[p + \frac{1}{2}(u_r^2 + u_\phi^2 + u_z^2)\right] = u_r\left(\frac{\partial}{\partial z} u_r - \frac{\partial}{\partial r} u_z\right) + u_\phi \frac{\partial}{\partial z} u_\phi. \tag{4.39}$$

Now, by also letting p to be an arbitrary function of ψ in the way that

$$p + \frac{1}{2}(u_r^2 + u_\phi^2 + u_z^2) = H(\psi), \tag{4.40}$$

both equations (4.38) and (4.39) accumulate into one equation

$$\begin{aligned} &\psi_{zz} + \psi_{rr} - \frac{1}{r}\psi_r = r^2 G(\psi) + F(\psi), \\ &\text{with } F(\psi) = -\frac{d}{d\psi}\left[\frac{1}{2}C^2(\psi)\right] \text{ and } G(\psi) = \frac{d}{d\psi}H(\psi). \end{aligned} \tag{4.41}$$

Thus without any loss of information the four Euler equations (4.33) can be represented as a single equation for the stream function ψ depending on (r, z). This equation is called Bragg-Hawthorne equation or in plasma physics Grad-Shafranov equation (Andreev *et al.*, 1998). Solving for ψ under an arbitrary choice of (F, G), one can easily construct the corresponding solutions of the original or primitive variables (u_r, u_ϕ, u_z, p). This scalar equation thus fully describes the class of incompressible stationary axisymmetric motions of an ideal fluid with swirl.

Although the Bragg-Hawthorne equation is a one-to-one derivation from the original Euler equations, these two systems of PDEs are not fully equivalent to each other for all mathematical investigations. This will be shown in section 4.3.3 under the example of a local Lie point symmetry investigation. It leads to a behavior that not every symmetry of equation (4.41) when transformed back to its primitive variables, is also a symmetry of equations (4.33).

4.3.2 Symmetry analysis of the Bragg-Hawthorne equation

This section gives a complete Lie point symmetry analysis of the Bragg-Hawthorne equation. Complete in the sense that at the end it will be possible to identify the full symmetry group (4.34) within a set of symmetries admitted by the Bragg-Hawthorne equation.
When performing a local Lie point symmetry analysis on a differential equation with arbitrary functions like the Bragg-Hawthorne equation

$$\psi_{zz} + \psi_{rr} - \frac{1}{r}\psi_r = r^2 G(\psi) + F(\psi), \tag{4.42}$$

the aim is to find all possible symmetry algebras for every choice that can be made on the arbitrary functions (F, G). From the structure of equation (4.42), it is easy to see that the minimal symmetry algebra is spanned by the single operator $X_1 = \partial_z$, irrespective of the choice for (F, G). Certainly more interesting is to know, for which special choice of F and G it is possible to gain the maximal symmetry algebra. For that one has to perform a group-theoretical classification upon equation (4.42). This has been partly done by Andreev *et al.* (1998). Partly in the sense that their classification emerged under the restriction that at least one of the functions F or G had to be non-linear.
The reason why a linear choice of F and G has to be investigated separately from a non-linear one, is that a Lie point symmetry analysis of equation (4.42) results into the following classifying relations for (F, G)

$$\left(\frac{F_\psi}{F_{\psi\psi}}\right)_\psi = \alpha, \quad \text{and} \quad \left(\frac{G_\psi}{G_{\psi\psi}}\right)_\psi = \frac{\alpha}{2}, \tag{4.43}$$

where α is a constant. Hence, one can only extract information from these two decoupled relations when the second derivatives of F or G relative to ψ do not vanish. In other words when at least one of these two functions are non-linear.

Nonlinear case

When the non-linear condition is satisfied ($F_{\psi\psi} \neq 0$ or $G_{\psi\psi} \neq 0$), the task is to solve the set of equations (4.43) for the functions (F, G). Since these classifying relations can be solved in the most general way, it is not necessary to simplify their structure by constructing equivalence transformations for the Bragg-Hawthorne equation (4.42), as it was done by Andreev *et al.* (1998). Furthermore, since the classifying relations are part of the determining system of the underlying symmetry analysis, they must be solved in such a way that their solutions do not induce contradictions to the rest of the determining system. Following that condition will lead to three different classes of local symmetry algebras which are distinguished by the following choices of α

$$\begin{aligned} \alpha = 0: \qquad & F(\psi) = \gamma_1 e^{\psi/\beta}, \quad G(\psi) = \gamma_2 e^{2\psi/\beta}, \quad \text{with} \quad \beta \neq 0, \\ & \{\, Y_1 = \frac{\partial}{\partial z} \;;\; Y_2 = r\frac{\partial}{\partial r} + z\frac{\partial}{\partial z} - 2\beta\frac{\partial}{\partial \psi} \,\}, \end{aligned}$$

$$
\begin{aligned}
\alpha \in \mathbb{R}\backslash\{0\}: \quad & F(\psi)=\gamma_1(\psi+\beta)^{1+1/\alpha},\ \ G(\psi)=\gamma_2(\psi+\beta)^{1+2/\alpha},\\
& \{\, Y_1=\frac{\partial}{\partial z}\ ;\ Y_2=r\frac{\partial}{\partial r}+z\frac{\partial}{\partial z}-2\alpha(\psi+\beta)\frac{\partial}{\partial \psi}\,\},\\
\alpha=-\tfrac{1}{4}: \quad & F(\psi)=\gamma_1(\psi+\beta)^{-3},\ \ G(\psi)=\gamma_2(\psi+\beta)^{-7},\\
& \{\, Y_1=\frac{\partial}{\partial z}\ ;\ Y_2=r\frac{\partial}{\partial r}+z\frac{\partial}{\partial z}+\tfrac{1}{2}(\psi+\beta)\frac{\partial}{\partial \psi}\ ;\\
& \quad Y_3=rz\frac{\partial}{\partial r}+\tfrac{1}{2}(z^2-r^2)\frac{\partial}{\partial z}+\tfrac{1}{2}z(\psi+\beta)\frac{\partial}{\partial \psi}\,\},
\end{aligned}
\tag{4.44}
$$

where the set $(\beta,\gamma_1,\gamma_2)$ are arbitrary constants. When the functions (F,G) are fixed as in the last part of (4.44) we obtain the maximal symmetry algebra based on a local Lie point transformation of the Bragg-Hawthorne equation (4.42). Such a size comparison between different classes of symmetry algebras fail, when it comes down to the pure linear case, for which a corresponding symmetry analysis will lead in general to infinite dimensional algebras.

Linear case

If the functions (F,G) are fixed in the most general way as

$$F(\psi)=c_1\psi+a,\ \ \text{and}\ \ G(\psi)=c_2\psi+b, \tag{4.45}$$

a proper local Lie point symmetry analysis of the Bragg-Hawthorne equation will be as complicated as solving the equation itself. Trying to solve for the infinitesimals of the symmetry group or to get the general solution of ψ itself always leads to complicated integrals over Whittaker functions. For these functions no analytical nor a numerical theory exists for calculating such quantities properly. In the appendix B an analytical attempt on how to find the general solution of the linear Bragg-Hawthorne equation is shown.

For our purposes in the next section, it is fully sufficient to look at the most simple specification: $c_1=c_2=0$. There we will show that already within this special symmetry group, together with the symmetry groups of the non-linear case, the full symmetry group (4.34) of the Euler equations can be identified. Performing a local Lie point symmetry analysis on equation

$$\psi_{zz}+\psi_{rr}-\frac{1}{r}\psi_r=br^2+a, \tag{4.46}$$

results into the following infinite dimensional symmetry algebra

$$
\begin{aligned}
Y_1 &= \frac{\partial}{\partial z},\\
Y_2 &= r\frac{\partial}{\partial r}+z\frac{\partial}{\partial z}+(az^2+\tfrac{1}{2}br^4)\frac{\partial}{\partial \psi},\\
Y_3 &= 2r\frac{\partial}{\partial r}+2z\frac{\partial}{\partial z}+(\tfrac{3}{2}az^2+\tfrac{7}{8}br^4+\psi)\frac{\partial}{\partial \psi},
\end{aligned}
$$

$$
\begin{aligned}
Y_4 &= 2rz\frac{\partial}{\partial r} + (z^2 - r^2)\frac{\partial}{\partial z} + (\tfrac{1}{2}az^3 + \tfrac{7}{8}zbr^4 + z\psi)\frac{\partial}{\partial \psi}, \\
Y_5 &= \phi(r,z)\frac{\partial}{\partial \psi}, \quad \text{with} \quad \phi_{zz} + \phi_{rr} - \tfrac{1}{r}\phi_r = 0.
\end{aligned} \tag{4.47}
$$

Making use of the method of separation of variables the general solution of ϕ in the radial coordinate can be expressed as Bessel functions (Abramowitz & Stegun, 1968). For our purposes again it's sufficient to simplify the symmetry algebra (4.47) down to a five-dimensional algebra by fixing ϕ to the trivial solution $\phi(r,z) = 1$.

4.3.3 Symmetry identification

In this section we identify the full symmetry group (4.34) of the Euler equations within the set of symmetries obtained in the previous section for the Bragg-Hawthorne equation. There we have listed eight distinct local symmetries

$$
\begin{aligned}
F,\ G \text{ arbitrary}: \quad & Y_1 = \frac{\partial}{\partial z}, \\
F \sim e^{\psi/\beta},\ G \sim e^{2\psi/\beta}: \quad & Y_2 = r\frac{\partial}{\partial r} + z\frac{\partial}{\partial z} - 2\beta\frac{\partial}{\partial \psi}, \\
F \sim (\psi+\beta)^{1+1/\alpha},\ G \sim (\psi+\beta)^{1+2/\alpha}: \quad & Y_3 = r\frac{\partial}{\partial r} + z\frac{\partial}{\partial z} - 2\alpha(\psi+\beta)\frac{\partial}{\partial \psi}, \\
F \sim (\psi+\beta)^{-3},\ G \sim (\psi+\beta)^{-7}: \quad & Y_4 = rz\frac{\partial}{\partial r} + \tfrac{1}{2}(z^2 - r^2)\frac{\partial}{\partial z} + \tfrac{1}{2}z(\psi+\beta)\frac{\partial}{\partial \psi}, \\
F = a,\ G = b: \quad & Y_5 = r\frac{\partial}{\partial r} + z\frac{\partial}{\partial z} + (az^2 + \tfrac{1}{2}br^4)\frac{\partial}{\partial \psi}, \\
& Y_6 = 2r\frac{\partial}{\partial r} + 2z\frac{\partial}{\partial z} + (\tfrac{3}{2}az^2 + \tfrac{7}{8}br^4 + \psi)\frac{\partial}{\partial \psi}, \\
& Y_7 = 2rz\frac{\partial}{\partial r} + (z^2 - r^2)\frac{\partial}{\partial z} \\
& \qquad + (\tfrac{1}{2}az^3 + \tfrac{7}{8}zbr^4 + z\psi)\frac{\partial}{\partial \psi}, \\
& Y_8 = \frac{\partial}{\partial \psi}.
\end{aligned} \tag{4.48}
$$

When these eight Bragg-Hawthorne symmetries in terms of the scalar stream function ψ are transformed back to the primitive variables (u_r, u_ϕ, u_z, p) of the Euler equations, they gain the following structure

$$
\begin{aligned}
Z_1 &= \frac{\partial}{\partial z}, \\
Z_2 &= r\frac{\partial}{\partial r} + z\frac{\partial}{\partial z} - 2\Big[u_r\frac{\partial}{\partial u_r} + u_\phi\frac{\partial}{\partial u_\phi} + u_z\frac{\partial}{\partial u_z} + 2p\frac{\partial}{\partial p}\Big], \\
Z_3 &= r\frac{\partial}{\partial r} + z\frac{\partial}{\partial z} - (2\alpha+2)\Big[u_r\frac{\partial}{\partial u_r} + u_\phi\frac{\partial}{\partial u_\phi} + u_z\frac{\partial}{\partial u_z} + 2p\frac{\partial}{\partial p}\Big],
\end{aligned}
$$

$$
\begin{aligned}
Z_4 &= rz\frac{\partial}{\partial r}+\frac{1}{2}(z^2-r^2)\frac{\partial}{\partial z}-\left(\frac{3}{2}zu_r-ru_z+\frac{\psi+\beta}{2r}\right)\frac{\partial}{\partial u_r}-\frac{3}{2}zu_\phi\frac{\partial}{\partial u_\phi}\\
&\quad-\left(\frac{3}{2}zu_z+ru_r\right)\frac{\partial}{\partial u_z}+\left(\frac{\psi+\beta}{2r}u_r-3zp\right)\frac{\partial}{\partial p},\\
Z_5 &= r\frac{\partial}{\partial r}+z\frac{\partial}{\partial z}-\left(2u_r+\frac{2az}{r}\right)\frac{\partial}{\partial u_r}-\left(u_\phi+\frac{abr^2}{2u_\phi}+\frac{a^2z^2}{r^2u_\phi}\right)\frac{\partial}{\partial u_\phi}-(2u_z-2br^2)\frac{\partial}{\partial u_z}\\
&\quad+\left(2u_r^2+u_\phi^2+2u_z^2+\frac{2az}{r}u_r+\frac{a^2z^2}{r^2}-2br^2u_z+\frac{1}{2}abr^2+abz^2+\frac{1}{2}b^2r^4\right)\frac{\partial}{\partial p},\\
Z_6 &= 2r\frac{\partial}{\partial r}+2z\frac{\partial}{\partial z}-\left(3u_r+\frac{3az}{r}\right)\frac{\partial}{\partial u_r}-\left(2u_\phi+\frac{7}{8}\frac{abr^2}{u_\phi}+\frac{\frac{3}{2}a^2z^2+a\psi}{r^2u_\phi}\right)\frac{\partial}{\partial u_\phi}\\
&\quad+\left(\frac{7}{2}br^2-3u_z\right)\frac{\partial}{\partial u_z}+\left(3u_r^2+2u_\phi^2+3u_z^2+\frac{3az}{r}u_r+\frac{\frac{3}{2}a^2z^2+a\psi}{r^2}-\frac{7}{2}br^2u_z\right.\\
&\quad\left.+\frac{7}{8}abr^2+\frac{3}{2}abz^2+\frac{7}{8}b^2r^4+b\psi\right)\frac{\partial}{\partial p},\\
Z_7 &= 2rz\frac{\partial}{\partial r}+(z^2-r^2)\frac{\partial}{\partial z}-\left(3zu_r+\frac{3az^2}{2r}+\frac{7}{8}br^3+\frac{\psi}{r}-2ru_z\right)\frac{\partial}{\partial u_r}\\
&\quad-\left(2zu_\phi+\frac{7}{8}z\frac{abr^2}{u_\phi}+\frac{\frac{1}{2}a^2z^3+az\psi}{r^2u_\phi}\right)\frac{\partial}{\partial u_\phi}+\left(\frac{7}{2}zbr^2-3zu_z-2ru_r\right)\frac{\partial}{\partial u_z}\\
&\quad+\left(3zu_r^2+2zu_\phi^2+3zu_z^2+\frac{3az^2}{2r}u_r+\frac{\frac{1}{2}a^2z^3+az\psi}{r^2}-\frac{7}{2}zbr^2u_z\right.\\
&\quad\left.+\frac{7}{8}zabr^2+\frac{7}{8}br^3u_r+\frac{\psi}{r}u_r+\frac{1}{2}abz^3+\frac{7}{8}zb^2r^4+zb\psi\right)\frac{\partial}{\partial p},\\
Z_8 &= -\frac{a}{r^2u_\phi}\frac{\partial}{\partial u_\phi}+\left(b+\frac{a}{r^2}\right)\frac{\partial}{\partial p},
\end{aligned}
\tag{4.49}
$$

where ψ is the path-independent line integral as given in (4.36). Due to this ψ-dependence the three operators Z_4, Z_6 and Z_7 will generate non-local symmetries. The rest of this set represent local symmetries in the sense of Lie point group transformations. On inspection we recognize the full symmetry group (4.34) of the Euler equations as the following subset

$$\{\, Z_1 = X_1\,;\; Z_3^{\alpha=-1} = X_2\,;\; \tfrac{1}{2}(Z_3^{\alpha=-1} - Z_2) = X_3\,;\; Z_8^{(a,b)=(-1,0)} = X_4\,;\; Z_8^{(a,b)=(0,1)} = X_5\,\}.$$

The rest of the set (4.49) represent no symmetries of the Euler equations. In other words, the Bragg-Hawthorne equation (4.42) admits more symmetries than the Euler equations (4.33) do. This statement is easily traceable if one for example looks at the local symmetry Z_5. It cannot be a symmetry of the Euler equations, since its maximal local symmetry group is already fixed by (4.34). What is the reason for this different behavior, if apparently the Bragg-Hawthorne equation was obtained without any loss of information from the Euler equations? Shouldn't they be equivalent and therefore admit the same set of symmetries? A reasonable explanation is that equations (4.33) are a fully unsolved system of the four unknown functions (u_r, u_ϕ, u_z, p), while the Bragg-Hawthorne equation (4.42) implicitly represents a partially solved system for (u_ϕ, p). This is reflected in the arbitrary functions (F, G), which are to be seen as PDE integration functions for (u_ϕ, p). But exactly

this is a crucial condition for a symmetry analysis of differential equations, since such an investigation strongly depends on the number of equations involved.
So what are the fully equivalent equations in terms of the primitive variables for the Bragg-Hawthorne equation?

4.3.4 Intermediate Euler equations

Following the same procedure as for the construction of the Bragg-Hawthorne equation, we start again with the Euler equations (4.33) and rewrite the first and third equation equivalently as (4.38) and (4.39) respectively. When substituting the expressions (4.37) and (4.40) into these two equations and using the scalar stream function in the definition of (4.36), we obtain the following equivalent set of integro-differential equations for the two unknown functions (u_r, u_z)

$$\begin{aligned} \frac{1}{r}\frac{\partial}{\partial r}(ru_r) + \frac{\partial}{\partial z}u_z &= 0, \\ \frac{\partial}{\partial r}u_z - \frac{\partial}{\partial z}u_r &= \frac{1}{r}F(\psi) + rG(\psi), \end{aligned} \tag{4.50}$$

where (F, G) are arbitrary functions depending on the path-independent line integral $\psi = \psi(r, z)$ as given in (4.36). Fixing a choice for $F(\psi)$ and $G(\psi)$, the above system (4.50) can be solved for the unknowns (u_r, u_z), at least theoretically. Then the corresponding solutions for the azimuthal velocity and the pressure are given by

$$\begin{aligned} u_\phi &= \pm\frac{1}{r}\sqrt{-2\int F(\psi)d\psi}, \\ p &= \int G(\psi)d\psi - \frac{1}{2}(u_r^2 + u_\phi^2 + u_z^2). \end{aligned} \tag{4.51}$$

From now on we will call the set of equations (4.50) together with the solutions (4.51) the intermediate Euler equations. By construction they are on the one hand equivalent to the Euler equations. As stated above the second and fourth equation of (4.33) accumulate into the second equation of (4.50), while the third equation of (4.33) is satisfied identically by the solution of u_ϕ given in (4.51). On the other hand, the intermediate Euler equations are also equivalent to the Bragg-Hawthorne equation. Applying definition (4.35) will satisfy the continuity equation in (4.50) identically, while the second equation changes to (4.42). But on the basis of a Lie point symmetry analysis, only the Bragg-Hawthorne equation is fully equivalent to the intermediate Euler equations. The reason is that a Lie symmetry analysis is highly sensitive to the number of equations being investigated. The Euler equations represent an unsolved systems for four unknown functions (u_r, u_ϕ, u_z, p), while the Bragg-Hawthorne and the intermediate Euler equations represent an unsolved system in only two unknown functions (u_r, u_z) — the Bragg-Hawthorne equation represents it implicitly, while the intermediate Euler equations represent it explicitly. This full equivalence between the Bragg-Hawthorne and the intermediate Euler equations expresses itself in the way that all the distinct symmetries Z_i listed in (4.49) relative to the variables

(r, z, u_r, u_z) are admitted by the integro-differential system (4.50).
Interesting to note is that this integro-differential system exhibits local symmetries like Z_1, Z_2 or Z_3. Normally for an integro-differential equation one would expect only non-local symmetries like Z_4, since they usually describe non-local features of a system. The fact that the integro-differential (4.50) equation admits local Lie point symmetries is fully consistent with the results found by Zawistowski Zawistowski (2001). He showed that it is possible to apply a local Lie point symmetry analysis to integro-differential equations. In the case of integro-differential equations there is no need for a non-local extension of a symmetry group. It is sufficient to stay in the same variable space as in the case of differential equations. This property allows an integro-differential equation to admit local Lie point symmetries. Through the method proposed by Zawistowski (2001) it is possible to determine the local symmetries Z_1, Z_2 or Z_3 directly by applying a local Lie point analysis onto the integro-differential system (4.50). The insight that an integro-differential equation can exhibit local Lie point symmetries was gained here by the process of finding the fully equivalent equations for the Bragg-Hawthorne equation in primitive variables.
On the other hand we know from the investigations of Ibragimov (1995*b*) that for differential equations it is also possible to admit non-local symmetries, which cannot be obtained by a direct Lie point symmetry analysis. For the choice of constant arbitrary functions $F(\psi) = a$ and $G(\psi) = b$, the integro-differential equations (4.50) turn into a system of pure differential equations for the unknowns (u_r, u_z). The transformation process from the Bragg-Hawthorne to the intermediate Euler equations shows how the local symmetry Y_7 gives rise to a non-local symmetry Z_7 within differential equations. In other words, one clearly sees how a non-local symmetry for a differential system is generated implicitly from a local Lie point analysis.

5 Shear-free turbulent diffusion

The investigations on shear-free turbulent diffusion using symmetry methods have been carried out by Oberlack & Guenther (2003). The investigations on turbulent diffusion in a rotating frame have been published in Guenther *et al.* (2004).

5.1 Introduction

We reconsider the problem of shear-free turbulent diffusion with no production due to a mean-velocity gradient. Turbulence is generated at the plane $x_1 = 0$ and diffuses in the direction $x_1 > 0$. Turbulence is homogeneous in the x_2-x_3 plane. Experimentally this problem is investigated by a plane vibrating grid in a sufficiently large tank. In order to produce a reasonable high degree of turbulence the grid is usually vibrating in the x_1 direction at a sufficiently small amplitude but at a large frequency. The flow geometry is given in figure (5.1) This is a classical problem which has been treated both experimentally

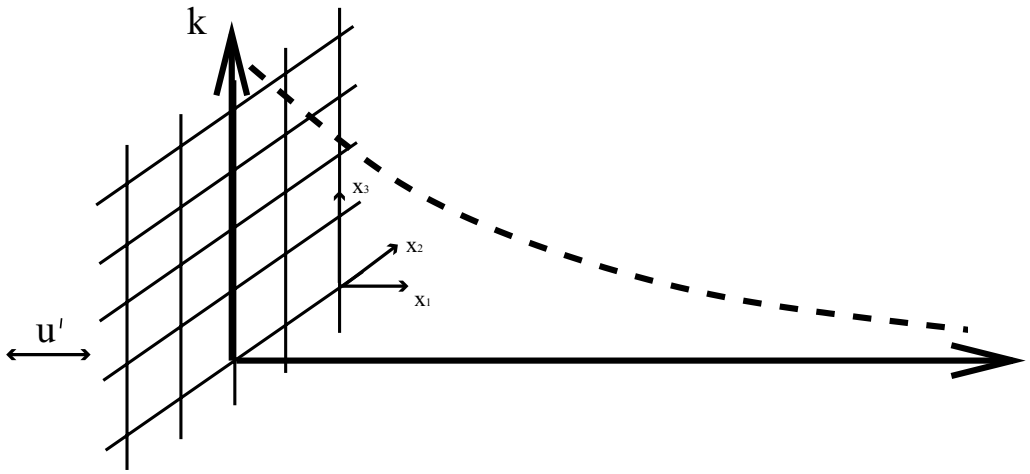

Figure 5.1: Flow geometry

and theoretically by several authors. It has long been known that in this classical case the turbulent kinetic energy behaves according to

$$K \sim x_1^{-n}.$$

Essentially all Reynolds averaged models such as two-equation or Reynolds stress transport models are compatible with this finding. Model constants determine the value of n. In reverse, the measured value of n may be used to determine the model constants (see

e.g. Chen & Jaw, 1989). Sometimes the exponent is used to determine the diffusion coefficient in the Reynolds stress or the turbulent kinetic energy equation, since other model parameters are determined by homogeneous or near-wall flows.

A broad variety of experiments both with one and two grids have been conducted. Experiments with one grid were for example conducted by Shy & Beidenthal (1991), Fernando & De Silva (1993), De Silva & Fernando (1994) or Srdic *et al.* (1996) investigating the spatial decay behavior, as well as other influencing parameters such as stratification. The numerical values for n found therein vary in the range of 0.86 to 1.5. Two parallel grids in opposite configuration were primarily used to produce a relatively large region of weak turbulence variation or in other words to generate nearly isotropic turbulence. Extensive experiments of this kind were for example conducted by Shy *et al.* (1997) or Mann *et al.* (1999) to name only a few. Also direct numerical simulations were for example carried out by Briggs *et al.* (1996) determining a value for n in the range given above.

It is the simplicity of the problem which makes it attractive to also theoretically investigate it. Any scalar statistical equation, such as the one for the turbulent kinetic energy or the dissipation of turbulent kinetic energy only contains three terms: an unsteady term, a destruction term, and a diffusion term. The latter two have to be modeled. However, since there is no mean flow in the problem, no production term is contained. Since usually a plane problem is studied the general model equations reduce to a simplified form with one spatial coordinate and time.

Aiming to analyze unsteady flows of this type the problem was reconsidered by Lele (1985) raising the question whether a turbulent diffusion-wave exists by investigating two equation models such as the K-ϵ model. Unfortunately, the non-local transformation he suggested did not lead to the simplification as it was intended to do. Still, and this will be shown in section 5.4.2, the suggested transformation has its validity for steady problems. In this case, it leads to the proposed linearization of the model equation. Hence, a complete analytic solution is admitted for the K-ϵ model. Since this solution has not been obtained from classical symmetry methods it can be concluded that the model equations admit additional hidden symmetries.

In a series of papers Cazalbou and collaborators (Cazalbou & Bradshaw, 1993; Cazalbou *et al.*, 1994; Cazalbou & Chassaing, 2001, 2002) analyzed turbulent diffusion investigating turbulence models at the edge of turbulent flows as well as the present problem of grid-turbulence. For the latter problem it was recognized in Cazalbou & Chassaing (2002) that for certain model constants the latter algebraic decay changes to an exponential decay. Two-equation and Reynolds stress transport models were analyzed using the algebraic decay law and an unsteady extension of it. It was shown that depending on the specific model different decay rates and anisotropy levels are obtained.

5.2 Large- and small-scale expansion of the multi-point correlation equations for shear-free turbulent diffusion

For the derivation of invariant solutions of shear-free turbulent flows below we need to investigate the symmetry properties of the multi-point correlation MPC equations (see section 2.3). In Oberlack (2000*a*) it is shown that all known symmetry groups of the Euler and Navier-Stokes equations are linear (see e.g. Ibragimov, 1995*a*,*b*, 1996) and hence uniquely map to a set of new symmetries for the MPC equations.

At this point we may discuss boundary conditions (BC) on the two-point (TP) quantities. From its basic definitions any quantity in (2.26) will become zero on a solid wall due to non-slip BC $u_i' = 0$. For any TP quantity we also have to specify the BC in r-space. Considering a turbulent flow in infinite space any TP quantity, such as R_{ij} becomes zero for $|\boldsymbol{r}| \to \infty$. In one of the present cases also periodic BC will be invoked such as $R_{ij}(r_2, r_3) = R_{ij}(r_2 + a, r_3 + a)$ to be specified in section 5.3.2. In principle, no BCs need to be specified at $\boldsymbol{r} = 0$ since the values are determined during the solution process. However, in some problems the limit $\lim_{r\to 0} R_{ij} = \overline{u_i' u_j'}$ needs to be invoked if for example Reynolds stresses are specified on BCs as is the case for all the present flows at the vibrating grid. Also, if mean flows are considered there is a direct coupling to the momentum equation which, however, is a one-way coupling.

A general problem with BC in the context of *similarity solutions* and its generalizations *invariant solutions*, derived from Lie group theory is the fact that they are special solutions. For most non-linear partial differential equations (PDE) these are the only analytic solutions that may be obtained. Hence arbitrary BC may not be imposed. Still, even if arbitrary BCs may not be invoked employing different symmetry groups for the construction of the solution allows at least a small number of different solutions to be shown below. These solutions are determined by global constrains, stemming from scaling groups other than classical BCs.

For the understanding of large Reynolds number turbulent flows it is important to note that the Euler equations admit one more scaling group compared to the Navier-Stokes equations (see section 4.2). It is in particular this additional scaling group which is crucial to understand turbulent scaling laws.

In order to "recover" this additional scaling group though the MPC equations contain viscosity we have to adopt these equations in a form derived from a singular asymptotic expansion, first suggested in Oberlack (2000*a*). Therein it was proven that, similar to the laminar boundary layer equations we may separate the correlation equations into an inner and outer equation, corresponding to small- and large-scale turbulence. The inner equations cover the inertial range and the dissipation range. The outer equations include all large-scales down to the inertial range. The inertial range is the matching region. A sketch of the asymptotic region in r-space is depicted in figure 5.2.

The following boundary layer type of expansion for small r is based on the turbulent

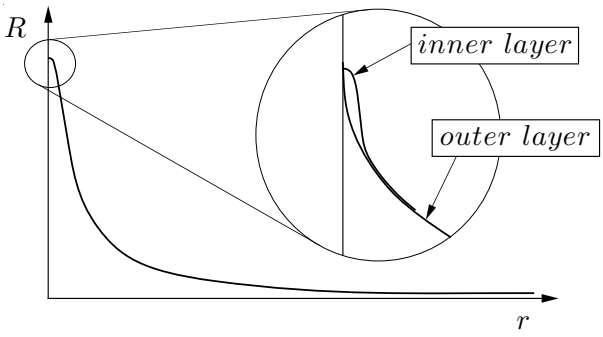

Figure 5.2: The asymptotic region in r-space.

Reynolds number

$$Re_T = \frac{\sqrt{K}\ell_t}{\nu}, \tag{5.1}$$

where the integral length-scale ℓ_t and the Kolmogorov length scale η_K are respectively defined as

$$\ell_t = \frac{1}{K}\int_{V_r} R_{kk}\frac{\mathrm{d}^3 r}{r^2} \quad \text{and} \quad \eta_K = \left(\frac{\nu^3}{\epsilon}\right)^{\frac{1}{4}}, \tag{5.2}$$

whereby V_r describes the volume of integration covering entire $\mathbb{R}^3$. K and ϵ are the turbulent kinetic energy and the dissipation of turbulent kinetic energy.

The outer part of the asymptotic expansion in r-space, that is the domain $\eta_K \ll r$, is obtained by taking the limit $1/Re_t \to 0$ or $\nu \to 0$ in the equations (2.26) yielding for the two-point correlation equation to

$$\begin{aligned}\Theta_{i_{\{2\}}} = {} & \frac{\bar{\mathrm{D}}R_{ij}}{\bar{\mathrm{D}}t} + R_{kj}\,\frac{\partial \bar{u}_i(\boldsymbol{x},t)}{\partial x_k} + R_{ik}\,\frac{\partial \bar{u}_j(\boldsymbol{x},t)}{\partial x_k}\bigg|_{\boldsymbol{x}+\boldsymbol{r}} \\ & + \left[\bar{u}_k\left(\boldsymbol{x}+\boldsymbol{r},t\right) - \bar{u}_k\left(\boldsymbol{x},t\right)\right]\,\frac{\partial R_{ij}}{\partial r_k} + \frac{\partial \overline{p'u'}_j}{\partial x_i} - \frac{\partial \overline{p'u'}_j}{\partial r_i} + \frac{\partial \overline{u'_i p'}}{\partial r_j} \\ & + \frac{\partial R_{(ik)j}}{\partial x_k} - \frac{\partial}{\partial r_k}\,\left[R_{(ik)j} - R_{i(jk)}\right] + 2\,\Omega_k\,\left[e_{kli}R_{lj} + e_{klj}R_{il}\right] = 0.\end{aligned} \tag{5.3}$$

It is apparent that the latter equation is not valid in the limit $r \to 0$ since no dissipation is contained which becomes important as $r \to \eta_K$.

The inner part of the asymptotic expansion of the correlation function may be obtained by introducing the singular expansion

$$\begin{aligned} R_{ij}(\boldsymbol{x},\boldsymbol{r}) &= \overline{u'_i u'_j}(\boldsymbol{x}) - Re_t^{-\frac{1}{2}} R^{(1)}_{ij}(\boldsymbol{x},\hat{\boldsymbol{r}}) - O(Re_t^{-\frac{3}{4}}), \\ R_{(ik)j}(\boldsymbol{x},\boldsymbol{r}) &= \overline{u'_i u'_j u'_k}(\boldsymbol{x}) + Re_t^{-\frac{3}{4}} R^{(1)}_{(ik)j}(\boldsymbol{x},\hat{\boldsymbol{r}}) - O(Re_t^{-1}), \\ R_{i(jk)}(\boldsymbol{x},\boldsymbol{r}) &= \overline{u'_i u'_j u'_k}(\boldsymbol{x}) + Re_t^{-\frac{3}{4}} R^{(1)}_{i(jk)}(\boldsymbol{x},\hat{\boldsymbol{r}}) - O(Re_t^{-1}), \\ & \text{with} \quad \hat{\boldsymbol{r}} = Re_t^{\frac{3}{4}}\boldsymbol{r} \end{aligned} \tag{5.4}$$

into (2.26) resulting in the leading order equation

$$\begin{aligned}
&\frac{\bar{\mathrm{D}}\overline{u_i' u_j'}}{\bar{\mathrm{D}}t} + \overline{u_j' u_k'}\,\frac{\partial \bar{u}_i(\boldsymbol{x},t)}{\partial x_k} + \overline{u_i' u_k'}\frac{\partial \bar{u}_j(\boldsymbol{x},t)}{\partial x_k} - \frac{\partial \bar{u}_k(\boldsymbol{x},t)}{\partial x_l}\,\hat{r}_l\,\frac{\partial R_{ij}^{(1)}}{\partial \hat{r}_k} \\
&+ \left[\frac{\partial \overline{p'u'}_j}{\partial x_i} - \frac{\partial \overline{p'u'}_j}{\partial r_i} + \frac{\partial \overline{u_i' p'}}{\partial r_j}\right]\Bigg|_{r=0} + 2\,\frac{\partial^2 R_{ij}^{(1)}}{\partial \hat{r}_k \partial \hat{r}_k} \\
&+ \frac{\partial \overline{u_i' u_j' u_k'}}{\partial x_k} - \frac{\partial}{\partial \hat{r}_k}\left[R_{(ik)j}^{(1)} - R_{i(jk)}^{(1)}\right] + 2\,\Omega_k\,\left[e_{kli}\overline{u_j' u_l'} + e_{klj}\overline{u_i' u_l'}\right] = 0.
\end{aligned} \tag{5.5}$$

The pressure velocity correlations $\overline{p'u'}_j$ and $\overline{u_i' p'}$ are determined by the Poisson equation and hence are not independent of the velocity correlations.

Comparing the equations (5.3) and (5.5) with boundary layer theory for laminar flows we find that (5.3) corresponds to the inviscid outer flow while (5.5) is the analog to the boundary layer equation. In complete resemblance to boundary layer theory where the pressure-gradient in streamwise direction is determined by the outer inviscid flow we may compute $R_{ij}^{(1)}(\boldsymbol{x},\hat{\boldsymbol{r}})$ in (5.5). Therein the quantities $\overline{u_i' u_j'}$, $\overline{u_i' u_j' u_k'}$, $\overline{p'u'}_j$ and $\overline{u_i' p'}$ are determined by the outer equations (5.3) by invoking the appropriate limit $\boldsymbol{r} = 0$. The only term that has no counterpart in equation (5.3) is the last term in the second line of equation (5.5) which denotes dissipation.

For the analysis to be carried out in the following section we first investigate the large-scale equation (5.3) to obtain quantities such as the Reynolds stress tensor. Once this is acquired we may derive the small-scale quantities such as the dissipation from (5.5).

5.3 Symmetries and invariant solutions of the correlation equation

Since the MPC equations of different tensor order have similar structure, in the following we solely present the two-point correlation (TPC) equations. It is important to note that all results to be presented below are fully consistent with all higher order correlation functions up to infinite order.

We are primarily interested in large-scale quantities such as the Reynolds stress tensor or the integral length-scale and hence we adopt the large-scale TPC equation (5.3) which for the present flow of shear-free diffusion reduces to

$$\begin{aligned}
&\frac{\partial R_{ij}}{\partial t} + \delta_{i1}\frac{\partial \overline{p'u'}_j}{\partial x_1} - \frac{\partial \overline{p'u'}_j}{\partial r_i} + \frac{\partial \overline{u_i' p'}}{\partial r_j} + \frac{\partial R_{(i1)j}}{\partial x_1} \\
&- \frac{\partial}{\partial r_k}\left[R_{(ik)j} - R_{i(jk)}\right] + 2\,\Omega_k\,\left[e_{kli}R_{lj} + e_{klj}R_{il}\right] = 0,
\end{aligned} \tag{5.6}$$

extended by the kinematic conditions for the correlation functions derived from the con-

tinuity equation

$$\delta_{i1}\frac{\partial R_{1j}}{\partial x_1} - \frac{\partial R_{ij}}{\partial r_i} = 0, \quad \frac{\partial R_{ij}}{\partial r_j} = 0, \quad \frac{\partial \overline{u_1' p'}}{\partial x_1} - \frac{\partial \overline{u_j' p'}}{\partial r_j} = 0, \quad \frac{\partial \overline{p' u'}_i}{\partial r_i} = 0. \tag{5.7}$$

For a non-rotating frame of reference ($\boldsymbol{\Omega} = 0$) the equations (5.6) and (5.7) admit the following classical symmetries in generator form

$$\mathrm{X}_{s_x} = x_1\frac{\partial}{\partial x_1} + r_i\frac{\partial}{\partial r_i} + 2R_{ij}\frac{\partial}{\partial R_{ij}} + \dots\,, \tag{5.8}$$

$$\mathrm{X}_{s_t} = t\frac{\partial}{\partial t} - 2R_{ij}\frac{\partial}{\partial R_{ij}} + \dots\,, \tag{5.9}$$

$$\mathrm{X}_{x_1} = \frac{\partial}{\partial x_1}\,, \tag{5.10}$$

$$\mathrm{X}_{t} = \frac{\partial}{\partial t}\,, \tag{5.11}$$

where dots denote additional higher order correlation functions which have been omitted.

Employing Lie's first theorem we may rewrite the symmetries in global form

$$\bar{T}_{s_x}:\ t^* = t\ ,\qquad x_1^* = \mathrm{e}^{a_1}x_1\ ,\quad \boldsymbol{r}^* = \mathrm{e}^{a_1}\boldsymbol{r}\ ,\ \mathbf{R}^* = \mathrm{e}^{2a_1}\mathbf{R}\ ,\quad \dots \tag{5.12}$$

$$\bar{T}_{s_t}:\ t^* = \mathrm{e}^{a_2}t\ ,\quad x_1^* = x_1\ ,\qquad \boldsymbol{r}^* = \boldsymbol{r}\ ,\quad \mathbf{R}^* = \mathrm{e}^{-2a_2}\mathbf{R}\ ,\ \dots \tag{5.13}$$

$$\bar{T}_{x_1}:\ t^* = t\ ,\qquad x_1^* = x_1 + a_3\ ,\ \boldsymbol{r}^* = \boldsymbol{r}\ ,\quad \mathbf{R}^* = \mathbf{R}\ ,\qquad \dots \tag{5.14}$$

$$\bar{T}_{t}:\ t^* = t + a_4\ ,\ x_1^* = x_1\ ,\qquad \boldsymbol{r}^* = \boldsymbol{r}\ ,\quad \mathbf{R}^* = \mathbf{R}\ ,\qquad \dots \tag{5.15}$$

which respectively correspond to scaling of space, scaling of time, translation in space and translation in time. The a_i's are the corresponding group parameter. Again dots refer to the omitted correlation functions.

Note that the equations (5.6) and (5.7) admit additional symmetries, which may not be employed for the present purpose to derive scaling laws: Galilean invariance, rotation invariance about x_1 and all three reflection groups for $\boldsymbol{\Omega} = 0$. If rotation about x_1 is considered the reflection groups in the x_2-x_3 plane are not admitted.

From a given set of symmetries we know from basic group theory that also any linear combination of them is a new symmetry. Hence we may combine all of the latter symmetries and rewrite the resulting symmetry in generator form

$$\mathrm{X} = a_1\mathrm{X}_{s_x} + a_2\mathrm{X}_{s_t} + a_3\mathrm{X}_{x_1} + a_4\mathrm{X}_{t}. \tag{5.16}$$

The latter combined generator may be rewritten to obtain the separated infinitesimals

$$\begin{aligned} \xi_{x_1} &= a_1x_1 + a_3, \\ \xi_{t} &= a_2t + a_4, \\ \xi_{r_k} &= a_1r_k, \\ \eta_{R_{ij}} &= 2(a_1 - a_2)R_{ij}, \\ \vdots \quad &\vdots \qquad\quad \vdots\ . \end{aligned} \tag{5.17}$$

Invoking the condition of an invariant solution we obtain (see e.g. Bluman & Kumei, 1989)

$$\frac{\mathrm{d}x_1}{a_1x_1+a_3}=\frac{\mathrm{d}t}{a_2t+a_4}=\frac{\mathrm{d}r_{[k]}}{a_1r_{[k]}}=\frac{\mathrm{d}R_{[ij]}}{2(a_1-a_2)R_{[ij]}}=\dots\ , \tag{5.18}$$

where indices in brackets indicate no summation. Depending on the scaling group parameter a_1 and a_2 we distinguish three different cases. Hence, in the subsequent three subsections BCs or rather global constrains coming from a_1 and a_2 for the different cases are discussed separately.

It is important to note that the invariant solutions (scaling laws) to be derived in the subsequent sections 5.3.1-5.3.3 are special solutions, having a limited range of applicability and usually also possess one or more singular points. In order to substantiate this we may consider the classical logarithmic law of the wall which has singular points, both at $y^+=0$ and $y^+=\infty$. Thus we cannot expect to find an analytic law in turbulence which is regular for the entire region of consideration. Experience shows that the range of applicability is always sufficiently far away from the singularities. The log-law is for example valid in the range $y^+\sim 100$ up to several thousand depending on the Reynolds number. The same may hold true here, however the range, where the new scaling laws are valid cannot be given, since no method is know to determine it.

5.3.1 Turbulent diffusion with spatially growing integral length-scale ($a_1\neq 0$, $a_2\neq 0$)

Integration of (5.18) leads to a set of invariants which are taken as the new independent and dependent variables

$$\begin{aligned}\tilde{x}_1&=\frac{x_1+x_o}{(t+t_o)^{1/(m+1)}}\,,\quad \tilde{\boldsymbol{r}}=\frac{\boldsymbol{r}}{x_1+x_o}\,,\\ R_{ij}(x_1,t,\boldsymbol{r})&=(x_1+x_o)^{-2m}\tilde{R}_{ij}(\tilde{x}_1,\tilde{\boldsymbol{r}})\,,\quad \dots\,,\end{aligned} \tag{5.19}$$

where $x_o=\frac{a_3}{a_1}$, $t_o=\frac{a_4}{a_2}$ and

$$m=\frac{a_2}{a_1}-1. \tag{5.20}$$

The value for m is not allocable with the help of BCs since an semi-infinite domain is considered into which turbulence can propagate and length-scales can evolve freely. This is for example in contrast to the case in the next section 5.3.2 where there is a limitation on the length-scale evolution due to periodic BCs.

The mathematical problem of determining m emerges due to the fact, that it is derived from the scaling group parameter a_1 and a_2 gathered from the symmetry analysis of the MPC equations. A major difference between the similarity solution of the MPC equations and for example Prandtl's boundary layer equations is that the MPC equations are PDEs while Prandtl's boundary layer equations are ODEs. This has important consequences one of which is that certain parameters such as the scaling exponent m may not be determined.

However, this is a well known fact for turbulent scaling laws. Classical examples are the decay of isotropic turbulence with $K \sim t^{-n}$ or the logarithmic law of the wall $\bar{u}^+ = \frac{1}{\kappa}\ln(y^+) + C$ which are both rigorously derived from the MPC equations (see Oberlack 2001, 2002a and 2002b). Nevertheless, scaling parameters such as the decay exponent n or the von Kármán constant κ are derived from the Lie group theory but numerical values cannot be given. A unifying theory for this open problem is still outstanding.

This is in clear contrast to the derivation of invariant solutions of closed systems such as the Prandtl's boundary layer equations. From this system Lie group theory leads for example to the Blasius or the Falkner-Skan solution for the flat or inclined plate where all flow parameters can be determined. Note that even in this case a full solution cannot be given and the reduced ordinary differential equations have to be solved numerically. Since in the present case a reduced but still infinite dimensional system is treated a numerically solution is not feasible.

Though a unifying theory for the numerical value of the scaling parameter in turbulent scaling laws are still outstanding the key achievement from Lie group theory is that the variables (5.19) lead to a similarity reduction of (5.6)/(5.7). From (5.2) and by invoking the one-point limit in (5.21) we obtain

$$\begin{gathered}\overline{u_i'u_j'}(x_1,t) = (x_1+x_o)^{-2m}\widetilde{\overline{u_i'u_j'}}(\tilde{x}_1) \text{ and} \\ \ell_t(x_1,t) = (x_1+x_o)\tilde{\ell}_t(\tilde{x}_1),\end{gathered} \tag{5.21}$$

where $\tilde{x}_1$ is taken from (5.19).

The corresponding dissipation function may immediately be taken from the small-scale equation (5.5) or even simpler directly from (5.21)

$$\epsilon(x_1,t) = (x_1+x_o)^{-3m-1}\tilde{\varepsilon}(\tilde{x}_1), \tag{5.22}$$

invoking the relation

$$\epsilon \sim \frac{K^{3/2}}{\ell_t}. \tag{5.23}$$

ℓ_t is linearly growing with x_1 independent of m. From experiments we usually have $m = 0.43\ldots0.75$ such that $\overline{u_i'u_j'}$ decreases algebraically with the distance from the turbulence source at $x_1 = 0$. $\tilde{x}_1$ is a typical diffusion type of similarity variable such as for the heat equation.

It is important to note that for the steady problem, that is $t \to \infty$ we can show that all MPCs such as R_{ij} become independent of $\tilde{x}_1$. Correspondingly the similarity variables for the one-point quantities such as $\widetilde{\overline{u_i'u_j'}}$, $\tilde{\ell}_t$ and $\tilde{\epsilon}$ in (5.21) and (5.22) become constants. This may also directly be derived from (5.18) by omitting the part for the invariant surface corresponding to t and $\boldsymbol{r}$.

A sketch of the unsteady and the steady self-similar turbulent diffusion according to (5.21) is given in figure 5.3.

A similarity solution of the form (5.21) and (5.22) has already been derived in Cazalbou & Chassaing (2001) by classical methods using an ansatz function. Cazalbou & Chassaing suggested a somewhat extended form of $\tilde{x}_1$ defined by

$$\eta = \frac{\delta(t) - z}{K^{3/2}(t)/E(t)}.$$

However, from their results one can easily show that $\delta(t) \sim K^{3/2}(t)/E(t)$ and hence $\tilde{x}_1$ is fully equivalent to η with just a constant offset.

Due to the special character of similarity solutions BCs usually cannot be employed for the construction of the solution. Nevertheless, BCs may be determined a posteriori once the similarity solution has been derived. Since this is not a process of constraining something we do not have BCs in the classical sense. Still in the following we call this a BC of the present flows having the modified meaning in mind.

In the present case, we need to employ that at the vibrating grid any velocity correlation is determined. As a result the TPC has to obey the condition

$$R_{ij}(x_1 = 0, t, \boldsymbol{r} = 0) = x_o^{-2m}\widetilde{\overline{u_i' u_j'}}\left(\frac{x_o}{(t + t_o)^{1/(m+1)}}\right), \tag{5.24}$$

taken from (5.19) and (5.21). From the latter we may also derive the BC for the steady problem which is derived from $t \to \infty$ leading to

$$R_{ij}(x_1 = 0, t \to \infty, \boldsymbol{r} = 0) = x_o^{-2m}\widetilde{\overline{u_i' u_j'}}_{(0)}, \tag{5.25}$$

which only requires regularity of $\widetilde{\overline{u_i' u_j'}}$ at $\tilde{x}_1 = 0$. Since no other energy source is implemented on the x_1-axis we have

$$R_{ij}(x_1 \to \infty, t, \boldsymbol{r}) = 0. \tag{5.26}$$

Finally we have the condition

$$R_{ij}(x_1, t, \boldsymbol{r} \to \infty) = 0, \tag{5.27}$$

which reflects the physical fact that velocity fluctuations decorrelate if measured at infinite separation.

Note, that no BCs need to be imposed for pressure velocity correlations since, continuity and Poisson equations may be derived for these quantities. Also in an incompressible flow pressure is a kinematic quantity, which admits the symmetry

$$t^* = t \ , \ \boldsymbol{x}^* = \boldsymbol{x} \ , \ \boldsymbol{u}^* = \boldsymbol{u} \ , \ p^* = p + f(t), \tag{5.28}$$

which means that the absolute value of p is irrelevant.

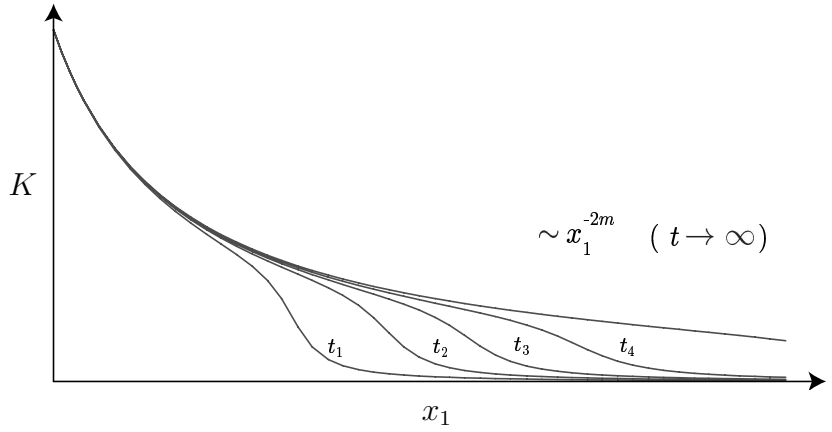

Figure 5.3: Sketch of the temporal evolution of the heat-equation-like turbulent diffusion process with linearly increasing integral length-scale according to (5.21).

5.3.2 Turbulent diffusion wave at a constant integral length-scale ($a_1 = 0$, $a_2 \neq 0$)

Since from the invariant surface condition (5.18) we can derive invariant solutions for arbitrary a_i's we may also impose certain symmetry breaking constrains. For the present case we impose $a_1 = 0$, which according to $x_1^* = \mathrm{e}^{a_1} x_1$ in (5.12), corresponds to the symmetry breaking of scaling of space or in other words $a_1 = 0$ amounts to a constant integral length-scale.

Under this constraint and similar to (5.19) we obtain from (5.18)

$$\tilde{x}_1 = x_1 - x_o \ln(t + t_o)\,, \quad \tilde{\boldsymbol{r}} = \boldsymbol{r}, \quad R_{ij}(x_1, t, \boldsymbol{r}) = \mathrm{e}^{-2\frac{x_1}{x_o}} \tilde{R}_{ij}(\tilde{x}_1, \tilde{\boldsymbol{r}}), \ \ldots\,, \tag{5.29}$$

where $x_o = \frac{a_3}{a_2}$ and $t_o = \frac{a_4}{a_2}$. From (5.29) together with (5.23) we derive the corresponding one-point quantities

$$\begin{gathered} \overline{u_i' u_j'}(x_1, t) = \mathrm{e}^{-2\frac{x_1}{x_o}} \widetilde{\overline{u_i' u_j'}}(\tilde{x}_1), \quad \ell_t(x_1, t) = \tilde{\ell}_t(\tilde{x}_1) \\ \text{and} \quad \epsilon(x_1, t) = \mathrm{e}^{-3\frac{x_1}{x_o}} \tilde{\epsilon}(\tilde{x}_1)\,, \end{gathered} \tag{5.30}$$

where the variable $\tilde{x}_1$ is taken from (5.29).

Similar to subsection 5.3.1 we may consider the corresponding steady case. The similarity variables of the MPCs for example in (5.29) become independent of $\tilde{x}_1$. Similarly, $\widetilde{\overline{u_i' u_j'}}$, $\tilde{\ell}_t$ and $\tilde{\epsilon}$ in (5.30) become constants. In particular the integral length-scale becomes a constant in space as $t \to \infty$.

Equation (5.29) or rather (5.30) imply two important results. Due to the symmetry breaking of scaling of space, a diffusion-wave type solution is induced with decreasing amplitude in x_1-direction and decreasing wave speed proportional to $1/t$ as may be taken from $\tilde{x}_1$ in (5.29). Second, the spatial decay behavior in x_1-direction has changed from an algebraic to an exponential function.

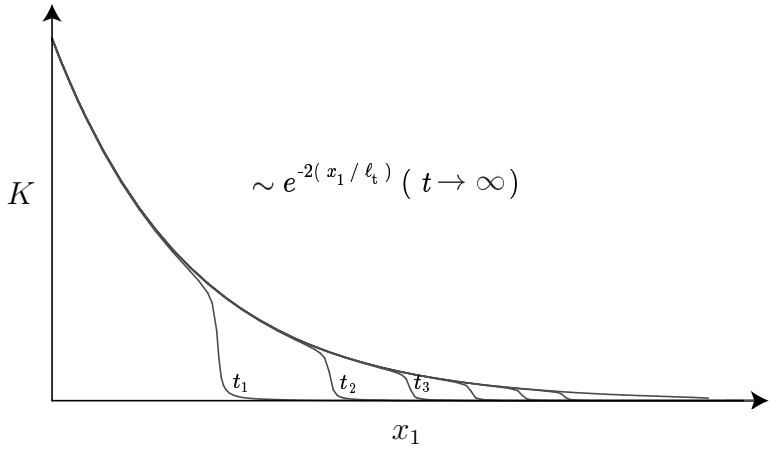

Figure 5.4: Sketch of the temporal evolution of the turbulent diffusion wave at constant integral length-scale according to (5.30).

Except for the last one, BCs are comparable to the one in the previous subsection. BC (5.24) changes to

$$R_{ij}(x_1 = 0, t, \boldsymbol{r} = 0) = \widetilde{\overline{u_i' u_j'}}\,(-x_o \ln(t + t_o)), \tag{5.31}$$

taken from (5.29) and (5.30). Apparently we have to ensure that the functional behavior of $\widetilde{\overline{u_i' u_j'}}$ is as such that a constant value is approached for $t \to \infty$. In other words we need to have

$$R_{ij}(x_1 = 0, t \to \infty, \boldsymbol{r} = 0) = \widetilde{\overline{u_i' u_j'}}_{(0)}, \tag{5.32}$$

where $\widetilde{\overline{u_i' u_j'}}_{(0)}$ is a constant. The third BC (5.26) is the same as for the present case.

The symmetry breaking of scaling of space or in other words the constant integral length-scale along the x_1 direction may be imposed by periodic BCs in the x_2-x_3 plane that is

$$R_{ij}(x_1, t, r_1, r_2, r_3) = R_{ij}(x_1, t, r_1, r_2 + c_2, r_3 + c_3). \tag{5.33}$$

In an experiment such a BC may not be achieved. Still, in a direct numerical simulation of the Navier-Stokes equations periodic BC may be imposed such that the integral length-scale cannot grow along x_1.

A sketch of the diffusion wave and the corresponding long time behavior is depicted in figure 5.4.

5.3.3 Turbulent diffusion in a constantly rotating frame ($a_1 \neq 0$, $a_2 = 0$)

In contrast to the previous case we may now consider the symmetry breaking of scaling of time in (5.13) due to $a_2 = 0$, imposed by an external time-scale given by the frame

rotation ($\tau = 1/|\mathbf{\Omega}|$). In the correlation equations (5.3), (5.5) or (5.6) frame rotation is modeled by invoking a non-zero $\mathbf{\Omega}$ or to be more specific in the present case $\Omega_1 \neq 0$.

If the rotation rate Ω_1 is considered as further independent variable in the MPC equations we receive the invariant solutions

$$\begin{aligned} x_1 = \acute{x}_1\gamma(\Omega_1), \quad \boldsymbol{r}_i = \acute{\boldsymbol{r}}_i\gamma(\Omega_1), \\ R_{ij}(x_1, \boldsymbol{r}) = \acute{R}_{ij}(\acute{x_1}, \acute{\boldsymbol{r}})\gamma(\Omega_1)^2\Omega_1^2, \end{aligned} \tag{5.34}$$

and corresponding the TP quantities

$$\begin{gathered} \overline{u_i'u_j'}(x_1) = \overline{\acute{u_i'u_j'}}(\acute{x}_1)\gamma(\Omega_1)^2\Omega_1^2, \quad \ell_t(x_1) = \left(\frac{1}{2}\right)^{3/2} \acute{\ell}_t(\acute{x_1})\gamma(\Omega_1) \\ \text{and} \quad \epsilon(x_1) = \acute{\epsilon}(\acute{x}_1)\gamma(\Omega_1)^2\Omega_1^3, \end{gathered} \tag{5.35}$$

where $\gamma(\Omega_1)$ describes an unknown free function which naturally appears due to the group analysis. Implementing these new dependent and independent variables in the primary equations, we receive a reduced set of equations. Performing a further Lie group analysis of these reduced equations we receive the final form of the invariant solutions:

$$\begin{aligned} \tilde{x}_1 = \left(\frac{x_1}{\gamma(\Omega_1)} + x_o\right) e^{-\frac{t\Omega_1}{t_o}}, \quad \tilde{r} = \frac{r}{x_1 + \gamma(\Omega_1)x_o} \\ R_{ij}(x_1, \boldsymbol{r}) = \Omega_1^2 \left(x_1 + \gamma(\Omega_1)x_0\right)^2 \tilde{R}_{ij}(\tilde{x}_1, \tilde{\boldsymbol{r}}), \end{aligned} \tag{5.36}$$

where $x_o = \frac{a_3}{a_1}$ and $t_o = \frac{a_4}{a_1}$.

The one-point quantities are similar to (5.21) and (5.22) with $a_2 = 0$ or rather $m = -1$ in (5.20) and may be written as

$$\begin{gathered} \overline{u_i'u_j'}(x_1) = \Omega_1^2 \left(x_1 + \gamma(\Omega_1)x_0\right)^2 \widetilde{\overline{u_i'u_j'}}(\tilde{x}_1), \quad \ell_t(x_1) = \left(\frac{1}{2}\right)^{3/2} \left(x_1 + \gamma(\Omega_1)x_0\right) \tilde{\ell}(\tilde{x}_1), \\ \text{and} \quad \epsilon(x_1) = \Omega_1^3 \left(x_1 + \gamma(\Omega_1)x_0\right)^2 \widetilde{\epsilon}(\tilde{x}_1), \end{gathered} \tag{5.37}$$

where $\tilde{x}_1$ is defined in (5.36). Similar to the above case, the steady case corresponds to the fact that the similarity variables in (5.36) and (5.37) become independent of $\tilde{x}_1$.

This is because for the steady case the second time-dependent term of the characteristic equation (5.18) is absent and therefore no similarity variable such as $\tilde{x}_1$ can be identified. As a result we find that all "˜"-quantities are simply constants of integration.

One may expect that for $t \to \infty$ the unsteady solution converges to the steady solution. From (5.36) we determine that in this limit we obtain $\tilde{x}_1 = 0$. Hence, we may conclude that all of the "˜"-quantities become constant at $\tilde{x}_1 = 0$ since there is no reason to believe that they admit singular points such as a pole.

The reasoning is based on a rather "physical" assumption related to the principle problem that we are dealing with an infinite dimensional set of correlation equations, which cannot be solved explicitly. Hence we cannot give explicit solutions for the functions $\tilde{R}_{ij}$, $\tilde{R}_{ijk}$ and

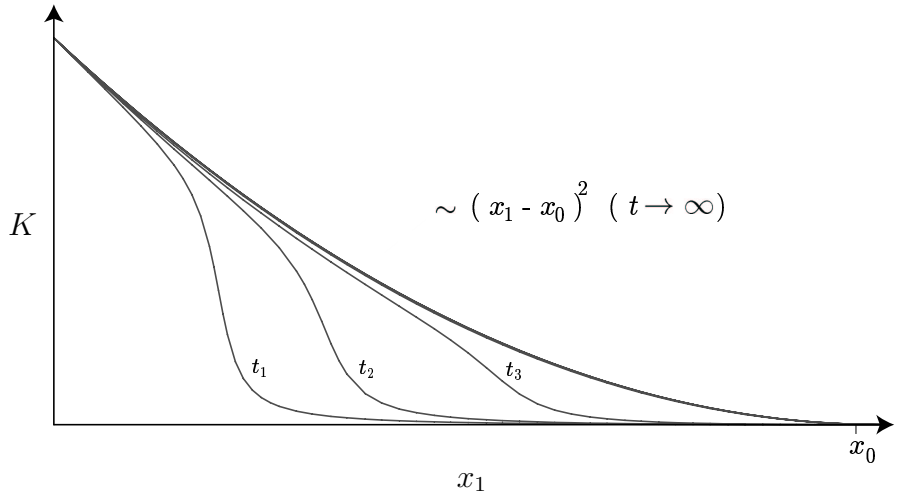

Figure 5.5: Sketch of the temporal evolution of the turbulent diffusion on a finite domain at a constant integral time-scale due to rotation according to (5.37).

so on. As a consequence we have to *assume* regularity for all "˜" quantities, in particular at critical points such as $\tilde{x}_1 = 0$.

Discussing the spatial dependence of the scaling law (5.37), $\tilde{x}_1 = 0$ also corresponds to the point $x_1 = -x_o$. At this point any turbulence quantity approaches zero. Due to physical reasons an increasing for example of the turbulent kinetic energy K has to be excluded if there is no additional energy source at $x_1 \geq -x_o$. $x_1 = -x_o$ appears to be a singular point since for example the second derivative of $\overline{u_i' u_j'}(x_1)$ may be discontinuous as may be taken from figure 5.5. We have to recall that turbulent scaling laws usually possess singularities as has been pointed out above. Close to singularities other effects may become dominant. For the present case the local Reynolds number becomes small close to $x_1 = -x_o$. Hence there is a possibility that viscous effects may become large however a decisive answer is beyond the present analysis.

The surprising result for the present case is that even for $t \to \infty$ the turbulent diffusion only influences a finite domain due to the quadratic behavior of the large-scale turbulence quantities. BCs for the present case are rather similar to one for the case in subsection 5.3.1. Only condition (5.24) changes to

$$R_{ij}(x_1 = 0, t, \boldsymbol{r} = 0) = x_o^2 \widetilde{\overline{u_i' u_j'}} \left(x_o \mathrm{e}^{-\frac{t}{t_o}} \right), \tag{5.38}$$

while the corresponding steady case is identical to (5.25).

From the results of the present subsection parallels can be drawn to Long's theory on grid-turbulence in a stably stratified fluid (see Long, 1978 and Fernando & Long, 1983). Due to the stratification the development of the turbulence perpendicular to the stratification is suppressed, which apparently can also be achieved through system rotation. Long describes in his work the temporal development of the mixed layer. In case of frame

rotation the depth of the turbulent layer becomes a constant for $t \to \infty$. From a symmetry point of view stratification imposes an external scale on the turbulent flow, which is symmetry breaking similar to the time-scale $\tau = 1/|\mathbf{\Omega}|$.

The present case is from two points of view quite curious. It is in general quite hard to imagine, that the turbulent diffusion only influences a finite domain and that any turbulence quantity approaches zero at a given point.
Furthermore corresponds the given case to the first case, whereby a coordinate transformation has been conducted. Actually a transformation from a fixed to a rotating coordinate system should not change the symmetry properties of an equation. So the symmetries and invariant solutions for the given case and the first case should be the same. Thus the third case should be examined in more detail in future projects.

5.4 Model implications and analytic model solutions for the turbulent diffusion without rotation

Classical two-equation models and Reynolds stress transport models are investigated on their capability to capture one or several of the above three invariant solutions. The particular model equations we will investigate here are the classical K-ϵ (Jones & Launder, 1972) and the Launder-Reece-Rodi (LRR) second-moment-closure model (Launder *et al.*, 1975). For further details on the model equations see chapter 3. In addition, in section 5.4.2 it will be shown that for the steady case a full analytic solution is given for the K-ϵ model. The invariant solutions in the subsequent section are special cases of this complete analytic solution.

5.4.1 Model implications derived from invariant solutions

Umlauf (2001) may have been the first who empirically recognized by numerically solving the steady diffusion problem employing the K-ϵ model that for certain model parameters a very distinguished change in model behavior appears. Without giving the invariant solution Umlauf derived the condition for the model parameter where the change in behavior occurred. Substantiating this result from certain model constants of the K-ϵ model but independent of Umlauf, Cazalbou & Chassaing (2001) were the first suggesting the exponential solution. We may suspect and this is what we see below, that this change corresponds to a singular point in all model equations, separating between an algebraic and an exponential decay with the singular point at $m = -1$ or rather $a_1 = 0$. For each model this point corresponds to a certain set of model constants.

In order to test the compatibility of the invariant solutions derived in the last section with turbulence models we simply implement the solutions into the model equations, here the K-ϵ and the LRR model.

It is important to note that we only need to employ the steady solutions into the model

equation, the rational behind this being the following. Formally, the invariant solutions derived above for the unsteady problem lead to a reduction of the K-ϵ or the LRR model equations. These reduced set of equations has to be compatible with physically appropriate BCs given above. In particular the condition of boundedness for $x_1 \to \infty$ has to hold true for all time and hence also for $t \to \infty$, which corresponds to the steady solution. Hence implementing the steady solution into the model equations imposes a minimum requirement on the boundedness. In fact, one can show by asymptotic arguments that the condition of boundedness for the reduced equations of the unsteady case is the same as for the steady case.

In order to prove the latter we employ as an example the K-ϵ model where the algebraic decay (5.21) and (5.22) has been implemented into (3.17) and (3.18). As a result we respectively obtain

$$
\begin{aligned}
-\frac{1}{m+1}\tilde{x}_1^{m+2}\frac{\mathrm{d}\tilde{K}}{\mathrm{d}\tilde{x}_1} = \\
-\tilde{\epsilon} + \frac{c_\mu}{\sigma_K}\left[\frac{\tilde{x}_1}{\tilde{\epsilon}^2}\left(\frac{\mathrm{d}\tilde{K}^2}{\mathrm{d}\tilde{x}_1}\tilde{\epsilon} - \tilde{K}^2\frac{\mathrm{d}\tilde{\epsilon}}{\mathrm{d}\tilde{x}_1}\right)\left(-2m\tilde{K} + \frac{\mathrm{d}\tilde{K}}{\mathrm{d}\tilde{x}_1}\tilde{x}_1\right)\right. \\
\left. +\frac{\tilde{K}^2}{\tilde{\epsilon}}\left(6m^2\tilde{K} + (-5m+1)\tilde{x}_1\frac{\mathrm{d}\tilde{K}}{\mathrm{d}\tilde{x}_1} + \frac{\mathrm{d}^2\tilde{K}}{\mathrm{d}\tilde{x}_1^2}\tilde{x}_1^2\right)\right] \quad (5.39)
\end{aligned}
$$

and

$$
\begin{aligned}
-\frac{1}{m+1}\tilde{x}_1^{m+2}\frac{\mathrm{d}\tilde{\epsilon}}{\mathrm{d}\tilde{x}_1} = \\
-c_{\varepsilon 2}\frac{\tilde{\epsilon}^2}{\tilde{K}} + \frac{c_\mu}{\sigma_\varepsilon}\left[\frac{\tilde{x}_1}{\tilde{\epsilon}^2}\left(\frac{\mathrm{d}\tilde{K}^2}{\mathrm{d}\tilde{x}_1}\tilde{\epsilon} - \tilde{K}^2\frac{\mathrm{d}\tilde{\epsilon}}{\mathrm{d}\tilde{x}_1}\right)\left((-3m-1)\tilde{\epsilon} + \tilde{x}_1\frac{\mathrm{d}\tilde{\epsilon}}{\mathrm{d}\tilde{x}_1}\right)\right. \\
\left. +\frac{\tilde{K}^2}{\tilde{\epsilon}}\left((3m+1)(4m+1)\tilde{\epsilon} - (7m+1)\tilde{x}_1\frac{\mathrm{d}\tilde{\epsilon}}{\mathrm{d}\tilde{x}_1} + \tilde{x}_1^2\frac{\mathrm{d}^2\tilde{\epsilon}}{\mathrm{d}\tilde{x}_1^2}\right)\right]. \quad (5.40)
\end{aligned}
$$

The latter two equations require two boundary conditions for both limits $\tilde{x}_1 \to 0$ and $\tilde{x}_1 \to \infty$. The former stems from the BCs (5.24) which together with the definition for $\tilde{x}_1$ in (5.19) and $t \to \infty$ immediately leads to $\tilde{x}_1 \to 0$. From (5.21) and (5.22) we obtain that as $\tilde{x}_1$ approaches zero both $\tilde{K}(0)$ and $\tilde{\epsilon}(0)$ have to be constants since any singularity has be excluded due to physical reasons. Expanding $\tilde{K}$ and $\tilde{\epsilon}$ about $\tilde{x}_1 = 0$ and implementing this into (5.39) and (5.40) we obtain

$$
0 = -\tilde{\epsilon} + \frac{c_\mu}{\sigma_K}6m^2\frac{\tilde{K}^3}{\tilde{\epsilon}} \quad (5.41)
$$

and

$$
0 = -c_{\varepsilon 2}\frac{\tilde{\epsilon}^2}{\tilde{K}} + \frac{c_\mu}{\sigma_\varepsilon}(12m^2 + 7m + 1)\tilde{K}^2 \quad (5.42)
$$

where the argument (0) from $\tilde{K}$ and $\tilde{\epsilon}$ has been omitted. The latter two equations are identical to the equations obtained from the steady problem that is if all ˜-quantities in (5.21) and (5.22) are assumed to be constants when implemented into the K-ϵ model.

Solving the latter two equations, whereby $\tilde{K}^3/\tilde{\epsilon}^2$ and m are the unknowns, we derive a quadratic equation for m, depending on the model parameter only and independent of $\tilde{K}$ and $\tilde{\epsilon}$ to be discussed below. Employing any of the two solutions for m into the latter equations (5.41) and (5.42) we obtain two identical equations of the form $\tilde{K}^3 \sim \tilde{\epsilon}^2$. The latter equation possesses two physical solutions. If $\tilde{K}$ is given $\tilde{\epsilon}$ is determined and vice versa. This corresponds to the BC at $\tilde{x}_1 = 0$. Note that this also means that the BCs for $\tilde{K}$ and $\tilde{\epsilon}$ may not be chosen independently.

The second solution is given from the fact that both $\tilde{K}$ and $\tilde{\epsilon}$ may become zero. This solution corresponds to the BC $\tilde{x}_1 \to \infty$ the reason being the following. Though any other value for $\tilde{K}$ and $\tilde{\epsilon}$, compatible with (5.41) and (5.42) may be chosen there is no physical reason that $\tilde{K}$ and $\tilde{\epsilon}$ are non-zero for $\tilde{x}_1 \to \infty$, since the only energy source exists close to $x_1 = 0$. Hence $\tilde{K} = 0$ and $\tilde{\epsilon} = 0$ are the appropriate BCs at $\tilde{x}_1 \to \infty$.

The latter analysis may be extended to any one-point model and invariant solution given above. Hence from the reasons given earlier we only need to consider the steady case for the model investigations below.

From the equations (5.41) and (5.42) we find that for the generic case of no symmetry breaking the value of m in subsection 5.3.1, which determines the spatial decay and the temporal behavior in (5.21) and (5.22), is determined by a quadratic equation

$$\begin{aligned} & 6(2\sigma_K - c_{\varepsilon_2}\sigma_\varepsilon)m^2 + 7\sigma_K m + \sigma_K = 0 \\ \Rightarrow \quad & m_{1,2} = \frac{7\sigma_K \pm \sqrt{\sigma_K(\sigma_K + 24c_{\varepsilon_2}\sigma_\varepsilon)}}{12(c_{\varepsilon_2}\sigma_\varepsilon - 2\sigma_K)}. \end{aligned} \tag{5.43}$$

Similarly a quartic equation

$$\begin{aligned} & (456c_\varepsilon c_1 c_s c_{\varepsilon_2} - 144c_1^2c_\varepsilon^2 + 144c_1c_\varepsilon^2 - 336c_\varepsilon c_s c_{\varepsilon_2} - 216c_s^2c_{\varepsilon_2}^2)m^4 \\ & +(168c_1c_\varepsilon^2 - 168c_1^2c_\varepsilon^2 - 196c_\varepsilon c_s c_{\varepsilon_2} + 266c_\varepsilon c_1 c_s c_{\varepsilon_2})m^3 \\ & +(73c_1c_\varepsilon^2 - 28c_\varepsilon c_s c_{\varepsilon_2} - 73c_1^2c_\varepsilon^2 + 38c_\varepsilon c_1 c_s c_{\varepsilon_2})m^2 \\ & +(14c_1c_\varepsilon^2 - 14c_1^2c_\varepsilon^2)m - c_1^2c_\varepsilon^2 + c_1c_\varepsilon^2 = 0 \end{aligned} \tag{5.44}$$

is derived by implementing the invariant solution (5.21) and (5.22) into the LRR model. From (5.43) and (5.44) and the standard model constants (see chapter 3) we respectively obtain the solutions for m: $m_1 = -0.14$, $m_2 = 2.49$ and $m_1 = -0.76$, $m_2 = -0.18$, $m_3 = -0.13$, $m_4 = 2.17$.

Since any of the values for m represent a solution of the corresponding model equations multiple algebraic solutions are admitted. This property of Reynolds averaged models is known to be important under certain conditions. In Durbin & Pettersson Reif (2001) it is shown that multiple solutions and the corresponding bifurcation of homogeneous shear-flows are an important property which in fact models important turbulence physics. Nevertheless, only m_2 and m_4 respectively represent physically reasonable solutions of the K-ϵ and the LRR model, because all other values for m would lead to a positive exponent in the similarity solutions (5.19) and (5.21). A positive exponent would describe an increase of turbulent kinetic energy which is physically impossible.

Unfortunately the exponents m_2 and m_4 are not in agreement with the values which could be determined from different experiments. Nokes (1988) obtained for example values for m between 0.43 and 0.75, depending on the amplitude of the oscillating grid and the distance from the grid at which measurements have been taken. 0.75 corresponds also to the value, which Thompson & Turner (1975) determined from their experiments. Hannoun *et al.* (1988) obtained a value of $m = 0.5$ from their experiments, while the experiments from Hopfinger & Toly (1976) led to $m = 1$.

The second invariant solution (5.30) in subsection 5.3.2 where the symmetry breaking of scaling of space is imposed, that is when a constant integral length-scale is considered, is only admitted if the model constants are modified. For example implementing (5.30) into the K-ϵ model, model constants need to obey the equation

$$\frac{c_{\varepsilon_2}\sigma_\varepsilon}{\sigma_K} = 2. \tag{5.45}$$

This singular point is already visible in equation (5.43), since the denominator in the second equation should not become zero for the exponent m of the algebraic solution. Still, employing (5.45) into the first equation of (5.43) a linear equation for m is obtained with the solution $m = -\frac{1}{7}$ independent of any model constant. Hence, the singular point (5.45) corresponds to multiple solutions one of which exhibits an exponential decay and another with an algebraic behavior.

The corresponding polynomial equations derived from implementing the exponential solution (5.30) into the LRR model is given by

$$\begin{aligned}(3c_1^2c_\varepsilon^2 - 12c_1c_\varepsilon^2 - 8c_1c_\varepsilon c_s c_{\varepsilon_2} + 112c_s c_\varepsilon c_{\varepsilon_2} - 144c_s^2c_{\varepsilon_2}^2)*\\ (9c_1^2c_\varepsilon^2 - 12c_1c_\varepsilon^2 - 104c_1c_\varepsilon c_s c_{\varepsilon_2} + 112c_s c_\varepsilon c_{\varepsilon_2} + 144c_s^2c_{\varepsilon_2}^2) = 0.\end{aligned} \tag{5.46}$$

Again we see at least for the LRR model that due to the two large factored terms, different model parameters lead to multiple, here exponential, solutions.

It is important to note that for a given set of model constants only one solution type is admissible, either the algebraic solution (5.21)/(5.22) or the exponential solution (5.30). Note that the classical model constants do not solve the above equations (5.45) and (5.46). Hence, a one-dimensional solution in form of an exponential spatial decay is not admitted.

This limitation is inherent to all one-point turbulence models since no structure knowledge such as a length-scales may be chosen independently of the scaling information delivered by K and ϵ. Apparently this limitation is abolish for two-point models since periodic boundary condition such as given by (5.33) may be invoked.

Interesting enough, if higher dimensional problems are considered, such as the 2D problem of turbulent diffusion constrained between two parallel walls we find that also the one-point models allow for solutions of the type (5.30). We may conclude that the reduced dimensionality of one-point models limits the ability to model certain solutions if only one-dimensional versions of the model equations are considered. Higher-dimensional versions or two-point models considerable extend the solution space.

The steady version of the solutions (5.21)/(5.22) and (5.30) implemented into the model equations do not necessarily allow for independent BCs for the Reynolds stresses and

the dissipation as mentioned above. For example implementing the steady form of the algebraic solution (5.21) and (5.22) into the K-ϵ model leads to the relation

$$\left(\frac{\tilde{K}^3}{\tilde{\epsilon}^2}\right)_{\text{alg}} = \frac{24\sigma_K(c_{\varepsilon_2}\sigma_\varepsilon - 2\sigma_K)^2}{c_\mu\left(7\sigma_K \pm \sqrt{\sigma_K(\sigma_K + 24c_{\varepsilon_2}\sigma_\varepsilon)}\right)^2}, \tag{5.47}$$

where, only the positive sign has a physical meaning if the standard model constants are used. Hence, once $\tilde{K}$ is picked $\tilde{\epsilon}$ is determined. In contrast the steady version of the exponential decay (5.30) invoked into the K-ϵ model yields after employing the restriction (5.45)

$$\left(\frac{\tilde{K}^3}{\tilde{\epsilon}^2}\right)_{\text{exp}} = \frac{x_0^2\sigma_K}{6c_\mu}, \tag{5.48}$$

which, apparently, allows to freely chose $\tilde{K}$ and $\tilde{\epsilon}$ due to the unconfined length-scale x_0, which is proportional to ℓ_t.

Note that the dimensions of $\tilde{K}$ and $\tilde{\epsilon}$ are different for the two cases above. According to (5.21)/(5.22) $\tilde{K}$ and $\tilde{\epsilon}$ have fractional dimensions in (5.47), while from (5.30) we find that in (5.48) $\tilde{K}$ and $\tilde{\epsilon}$ have the same dimensions as the original variables K and ϵ.

Interesting enough the singular point (5.45) is also visible in the boundary relation (5.47). At this point the nominator becomes zero. In addition also the denominator vanishes, if the minus sign is chosen.

5.4.2 Lele's transformation for the K-ϵ model of a steady turbulent diffusion flow

We have to realize that the invariant solution obtained in section 5.4 are special solutions of the model equations. Still, for certain models a full analytic solution may be attained to be shown in the present section.

Though the transformation introduced by Lele (1985) did not lead to a simplification for the unsteady diffusion problem it may still be very useful for the steady flow. In this case the full K-ϵ model detailed in the equations (3.19)-(3.19) in section 3 simplify to

$$0 = -\epsilon + \frac{\mathrm{d}}{\mathrm{d}x_1}\left[\frac{c_\mu}{\sigma_K}\frac{K^2}{\epsilon}\frac{\mathrm{d}K}{\mathrm{d}x_1}\right] \tag{5.49}$$

and

$$0 = -c_{\epsilon_2}\frac{\epsilon^2}{K} + \frac{\mathrm{d}}{\mathrm{d}x_1}\left[\frac{c_\mu}{\sigma_\varepsilon}\frac{K^2}{\epsilon}\frac{\mathrm{d}\epsilon}{\mathrm{d}x_1}\right]. \tag{5.50}$$

Introducing the non-local transformation Lele (1985) based on the integral length-scale ℓ_t

$$\mathrm{d}z = \sqrt{\frac{3}{2}\frac{\sigma_K}{c_\mu}}\frac{\mathrm{d}x_1}{\ell_t} \quad \text{with} \quad \ell_t \equiv \frac{K^{3/2}}{\epsilon} \tag{5.51}$$

as well as a new variable for the turbulent kinetic energy

$$H = K^{3/2} \tag{5.52}$$

into (5.49) and (5.50) we respectively obtain the set of equations

$$\frac{\mathrm{d}^2 H}{\mathrm{d}z^2} - H = 0 \tag{5.53}$$

and

$$\frac{\mathrm{d}^2 \epsilon}{\mathrm{d}z^2} + \frac{1}{3}\frac{1}{H}\frac{\mathrm{d}H}{\mathrm{d}z}\frac{\mathrm{d}\epsilon}{\mathrm{d}z} - \frac{2}{3}C^*\epsilon = 0, \quad \text{with} \quad C^* = \frac{c_{\varepsilon_2}\sigma_\varepsilon}{\sigma_K}, \tag{5.54}$$

which in fact decouple from each other. Hence, once separated, they may be treated as two linear equations. Note that C^* comprises the singular point, identified in the previous sections. The singular value 2 may be taken from (5.45).

The equations (5.53) and (5.54) may immediately be solved to yield together with (5.52)

$$H(z) = C_1\mathrm{e}^z + C_2\mathrm{e}^{-z} \quad \text{or} \quad K(z) = \left[C_1\mathrm{e}^z + C_2\mathrm{e}^{-z}\right]^{2/3} \tag{5.55}$$

and

$$\epsilon(z) = \frac{C_3 P^{-\frac{1}{6}\sqrt{1+24C^*}}_{-\frac{1}{6}}\left(-\frac{1}{H}\frac{\mathrm{d}H}{\mathrm{d}z}\right) + C_4 P^{\frac{1}{6}\sqrt{1+24C^*}}_{-\frac{1}{6}}\left(-\frac{1}{H}\frac{\mathrm{d}H}{\mathrm{d}z}\right)}{[H(z)]^{1/6}}, \tag{5.56}$$

where $P^\mu_\nu(x)$ is the associated Legendre function of the first kind (see e.g. Abramowitz & Stegun, 1968).

In order to write the solution in terms of the spatial variable x_1 we may rewrite (5.51) in integrated form

$$x_1 = \sqrt{\frac{2}{3}\frac{c_\mu}{\sigma_K}}\int_z \frac{H(z)}{\epsilon(z)}\mathrm{d}z, \tag{5.57}$$

which could not be evaluated explicitly. Since H and ϵ are positive functions of z, x_1 increases monotonically in z. As a result, the functional x_1 dependence of H and ϵ is unique. To conclude, the full analytic solution to the equations (5.49) and (5.50) is given in parametric form defined by (5.55), (5.56) and (5.57), where BCs have to be specified by determining the C_i's. Since four C_i's are to be determined we may independently specify K and ϵ at two different locations. Unfortunately, the free constants $C_1 - C_4$ may not explicitly be derived from the BCs for K and ϵ due to the non-local dependence (5.57). An iterative method has to be invoked in order to solve for BCs e.g. at $x_1 = 0$ and $x_1 = a$.

It is interesting to note that the analytic solution above may not be obtained from classical Lie symmetries since the transformation (5.51) is not a point transformation, as may be taken from (5.57). Applying classical Lie symmetry method to (5.49) and (5.50) we solely obtain the three groups

$$\bar{T}^{K-\epsilon}_{s_x}: \quad x_1^* = \mathrm{e}^{a_1}x_1 \ , \quad K^* = \mathrm{e}^{2a_1}K \ , \quad \epsilon^* = \mathrm{e}^{2a_1}\epsilon \ , \tag{5.58}$$

$$\bar{T}^{K-\epsilon}_{s_t}: \quad x_1^* = x_1 \ , \quad K^* = \mathrm{e}^{-2a_2}K \ , \ \epsilon^* = \mathrm{e}^{-3a_2}\epsilon \ , \tag{5.59}$$

$$\bar{T}^{K-\epsilon}_{x_1}: \quad x_1^* = x_1 + a_3 \ , \ K^* = K \ , \quad \epsilon^* = \epsilon \ . \tag{5.60}$$

Since three Lie symmetries are not sufficient to completely integrate (5.49) and (5.50) other methods need to be applied. As a result, the underlying symmetries may not be uncovered by this technique and other methods such as non-classical symmetries, potential or generalized symmetries (see e.g. Bluman & Kumei, 1989) need to be invoked to uncover the underlying "hidden" symmetries.

It should be noted that a multi-dimensional form of the transformation (5.51) also leads to a multi-dimensional linear set of equations, a simple extension of (5.53) and (5.54).

5.5 Investigations and model implications for the turbulent diffusion with rotation

The third invariant solution (5.37) of diffusion in a rotating frame in subsection 5.3.3, here rotating about x_1, cannot be reproduced by one-point models. Classical two-equation models are insensitive to rotation anyway. However, even most fully non-linear two-equation models and non-linear Reynolds stress transport models (non-linear in the Reynolds stresses for the pressure strain model) are insensitive to rotation about x_1 for the present type of flow, elucidating a serious shortcoming of these models. Anyway, there are still a few turbulence models which seem to be capable to give a dependence of the Reynolds stresses, respectively the kinetic energy on the rotation rate. Thereby the vanishing dissipation rate for rapid rotations is mostly built into the modeled dissipation rate equation, whereby the condition of the vanishing viscosity is violated. A model satisfying the second condition has been derived by Rubinstein & Zhou (1997). In the following we will concentrate on the models satisfying the condition on the dissipation rate. The two models which are tested numerically in section (5.5.2) are the model from Shimomura (1993) as an example for a two-equation model, and the model from Sjögren & Johansson (2000) as an example for a second-moment-closure model.

5.5.1 Large eddy simulations of turbulent diffusion with rotation

To obtain a better understanding of the given flow case, large-eddy simulations (LES) in a rotating frame at a constant angular velocity Ω_1 about the x_1 axis have been performed. For the LES a standard pseudo-spectral method is used with periodic BCs in all three directions. In order to simulate shear-free turbulence, the flow field with zero mean velocity is forced in a limited part at the center of the domain. Outside this region the flow field is not forced. A method introduced by Alevlius (1999) is used to generate a random but statistically stationary forcing. The forcing is implemented in spectral space where it is concentrated at small wavenumbers. Hence the power input is introduced into the flow at large-scales. The randomness in time makes the forcing uncorrelated with the velocity field and the effect from the forcing on the velocity field is a priori determined by the forcing. The fact that the time-scale of the forcing is separated from all time-scales of the turbulent flow makes it neutral in the sense that it does not particularly enhance a certain time-scale in an unknown way. This random forcing in a limited part of the

computational domain provides conditions, which are similar to a vibrating grid in an experiment. Turbulent fluctuations develop in the forcing region, which then diffuse in x_1 direction. The subgrid scales of the velocity field are modeled by means of a simple eddy viscosity model due to Smagorinsky (1963) with the Smagorinsky constant $C_s = 0.115$ and a low Reynolds number correction. We observed that the subgrid scales have only a significant contribution inside and close to the part of the domain where the forcing is applied. Further apart from the forcing region the subgrid contribution is small because of the lower turbulence intensity. The simulations have been running using a $1024 \times 48 \times 48$ grid in a $40\pi \times 2\pi \times 2\pi$ box at various rotation rates.
Figure 5.6 shows the spatial decay of the turbulent kinetic energy depending on the rotation rate if anisotropic forcing is considered. From (5.6) it is easily see, that the spatial

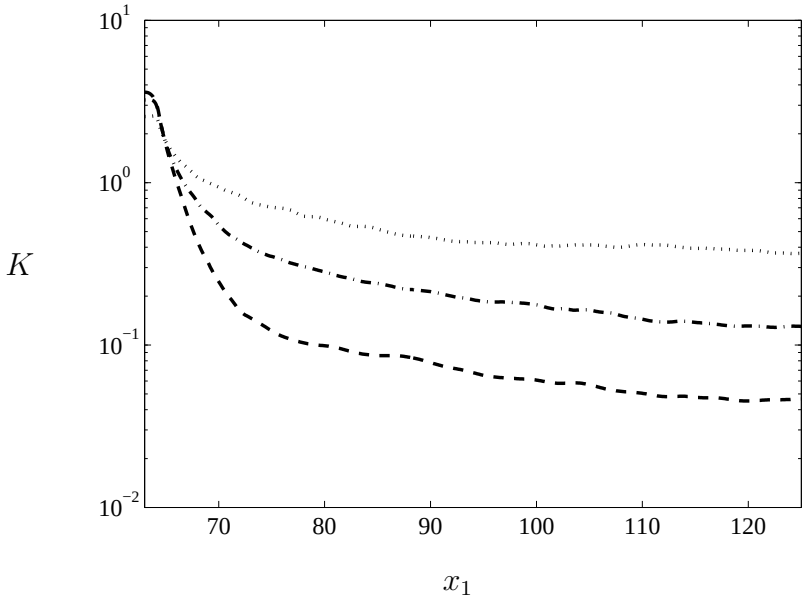

Figure 5.6: Decay of turbulent kinetic energy obtained by large eddy simulation for various rotation rates: $- - - \Omega_1 = 0.5$, $- \cdot - \Omega_1 = 1$, $\cdots \Omega_1 = 2$.

decay of the turbulent kinetic energy is faster for small rotation rates than for larger ones. Hence the rotation decreases the decay of the turbulent kinetic energy. The larger the rotation is the more intense is this effect. The same results have already been obtained for the temporal decay of isotropic turbulence in various former numerical simulations and experiments (for a list of relevant numerical simulations and experiments (see Jacquin *et al.*, 1990). The slower decay of kinetic energy is due to the fact that the rotation inhibits the transfer of energy from large to small scales and therefore results in a decrease of the dissipation rate. In Mansour *et al.* (1991*a*) it is shown that the transfer of energy is essentially shut off at Rossby numbers of $Ro = \epsilon/\Omega K < 0.01$.

The integral length-scale is increasing as predicted by the theory (5.37). The LES does not predict the finite domain diffusion, which is given by the theory. Thus the assumption that this solution is physically not correct is supported by the LES results.

5.5.2 Modeling of the rotating turbulent diffusion with two-equation models

Existing extensions of the ϵ-equation

Since the rotation reduces the dissipation rate (see chapter 5.5.1) it is near to hand to introduce a modification in the ϵ-equation to account for the rotation. Although there is no term in the exact dissipation rate equation that accounts for system rotation directly, ϵ is indirectly influenced through changes in anisotropies of the dissipation correlation ϵ_{ij}. All of the commonly used dissipation rate equations predict that for a given mean flow a system rotation has no effect on the evolution of the dissipation rate, what is in contradiction to numerical and experimental data. For this reason there exist a couple of two-equation models in which the ϵ-equation is augmented by a term which is quadratic in the mean rotation rate tensor

$$W_{ij} = \frac{1}{2}\left(\frac{\partial \bar{u}_i}{\partial x_j} - \frac{\partial \bar{u}_j}{\partial x_i}\right) + e_{jim}\Omega_m.$$

Bardina *et al.* (1985) for example proposed to model the influence of rotation by a modification of the $C_{\varepsilon 2}$ parameter

$$C_{\varepsilon 2}^{(mod)} = C_{\varepsilon 2} + C_{\varepsilon\Omega}\Omega^* \,, \tag{5.61}$$

where

$$\Omega^* = \Omega\frac{2K}{\epsilon} \tag{5.62}$$

might be interpreted as an inverse Rossby number and $\Omega = |\mathbf{\Omega}|$. From comparisons with the experimental data of Wiegeland & Nagib (1978) they found a value of $C_{\epsilon\Omega} = 0.075$ to give the best fit. The effect of the extra term is to lower the decay rate of the turbulent kinetic energy for higher rotation rates. In Cambon *et al.* (1992) and Hallbäck & Johansson (1993) it is stated that an anomalous feature of the model (5.61) is that for large times ($\Omega t \gg 1$) a constant value of the kinetic energy, determined by the rotation rate Ω is approached which causes a significant overprediction of K in cases with high rotation rates.
For this purpose Hallbäck & Johansson (1993) proposed a model which behaves well also at high rotation rates. In their model $C_{\varepsilon 2}$ is described by Ω^* and the turbulence Reynolds number $Re_T = \frac{4K^2}{\nu\epsilon}$, giving

$$C_{\varepsilon 2}^{HM} = C_{\varepsilon 2} + \frac{C_1^{HM}\Omega^*\sqrt{Re_T}}{C_2^{MH} + \Omega^*} \,, \tag{5.63}$$

with $C_1^{HM} = 0.15$ and $C_2^{HM} = 25$. Hallbäck & Johansson pointed out that their model agrees fairly well with the direct numerical simulation data from Speziale *et al.* (1987). For very large Reynolds numbers $C_{\epsilon 2}^{HM}$ becomes very large, leading to a very slow decrease of the kinetic energy in time.
Hanjalić & Launder (1972) improved the standard model by subtracting the term

$$C_{\varepsilon 3} K W_{ij} W_{ij} \,, \tag{5.64}$$

with $C_{\varepsilon 3} = 0.54$ from the standard equation. Transforming this term into a rotating frame of reference it takes the form:

$$-C_{\varepsilon 3} K (W_{ij} W_{ij} - 2(\Omega^2 - e_{ijk}\Omega_i W_{jk})). \tag{5.65}$$

In Shimomura (1993) it is pointed out that with this model modification the analytical solution for K for homogeneous turbulent flow without mean shear shows a sinosoidal behavior causing negative values of ϵ. Therefore the model is not realizable with respect to K and ϵ. The solution has further a singularity at finite time, which is even worse.
A further modification of the dissipation destruction term was proposed by Rubinstein & Zhou (2004):

$$-C_{\varepsilon 2}\left(1 + C_{\varepsilon\Omega}\Omega^2 \frac{K^2}{\epsilon^2}\right)^{\frac{1}{2}} \frac{\epsilon^2}{K}, \tag{5.66}$$

without giving a value for $C_{\varepsilon\Omega}$. Testing the model, Jakirlić *et al.* (2002) could not find any improvements. They concluded that the exponent in (5.66) should be higher than 1 instead of 1/2 to capture the non-linear rotational effects.
Shimomura (1993) introduced the term

$$\epsilon_\omega = -C_{\varepsilon 3} \frac{K W_{ij} W_{ji}}{1 + C_{\varepsilon 4} W_{ij} W_{ji} \frac{K^2}{\epsilon^2}}, \tag{5.67}$$

which will be investigated in section (5.5.2). This model guarantees realizability due to an additional term ϵ_ω / K in the K-equation. Shimomura proposed as coefficients for the model constants $C_{\epsilon 3} = C_{\epsilon 4} = 0.05$.
Shimomura (1989) further proposed to introduce an additional source term

$$C_\Omega K e_{ijk} \frac{\partial \bar{u}_i}{\partial x_j} \tag{5.68}$$

with $C_\Omega = 0.074$, which was determined from theoretical considerations. In Jakirlić *et al.* (2002) it is pointed out that despite the theoretical derivation of Shimomura, a negative C_Ω would yield to the desired improvements in capturing asymmetric effects of rotation in rotating channel flows at higher Reynolds numbers.

Capability of the given ϵ-equation modification to model the rotating turbulent diffusion problem

The $K-\epsilon$ model augmented by the ϵ_ω-term from Shimomura (1993) has been investigated numerically for the given flow geometry with the help of a numerical tool, called 1D solver (© S. Wallin, FOI) (see e.g. Wallin & Martensson, 2004). The K- and ϵ-equations reduce for the given flow case to

$$\frac{\partial K}{\partial t} = -\epsilon + \frac{\partial}{\partial x_1}\left(\frac{C_\mu K^2}{\sigma_K \epsilon} \frac{\partial K}{\partial x_1}\right), \tag{5.69}$$

$$\frac{\partial \epsilon}{\partial t} = -C_{\varepsilon 2}\frac{\epsilon^2}{K} + \frac{\partial}{\partial x_1}\left(\frac{C_\mu k^2}{\sigma_\varepsilon \epsilon}\frac{\partial \epsilon}{\partial x_1}\right) - C_{\varepsilon 3}\frac{K\Omega_1^2}{1 + C_{\varepsilon 4}\Omega_1^2 \frac{K^2}{\epsilon^2}}\,. \tag{5.70}$$

Figure 5.7 shows, that the model gives a finite domain diffusion due to rotation. The position of the fixed point depends thereby on the rotation rate Ω_1 as predicted in section 5.3.3. Considering the dependence of the decay of kinetic energy on the rotation rate, it is found, that the Shimomura model reproduces the trend of the invariant solution in equation 5.36. It is quite interesting to note that the model predicts the finite domain diffusion, which is in contradiction to the LES results. As already mentioned is this finite domain diffusion an arguable result. Anyway this result is partly reproduced by the model equations. It is not clear yet, why the models reproduce this seemingly deficient theoretic result. For an improvement of turbulence models for rotating flows it seems therefore quite promising to investigate the given flow case in more detail.
What can not be found is the quadratic decreasing behavior given by equation 5.36 and the constant integral time-scale predicted by the invariant solutions. Assuming that the

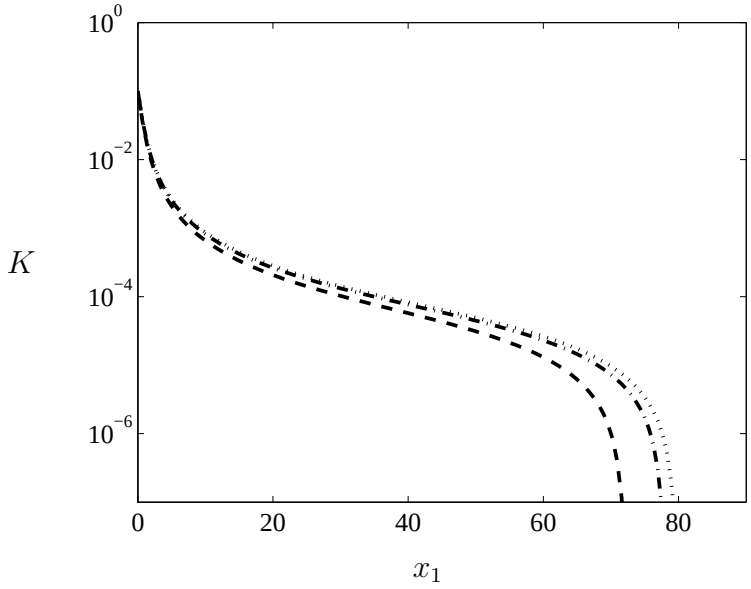

Figure 5.7: Decay of turbulent kinetic energy using the $K - \epsilon$ model (3.17)/(5.70) augmented by ϵ_ω calculated with the 1D solver: $- - -\,\Omega_1 = 0.5$, $- \cdot -\,\Omega_1 = 1$, $\cdots\ \Omega_1 = 2$.

theoretical results are correct and thus inserting the invariant solutions (5.36) into the model equations leads to the condition

$$0 = -C_{\varepsilon 2}\sigma_\varepsilon + \sigma_K + 2C_{\varepsilon 4}(\sigma_K - C_{\varepsilon 2}\sigma_\varepsilon) - C_{\varepsilon 3}\sigma_\varepsilon, \tag{5.71}$$

which is not satisfied by the standard model constants. To fix this constraint for the Shimomura model one either has to add the rotation-dependent term in the ϵ-equation, instead of subtracting it or to subtract a further rotation-dependent term in the K-equation. Both modifications would lead to a faster decay of the turbulent kinetic energy

for increasing rotation rates what is in contradiction to the flow physics. Therefore it is found that this model is not capable to reproduce the results from the symmetry analysis with its standard model constants.

5.5.3 Modeling of the rotating turbulent diffusion with second-moment-closure models

"New" modeling approach for the pressure strain correlation

There appears to be one second-moment-closure model which may account for system rotation for this type of flow. It is the model by Sjögren & Johansson (2000) which includes non-linearity of the mean velocity gradient $\nabla \bar{\boldsymbol{u}}$ in the rapid part of the pressure strain model or in other words: $\mathbf{M}$ may also depend on $\nabla \bar{\boldsymbol{u}}$ which is in clear contrast to all other pressure strain models. Therefore to account for the rotation in the given flow case a new modeling approach for the pressure strain correlation has been developed along the lines of the model from Sjögren and Johansson (2000). This approach is based on the assumption, that the pressure strain term depends on the mean shear tensor S_{ij}:

$$S_{ij} = \frac{1}{2}\left(\frac{\partial \bar{u}_i}{\partial x_j} + \frac{\partial \bar{u}_j}{\partial x_i}\right) , \tag{5.72}$$

and the mean rotation tensor W_j:

$$W_{ij} = \frac{1}{2}\left(\frac{\partial \bar{u}_i}{\partial x_j} - \frac{\partial \bar{u}_j}{\partial x_i}\right) + e_{jim}\Omega_m \tag{5.73}$$

and the Reynolds stress anisotropy tensor a_{ij}:

$$a_{ij} = \frac{\overline{u_i' u_j'}}{K} - \frac{2}{3}\delta_{ij} , \tag{5.74}$$

which are normalized by using the two scaling parameters K and ϵ according to (3.20)-(3.22). Furthermore this term can be split up into three parts which are the classical return and rapid term and a new term which will be called non-linear scrambling (nls) term. For the model of the return and rapid term the linearity of the gradient of the mean velocity and the Cayley-Hamilton theorem is applied, leading to an approach which is non-linear in a_{ij} only (see section 3.2.3). Finally for a non-linear term accounting for the rotation the nls term is adopted. This term is developed with the help of tensor invariant theory. It is built up from tensor invariants and coefficients depending on the scalar invariants. With the condition of no mean flow velocity for the present flow case the model consists of five tensor invariants since S_{ij} is zero and W_{ij} contains only $e_{jim}\Omega_m$. Introducing the variables

$$\phi_{ij}^{nls^*} = \frac{\phi_{ij}^{nls}}{\epsilon} \tag{5.75}$$

the *nls* term can be written in dimensionless form:

$$\begin{aligned}\phi_{ij}^{nls^*} = &\alpha_1 \left(W_{ij}^{*2} - \frac{1}{3} W_{ll}^{*2} \delta_{ij} \right) + \alpha_2 \left(W_{ik}^{*2} a_{kj}^{*} - \frac{1}{3} W_{lk}^{*2} a_{kl}^{*} \delta_{ij} \right) \\ &+ \alpha_3 \left(W_{ik}^{*2} a_{kj}^{*2} - \frac{1}{3} W_{lk}^{*2} a_{kl}^{*2} \delta_{ij} \right) + \alpha_4 \left(W_{ik}^{*2} a_{kl}^{*} W_{lj}^{*} - \frac{1}{3} W_{hk}^{*2} a_{kl}^{*} W_{lh}^{*} \delta_{ij} \right) \\ &+ \alpha_5 \left(W_{ik}^{*2} a_{kl}^{*2} W_{lj}^{*} - \frac{1}{3} W_{hk}^{*2} a_{kl}^{*2} W_{lh}^{*} \delta_{ij} \right),\end{aligned} \tag{5.76}$$

with

$$\alpha_i = f\left[\{a_{ij}^{*}\}, \{a_{ij}^{*2}\}, \{a_{ij}^{*3}\}, \ldots, \{W_{ij}^{*2} a_{jk}^{*2}\}, \{W_{ij}^{*2} a_{jk}^{*} W_{kl}^{*} a_{lh}^{*2}\} \right], \tag{5.77}$$

where $\{\cdot\}$ denotes the trace. For the present flow case the mean rotation tensor only consists of the components $W_{23} = -\Omega_1$ and $W_{32} = \Omega_1$. The other components become zero because the mean flow velocity is zero and only rotation about x_1 is considered ($\Omega_2 = \Omega_3 = 0$).

Existing extension of the pressure strain correlation

In the approach of Sjögren & Johansson (2000) a term which is quadratic in the rotation tensor W_{ij} is added to the rapid term of the pressure strain correlation (see section 3.2.3). This term is scaled with $\sqrt{-II_W}$, ($II_W = W_{ij}W_{ji}$) in order to be linearly dependent on the magnitude of the rotation. It corresponds to the *nls* term with all coefficients except β_2 being zero. Thus this model can be written as

$$N_{ij} = \frac{1}{\sqrt{-II_W}} \left(a_{ik} W_{kl} W_{lj} + W_{ik} W_{kl} a_{lj} - \frac{2}{3} I_{aWW} \delta_{ij} \right), \tag{5.78}$$

whereby Sjögren and Johansson put the coefficient of this term $\beta_2 = 0.5$.

Capability of the given model to model the rotating turbulent diffusion problem

Classical Reynolds stress transport models augmented by the *nls* term have been investigated for their capability to account for system rotation for the given flow geometry. In the following the Launder-Reece-Rodi model (Launder *et al.*, 1975) (LRR) is used as an example. Introducing the *nls* term, the model equations for the Reynolds stresses and the dissipation respectively are

$$\begin{aligned}\frac{\partial \overline{u_i' u_j'}}{\partial t} = &C_4 K \left(b_{ik} W_{jk} + b_{jk} W_{ik} \right) - C_1 b_{ij} \epsilon - \frac{2}{3} \delta_{ij} \epsilon + \epsilon \phi_{ij}^{nls^\star} \\ &+ C_s \frac{\partial}{\partial x_k} \left(\frac{K}{\epsilon} \left(\overline{u_i' u_l'} \frac{\partial \overline{u_j' u_k'}}{\partial x_l} + \overline{u_j' u_l'} \frac{\partial \overline{u_k' u_i'}}{\partial x_l} + \overline{u_k' u_l'} \frac{\partial \overline{u_i' u_j'}}{\partial x_l} \right) \right) \\ &- 2\Omega_k \left[e_{kli} \overline{u_j' u_l'} + e_{klj} \overline{u_i' u_l'} \right],\end{aligned}$$

$$\frac{\partial \epsilon}{\partial t} = -C_{\varepsilon 2}\frac{\epsilon^2}{K} + C_\varepsilon \frac{\partial}{\partial x_k}\left(\frac{K}{\epsilon}\overline{u_k' u_l'}\frac{\partial \epsilon}{\partial x_l}\right), \tag{5.79}$$

whereby $b_{ij} = a_{ij}/2$. These equations are further simplified by the homogeneity in the $x_2 - x_3$ plane and the fact that there are no shear stresses occurring in the given flow. Therefore $\overline{u_2' u_2'}$ becomes equal to $\overline{u_3' u_3'}$ and all off-diagonal elements of the Reynolds stress tensor become zero. Taking a closer look at the model equations it turns out that the rapid

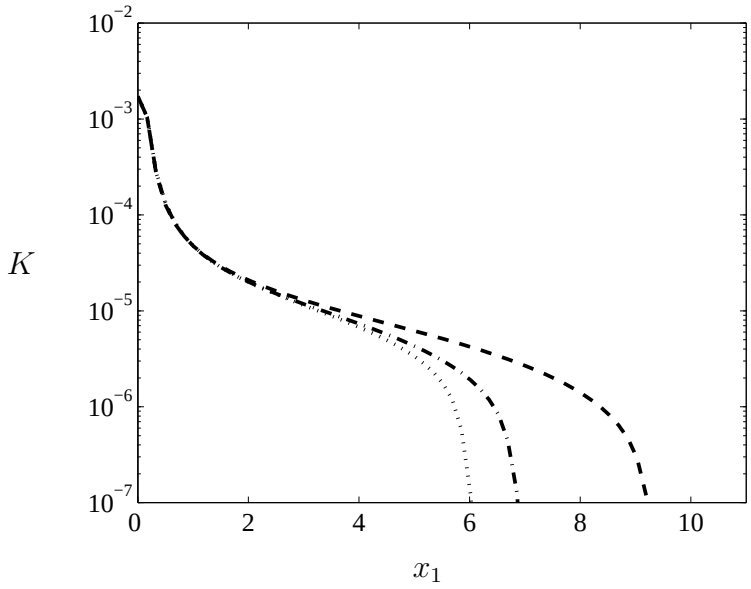

Figure 5.8: Decay of turbulent kinetic energy using the LRR model augmented by the *nls* term calculated with the 1D solver: $- - - \Omega_1 = 0.5$, $- \cdot - \Omega_1 = 1$, $\cdots \Omega_1 = 2$.

term of the pressure strain correlation as well as the advection term do not contribute to the solutions for the present flow geometry. Therefore in the pressure strain term only the *nls* term accounts for rotation.

The LRR model augmented by the *nls* term has been investigated numerically for the given flow geometry with the help of the 1D solver (© S. Wallin, FOI). Thereby the coefficients in the *nls* term have all been put to zero except for β_2 which has been set to 0.5 (see Sjögren & Johansson, 2000). It has thus been found that as a consequence of the *nls* term the questionable result of a finite domain diffusion is predicted once again. The turbulent kinetic energy K decreases to zero at a finite value of x_1. In addition it is found that the position of the fixed point depends on the rotation rate as can be taken from figure 5.8. The higher the rotation rate the closer the fixed point lies towards the turbulence source at the grid. However, again the model fails in predicting the quadratic decreasing behavior and the constant integral time-scale which are given by the invariant solutions (5.36). To predict the quadratic decreasing behavior the model constants would have to obey the condition

$$114C_\varepsilon C_1 C_s C_{\varepsilon 2} - 9C_1^2 C_\varepsilon^2 + 18C_1 C_\varepsilon^2 + 135C_\varepsilon C_s C_{\varepsilon 2} - 216C_s^2 C_{\varepsilon 2}^2 = 0\,, \tag{5.80}$$

which was obtained from substituting (5.36) into (5.79)/(5.79).
Assuming the quadratic decreasing behavior one receives solutions for the Reynolds stresses which are not realizable. This failing depends on the model, respectively the model constants of the diffusion and the dissipation term. For the model constants we receive the condition $C_\varepsilon < 3C_sC_{\varepsilon 2} < 3C_\varepsilon$ for which the Reynolds stresses would become positive. Therefore these solutions can not be obtained using physical reasonable boundary conditions. Since it is arguable to change the values for the model constants a better option for rectifying this problem is to introduce an improved model for the diffusion term, for example

$$\frac{\partial}{\partial x_k}\left[C_{s1}\frac{K}{\epsilon}\left(\overline{u_i'u_l'}\frac{\partial\overline{u_j'u_k'}}{\partial x_l}+\overline{u_j'u_l'}\frac{\partial\overline{u_k'u_i'}}{\partial x_l}\right)+C_{s2}\frac{K}{\epsilon}\left(\overline{u_k'u_l'}\frac{\partial\overline{u_i'u_j'}}{\partial x_l}\right)\right] \tag{5.81}$$

with $C_{s1} > 0.00048$ and $C_{s2} < 0.081$. The model further gives a faster decay of the turbulent kinetic energy for increasing rotation rates, what is in contradiction to our findings in section (5.5.1).
It should further be noted that the non-linear term disappears from the model equations for isotropic boundary conditions at the grid. Hence the numerical solution becomes independent of the rotation rate if isotropic turbulence is considered.

5.5.4 Modeling of the rotating turbulent diffusion with the M-tensor model

The M-tensor model, introduced by Johansson (2003) (see section 3.3) has been applied to the given flow case and the results were compared with the results of the second-moment-closure model by Sjögren & Johansson (2000). The analysis was carried out for isotropic as well as for anisotropic boundary conditions.
Since the given flow is also axisymmetric the M-tensor can once again be described by the five scalars given in (3.65). Therefore we derive from (3.48) the corresponding five model equations which describe the turbulent diffusion in a rotating frame:

$$\frac{\partial K}{\partial t} = -\epsilon + C_s\frac{\partial}{\partial x_1}\left(\frac{R_{11}K}{\epsilon}\frac{\partial K}{\partial x_1}\right), \tag{5.82}$$

$$\frac{\partial R_{11}}{\partial t} = 4\Omega_1 M_2 - C_1\frac{\epsilon}{K}\left(R_{11}-\frac{2}{3}K\right)-\frac{2}{3}\epsilon + C_s\frac{\partial}{\partial x_1}\left(\frac{R_{11}K}{\epsilon}\frac{\partial R_{11}}{\partial x_1}\right), \tag{5.83}$$

$$\frac{\partial Y_{11}}{\partial t} = -C_1\frac{\epsilon}{K}\left(Y_{11}-\frac{2}{3}K\right)-\frac{2}{3}\epsilon + C_s\frac{\partial}{\partial x_1}\left(\frac{R_{11}K}{\epsilon}\frac{\partial Y_{11}}{\partial x_1}\right), \tag{5.84}$$

$$\frac{\partial M_1}{\partial t} = \frac{4}{3}\Omega_1 M_2 - C_1\frac{\epsilon}{K}\left(M_1-\frac{2}{5}K\right)-\frac{2}{5}\epsilon + C_s\frac{\partial}{\partial x_1}\left(\frac{R_{11}K}{\epsilon}\frac{\partial M_1}{\partial x_1}\right), \tag{5.85}$$

$$\frac{\partial M_2}{\partial t} = \Omega_1 \left(-4M_1 + 2Y_{11} - 2 \left(-\frac{2}{5} K \left(110\alpha - \frac{101}{147} \right) \right. \right.$$
$$\left. + \; R_{11} \left(110\alpha + \frac{38}{147} \right) + Y_{11} \left(110\alpha + \frac{164}{147} \right) - M_1 \left(770\alpha + \frac{38}{21} \right) \right) \Bigg) \tag{5.86}$$
$$- C_1 \frac{\epsilon}{K} M_2 - \frac{2}{5}\epsilon + C_s \frac{\partial}{\partial x_1} \left(\frac{R_{11} K}{\epsilon} \frac{\partial M_2}{\partial x_1} \right) ,$$

with $M_1 = M_{1111}$ and $M_2 = M_{i1p1} e_{1ip}$ and C_s, C_1 and α being the model constants.

For isotropic boundary conditions M_1 has to be $\frac{2}{15}K$ and M_2 becomes zero. The new model has been investigated numerically for the given flow geometry with the help of the 1D solver. The results have then been compared to the results received with the mentioned model given by Sjögren & Johansson (2000) and the Launder-Reece-Rodi model (LRR) (Launder *et al.*, 1975).

Only the LRR model augmented by the *nls* term predicts the finite domain diffusion

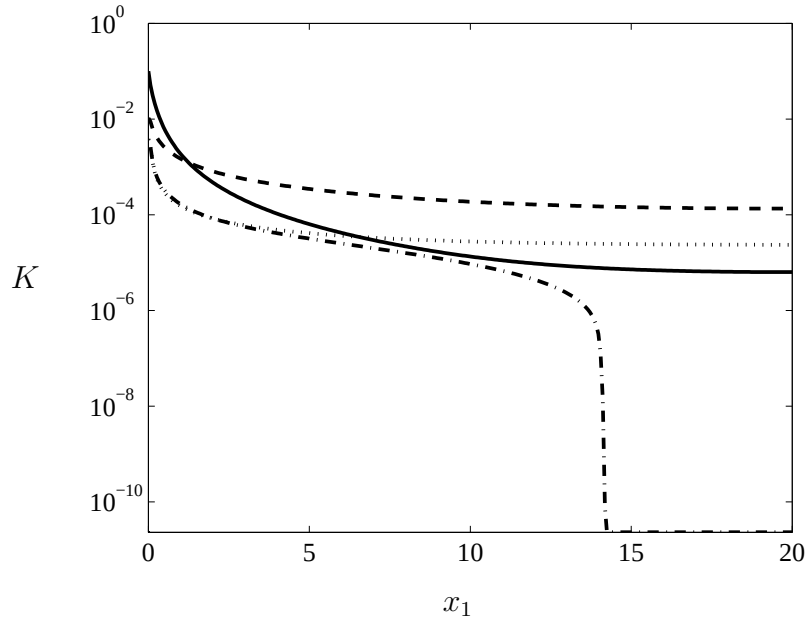

Figure 5.9: Decreasing of the turbulent kinetic energy for $\Omega_1 = 2$ calculated with the 1D solver: Comparison between the M tensor model, the standard LRR model and the LRR model augmented by the *nls* term for isotropic and anisotropic BCs: - - - LRR model + *nls* term (isotr. BCs) , $- \cdot -$ LRR model + *nls* term (anisotr. BCs) , $\cdots$ LRR model (anisotr. BCs), —— M-tensor model (isotr. and anisotr. BCs).

and only for anisotropic BCs. For isotropic boundary conditions the M-tensor model gives lower values for the turbulent kinetic energy with the same departure from the turbulence source as the non-linear model. The LRR model gives nearly the same behavior whereby the values for K are again a bit higher, than for the M-tensor model. In contradiction

to the standard LRR model is the M-tensor model sensitive to rotation for the given flow case. Being sensitive to rotation, while not predicting the questionable finite domain diffusion makes the M-tensor model superior to the standard LRR model and the LRR model, augmented by the *nls*-term.
The decreasing behavior given by all three models is not quadratic and the integral time-scale is not even constant, as predicted by the Lie group analysis.

6 Parallel turbulent shear-flow - exponential scaling law

In the following the results of investigations of parallel turbulent shear-flow performed by Guenther & Oberlack (2005a) are presented.

6.1 Introduction

Analyzing the multi point correlation equations for parallel turbulent shear-flows, and zero pressure gradient (ZPG) turbulent boundary layer flows with the help of Lie symmetry methods a new exponential scaling law has been derived in Oberlack (2001).
From experiments (e.g. Lindgren *et al.*, 2004) and direct numerical simulations (DNS) (e.g Khujadze & Oberlack, 2004) the exponential velocity profile was clearly validated in the mid-wake region of high Reynolds number flat-plate boundary layers. It was identified as an explicit analytic form of the velocity defect law.
Implementing the latter invariant solution into various Reynolds stress models it was found that none of the investigated models is in accordance with the exponential velocity law.

6.2 Symmetry analysis

In Oberlack (2001) a Lie group analysis of the two-point correlation (TPC) equations has been performed for plane shear-flows including a ZPG turbulent boundary layer flow. For the analysis it was assumed that all statistical quantities depend only on the wall normal coordinate ($\bar{u}_1 = \bar{u}_1(x_2)$) and an infinite Reynolds number was assumed. Hence only large-scale quantities such as the mean velocities or the Reynolds stresses are determined. The TPC equations have been considered in the outer part of the boundary layer flow where viscosity can be neglected. The analysis was further limited to flows without system rotation ($\mathbf{\Omega} = 0$).
Focusing only on scaling symmetries (G_{s1}, G_{s2}, G_{s3}), Galilean invariance (G_{Gali}) and the translation group (G_{Trans}) the analysis gives the following global transformations (Khu-

jadze & Oberlack, 2004):

$$
\begin{aligned}
\mathbf{G_{s1}} \;&:\; \tilde{x}_2 = x_2 e^{a_1},\ \tilde{r}_i = r_i e^{a_1},\ \tilde{\bar{u}}_1 = \bar{u}_1 e^{a_1},\ \tilde{R}_{ij} = R_{ij} e^{2a_1},\ \widetilde{\overline{p'u_i'}} = \overline{p'u_i'} e^{3a_1},\\
&\quad \widetilde{\overline{u_i'p'}} = \overline{u_i'p'} e^{3a_1},\ \ldots\\
\mathbf{G_{s2}} \;&:\; \tilde{x}_2 = x_2,\ \tilde{r}_i = r_i,\ \tilde{\bar{u}}_1 = \bar{u}_1 e^{-a_2},\ \tilde{R}_{ij} = R_{ij} e^{-2a_2},\ \widetilde{\overline{p'u_i'}} = \overline{p'u_i'} e^{-3a_2},\\
&\quad \widetilde{\overline{u_i'p'}} = \overline{u_i'p'} e^{-3a_2},\ \ldots\\
\mathbf{G_{s3}} \;&:\; \tilde{x}_2 = x_2,\ \tilde{r}_i = r_i,\ \tilde{\bar{u}}_1 = \bar{u}_1,\ \tilde{R}_{ij} = R_{ij} e^{-a_3},\ \widetilde{\overline{p'u_i'}} = \overline{p'u_i'} e^{-a_3},\\
&\quad \widetilde{\overline{u_i'p'}} = \overline{u_i'p'} e^{-a_3},\ \ldots\\
\mathbf{G_{Trans}} \;&:\; \tilde{x}_2 = x_2 + a_4,\ \tilde{r}_i = r_i,\ \tilde{\bar{u}}_1 = \bar{u}_1,\ \tilde{R}_{ij} = R_{ij},\ \widetilde{\overline{p'u_i'}} = \overline{p'u_i'},\ \widetilde{\overline{u_i'p'}} = \overline{u_i'p'},\ \ldots\\
\mathbf{G_{Gali}} \;&:\; \tilde{x}_2 = x_2,\ \tilde{r}_i = r_i,\ \tilde{\bar{u}}_1 = \bar{u}_1 + a_5,\ \tilde{R}_{ij} = R_{ij},\ \widetilde{\overline{p'u_i'}} = \overline{p'u_i'},\ \widetilde{\overline{u_i'p'}} = \overline{u_i'p'},\ \ldots\,,
\end{aligned}
\tag{6.1}
$$

where x_2 is the wall normal coordinate, r_i the correlation length and $\bar{u}_1$ corresponds to the streamwise velocity component. The correlation vectors and tensors are defined as:

$$
R_{ij} = \overline{u_i'(x,t)u_j'(x+r,t)},\ \ \overline{u_i'p'} = \overline{u_i'(x,t)p'(x+r,t)},\ \ \overline{p'u_i'} = \overline{p'(x,t)u_i'(x+r,t)}\,.
$$

The variables $a_1 - a_5$ are group parameters of the corresponding transformations. According to the definition of symmetries all $\tilde{}$-quantities refer to transformed variables which, introduced into the TPC equations, leave the equation invariant, that is unchanged in the new variables. The corresponding characteristic equations for the invariant solutions read:

$$
\begin{aligned}
\frac{dx_2}{a_1x_2 + a_4} = \frac{dr_i}{a_1 r_i} = \frac{d\bar{u}_1}{(a_1 - a_2)\bar{u}_1 + a_5} = \frac{dR_{ij}}{[2(a_1 - a_2) + a_3]R_{ij}} =\\
\frac{d\overline{p'u_i'}}{[3(a_1 - a_2) + a_3]\overline{p'u_i'}} = \frac{d\overline{u_i'p'}}{[3(a_1 - a_2) + a_3]\overline{u_i'p'}}, \ldots .
\end{aligned}
\tag{6.2}
$$

From G_{s1} we find that imposing a symmetry breaking of space means $a_1 = 0$. Correspondingly setting in equation (6.2) a_1 to zero and integrating the corresponding equations a new exponential scaling law is received as it is shown by Oberlack (2001):

$$
\bar{u}_1(x_2) = k_1 + k_2 e^{-k_3 x_2}, \tag{6.3}
$$

with

$$
k_1 \equiv \frac{a_5}{a_2} \equiv \bar{u}_\infty, \quad k_3 \equiv \frac{a_2}{a_4} \equiv \frac{\beta}{\Delta}\,,
$$

and $k_2 \equiv -\alpha u_\tau$ being a constant of integration. The physical assignments for $k_1 - k_3$ are according to Oberlack (2001) to be defined below. For the present case the correlation length r_i becomes constant, that is an invariant or physically interpreted the integral length-scale $\ell_t = K^{3/2}/\epsilon$ is constant (see equation (6.5) below).
Scaling the wall-normal coordinate in the outer region with the Clauser-Rotta length-scale ($\Delta = (\delta_* \bar{u}_\infty)/\bar{u}_\tau$, where δ_* is the displacement thickness) the exponential law may be written in general wake form as

$$
\frac{\bar{u}_\infty - \bar{u}_1}{\bar{u}_\tau} = F(\eta) = \alpha \exp(-\beta\eta)\,, \tag{6.4}
$$

where $\eta = x_2/\Delta$ and α, β are universal parameters.

6.3 Evaluation of the exponential law by experiments

Recently the theory has been carefully tested against very high quality experimental data from the KTH database (Lindgren *et al.*, 2004) and the Laminar Wind Tunnel (LaWiKa) of the Hermann-Föttinger-Institute in Berlin (Knobloch & Fernholz, 2003). The experiments have been performed at very high Reynolds numbers where for the large-scale quantities the viscous terms are negligible small compared to the other terms. Thus the assumption of the infinite Reynolds number limit made for the Lie group analysis and therefore the findings received from the analysis are supported by the data. It could further be found that the exponential region increases for increasing Reynolds numbers respectively decreasing shape factors.
At KTH experiments for a range of Reynolds numbers from 22579 to 27320 have been performed. These Reynolds numbers are based on the momentum-loss thickness. In figure 6.1 six profiles from the KTH database are plotted in outer scaling showing a very good collapse of the data. It can be shown that the exponential law fits the experimental data very well in the range of about $0.03 \leq x_2/\Delta \leq 0.10$, corresponding to almost half of the boundary layer thickness. The exponential region is thus substantially larger than the region in which the log-law is valid. The constants are determined to $\alpha = 10.6$ and $\beta = 9.34$. Figure 6.2 shows the results of experiments performed at $R_\theta = 11840$ in the

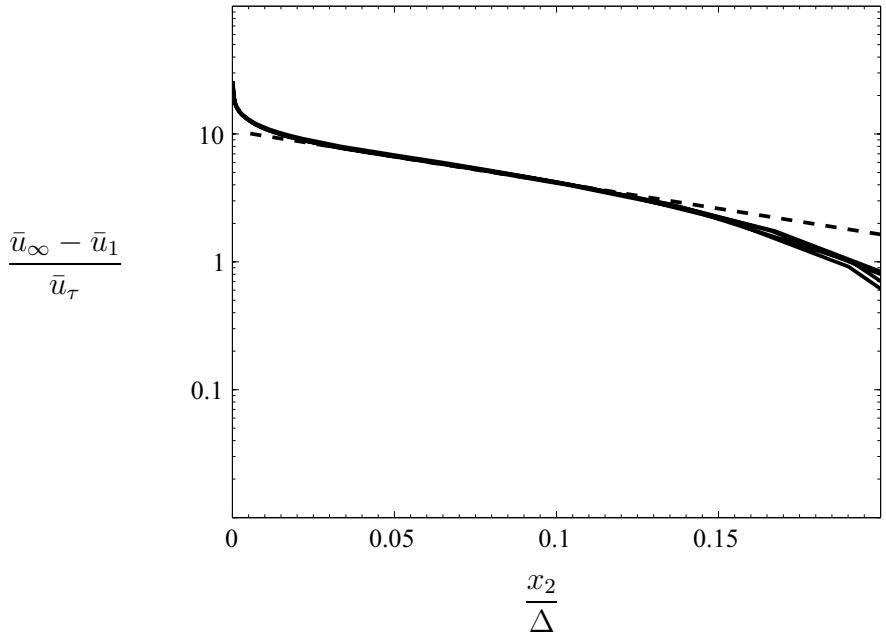

Figure 6.1: Mean velocity profiles from experiments at different Reynolds numbers $Re_\theta =$ 22 579, 23 119, 23 870, 25 779, 26 612, 27 320, performed at KTH (Stockholm), Lindgren *et al.* (2004), - - - exponential law.

LaWiKa. These experimental results show as well a good fit with the exponential law in the region $0.03 \leq x_2/\Delta \leq 0.10$.

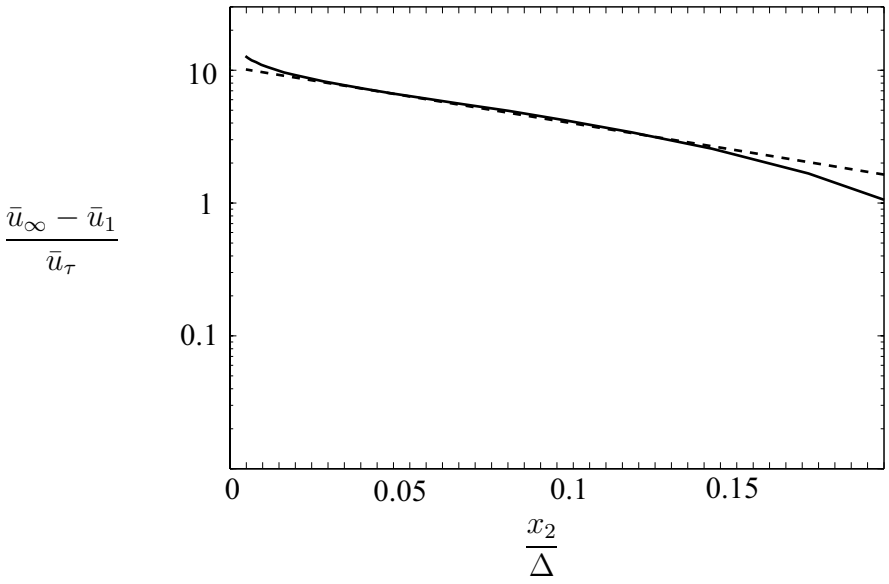

Figure 6.2: Mean velocity profiles from experiments with $Re_\theta = 11840$, Knobloch & Fernholz (2003), - - - exponential law.

Figure 6.3 shows the results of a direct numerical simulation (DNS) of a ZPG boundary layer performed for $R_\theta = 2240$ (see Khujadze & Oberlack, 2004). The DNS results show an exponential law in the region $0.025 \leq x_2/\Delta \leq 0.15$.

In the outermost part of the boundary layer the velocity decreases more rapidly than the exponential law. The reason for this is not clear yet. In Lindgren *et al.* (2004) two possible reasons are discussed: One possible explanation is that the relative influence of viscosity may be higher in this region than otherwise in the outer region. Another explanation is that the undisturbed free-stream fluid penetrates the boundary layer to give an intermittent behavior. Since the fluid has a higher velocity than the local mean of the turbulent flow, the mean velocity increases and thereby the velocity defect decreases. These non-parallel effects which might become dominant are not taken into account in the derivation of the exponential law.

6.4 Turbulence model implications

Since a remarkable good agreement between theory, experiments and numerical simulations is observed it should also be demanded from the Reynolds stress models to be in accordance with the theory. Thus a further symmetry analysis of the $K-\epsilon$ model for ZPG boundary layer flows has been performed. Imposing here as well the symmetry breaking

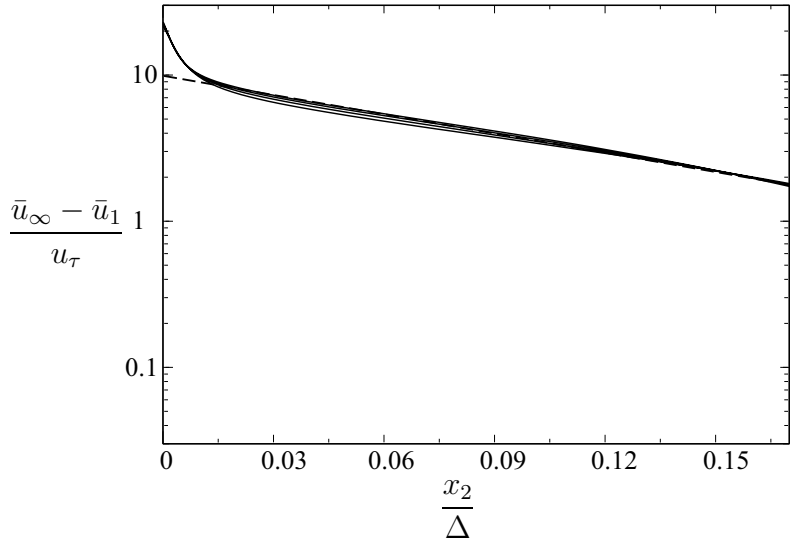

Figure 6.3: Mean velocity profiles from DNS at $Re_\theta = 2240$, (Khujadze and Oberlack, 2004); - - - exponential law (Oberlack, 2001).

of scaling of space we obtain besides (6.4) the following set of invariant solutions:

$$K = C\exp(-2\beta\eta)\,,\ \epsilon = D\exp(-3\beta\eta)\,,\ell = \frac{C^{3/2}}{D} \tag{6.5}$$

whereby C and D are again combinations of the group parameter. Implementing the invariant solution (6.4) and (6.5) into the model equations it has to be analyzed if the models admit the new exponential scaling law.
The models which have been tested concerning this requirement are the one-equation model of Spalart & Allmaras (1992), the classical $K-\epsilon$ model of Hanjalić & Launder (1976), the $K-\omega$ model of Wilcox (1993), the v^2f model of Durbin (1991), the SST model of Menter (1994), the $\sqrt{K}\ell$ model of Menter & Egorov (2004), the $K-K\ell$ model of Rotta (1968) and as an example for a Reynolds stress second moment closure model the LRR model of Launder *et al.* (1975). Thereby it was found that all these models are in contradiction to the theory.
For our investigations we assumed that the exponential region is characterized by an equilibrium between production, diffusion and dissipation (see Fig. 6.4). The diffusion term can thus not be neglected as it is done at the calibration of the turbulence models with the logarithmic velocity law.

All statistical quantities depend only on the wall-normal coordinate leading to a simplification of the model equations. Introducing the invariant solutions (6.4) and (6.5) into these simplified model equations we find that any exponential dependence on x_2 cancels out. Hence a set of algebraic equations is retained, connecting the model coefficients, as well as α and β. Interesting enough solving these equations we obtain coefficients for the exponential law, which are in contradiction to common model values.
In the following we will exemplary point out the problems appearing in the *Spalart-Almaras*, the $K-\epsilon$ and the LRR model. Replacing the dependent variable $\tilde{\nu}$ in the

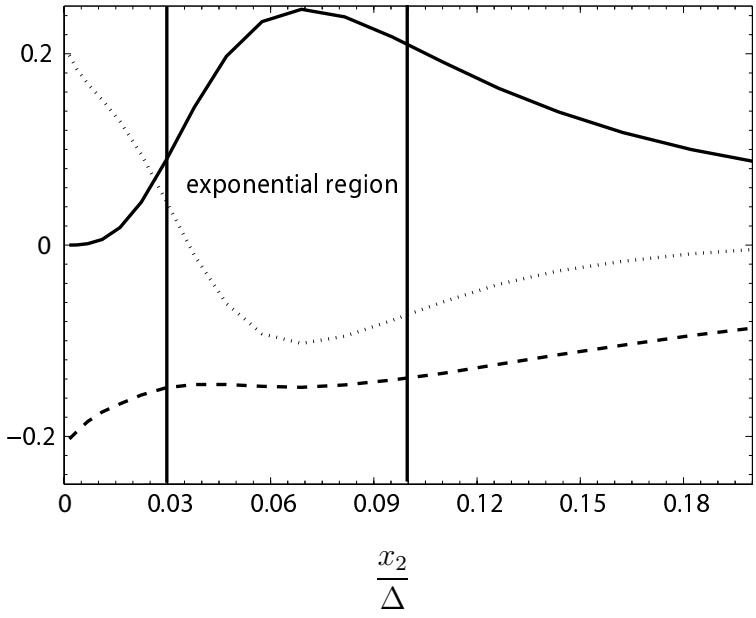

Figure 6.4: The turbulent-kinetic-energy budget in a turbulent boundary layer at Re_θ=1410, Spalart (1988); —— production, - - - dissipation, $\cdots$ diffusion.

Spalart-Almaras model by the invariant solution

$$\tilde{\nu} = E \exp(-\beta x_2) \tag{6.6}$$

and neglecting molecular viscosity we receive the coefficient

$$E = -\frac{C_{b1}\sigma\alpha u_\tau \Delta}{2\beta(2 + C_{b2})}\,, \tag{6.7}$$

whereby C_{b1}, σ and C_{b2} are model constants. We can thus derive the condition

$$\frac{C_{b1}\sigma}{2(2 + C_{b2})} < 0\,, \tag{6.8}$$

under which a proper modeling of the exponential region is assured. Since C_{b1}, σ and C_{b2} are positive, changing the algebraic sign of one of the coefficients would probably lead to a deficient modeling if other flow cases are considered.
The same problem appears if the invariant solutions (6.4) and (6.5) are introduced into the $K - \epsilon$ model. Here we receive the following dependence of the coefficients in the exponential law on the model constants:

$$\begin{aligned} C &= \frac{\sigma_K \sigma_\varepsilon (C_{\varepsilon 1} - C_{\varepsilon 2})\alpha^2 u_\tau^2}{6C_{\varepsilon 2}\sigma_\varepsilon - 12\sigma_K}\,, \\ D &= \sqrt{\frac{C_\mu \sigma_K^2 \sigma_\varepsilon^2 (C_{\varepsilon 1} - C_{\varepsilon 2})^2 \left(1 + \frac{\sigma_\varepsilon (C_{\varepsilon 1} - C_{\varepsilon 2})}{C_{\varepsilon 2}\sigma_\varepsilon - 2\sigma_K}\right)}{(6C_{\varepsilon 2}\sigma_\varepsilon - 12\sigma_K)^2}}\,\frac{\alpha^3 u_\tau^3 \beta}{\Delta}\,, \end{aligned} \tag{6.9}$$

leading with the standard model constants (see chapter 3) to

$$C = -0.21\alpha^2 u_\tau^2\,, \quad D = 0.03\sqrt{-1}\frac{\alpha^3 u_\tau^3 \beta}{\Delta}, \tag{6.10}$$

which apparently is completely unphysical. From equation (6.9) various conditions for the model constants of the $K-\epsilon$ model can be derived, guaranteeing a proper modeling of the exponential velocity law:

$$C_{\epsilon 1} < C_{\epsilon 2} \quad , \frac{C_{\epsilon 2}\sigma_\epsilon}{\sigma_K} < 2\,. \tag{6.11}$$

Thus changing for example σ_ϵ to 1.04 which comes from the second condition $\sigma_\epsilon < 2\frac{\sigma_K}{C_{\epsilon 2}}$ and keeping the numerical value of the other model constants would give positive values for C and D. Since the model constants are related by

$$\kappa^2 = \sigma_\epsilon C_\mu^{1/2}\left(C_{\epsilon 2} - C_{\epsilon 1}\right) \tag{6.12}$$

due to the balance of production and dissipation in the log-law region a change of σ_ϵ to 1.04 demands an adjustment of the von Karman constant to 0.38. In the literature the values for κ range from 0.38 to 0.43. Therefore $\kappa = 0.38$ is an acceptable choice and guarantees together with $\sigma_\epsilon = 1.04$ a correct reproduction of the log-law region.
For the LRR model such a discrepancy appears in the model constants that all coefficients of the scaling laws become zero if the invariant solutions are introduced into the model equations.
The reason for these mismatches seems to be due to the fact that the given models are all calibrated employing the classical flow cases. A calibration of the models using symmetry methods would probably improve the described shortcomings.

7 Fully developed axially rotating turbulent pipe flow

The investigations on the fully developed axially rotating turbulent pipe flow have been carried out by Guenther & Oberlack (2005*b*).

7.1 Introduction and review

Axially rotating turbulent pipe flow is an example where rotation strongly affects turbulence and thereby the Reynolds stresses and the mean flow properties i.e. the axial and azimuthal mean velocity. For almost two decades this flow has been a popular benchmark for the testing and evaluation of turbulence theories and models.

The present investigations are based on the work of Oberlack (1999) in which he derived new scaling laws for the non-rotating and rotating turbulent pipe flow based on the mean and fluctuation momentum equation (see also §7.3). From a symmetry analysis of the Navier-Stokes equations an algebraic scaling law for the axial and azimuthal mean velocity is obtained for the most general case of no symmetry breaking. If an external velocity scale is dominantly acting on the flow, a logarithmic mean velocity profile is received for the axial velocity component. From comparison with numerical and experimental data Oberlack could validate the theoretical results, both for the algebraic and the new logarithmic scaling law.

Eggels, Boersma & Nieuwstadt (1994) performed a direct numerical simulations (DNS) and a large eddy simulations (LES) considering the turbulent rotating pipe flow. From their simulations they found that the mean axial velocity profile is considerably deformed due to rotation and that the skin friction coefficient is reduced significantly. The mean circumferential velocity profile appears to be close to parabolic for sufficiently high rotation rates and nearly independent of the Reynolds number. It is further shown, that any closure model, based on the gradient hypothesis will provide an incorrect mean circumferential velocity profile, namely a solid body rotation.

Turbulent flow in a circular pipe with and without rotation about its axis has also been numerically investigated by Orlandi & Fatica (1997). A comparison between the vorticity in the non-rotating and in the high rotation case has shown a spiral motion leading to the transport of streamwise vorticity far from the wall. It was also found that the rotation produces drag reduction and that at high rotation rates the mean streamwise velocity tends to a parabolic laminar-like Poiseuille profile.

The effects of rotation on the helicity density fluctuation in a turbulent pipe flow have

been investigated by Orlandi (1997). Orlandi also confirmed a drag reduction due to the imposed rotation on the turbulent pipe flow and a reduction of the turbulent kinetic energy near the wall.

Orlandi & Ebstein (2000) performed direct numerical simulations placing particular interest on the near wall region. Their data shows that the friction factor decreases with about 15% when the rotation number N is increased from 0 to 2. For $N = 5$ the friction factor increases again and interesting enough at $N = 10$ it is actually higher than for the non-rotating case. This has not been confirmed by an experiment so far.

Early experimental results concerning the flow pattern and hydraulic resistance in a rotating pipe are described by Murakami & Kikuyama (1980). They also found that an increase of the rotation rate reduces the hydraulic loss due to a swirling flow component. The reduction in the hydraulic loss is thereby a function of the rotation rate and the pipe length.

Kikuyama, Murakami & Nishibori (1983*a*) measured the mean velocities and the turbulent fluctuations inside the turbulent boundary layer which developed in an axially rotating pipe. It is found that the pipe rotation gives rise to two counter effects on the flow: one is a destabilising effect due to a large shear caused by the rotating pipe wall and the other is a stabilising effect due to the centrifugal force of the swirling velocity component of the flow. The destabilising effect prevails in the inlet region, but the stabilising effect becomes dominant in the downstream sections.

Reich (1988) also experimentally investigated turbulent flow as well as the heat transfer in a rotating pipe. Reich found that there is almost no dependence of the exponent in the algebraic scaling law on the axial and azimuthal Reynolds number when the velocity is normalized with the wall friction velocity. Furthermore Reich confirmed that the algebraic azimuthal mean velocity profile is in sharp contrast to the laminar flow in a rotating pipe where solid-body rotation occurs.

A further experimental study of the instability of a flow in an axially rotating pipe is performed by means of LDV and flow visualisation technique in Imao, Itoh & Zhang (1992). Therein it is also confirmed that pipe rotation destabilizes the flow and spiral waves appear in the developing region. Owing to the occurrence of spiral waves, the velocity initially fluctuates like a sine wave, while further downstream a somewhat sawtooth-like wave form occurs.

In a recent study Facciolo (2003) experimentally investigated rotating pipe and jet flow. The flow data have been compared with the scaling laws derived in Oberlack (1999) and it is found that the experimental results closely follow the theoretical results of the algebraic and the logarithmic scaling law.

Besides DNS and experimental studies calculations of axially rotating pipe flow, using a variety of turbulence closure models have been reported by several authors.

The most simple approaches have been based on the mixing-length model introduced by

Kikuyama *et al.* (1983*b*):

$$\frac{\ell}{\ell_0} = 1 - \beta R_i, \tag{7.1}$$

where β is a constant and R_i is the Richardson number defined by

$$R_i = \frac{2\frac{u_\phi}{r^2}\frac{\partial r u_\phi}{\partial r}}{\left(\frac{\partial u_z}{\partial r}\right)^2 + \left(r\frac{\partial u_\phi r}{\partial r}\right)^2}. \tag{7.2}$$

Kikuyama *et al.* (1983*b*) found that the mixing-length decreases with an increase of the rotation number N. Finally the mixing-length becomes essentially zero when N exceeds 3.5. At that point the axial velocity profile changes into a nearly laminar-like profile.

Hirai, Takagi & Matsumoto (1988) tested three different turbulence models, the standard $K-\epsilon$ model, the $K-\epsilon$ model modified by the Richardson number and a Reynolds stress transport model (RSTM). The results of the numerical calculations have then been compared with experiments. It was found that the stress equation model behaves fairly well for this kind of flow whereby the standard $K-\epsilon$ model is unaffected by the rotation. The modified $K-\epsilon$ model accounts for system rotation but is not able to capture any of the correct physical trends for the mean flow found in experiments. Further inquiries concerning the modified model can be found in §7.4.

Kurbatskii & Poroseva (1995) present a gradient transfer model for calculating the turbulent velocity field in a rotating pipe and found an adequate agreement of their numerical results with experiments from Pilipchuk (1986), Zaets, Safarov & Safarov (1985) and Safarov (1986).

In Kurbatskii & Poroseva (1999) and Poroseva (2001) it is stated that at present the tensor-invariant model of Hanjalić & Launder (1976) for the diffusion term and the linear SSG model (Speziale *et al.*, 1991) for the pressure-strain term are the best choices to model turbulent rotating pipe flow. By testing two different diffusion and five different pressure strain models Kurbatskii and Poroseva found that with increasing Reynolds number the difference between the profiles calculated with the different models becomes negligible. In Poroseva (2001) it is further shown that all models need additional wall corrections to describe the turbulent kinetic energy and its partition between components near a wall adequately.

Zaets *et al.* (1998) compared three different models for their performance in rotating pipe flow. Thereby the LRR gave a better match with the experimental data than the models with algebraic relationships for second-order moments. The model with a non-equilibrium relationship for normal stresses (Rodi, 1980 and Hossain, 1980) allows a better calculation of the behaviour of the turbulence energy and its components in the axial flow region at a moderate pipe rotation than the model introduced by Gibson & Launder (1978) and So & Yoo (1986).

Pettersson, Andersson & Brunvoll (1998) as well as Speziale, Younis & Berger (2000) found from comparison with the results from physical and numerical experiments that the best overall performance RSTM at modeling fully developed turbulent pipe flow is obtained

by a pressure strain model that retains terms which are quadratic in the Reynolds stress tensor (e.g. SSG, Speziale *et al.*, 1991) whereby highly non-linear pressure strain models fail in the present case. The stabilising effect of the imposed rotation on the turbulence is generally overpredicted by the models and the adoption of a particular gradient diffusion model seems to be of minor influence on the results.

In Poroseva *et al.* (2002) the structure based model suggested by Kassinos *et al.* (2000) has been evaluated in a rotating pipe. It was observed that this model is able to predict the flow more accurately at various Reynolds numbers and under stronger rotation than it was possible with any of the RSTM. Most important, the structure based model is able to reproduce the correct behaviour of flow characteristics at relatively high rotation rates, whereas the RSTMs predict flow relaminarization in contrast to experiments (see also Poroseva, 2001).

Rubinstein & Zhou (2004) developed a non-linear single-point eddy viscosity model based on two-point closure theory. The developed model focuses on the diminished energy transfer due to rotation which might not be the dominant physical effect of rotation and thus discrepancies between the model predictions and the numerical and experimental results appear.

Grundestam *et al.* (2004) investigated the differences between two explicit algebraic Reynolds stress models (EARSM), the EARSM by Wallin & Johansson (2000) and the extension of this model to a non-linear pressure strain rate model proposed by Grundestam *et al.* (2003) and their corresponding differential Reynolds stress models (DRSM), studying fully developed rotating turbulent pipe flow. Thereby they found for all models a quite good agreement with experimental results for the mean velocity profiles. Grundestam *et al.* (2003) found that the predictions obtained with the EARSMs closely follow those of the corresponding DRSMs.
The non-linear terms have a significant positive influence on the flow predictions, which is more profound for the EARSMs than for the DRSMs. It is further demonstrated that the predictions for the turbulent kinetic energy vary dramatically with the applied diffusion model and that this is closely related to the model for the evolution of the length-scale determining quantity, such as ϵ or ω. Thereby Grundestam *et al.* (2003) found that it is important to choose a Daly-Harlow type of diffusion model for a reasonably correct prediction of the kinetic energy levels.

7.2 Governing equations

Analyzing the flow in a circular axially rotating pipe the examined equations have to be transferred into cylindrical coordinates. Since we are interested in the turbulence modeling aspects of the given flow problem we will consider the Reynolds-averaged form of the Navier-Stokes equations. There are two possibilities to account for the rotation. The first one is to consider the equations in an inertial frame whereby the boundary conditions account for the rotation. The second choice is to use a rotating frame and to introduce centrifugal and Coriolis effects to the equations while the boundaries are non-rotating in

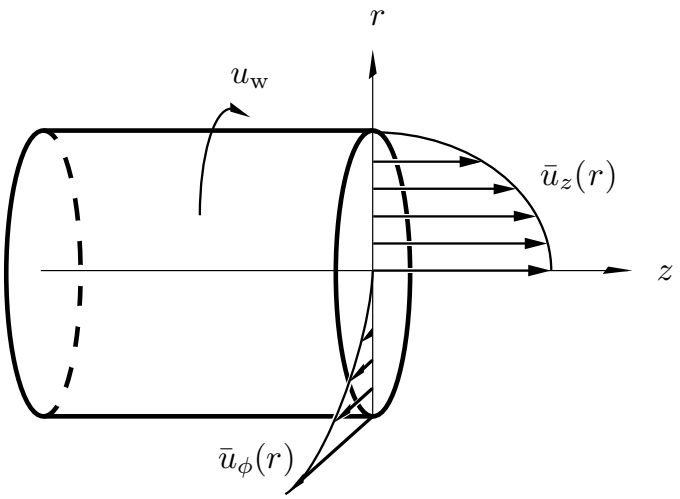

Figure 7.1: Flow geometry

this frame. In the following we restrict to the first possibility being the more facile one since the determined equations consist of less terms.
Corresponding to figure 7.1 we denote the radial, azimuthal and axial direction with (r, ϕ, z) and the respective velocity components with (u_r, u_ϕ, u_z).

Since we confine our considerations to fully developed flow with azimuthal symmetry there is no streamwise and azimuthal dependence of the mean flow. Thus the continuity equation (2.1), written in cylindrical coordinates reduces to

$$\frac{1}{r}\frac{\partial}{\partial r}(r\bar{u}_r) = 0, \tag{7.3}$$

which has the only solution $\bar{u}_r = \frac{C_1}{r}$ where C_1 is a constant. The no-slip boundary condition $\bar{u}_r(r = R) = 0$ along with the condition of regularity of the velocity field at $r = 0$ yields $C_1 = 0$ and hence

$$\bar{u}_r = 0. \tag{7.4}$$

Taking this as well as the above mentioned restrictions into account the Reynolds-averaged Navier-Stokes equations (2.2) for the radial, azimuthal and axial components respectively reduce to

$$\frac{\partial \bar{u}_r}{\partial t} - \frac{\bar{u}_\phi^2}{r} = \frac{\partial p}{\partial r} - \frac{1}{r}\frac{\partial}{\partial r}\left(r\overline{u_r' u_r'}\right) + \frac{\overline{u_\phi' u_\phi'}}{r}, \tag{7.5}$$

$$\frac{\partial \bar{u}_\phi}{\partial t} = \frac{1}{r^2}\frac{\partial}{\partial r}\left(r^3\nu\frac{\partial}{\partial r}\left(\frac{\bar{u}_\phi}{r}\right) - r^2\overline{u_r' u_\phi'}\right), \tag{7.6}$$

$$\frac{\partial \bar{u}_z}{\partial t} = -\frac{\partial p}{\partial z} + \frac{1}{r}\frac{\partial}{\partial r}\left(r\nu\frac{\partial \bar{u}_z}{\partial r} - r\overline{u_r' u_z'}\right). \tag{7.7}$$

Restricting to stationary high Reynolds-number flow ($\nu = 0$) equation (7.6) and (7.7) further reduce to

$$0 = \frac{1}{r^2}\frac{\partial}{\partial r}\left(-r^2\overline{u_r' u_\phi'}\right), \tag{7.8}$$

$$0 = -\frac{\partial p}{\partial z} + \frac{1}{r}\frac{\partial}{\partial r}\left(-r\overline{u_r' u_z'}\right). \tag{7.9}$$

Integration of (7.8) gives $\overline{u_r' u_\phi'} = \frac{C_2}{r^2}$, with C_2 being the constant of integration. Due to symmetry conditions $\overline{u_r' u_\phi'}$ must become zero at the centre of the pipe. Therefore we receive $C_2 = 0$ and hence

$$\overline{u_r' u_\phi'} = 0. \tag{7.10}$$

In the DNS data of Orlandi & Fatica (1997) and Eggels *et al.* (1994) it is indicated that $\overline{u_r' u_\phi'}$ is unequal zero. Still, as can be taken from Orlandi & Fatica (1997), its value is one order of magnitude lower than the other Reynolds stresses, e.g. $\overline{u_\phi' u_z'}$ due to its viscous origin. Since we are considering the large Reynolds number limit, $\overline{u_r' u_\phi'}$ is set to zero in the following.
Integrating the reduced axial Reynolds-averaged Navier-Stokes equation (7.9) gives:

$$\overline{u_r' u_z'} = \frac{1}{r}\int r\frac{\partial \bar{p}}{\partial z} dr + C_3. \tag{7.11}$$

The pressure gradient in z direction is independent of the radius and for the fully developed flow known to be a constant. Since $\overline{u_r' u_z'}$ must be zero at $r = 0$ we receive $C_3 = 0$ and therewith

$$\overline{u_r' u_z'} = \frac{r}{2}\frac{\partial \bar{p}}{\partial z}. \tag{7.12}$$

7.3 Symmetry analysis for the turbulent pipe flow

In Oberlack (1999) new scaling laws for high Reynolds number turbulent pipe flow are derived by using symmetry methods. For the analysis an infinite Reynolds number was assumed and viscosity has been neglected. Hence only large-scale quantities such as the mean velocities are determined.
From a Lie group analysis of the two-point correlation equations Oberlack receives the following symmetries:

$$T_{s1} \;:\; r^* = re^{a_1},\;\; \bar{u}_z^* = \bar{u}_z e^{a_1},\;\; \bar{u}_\phi^* = \bar{u}_\phi e^{a_1}, \tag{7.13}$$

$$T_{s2} \;:\; r^* = r,\;\; \bar{u}_z^* = \bar{u}_z e^{-a_2},\;\; \bar{u}_\phi^* = \bar{u}_\phi e^{-a_2}, \tag{7.14}$$

$$T_{u_z} \;:\; r^* = r,\;\; \bar{u}_z^* = \bar{u}_z + a_3,\;\; \bar{u}_\phi^* = \bar{u}_\phi. \tag{7.15}$$

$$\tag{7.16}$$

From the infinitesimal form of (7.13) to (7.15) the characteristic equation for the invariant solutions can be derived:

$$\frac{dr}{a_1 r} = \frac{d\bar{u}_z}{[a_1 - a_2]\bar{u}_z + b_1} = \frac{d\bar{u}_\phi}{[a_1 - a_2]\bar{u}_\phi}, \tag{7.17}$$

where a_1, a_2 and b_1 are group parameters of the corresponding transformations, scaling of space and time and Galilean invariance in z-direction. Integration of (7.17) gives the

invariant solutions whereby all scaling laws have their origin at the pipe centre. Thereby two cases each one referring to a broken symmetry can be distinguished.

The first case is the most general case since no symmetry breaking is imposed on the flow, meaning that a_1, a_2 and b_1 are arbitrary and unequal zero. Integration of (7.17) gives then an algebraic scaling law for the axial and azimuthal mean velocity profile:

$$\bar{u}_z = C_{u_z} r^{1-a_2/a_1} - \frac{b_1}{a_1 - a_2}, \tag{7.18}$$

$$\bar{u}_\phi = C_{u_\phi} r^{1-a_2/a_1}, \tag{7.19}$$

whereby C_{u_z} and C_{u_ϕ} are constants. In Oberlack (1999) experimental and direct numerical simulation (DNS) data are used to verify the equations (7.18) and (7.19) giving the velocity defect law for the axial mean velocity

$$\frac{\bar{u}_c - \bar{u}_z}{\bar{u}_\tau} = \chi\left(\frac{u_w}{\bar{u}_\tau}\right)\left(\frac{r}{R}\right)^\psi. \tag{7.20}$$

Therein χ is a function of the velocity ratio $u_w/\bar{u}_\tau$ where u_w and $\bar{u}_\tau$ are respectively the wall velocity of the rotating pipe $u_w = R\Omega$ and $\bar{u}_\tau = \sqrt{\tau_w/\nu}$ is the friction velocity and $\bar{u}_c$ is the centerline velocity. ψ is defined as a combination of the group parameter a_1 and a_2:

$$\psi = 1 - \frac{a_2}{a_1}. \tag{7.21}$$

Experiments suggest $\psi \approx 2$, which is interesting enough, close to the value for the laminar flow.

The algebraic scaling law for the azimuthal velocity component is apparent in many experimental and DNS data. It can be rewritten as

$$\frac{\bar{u}_\phi}{u_w} = \zeta\left(\frac{r}{R}\right)^\psi. \tag{7.22}$$

From the symmetry analysis we know that the exponent in (7.20) and (7.22) should have the same value. For ζ Oberlack gives a value close to unity.
The corresponding scaling laws for the Reynolds stresses, respectively the turbulent kinetic energy if the Reynolds stress tensor is contracted and the dissipation rate are:

$$\frac{\overline{u_i' u_j'}}{\bar{u}_\tau^2} = C_{1\overline{u_i' u_j'}}\left(\frac{r}{R}\right)^{2\psi}, \tag{7.23}$$

$$\frac{K}{\bar{u}_\tau^2} = C_{1k}\left(\frac{r}{R}\right)^{2\psi}, \tag{7.24}$$

$$\frac{\epsilon R}{\bar{u}_\tau^3} = C_{1\epsilon}\left(\frac{r}{R}\right)^{3\psi-1}. \tag{7.25}$$

Experiments suggest that the algebraic scaling laws (7.20) and (7.25) only apply for a moderate rotation number. As the rotation number increases, the rotating wall velocity

u_w becomes the dominant velocity scale and the axial velocity changes drastically. For the algebraic law for the axial velocity Oberlack found from comparison with DNS data from Orlandi & Fatica (1997) that it is only valid up to $r/R \approx 0.5$ for this case. The algebraic law for the azimuthal velocity is valid for $0.3 \leqslant r/R \leqslant 0.6$. Below $r/R \approx 0.1$ solid-body rotation is present. These findings are also confirmed in Facciolo (2003).

The second scaling to be taken from (7.17) is derived for $a_1 = a_2 \neq 0$. The parameter b_1 is left arbitrary. This combination of parameters applies if an external velocity scale acts on the flow. For this case a logarithmic mean velocity profile for the axial velocity is received:

$$\bar{u}_z = \frac{b_1}{a_1} \ln(r) + C_{u_z}, \tag{7.26}$$

with C_{2u_z} being constant.

For this scaling law the singularity appears on the pipe axis, not at the wall ($y^+ = 0$) as it is in the classical law of the wall. Oberlack found that (7.26) applies in some section of the radius for rapidly rotating pipes in which the wall velocity dominates the friction velocity $\bar{u}_\tau$ and is therefore the symmetry breaking velocity scale. The corresponding azimuthal velocity is given by

$$\bar{u}_\phi = C_{2u_\phi}, \tag{7.27}$$

with C_{2u_ϕ} being a constant. From (7.26) Oberlack suggests the scaling law

$$\frac{\bar{u}_z}{u_w} = \lambda \ln\left(\frac{r}{R}\right) + \omega. \tag{7.28}$$

For the region of applicability of this new log-law it appears to be valid in the region $0.5 \leqslant r/R \leqslant 0.8$, using data from Orlandi & Fatica (1997). The coefficient λ is negative and approximately equal to -1 and the additive constant ω has been fitted to 0.354. Facciolo (2003) found from his experiments that either the logarithmic region or the value of the coefficient λ differ with the rotation rate. Facciolo performed experiments for the rotation numbers $N = 0.5$, 1.0 and 1.5 and found for $0.5 \leqslant r/R \leqslant 0.8$ corresponding to the three rotation numbers three different values for λ being -2.6, -1.5 and -1.1 respectively. Putting λ for all three rotation numbers equal to -1 he found three different regions of fit for the three different rotation numbers, reaching from $0.3 \leqslant r/R \leqslant 0.5$ to $0.5 \leqslant r/R \leqslant 0.8$.
The corresponding scaling laws for the Reynolds stresses, the turbulent kinetic energy and the dissipationrate are:

$$\frac{\overline{u_i' u_j'}}{\bar{u}_\tau^2} = C_{2\overline{u_i' u_j'}}, \tag{7.29}$$

$$\frac{K}{\bar{u}_\tau^2} = C_{2k}, \tag{7.30}$$

$$\frac{\epsilon R}{\bar{u}_\tau^3} = C_{2\epsilon} \frac{R}{r}. \tag{7.31}$$

7.4 Model performance for axially rotating pipe flow

In the past decades turbulent scaling laws such as for isotropic or homogeneous flows, as well as for inhomogeneous flows, e.g. the logarithmic law of the wall have been the key benchmarks for the model development. Nowadays streamline curvature and rotation became an important modeling issue and hence the rotating pipe is an important new benchmark. Thus, in the present subsection we incorporate the scaling laws mentioned in section 7.3 into linear and non-linear eddy viscosity models as well as into RSTM. The intention is not to discredit any of the models analyzed below but rather to analytically investigate model performance in detail and extract information on necessary model structure for future turbulence modeling.

7.4.1 Linear eddy viscosity models

Modelling the rotating pipe flow with linear eddy viscosity models bears a couple of problems which will be illustrated in the following using the standard $K-\epsilon$ model.
Introducing Boussinesque's eddy viscosity model (3.1) the momentum equations in azimuthal and axial direction are

$$0 = \frac{1}{r^2}\frac{d}{dr}\left(r^3\nu_t\frac{d}{dr}\left(\frac{\bar{u}_\phi}{r}\right)\right) \quad \text{and} \tag{7.32}$$

$$0 = -\frac{d\bar{p}}{dz} + \frac{1}{r}\frac{d}{dr}\left(r\nu_t\frac{d\bar{u}_z}{dr}\right), \tag{7.33}$$

with $\nu_t = C_\mu\frac{K^2}{\epsilon}$.
Writing the $K-\epsilon$ model (3.17) - (3.19) in cylindrical coordinates and invoking the simplifications pertinent for the present test case we obtain

$$0 = \underbrace{\nu_t\left[\left(r\frac{d}{dr}\left(\frac{\bar{u}_\phi}{r}\right)\right)^2 + \left(\frac{d\bar{u}_z}{dr}\right)^2\right]}_{\mathcal{P}} - \epsilon + C_k\frac{1}{r}\frac{d}{dr}\left(\nu_t r\frac{dK}{dr}\right), \tag{7.34}$$

$$0 = C_{\varepsilon 1}\underbrace{\nu_t\left[\left(r\frac{d}{dr}\left(\frac{\bar{u}_\phi}{r}\right)\right)^2 + \left(\frac{d\bar{u}_z}{dr}\right)^2\right]}_{\mathcal{P}}\frac{\epsilon}{K} - C_{\varepsilon 2}\frac{\epsilon^2}{K} + C_\varepsilon\frac{1}{r}\frac{d}{dr}\left(\nu_t r\frac{d\epsilon}{dr}\right). \tag{7.35}$$

The empirical constants are $C_k = 1$, $C_{\varepsilon 1} = 1.44$, $C_{\varepsilon 2} = 1.92$ and $C_\varepsilon = 1/1.3$. It is easy to see that these equations do not contain the rotation rate Ω due to the lack of the Coriolis term. The $K-\epsilon$ model alone is therefore not able to distinguish between a rotating and an inertial system. System rotation may only enter due to boundary conditions.

One can show that the model equations above contain all symmetries given in (7.13) to (7.15). Oberlack (2000*b*) found that the system (7.32)-(7.35) even has one more symmetry which is not contained in the two- and multi-point equations leading to non-physical

behaviour under certain flow conditions such as rotation or streamline curvature. A complete group analysis of the $K-\epsilon$ equations in cylinder coordinates, i.e. the equations (7.32)-(7.35), discloses an additional symmetry of the form:

$$r^* = r\,, \quad \bar{u}_z^* = \bar{u}_z\,, \quad \bar{u}_\phi^* = \bar{u}_\phi + br\,, \quad K^* = K\,, \quad \epsilon^* = \epsilon\,, \tag{7.36}$$

where b represents the group parameter. This additional symmetry allows to add a solid-body rotation to the azimuthal velocity without any change to the remaining flow quantities. Obviously this is unphysical since turbulence is highly sensitive to rotation. This additional unphysical symmetry leads to solid-body-like azimuthal mean velocity to be shown below.

Hirai *et al.* (1988) performed numerical calculations with two two-equation models and one RSTM. In their calculations with the standard $K-\epsilon$ model Hirai et al. found a physically wrong linear profile for the azimuthal velocity.

Furthermore Hirai et al. performed numerical calculations with a modified $K-\epsilon$ model proposed by Launder, Priddin & Sharma (1977). In their modified $K-\epsilon$ model Launder et al. introduced a correction of the source term in the dissipation rate equation by the Richardson number R_i. The modified transport equation for the dissipation rate is then

$$0 = \left[C_{\varepsilon 1}\nu_t\left(\left(r\frac{d}{dr}\left(\frac{\bar{u}_\phi}{r}\right)\right)^2 + \left(\frac{d\bar{u}_z}{dr}\right)^2\right) - C_{\varepsilon 2}(1-\beta R_i)\epsilon\right]\frac{\epsilon}{K} + C_\varepsilon \frac{1}{r}\frac{d}{dr}\left(\nu_t r\frac{d\epsilon}{dr}\right), \tag{7.37}$$

where

$$R_i = \frac{K^2}{\epsilon^2}\frac{\bar{u}_\phi}{r^2}\frac{d}{dr}(r\bar{u}_\phi). \tag{7.38}$$

Due to the additional term in the $\epsilon-$equation the unphysical symmetry (7.36), admitted by the standard $K-\epsilon$ model is broken.

For their numerical calculations Hirai et al. put $\beta = 0.005$. Though the unphysical symmetry (7.36) is broken the calculations still give straight line profiles for the azimuthal velocity component which are in contradiction to the parabolic profiles, which are received from experiments. Interesting enough the calculations with the modified model show an increasing axial velocity $\bar{u}_z$ near the centerline with increasing swirl strength. Nevertheless the predicted radial profile of $\bar{u}_z$ becomes rectilinear when the swirl is sufficiently strong and can not predict the experimental results of the algebraic laminar-like velocity profile (see figure 7.2). This is due to the fact that a symmetry breaking of the scaling of time is imposed due to the structure of the $\epsilon-$equation.
If we introduce the invariant solution (7.20) - (7.25) into the azimuthal momentum equation (7.32) we receive:

$$0 = 2(\psi-1)(\psi+1)C_\mu\frac{C_{1k}^2}{C_{1\epsilon}}\zeta u_w. \tag{7.39}$$

This shows that the linear law, received from the standard $K-\epsilon$ model represents a solution since b, representing the group parameter of the unphysical symmetry of the $K-\epsilon$ model, is cancelled completely out of the equation. The algebraic law is just a solution if $\psi = \pm 1$. Here only the positive sign makes sense since the azimuthal velocity

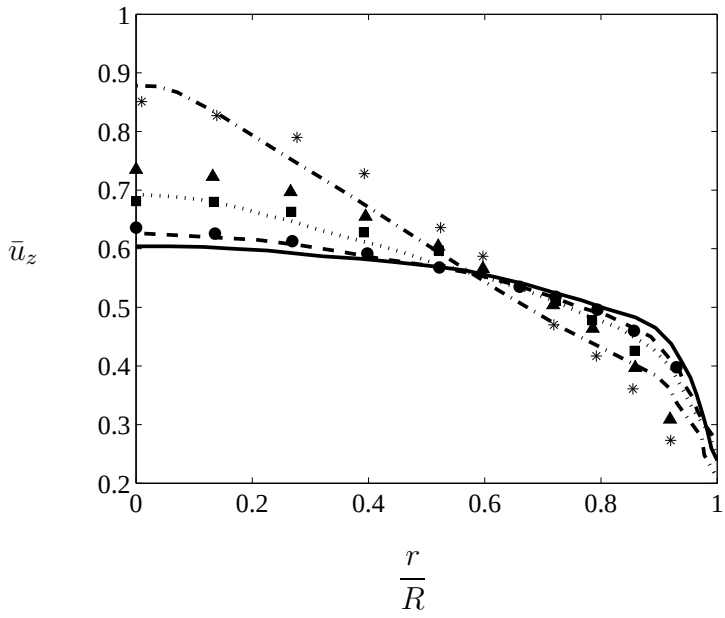

Figure 7.2: Axial velocity profiles calculated with the modified $K-\epsilon$ model Hirai *et al.* (1988) (lines=calculations, plots=experiments from Kikuyama *et al.* (1983*a*)) for $N = 0 : \bullet$, —— ; $N = 0.5 : \blacksquare$, $- - -$; $N = 1 : \blacktriangle$, $\cdots$ and $N = 1.5 :$ $*$, $- \cdot -$.

increases from the axis to the wall. With $\psi = 1$ we receive $a_2 = 0$ corresponding to a symmetry breaking of time in (7.17). This constitutes the linear azimuthal profile which the standard, as well as the modified $K-\epsilon$ model give.
If we now introduce the invariant solutions (7.20) - (7.25) with $\bar{u}_\phi = \zeta u_w r/R$ into the model equations the azimuthal and the axial velocity components decouple completely in the standard model. In the modified model a coupling is received due to the additional term which contains the Richardson number. The Richardson number is then given by

$$R_i = 2\frac{C_{1k}^2}{C_{1\epsilon}^2}\zeta^2\frac{u_w^2}{u_b^2}r^{(-2\psi+2)}R^{(-2\psi+2)}. \tag{7.40}$$

Since R_i has to be nondimensional ψ must equal 1 so that the $r-$dependence cancels out. Thus we receive a rectilinear profile for the axial profile too, which becomes more rectilinear for higher rotation rates, since then the influence of the additional term increases (see figure 7.2).

7.4.2 Non-linear eddy viscosity models

In recent years many non-linear stress-strain relations have been proposed to extend the applicability of linear eddy viscosity models to streamline curvature and rotation at modest computational costs. Pope (1975) was probably the first who suggested a general form of the effective-viscosity formulation in form of a tensor polynomial. Using non-linear

eddy viscosity models guarantees a physically improved modeling of the Reynolds stress tensor and an incorporation of the influence of streamline curvature on the Reynolds stresses. Thus it seems to be promising to apply a non-linear eddy viscosity model to the fully developed rotating pipe flow. Craft, Launder & Suga (1996) as well as Shih, Zhu & Liou (1997) applied a non-linear eddy viscosity model to the rotating pipe flow with good results. The basic assumption behind a non-linear eddy viscosity model is that the Reynolds stresses are uniquely related to the rates of strain (3.21), the rate of rotation (3.22) and scalar quantities. The basic idea of non-linear eddy viscosity models as well as the full tensor basis and the scalar invariants may be taken from section 3.1.4. For the rotating pipe flow the mean strain and rotation rate tensor read

$$\boldsymbol{S} = \frac{1}{2}\begin{pmatrix} 0 & \frac{d\bar{u}_\phi}{dr} - \frac{\bar{u}_\phi}{r} & \frac{d\bar{u}_z}{dr} \\ \frac{d\bar{u}_\phi}{dr} - \frac{\bar{u}_\phi}{r} & 0 & 0 \\ \frac{d\bar{u}_z}{dr} & 0 & 0 \end{pmatrix}, \tag{7.41}$$

$$\boldsymbol{W} = \frac{1}{2}\begin{pmatrix} 0 & -\frac{d\bar{u}_\phi}{dr} - \frac{\bar{u}_\phi}{r} & -\frac{d\bar{u}_z}{dr} \\ \frac{d\bar{u}_\phi}{dr} + \frac{\bar{u}_\phi}{r} & 0 & 0 \\ \frac{d\bar{u}_z}{dr} & 0 & 0 \end{pmatrix}. \tag{7.42}$$

In the following the tensors T^λ and the invariants I_λ are corresponding the tensors, respectively invariants, build from $\boldsymbol{S}$ and $\boldsymbol{W}$ and are thus not dimensionless. These tensors and invariants are given in cylindrical coordinates in appendix D.

Special attention is turned in the following to constrains which break the unphysical symmetry (7.36) which is admitted by linear two-equation models in order to be sensitive to rotation in a physically correct manner.

For a fully developed, rotating, turbulent pipe flow the production term reduces to

$$P = -\overline{u_r' u_z'}\frac{\partial \bar{u}_z}{\partial r} = b_{rz} 2K(S_{[3,1]} + W_{[3,1]}). \tag{7.43}$$

Thus only the $[r,z]$ component of the tensors $\boldsymbol{T}^1 - \boldsymbol{T}^{10}$ gives a contribution. If the ten tensors are written in cylindrical coordinates and the simplifications mentioned in section 7.2 are introduced only the tensors $\boldsymbol{T}^1, \boldsymbol{T}^5, \boldsymbol{T}^6$ and $\boldsymbol{T}^{10}$ have a $[r,z]$ component which is unequal to zero (see appendix D). Considering these four tensors it has been found that the linear solution for the azimuthal velocity is not admitted by $\boldsymbol{T}^5, \boldsymbol{T}^6$ and $\boldsymbol{T}^{10}$. Only these tensors contain a term of the form $r\frac{d\bar{u}_\phi}{dr} + \bar{u}_\phi$ which is not invariant under (7.36) and hence make them sensitive to rotation.

Lets e.g. consider the cubic model introduced by Shih *et al.* (1997), which can be written in terms of the mean strain and rotation rates as

$$\begin{aligned} -\overline{u_i' u_j'} = &-\frac{2}{3}K\delta_{ij} + C_\mu \frac{K^2}{\epsilon} 2\left[S_{ij} - \frac{1}{3}S_{kk}\delta_{ij}\right] + 2B_1\frac{K^3}{\epsilon^2}\left[S_{ik}W_{kj} - W_{ik}S_{kj}\right] - \\ &2B_2\frac{K^4}{\epsilon^3}\left[W_{ik}S_{kj}^2 - S_{ik}^2 W_{kj} + W_{ik}S_{km}W_{mj} - \frac{1}{3}W_{kl}S_{lm}W_{mk}\delta_{ij} + II_S(S_{ij} - \frac{1}{3}S_{kk}\delta_{ij})\right], \end{aligned} \tag{7.44}$$

with $II_S = S_{ij}S_{ji}$. Thus this model contains the tensors $\boldsymbol{T}^5$ and $\boldsymbol{T}^6$ due to which the unphysical symmetry (7.36) of the standard $K-\epsilon$ model is broken.
Interesting enough models containing $\boldsymbol{T}^5$, $\boldsymbol{T}^6$ and $\boldsymbol{T}^{10}$ such as (7.44) may be used to derive the unknown rotation rate dependence of (7.20) due to $\chi\left(u_w/\bar{u}_\tau\right)$.
Using the fundamental condition $\overline{u_r' u_\phi'} = 0$ (see 7.10) we solely consider the $[r,\phi]$ component of equation (7.44). Introducing into this equation the invariant solutions (7.20) - (7.25) equation (7.44) reduces to an algebraic equation, which can be solved easily for the coefficient of the axial velocity component $\chi\left(u_w/\bar{u}_\tau\right)$, giving

$$\chi\left(\frac{u_w}{\bar{u}_\tau}\right) = \sqrt{C_1 \frac{u_w^2}{\bar{u}_\tau^2} + C_2}, \tag{7.45}$$

with C_1 and C_2 being constants respectively combinations of the model constants, the exponent ψ and the coefficients ζ, C_{1k} and $C_{1\epsilon}$.
If we now introduce (7.45) into the expression for the axial velocity component (7.20), we receive the dependence of the axial velocity component on the rotation rate:

$$\frac{u_c - \bar{u}_z}{\bar{u}_\tau} = \sqrt{C_1 \frac{R^2\Omega^2}{\bar{u}_\tau^2} + C_2}\,\left(\frac{r}{R}\right)^\psi, \tag{7.46}$$

whereby $u_w = R\Omega$ has been used. This dependence is confirmed by the numerical calculations done by Shih *et al.* (1997) with their cubic model.

It can be taken from figure 7.3 that this finding is also confirmed by experiments since the profile for $\bar{u}_z$ becomes steeper or in other words $\chi\left(u_w/\bar{u}_\tau\right)$ increases for increasing rotation rates. Using the experiments from Kikuyama *et al.* (1983*a*) the coefficients may be fitted to $C_1 = -0.59$, $C_2 = 0.43$ and $\psi = 2$.

For the second case described in §7.3 for which a logarithmic law for the axial velocity component is received Oberlack (1999) did not comment on the form of the coefficient λ in (7.28). A mathematical term for λ can be received, by following the steps described above. We thus introduce the invariant solutions (7.28)-(7.31) into the non-linear eddy viscosity model and solve then the $[r,\phi]$ component of equation (7.44) for λ. Interesting enough gives this the same expression for λ, which we already received for χ (7.45), whereby the constants are slightly different. Thus the axial velocity component depends on the rotationrate for the second case described in section 7.3 as well. We might then rewrite (7.28) in the following form

$$\frac{\bar{u}_z}{u_w} = \sqrt{C_3 \frac{R^2\Omega^2}{\bar{u}_\tau^2} + C_4} ln\left(\frac{r}{R}\right) + \omega. \tag{7.47}$$

From appendix D it may be taken that the term $r\frac{d\bar{u}_\phi}{dr} + \bar{u}_\phi$ due to which the unphysical symmetry (7.36) of the $K-\epsilon$ model is broken also appears in the invariant I_2 being the only scalar invariant having this property. Furtheron the number of independent invariants reduces to 2, since I_3 and I_4 become zero and I_5 equals $1/2I_1^2$ for the given flow case, as can be taken from appendix D .

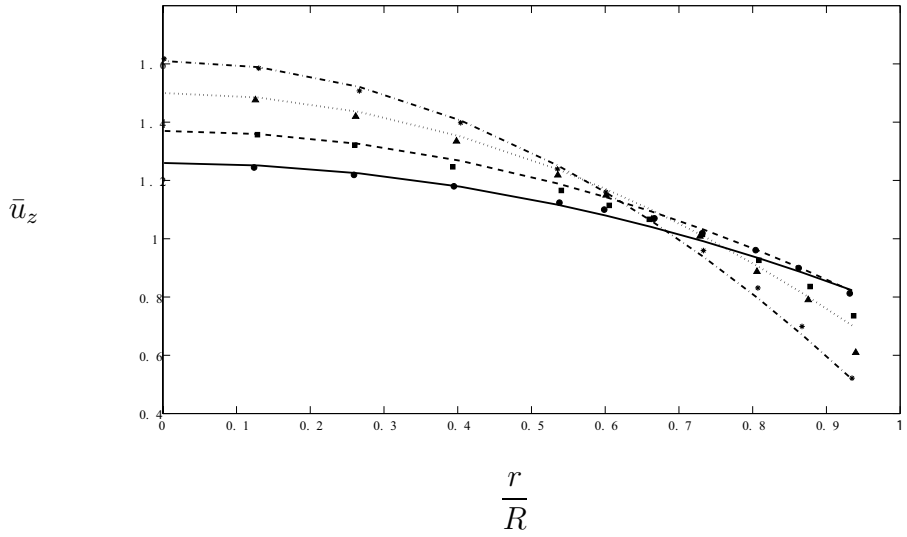

Figure 7.3: Plot of the axial mean velocity in dependence of the rotation rate; Experimental data from Kikuyama *et al.* (1983*a*) for $R_e = 20000$ and fits corresponding to equation (7.46): $N = 0 : \bullet$, —— ; $N = 0.5 : \blacksquare$, − − − ; $N = 1 : \blacktriangle$, $\cdots$ and $N = 1.5 : *$, $-\cdot-$.

This finding may suggest a new model for the eddy viscosity depending on I_2.

Rung (1999) as well as Pettersson Reif *et al.* (1999) proposed modified models for the eddy viscosity which account for streamline curvatures and rotation. The model by Rung is given by

$$C_\mu * = \sqrt{\frac{II_b}{I_1}}. \tag{7.48}$$

where $C_\mu *$ replaces the usual C_μ and $II_b = b_{ij}b_{ji}$. This model implies the dependence of the eddy viscosity on the anisotropy of the Reynolds stresses. Its validity is limited to axisymmetric flows. The same model has been proposed by Jovanović (2002) in order to confirm, that a linear relationship between $\overline{u_i'u_j'}$ and $\bar{S}_{ij}$ holds for axisymmetric strained turbulence. In his derivation of (7.48) Jovanović argued that the effective viscosity grows proportional to the anisotropy of turbulence defined by b_{ij} and the length-scale based on the magnitude of the mean strain rate. However, since only the invariant I_1 is employed in the model for ν_t no symmetry breaking of the unphysical symmetry (7.36) is received and the model does not lead to any improvements for the considered flow case.

Whereas Pettersson Reif *et al.* (1999) proposed a model which encloses the symmetry breaking invariant I_2:

$$C_\mu^{**} = C_\mu \frac{1 + \alpha_2 \mid I_3 \mid + \alpha_3 I_3}{1 + \alpha_4 \mid I_3 \mid} \left(\sqrt{\frac{1 + \alpha_5 I_1}{1 + \alpha_5 I_2}} + \alpha_1 \sqrt{I_2} \sqrt{\mid I_3 \mid - I_3} \right)^{-1}. \tag{7.49}$$

C_μ^{**} is thereby the modified coefficient, which approaches the original value of 0.09 if the streamline curvature or rotation becomes small. Thus this model should account for

rotation but reduce to the standard model for parallel shear flows in an inertial frame of reference. It has been calibrated with reference to the bifurcation diagram for the $\bar{v}^2 - f$ model. For the model coefficients α_i Pettersson Reif *et al.* proposed a dependence on the wall damping function f_μ. The invariants are written in cylindrical coordinates in appendix D. The dependence of the coefficient on the rotation tensor allows to account for system rotation. Since the invariant I_3 becomes zero for the given flow case (7.49) reduces to

$$C_\mu^{**} = \left(C_\mu \sqrt{\frac{1 + \alpha_5 I_1}{1 + \alpha_5 I_2}} \right)^{-1} . \tag{7.50}$$

If we introduce the invariant solutions into the invariants I_1 and I_2 we receive:

$$I_1 = \zeta^2 \frac{u_w^2}{\bar{u}_\tau^2} \left[(\psi - 1)^2 + \frac{1}{2}\psi^2 \right] \left(\frac{r}{R} \right)^{2\psi} \tag{7.51}$$

and

$$I_2 = -\frac{1}{2}\chi^2 \left[(\psi - 1)^2 + \psi^2 \right] \left(\frac{r}{R} \right)^{2\psi} . \tag{7.52}$$

Due to (7.51) and (7.52) the constant C_μ^{**} varies with the ratio of the velocities u_w and $\bar{u}_\tau$ and is thus not a pure constant.

From dimensional arguments the most simple eddy viscosity model which encloses the invariant I_2 and breaks therefore the unphysical symmetry (7.36) is given by:

$$\nu_t = C_\mu \frac{K^2}{\epsilon} f\left(I_2^*\right) . \tag{7.53}$$

The function f should thereby reduce to 1 if flow cases without rotation are considered, so that the calibration of the classical $K - \epsilon$ model with the law of the wall as well as with homogeneous shear is retained. The new model for the eddy viscosity should thus account for shear and rotation, while keeping the standard calibration.

The calibration should be conducted with the help of the invariant solutions (7.20) - (7.25), which are received from the symmetry analysis.

Two different models for the eddy viscosity are used for the production and the diffusion term, since otherwise two different, mutually contradictory expressions for the function f are received from the K- and the ϵ-equation. Hence we use:

$$\nu_{tP} = C_\mu \frac{K^2}{\epsilon} f\left(I_2^*\right) \tag{7.54}$$

and

$$\nu_{tDiff} = C_\mu \frac{K^2}{\epsilon} g\left(I_2^*\right) . \tag{7.55}$$

Introducing the invariant solutions (7.20) - (7.25) into the $K - \epsilon$ model, where the eddy viscosities are given by equation (7.54) and (7.55) and solving for the model functions gives for the function f in (7.54)

$$f\left(I_2^*\right) = \frac{K_1}{\zeta I_2^{*2} + \chi^2} \tag{7.56}$$

and together with (7.45)

$$f\left(I_2^*\right) = \frac{C_3}{I_2^{*2} + C_4}, \tag{7.57}$$

whereby C_3 and C_4 are constants, which are composed of the model constants, and the coefficients ζ, C_{1k}, and $C_{1\epsilon}$ and the exponent ψ in the invariant solutions (7.20) - (7.25). For the function g a constant, composed of the above mentioned parameters is received, so that (7.55) reduces to

$$\nu_{tDiff} = C_\mu^{\star\star} \frac{K^2}{\epsilon}, \tag{7.58}$$

where $C_\mu^{\star\star}$ has a unknown value so far. Keeping in mind, that the calibration with the logarithmic law should be retained, we consider the invariant I_2^* in the logarithmic region. In the logarithmic region I_2^* reduces to

$$\{\boldsymbol{W}^{*2}\} = \left(\frac{K}{\epsilon}\right)^2 \frac{\bar{u}_\tau^2}{4\kappa^2 x_2^2}. \tag{7.59}$$

Since the K and ϵ scale as

$$\epsilon = \frac{\bar{u}_\tau^3}{\kappa x_2} \text{ and } K \simeq \frac{\bar{u}_\tau^2}{0.3^2} \tag{7.60}$$

in the logarithmic region a constant value of $I_2^* = 30.86$ is received. Since the functions f and g should reduce to 1 for flows without rotation the constrains $f(30.86) = 1$ and $g(30.86) = 1$ need to be imposed. From this we receive $C_{1k} = 7.17$ and $C_{1\epsilon} = 6.23$ in the equations (7.24) and (7.25). It should be noted that the modified model is in fact also consistent with homogeneous shear since the value for P/ϵ is kept but the growth rate is slightly increased. Using the models (7.58) and (7.54) with (7.57) in the standard $K - \epsilon$ model leads insofar to a structural improvement for the given flow case, that the unphysical symmetry (7.36) of the standard $K - \epsilon$ model is not admitted anymore and hence the scaling laws of the rotating pipe flow (7.20) and (7.22) are observed.

7.4.3 Reynolds stress models

As it is mentioned in section 7.1 there are a couple of Reynolds stress models which perform quite well at modelling the rotating turbulent pipe flow.

Hirai *et al.* (1988) adopted the Reynolds stress model from Launder, Reece & Rodi (1975) (LRR) for their numerical calculations and compared the results with experiments. Thereby they found that the LRR model quite well predicts the azimuthal mean velocity as well as the dependence of the axial velocity component $\bar{u}_z$ on the rotation rate. In the following this coherence of the LRR model will be derived using the symmetry methods and tensor invariant theory.

For the subsequent analysis it is convenient to rewrite the Reynolds stress transport equation 2.13, which is based on the variables $\overline{u_i' u_j'}$ and ϵ into a set of equations for K, ϵ

and b_{ij}. Rewriting (2.13) in classical notation we obtain

$$\frac{\partial b_{ij}}{\partial t} + \bar{u}_k \frac{\partial b_{ij}}{\partial x_k} = \frac{1}{2K}(P_{ij} + \Pi_{ij} + D^t_{ij} + D^\nu_{ij}) - \frac{1}{k}\left(b_{ij} + \frac{2}{3}\delta_{ij}\right)(P - \epsilon + D^t + D^\nu), \tag{7.61}$$

where

$$\Pi_{ij} = \phi_{ij} - \epsilon^D_{ij}, \tag{7.62}$$

extended by the usual K- and ϵ equation.

Besides the usual closure from the LRR model we adopt a simplified model for the diffusion term

$$D_{ij} = C_s \frac{\partial}{\partial x_k}\left(C_\mu \frac{K^2}{\epsilon}\frac{\partial \overline{u_i' u_j'}}{\partial x_k}\right) \tag{7.63}$$

in order to straighten the subsequent analysis. Taking this simplified model (7.63) for the diffusion term has the advantage, that the diffusion model as well as the convection term in equation (7.61) cancel by introducing the invariant solutions (7.20) - (7.25). Hence the concept of explicit algebraic stress models EARSM (e.g. Gatski & Speziale, 1993), described in chapter 3.4 may be used to express the anisotropy tensor b_{ij} explicitly in terms of the mean velocity gradients to derive a solution for $\bar{u}_z$ in terms of the rotation rate Ω.
For the pressure strain correlation a in b_{ij} tensorially linear model is used (see Gatski & Speziale, 1993) so that an explicit expression for b_{ij} in terms of the mean velocity gradients is obtained.
The tensors T^λ and the scalar invariants I_λ are given in cylindrical coordinates in appendix D. We now make use of the fact (7.10) that $\overline{u_r' u_\phi'} = 0$ or $b_{r\phi} = 0$ and thus take only the $[r, \phi]$ component of equation (3.23). Only the tensors $\widehat{\boldsymbol{T}}^1$, $\widehat{\boldsymbol{T}}^5$, $\widehat{\boldsymbol{T}}^6$ and $\widehat{\boldsymbol{T}}^{10}$ have a $[r, \phi]$ component so that we receive:

$$b_{r\phi} = 0 = G_1 \widehat{\boldsymbol{T}}^1_{[r,\phi]} + G_5 \widehat{\boldsymbol{T}}^5_{[r,\phi]} + G_6 \widehat{\boldsymbol{T}}^6_{[r,\phi]} + G_{10} \widehat{\boldsymbol{T}}^{10}_{[r,\phi]}, \tag{7.64}$$

whereby the solutions for G_λ are given by (3.87).
The full equation (7.64) is quite lengthy and thus not presented here. Nevertheless, introducing the invariant solutions (7.20) - (7.25) into equation (7.64) gives an equation, which can be solved easily for the coefficient of the axial velocity component $\chi\,(u_w/\bar{u}_\tau)$, giving the same expression (7.45), which we already received for the non-linear eddy viscosity models. If this solution is then introduced into the invariant solution for the axial velocity component (7.20) the same dependence (7.46) of the axial velocity on the rotation rate Ω as for the non-linear eddy viscosity models obtained.

The same procedure can be carried out introducing the invariant solutions of the second case described in section 7.3 for which a logarithmic law for the axial velocity component is derived. Insertion of (7.26) - (7.31) into equation (7.64) gives again a reduced equation, which is then solved for λ. This solution is then introduced into (7.28), giving qualitatively the same dependence (7.47) on the rotationrate Ω, which has been derived for the nonlinear eddy viscosity models.

8 Summary and conclusions

In the given thesis symmetry methods are used for the investigation of turbulence models. Hereby three different flow cases are investigated: 1) The shear-free turbulent diffusion with rotation, without rotation and with a constant integral length-scale; 2) The zero-pressure gradient (ZPG) turbulent boundary layer flow; 3) The fully developed rotating turbulent pipe flow. To illustrate the approach to symmetry analysis the Bragg-Hawthorne equation, which is equivalent to the incompressible stationary axisymmetric Euler equations with swirl is investigated.

Thereby it is demonstrated that although the Bragg-Hawthorne equation is an equivalent representation of the incompressible stationary axisymmetric Euler equations with swirl, it is not fully equivalent on the basis of a Lie symmetry analysis. The fully equivalent counterpart is derived, the so called intermediate Euler equations, in general having the structure of integro-differential equations. A local Lie point symmetry analysis of the Bragg-Hawthorne equation, when transformed back to its primitive variables, allows us to see in a very natural way how an integro-differential equation can admit a local symmetry and how a differential equation can admit a non-local symmetry.

For the turbulent diffusion problem a set of three different invariant solutions are constructed based on Lie group analysis of the multi-point correlation equations. The solutions cover classical diffusion-like solution (heat-equation-like) with algebraic spatial decay, decelerating diffusion-wave solution with exponential spatial decay and finite domain diffusion due to rotation. Two-equation model equations and full Reynolds stress equations are investigated whether they capture any of the invariant solutions. Particularly the classical K-ϵ and the LRR model are investigated. All models comply with the diffusion-like solution with algebraic spatial decay. The decay exponent is determined by the model constants while multiple decay exponents are observed. The exponential solution is only admitted by the model equations if the model constants obey certain algebraic relations. For a given set of model constants either the algebraic or the exponential solution is admitted.

It is important to note that the discrepancy between the admitted invariant solutions for the multi-point correlation equations and the one-point model equations lies in the reduced dimensionality of the one-point equations. For the set of classical model constants only the algebraic solution is obtained. Nevertheless, we may not conclude from the one-dimensional case that with the classical model constants exponential solutions are not admitted for the two- or three-dimensional case. In fact it appears to be very likely that these solutions exist for probably all Reynolds stress models at dimensions higher than one.

Additional unresolved problems arise from the experimental verification of the scaling laws

and its Reynolds number dependency. Essentially nothing exists which clearly supports the presented analytical results going beyond the classical law $K \sim x_1^{-n}$. Reynolds number dependency is an unresolved question even from an analytical point of view. Up to this point group theoretical methods have not been able to unravel this problem.

The case of turbulent diffusion with rotation is very difficult to model. Investigating this flow case using symmetry methods, it can be found, that the decay of the turbulent kinetic energy is described by a quadratic equation, meaning that the turbulent diffusion only influences a finite domain for $t \to \infty$. These results can only partly be reproduced by performing large eddy simulations. Here further investigations have to be carried out concerning the scaling of the boundary conditions with the rotation rate. Two models are thoroughly analyzed for the given flow case. One investigated model is the one by Sjögren & Johansson (2000), in which the pressure strain term is modeled as a non-linear function of the mean velocity gradient. This is in contrast to classical approaches where this term is linearly modeled. The other investigated model is the one by Shimomura (1993), where an extension of the ϵ-equation depending on the rotation rate $\mathbf{\Omega}$ is introduced. Both models predict a finite domain diffusion in which the fixed point depends on the rotation rate. Concerning the results of the large eddy simulation, the model from Shimomura Though both models fail in predicting the quadratic decreasing behavior and the constant turbulent time-scale given by the invariant solutions. Hence further investigations have to be carried out in regard of this special flow case.

Investigating parallel turbulent shear-flow, a wide spectrum of Reynolds stress models are tested for their ability to properly capture the new exponential scaling law derived by Oberlack (2001). This scaling law has recently been validated in the mid wake region of high Reynolds number flat-plate boundary layers using experimental data. Thus it should be required that the exponential velocity law is also admitted by the model equations of Reynolds stress models. Implicating the invariant solutions into the model equations it is found that none of the tested models is in accordance with the exponential velocity law. Though from some models we receive conditions for the model constants under which a proper modeling of this scaling law would be possible.

As an example for a flow with rotation, the fully developed rotating turbulent pipe flow is investigated. Using symmetry methods, linear and non-linear eddy viscosity models as well as Reynolds stress models are investigated on their ability to reproduce the scaling laws derived in Oberlack (1999) for this very important testcase in the field of turbulence modeling.

Thereby it is demonstrated why the standard as well as the modified $K-\epsilon$ model do not correctly predict the flow pattern, found in a fully developed rotating pipe flow.
In particular an additional unphysical symmetry of the standard $K-\epsilon$ and other two-equation models is obtained which gives rise to a linear profile for the azimuthal velocity component. This profile is furthermore independent of the rotation rate since the $K-\epsilon$ model does not contain the Coriolis term and is therefore unable to distinguish between a rotating and an inertial system.
Investigating the modified $K-\epsilon$ model proposed by Launder *et al.* (1977) it is shown that this model gives a rectilinear velocity profile for the axial velocity component for

increasing rotation rates because of a symmetry breaking due to the structure of the $\epsilon-$equation.
Considering non-linear eddy viscosity models it is found, that only three tensors of the tensor basis do not admit the additional unphysical symmetry, which is admitted by the standard $K-\epsilon$ model. Furthermore an equation describing the dependence of the axial velocity component on the rotation rate is received from the cubic eddy viscosity model introduced by Shih *et al.* (1997). This dependence is confirmed by the numerical calculations from Shih *et al.* (1997).

Considering the tensor invariants it is found, that only the invariant $I_2 = \{\boldsymbol{W}^2\}$ breaks the unphysical symmetry. Based on this finding a new model for the eddy viscosity is proposed due to which the unphysical symmetry adopted by the standard $K-\epsilon$ model is broken. Using this new model gives qualitatively correct results for the azimuthal velocity components. The invariant solutions can further be used for a calibration of the new model constant C_μ^*. It seems thus to be sufficient to introduce a dependence of one of the model constants onto this invariant. Based on this finding different models for the eddy viscosity introduced by Rung (1999) and Pettersson Reif *et al.* (1999) are investigated.

Finally using the LRR model the same dependency of the axial velocity component on the rotation rate, given by the non-linear eddy viscosity model is derived. Therefore the method of explicit algebraic stress models is adopted. Here the question arises, if it is also possible to derive this coherence from the two-point correlation equations. This should be the subject of future research.

Based on the findings mentioned above, the importance of the symmetry conditions for Reynolds averaged turbulence models derived in Oberlack (2000*b*) are emphasized in the given thesis. It could be shown that the symmetry methods provide a very useful tool for the improvement of existing turbulence models or may be a guideline for the development of new models from first principles.

In the near future more research should be carried out with the purpose to develop new turbulence models and calibrate old ones using symmetry methods. Using this approach leads to turbulence models based on first principles and thus provides a way to "model the physics and not the equations".

Bibliography

Abramowitz, M. & Stegun, I. A. 1968 *Handbook of Mathematical Functions*. Dover Publications.

Ahmadi, G. 1984 On thermodynamics of turbulence. *Bull. American Physical Soc.* **29** (1529).

Ahmadi, G. 1991*a* A thermodynamically consistent rate-dependent model for turbulence. part I: Formulation. *Int. J. Non.-lin.Mech.* **26** (395).

Ahmadi, G. 1991*b* A two-equation turbulence model for compressible flows based on the second law of thermodynamics. *J. Non-equilibrium Thermodynamics* **14**.

Alevlius, K. 1999 Random forcing of three-dimensional homogeneous turbulence. *Phys. Fluids* **11** (7), 1880.

Andreev, V. K., Kaptsov, O. V., Pukhnachov, V. V. & Rodionov, A. A. 1998 *Applications of Group Theoretical Methods in Hydrodynamics*. Kluwer Academic Press.

Baldwin, B. & Lomax, H. 1978 Thin-layer approximation and algebraic model for separated turbulent flows. *AIAA Paper* pp. 78–257.

Bardina, J., Ferziger, J. & Rogallo, R. 1985 Effect of rotation on isotropic turbulence: computation and modelling. *J. Fluid Mech.* **154**, 321–336.

Batchelor, G. & Proudman, I. 1954 The effect of rapid distortion on a fluid in turbulent motion. *Quart. J. Mech. Appl. Math.* **7**, 83–103.

Batchelor, G. K. 1953 *The theory of homogeneous turbulence*. Cambridge University Press.

Bluman, G. W. & Kumei, S. 1989 *Symmetries and Differential Equations*. Springer-Verlag.

Boussinesq, J. 1877 Memoire sur l'influence des frottements dans les mouvements reguliers des fluides. *J. Math. Pures Appl.* **13**, 377–424.

Bragg, S. L. & Hawthorne, W. R. 1950 Some exact solutions of the flow through annular cascade actuator discs. *J. of Aeronautical Sciences* **17**, 243–249.

Briggs, D. A., Ferziger, J. H., Koseff, J. R. & Monismith, S. G. 1996 Entrainment in a shear-free turbulent mixing layer. *J. Fluid Mech.* **310**, 215–241.

Britter, R., Hunt, J. & Mumford, J. 1979 The distortion of turbulence by a circular cylinder. *J. Fluid Mech.* **92**, 269–301.

Bronstein, I. N. & Semendjajew, K. A. 1981 *Taschenbuch der Mathematik*. Verlag Harri Deutsch, 21. Auflage.

Cambon, C., Jacquin, L. & Lubrano, J. 1992 Towards a new Reynolds stress model for rotating turbulent flows. *Phys. of Fluids* **A4** (4), 812–824.

Carminati, J. & Vu, K. 2000 Symbolic computation and differential equations: Lie symmetries. *Journal of Symbolic computation* **29** (1), 95–116.

Cazalbou, J. B. & Bradshaw, P. 1993 Turbulent transport in wall-bounded flows. Evaluation of model coefficients using direct numerical simulation. *Phys. Fluids* **12** (5), 3233–3239.

Cazalbou, J. B. & Chassaing, P. 2001 New results on the model probleme of the diffusion of turbulence from a plane source. *Phys. Fluids* **13** (2), 464–475.

Cazalbou, J. B. & Chassaing, P. 2002 The structure of the solution obtained with Reynolds-stress-transport models at the free stream edge of turbulent flows. *Phys. Fluids* **14** (2), 597–611.

Cazalbou, J. B., Spalart, P. R. & Bradshaw, P. 1994 On the behaviour of two - equation models at the edge of a turbulent region. *Phys. Fluids* **6**, 1797 – 1804.

Cebeci, T. & Smith, A. 1974 Analysis of turbulent boundary layers. In *Ser. in Appl. Math. & Mech.*, , vol. XV. Orlando, Fl.: Academic Press.

Chen, C.-J. & Jaw, S.-Y. 1989 *Fundamentals of turbulence modeling*. London: Combustion: An international series.

Chou, P. 1945 On velocity correlations and the solution of the equations of turbulent fluctuation. *Quart. J. Appl. Math.* **3** (1), 38–54.

Chowdhury, S. & Ahmadi, G. 1990 A thermodynamically consistent rate-dependent model for turbulence. part I: Theory & II: Computational results. *Int. J. Non-Linear Mech.* .

Chung, M. K. & Kim, S. K. 1995 A nonlinear return-to-isotropy model with Reynolds number and anisotropy dependency. *Physics of Fluids* **7**, 1425–1436.

Craft, T. J., Launder, B. & Suga, K. 1996 Development and application of a cubic eddy-viscosity model of turbulence. *Int. J. Heat and Fluid Flow* **17**, 108–115.

Craya, A. 1958 Contribution a l'analyse de la turbulence associtée a des vitesses moyennes. In *Publications Scientific et Techniques du Ministère de l'air*. Paris.

Daly, B. J. & Harlow, F. H. 1970 Transport equations in turbulence. *Physics of Fluids* **13**, 2634–2649.

Davidov, B. I. 1961 On the statistical dynamics of an incompressible turbulent fluid. *Dokl. Akad. Nauk S.S.S.R.* **136**, 47–50.

De Silva, I. P. D. & Fernando, H. J. S. 1994 Oscillating grids as a source of nearly isotropic turbulence. *Phys. Fluids* **6** (7), 2455–2464.

Durbin, P. 1991 Near-wall turbulence closure modeling without 'damping functions'. *Theoret. Comput. Fluid Dyn.* **3**, 1–13.

Durbin, P. A. & Pettersson Reif, B. A. 2001 *Statistical theory and modeling of turbulent flows*. New York: Wiley.

Eggels, J., Boersma, B. & Nieuwstadt, F. 1994 Direct and large-eddy simulations of turbulent flow in an axially rotating pipe. *Tech. Rep.*. Lab. for Aero- and Hydrodynamics, Univ. of Technology, Delft, The Netherlands.

Facciolo, L. 2003 Experimental study of rotating pipe and jet flows. Licantiate Thesis 15. KTH, Stockholm, Sweden, TRITA-MEK.

Fernando, H. J. S. & De Silva, I. P. D. 1993 Note on secondary flows in oscillating grid, mixing box experiments. *Phys. Fluids* **5** (7), 1849–1851.

Fernando, H. J. S. & Long, R. R. 1983 The growth of a grid-generated turbulent mixing layer in a two fluid system. *J. Fluid Mech.* **133**, 377–395.

Frewer, M., Oberlack, M. & Guenther, S. 2005 Symmetry investigations on the incompressible stationary axisymmetric Euler equations with swirl. *submitted to Fluid Dynamics Research* .

Fu, S., Lunder, B. & Tselepidakis, D. 1987 *Tech. Rep.*. TFD/87/5, Mechanical Engineering Department, umist.

Gatski, T. & Wallin, S. 2004 Extending the weak-equilibrium condition for algebraic Reynolds stress models to rotating and curved flows. *J. Fluid Mech.* **518**, 147–155.

Gatski, T. B. & Speziale, C. G. 1993 On explicit algebraic stress models for complex turbulent flows. *J. Fluid Mech.* **254**, 59–78.

Gence, J. & Mathieu, J. 1979 On the application of successive plane strains to grid-generated turbulence. *J. Fluid Mech.* **93**, 501–513.

Gibson, M. & Launder, B. 1978 Ground effects on pressure fluctuations in the atmospheric boundary layer. *J. Fluid Mech.* **86**, 491–511.

Girimaji, S. 1997 A Galilean invariant explicit Reynolds stress model for turbulent curved flows. *Phys. Fluids* **9**, 1067–1077.

Girimaji, S. 2004 A new perspective on realizability of turbulence models. *J. Fluid Mech.* **512**, 1991–210.

Grundestam, O., Wallin, S. & Johansson, A. 2003 A generalized easm based on a nonlinear pressure strain rate model. In *Proc. of the Third Conference on Turbulent Shear Flow Phenomena, TSFP-3*. Sendai, Japan.

Grundestam, O., Wallin, S. & Johansson, A. 2004 Observations on the predictions of fully developed rotating pipe flow using differential and explicit algebraic Reynolds stress models. *submitted to Euro. J. Mech. B/Fluids* .

Guenther, S. & Oberlack, M. 2005*a* Incompatibility of the exponential scaling law for a zero pressure gradient boundary layer flow with Reynolds averaged turbulence models. *Physics of Fluids* **17** (4), 048105.

Guenther, S. & Oberlack, M. 2005*b* Symmetry methods in modelling rotating, turbulent pipe flow. *submitted to J. Fluid Mech.* .

Guenther, S., Oberlack, M., Brethouwer, G. & Johansson, A. 2004 Lie group analysis, LES and modeling of shear-free turbulent diffusion in a rotating frame. In *Advances in Turbulence X, Proc. of the 10th European Turbulence Conference*. Trondheim/Norway.

Halbäck, M., Groth, J. & Johansson, A. 1990 An algebraic model for nonisotropic turbulent dissipation rate term in Reynolds stress closures. *Phys. Fluids* **A 2**, 1859–1866.

Hallbäck, M. & Johansson, A. 1993 Modelling of rotation effects in the $\epsilon-$equation and Reynolds number influence on slow pressure strain in RST closures. In *Proceeding of the 5th International Symposium on Refined Flow Modelling and Turbulence Measurements*, pp. 65–72.

Hanjalić, K. & Launder, B. E. 1972 A Reynolds stress model of turbulence and its application to thin shear flows. *J. Fluid Mech.* **52** (4), 609–638.

Hanjalić, K. & Launder, B. E. 1976 Contribution towards a Reynolds stress closure for low Reynolds number turbulence. *J. Fluid Mech.* **74**, 593–610.

Hannoun, I. A., Fernando, H. J. S. & List, E. J. 1988 Turbulence structure near a sharp density interface. *J. Fluid Mech.* **180**, 189–209.

Harlow, F. H. & Nakayama, P. I. 1967 Turbulent transport equations. *Physics of Fluids* **10**, 2323.

Harlow, F. H. & Nakayama, P. I. 1968 Transport of turbulence energy decay rate. Report LA-3854. Los Alamos Science Laboratory, University of California.

Hirai, S., Takagi, T. & Matsumoto, M. 1988 Predictions of the laminarization phenomena in an axially rotating pipe flow. *J. Fluids Eng.* **110**, 424–430.

Hopfinger, E. J. & Toly, J. A. 1976 Spatially decaying turbulence and its relation to mixing across density interfaces. *J. Fluid Mech.* **78** (1), 155–175.

Hossain, M. 1980 Mathematische Modellierung von turbulenten Auftriebströmungen. PhD thesis, University of Karlsruhe, Karlsruhe.

Ibragimov, N. H. 1995*a* *CRC Handbook of Lie Group Analysis of Differential Equations*, , vol. 1: Symmetries, Exact Solutions, and Conservation Laws. CRC Press.

Ibragimov, N. H. 1995*b* *CRC Handbook of Lie Group Analysis of Differential Equations*, , vol. 2: Applications in Engineering and Physical Sciences. CRC Press.

Ibragimov, N. H. 1996 *CRC Handbook of Lie Group Analysis of Differential Equations*, , vol. 3: New Trends in Theoretical Developments and Computational Methods. CRC Press.

Imao, S., Itoh, M. & Zhang, Q. 1992 The characteristics of spiral waves in an axially rotating pipe. *Experiments in Fluids* **12**, 277–285.

Jacquin, L., Leuchter, O., Cambon, C. & Mathieu, J. 1990 Homogenous turbulence in the presence of rotation. *J. Fluid Mech.* **220**, 1–52.

Jakirlić, S., Hanjalić, K. & Tropea, C. 2002 Modeling rotating and swirling flows: A perpetual challenge. *AIAA Journal* **40** (10), 1984–1996.

Johansson, A. 2003 Turbulence modelling in the rapid homogeneous limit through a generalization of the Reynolds stress concept. Private communication.

Johansson, A. & Hallbäck, M. 1994 Modelling of rapid pressure strain rate in Reynolds stress closures. *J. Fluid Mech.* **269**, 143–168.

Jones, W. P. & Launder, B. E. 1972 The prediction of laminarization with a two-equation model of turbulence. *Int. J. Heat Mass Transfer* **15**, 301–314.

Jou, D., Casas-Vasquez, J. & Lebon, G. 1996 *Extended irreversible thermodynamics*, , vol. 2d ed. Berlin: Springer Verlag.

Jovanović, J. 2002 *The statistical dynamics of turbulence*. Springer COMPLEXITY.

Kassinos, S.C. Langer, C., Haire, S. & Reynolds, W. 2000 Structure-based turbulence modeling for wall bounded flows. *Int. J. Heat Fluid Flow* **21**, 599–605.

Kassinos, S. & Reynolds, W. C. 1994 A structure-based model for the rapid distortion of homogeneous turbulence. Dissertation, Stanford University.

Khor'kova, N. G. & Verbovetsky, A. M. 1995 On symmetry subalgebras and conservation laws for the k-ε turbulence model and the Navier-Stokes equations. *Amer. Math. Soc. Transl.* **167** (2), 61–90.

Khujadze, G. & Oberlack, M. 2004 DNS and scaling laws from new symmetry groups of ZPG turbulent boundary layer flow. *Theoretical and computational fluid dynamics* **18** (5), 391–411.

Kikuyama, K., Murakami, M. & Nishibori, K. 1983*a* Development of three dimensional turbulent boundary layer in an axially rotating pipe. *Trans. ASME J. Fluids Engng.* **105**, 154–160.

Kikuyama, K., Murakami, M., Nishibori, K. & Maeda, K. 1983*b* Flow in axially rotating pipe (a calculation of flow in the saturated region). *Bulletin JSME* **26** (214), 506–513.

Knobloch, K. & Fernholz, H. 2003 Hot-wire and PIV measurements in a high-Reynolds number turbulent boundary layer. In *Progress in Turbulence, Proceeding of the first iTi Conference*.

Kolmogorov, A. N. 1942 Equations of turbulent motion of an incompressible fluid. *Izvestia Academy of Sciences, USSR; Physics* **6**, 56–58.

Kurbatskii, A. & Poroseva, S. 1995 A model for calculating the three components of the excess for the turbulent filed of flow velocity in a round pipe rotating about its longitudinal axis. *High Temperature* **35**, 432–440.

Kurbatskii, A. & Poroseva, S. 1999 Modeling turbulent in a rotating cylindrical pipe flow. *Elsevier* **20**, 341–348.

Launder, B. E., Priddin, C. & Sharma, B. 1977 The calculation of turbulent boundary layers in spinning and curved surfaces. *ASME Journal of Fluids Engineering* **99**, 231–239.

Launder, B. E., Reece, G. E. & Rodi, W. 1975 Progress in the development of Reynolds-stress turbulence closure. *J. Fluid Mech.* **68**, 537–566.

Launder, B. E. & Sharma, B. I. 1974 Application of the energy-dissipation model of turbulence to the calculation of flow near a spinning disc. *Lett. Heat Mas Transf.* **1**, 131–138.

Lee, M., Kim, J. & Moin, P. 1989 Structure of turbulence at high shear rate. *J. Fluid Mech.* **216** (561-583).

Lele, S. K. 1985 A consistency condition for Reynolds stress closures. *Phys. Fluids* **28** (1), 64–68.

Lindgren, B., Österlund, J. M. & Johansson, A. V. 2004 Evaluation of scaling laws derived from Lie group symmetry methods in zero-pressure-gradient turbulent boundary layers. *J. Fluid Mech.* **502**, 127–152.

Long, R. R. 1978 A theory of mixing in a stably stratified fluid. *J. Fluid Mech.* **84**, 113–124.

Lumley, J. 1970 Toward a turbulence constitutive relation. *J. Fluid Mech.* **41**, 413–434.

Lumley, J. 1978 Computational modeling of turbulent flows. *Adv. Appl. Mech.* **18**, 123–176.

Mann, J., Ott, S. & Andersen, J. S. 1999 Experimental study of relative turbulent diffusion. Research report. Riso National Laboratory, Roskilde, Denmark.

Mansour, N., Cambon, C. & Speziale, C. 1991*a* Single point modeling of initially isotropic turbulence under uniform rotation. Annual research briefs. Center of turbulence research.

Mansour, N., Shih, T.-H. & Reynolds, W. 1991*b* The effect of rotation on initially anisotropic homogeneous flows. *Phys. Fluids* **A 3** (2421-2425).

Marshall, J. & Nagdhi, P. 1988 Thermodynamical theory of turbulence i. basic developments. *Phil. Trans. R. Soc. Lond.* **A327**, 415–488.

Maugin, G. 1990 Internal variables and dissipative structures. *J. Non-Equilib. Thermodyn.* **15**, 173–192.

Menter, F. R. 1994 Two-equation eddy viscosity turbulence models for engineering applications. *AIAA Journal* **32** (8), 1598–1605.

Menter, F. R. & Egorov, Y. 2004 Revisiting the turbulent scale equation. In *Proceeding of the IUTAM Aymposium 'One hundred Years of Boundary Layer Research'*. Göttingen.

Mueller, I. & Wilmanski, K. 1986 Extended thermodynamics of non-Newtonian fluid. *Rheol Acta* **25**.

Murakami, M. & Kikuyama, K. 1980 Turbulent flow in axially rotating pipes. *J. Fluid Mech.* **102**, 97–103.

Nokes, R. I. 1988 On the entrainment across a density interface. *J. Fluid Mech.* **188**, 185–204.

Oberlack, M. 1995 A general approach to the pressure-strain correlation using rapid distortion theory. Submitted to TSFP.

Oberlack, M. 1999 Similarity in non-rotating and rotating turbulent pipe flows. *J. Fluid Mech.* **379**, 1–22.

Oberlack, M. 2000*a* On symmetries and invariant solutions of laminar and turbulent wall-bounded flows. *Zeitschrift für Angewandte Mathematik und Mechanik* **80** (11-12), 791–800.

Oberlack, M. 2000*b* *Symmetrie, Invarianz und Selbstähnlichkeit in der Turbulenz*. Habilitationsschrift, Fakultät für Maschinenwese, Rheinisch-Westfählische Technische Hochschule Aachen.

Oberlack, M. 2001 Unified approach for symmetries in plane parallel turbulent shear flows. *J. Fluid Mech.* **427**, 299–328.

Oberlack, M. 2005 Navier-Stokes equations in a rotating frame. Private communication.

Oberlack, M. & Guenther, S. 2003 Shear-free turbulent diffusion - classical and new scaling laws. *Fluid Dynamics Research* **33**, 453–476.

Olver, P. J. 1986 *Applications of Lie Groups to Differential Equations. Graduate Texts in Mathematics* . Springer-Verlag.

Orlandi, P. 1997 Helicity fluctuations and turbulent energy production in rotating and non-rotating pipes. *Phys. Fluids* **9**, 2045–2055.

Orlandi, P. & Ebstein, D. 2000 Turbulent budgets in rotating pipe by DNS. *Int. J. Heat and Fluid Flow* **21** (5), 499–505.

Orlandi, P. & Fatica, M. 1997 Direct simulations of turbulent flow in a pipe rotating about its axis. *J. Fluid Mech.* **343**, 43–72.

Pearson, J. 1959 The effect of uniform distortion on weak homogenous turbulence. *J. Fluid Mech.* **5**, 274–288.

Pettersson, B., Andersson, H. & Brunvoll, A. 1998 Modeling near-wall effects in axially rotating pipe flow by elliptic relaxation. *AIAA* **36**, 1164–1170.

Pettersson Reif, B., Durbin, P. & Ooi, a. 1999 Modeling rotational effects in eddy viscosity closures. *International Journal of Heat and Fluid Flows* **20**, 563–573.

Pilipchuk, M. 1986 Dissertation. PhD thesis, Moscow Physicotechnical Inst.

Pope, S. B. 1975 A more general effective-viscosity hypothesis. *J. Fluid Mech.* **72**, 331–340.

Pope, S. B. 2000 *Turbulent Flows*. Cambridge University Press.

Poroseva, S. 2001 Wall corrections in modeling rotating pipe flow. *Annual Research Briefs, Center for Turbulence Research* .

Poroseva, S., Kassinos, C., Langer, C. & Reynolds, W. 2002 Structure-based turbulence model: Application to a rotating pipe flow. *Physics of Fluids* **14** (4), 1523–1532.

Prandtl, L. 1925 Bericht über Untersuchungen zur Ausgebildeten Turbulenz. *ZAMM* **5** (2), 136–139.

Prandtl, L. 1945 Über ein neues Formelsystem für die ausgebildete Turbulenz. Math.-Phys. Klasse p.6. Nachr. Akad. Wiss.

Reich, G. 1988 Strömung und Wärmeübertragung in einem axial rotierenden Rohr. Dissertation, Technische Universität Darmstadt.

Reynolds, O. 1895 On the dynamical theory of incompressible viscous fluids and the determination of the criterion. *Philos. Trans. R. Soc. London Ser.* **A 186**, 123–164.

Ristorcelli, J. R., Lumley, J. L. & Abid, R. 1995 A rapid-pressure covariance representation consistent with the Taylor-Proudman theorem materially frame indifferent in the two-dimensional limit. *J. Fluid Mech.* **292**, 111–152.

Rodi, W. 1976 A new algebraic relation for calualting the Reynolds stresses. *Z. angew. Math. Mech.* **56**, 219–221.

Rodi, W. 1980 *Prediction mehtods for turbulent flows*, chap. Turbulence models of the ambient medium. Hemisphere Publishing Corporation.

Rodi, W. & Spalding, D. 1970 A two parameter model of turbulene and its application to free jets. *Wärme und Stoffübertragung* **3** (85).

Rotta, J. C. 1951 Statistische Theorie nichthomogener Turbulenz. *1. Mitteilung, Zeitschrift für Physik* **129**, 547–572.

Rotta, J. C. 1968 Über eine Methode zur Berechnung turbulenter Scherströmungen. *Tech. Rep.*. Aerodynamische Versuchsanstalt Göttingen.

Rotta, J. C. 1972 *Turbulente Strömungen*. Teubner, Stuttgart.

Rubinstein, R. & Barton, J. 1990 Nonlinear Reynolds stress models and the renormalization group. *Phys. Fluids* **A 2**, 1472–1476.

Rubinstein, R. & Zhou, Y. 1997 The dissipation rate transport equation and subgrid scale models in rotating turbulence. (97) 63. ICASE Report.

Rubinstein, R. & Zhou, Y. 2004 Turbulence modeling for the axially rotating pipe from the viewpoint of analytical closures. *Theoretical and Computational Fluid Dynamics* **17** (5-6), 299–312.

Rung, T. 1999 Realizability linearer Stress-Strain Beziehungen. Institutsbericht 04/98. Hermann-Föttinger-Institut für Strömungsmechanik, TU Berlin.

Sadiki, A. 1998 Turbulenzmodellierung und Thermodynamik. Habilitationsschrift, TU-Darmstadt.

Sadiki, A., Bauer, W. & Hutter, C. 2000 Thermodynamically consistent coefficient calibration in nonlinear and anisotropic closure models of turbulence. *Continuum Mech. Thermodyn.* **12**, 131–149.

Sadiki, A. & Hutter, C. 1996 On the frame dependence and form invariance of the transport equations for the Reynolds stress tensor and the turbulent heat flux vector: its consequences on closure models in turbulence modelling. *Cont. Mech. and Thermod.* **8**, 341–349.

Sadiki, A. & Hutter, C. 2000 On thermodynamics of turbulence: development of first order closure models and critical evaluation of existing models. *Inter. J. Nonequil. Thermod.* **25** (2), 131–160.

Sadiki, A., Jakirlić, S. & Hanjalić, K. 2003 Towards a thermodynamically consistent, anisotropy-resolving turbulence model for conjugate flow, heat and mass transfer. In *4th Int. Symp. on Turbulence, Heat and Mass Transfer, Antalya, Turkey*.

Safarov, N. 1986 Dissertation. PhD thesis, Moscow Physicotechnical Inst.

Saffman, P. G. 1970 A model for inhomogenous turbulent flows. *Proc R. Soc. Lond.* **A317**, 417–433.

Sambasivam, A., Girimaji, S. & Poroseva, S. 2004 Realizability of the Reynolds stress and rapid pressure-strain correlation in turbulence modelling. *Journal of Turbulence* .

Sarkar, S. & Speziale, C. 1990 A simple nonlinear model for return to isotropy of turbulence. *Phys. Fluids A* **2**, 84–93.

Schumann, U. 1977 Realizability of Reynolds stress turbulence models. *Phys. Fluids* **20**, 721–725.

Shih, T.-H. & Lumley, J. 1985 *Tech. Rep.* 85-3. FDA, Cornell University.

Shih, T.-H., Zhu, J. & Liou, W. W. 1997 Modeling of turbulent swirling flows. In *Proc. eleventh symposium on turbulent shear flows*, , vol. 3.

Shimomura, Y. 1989 A statistically derived two-equation model of turbulent flows in a rotating system. *Journal of the Physical Society of Japan* **58**, 352–355.

Shimomura, Y. 1993 Near-wall turbulent flows. In *Proceedings of the In- ternational Conference on Near-Wall Turbulent Flows*. Tempe, Arizona, U.S.A.

Shy, S. S. & Beidenthal, R. E. 1991 Turbulent stratified interfaces. *Phys. Fluids* **5**, 1278–1285.

Shy, S. S., Tang, C. Y. & Fann, S. Y. 1997 A nearly isotropic tubulence generated by a pair of vibrating grids. *Exp. thermal Fluid Sci.* **14**, 251–262.

Sjögren, T. 1997 Development and validation of turbulence models through experiment and computation. Doctoral thesis, Dept. of Mechanics, KTH, Stockholm, Sweden.

Sjögren, T. & Johansson, A. V. 2000 Development and calibration of algebraic nonlinear models for terms in the Reynolds stress transport equation. *Phys. Fluids* **12** (6), 1554–1572.

Smagorinsky, J. 1963 General circulation experiments with the primitive equations. *Mon. Weath. Rev.* **91**, 99–164.

So, R. & Yoo, G. 1986 On the modeling of low-Reynolds-number turbulence. *Tech. Rep.* 3994. NASA Contractor Report.

Spalart, P. R. 1988 Direct numerical simulation of a turbulent boundary layer up to $Re_\theta = 1410$. *J. Fluid Mech.* **187**, 61–98.

Spalart, P. R. & Allmaras, S. R. 1992 A one-equation turbulence model for aerodynamic flow. In *30th AIAA Aerospace Sciences Meeting, Reno, USA*, , vol. 92-0439. Reno, U.S.A.

Spalding, D. 1967 The calculation of the length scale of turbulence in some turbulent boundary layers remote from walls. Heat Transfer Section Rep. (TWF/TN/31). Imperial College, Dept. Mech. Eng.

Spalding, D. 1971 The k$-\omega$ model of turbulence. Report (TM/TN/A/16). Imperial College, Dept. Mech. Eng.

Spencer, A. J. M. 1971 Theory of invariants. In *Continuum Physics* (ed. A. C. Eringen), , vol. 1, Mathematics, chap. III, pp. 239–353. Academic Press.

Speziale, C. G. 1987 On non-linear $k-l$ and $k-\epsilon$ models of turbulence. *J. Fluid Mech.* **178**, 459–475.

Speziale, C. G., Mansour, N. N. & Rogallo, R. S. 1987 The decay of isotropic turbulence in a rapidly rotating frame. In *Studying Turbulence Using Numerical Simulation Databases* (ed. P. Moin, W. C. Reynolds & J. Kim), pp. 205–211. Center for Turbulence Research, Stanford University/NASA Ames, CA, USA.

Speziale, C. G., Sarkar, S. & Gatski, T. B. 1991 Modelling the pressure-strain correlation of turbulence: an invariant dynamical systems approach. *J. Fluid Mech.* **227**, 245–272.

Speziale, C. G., Younis, B. A. & Berger, S. A. 2000 Analysis and modelling of turbulent flow in an axially rotating pipe. *J. Fluid Mech.* **407**, 1–26.

Srdic, a., Fernando, H. J. S. & Montenegro, L. 1996 Generation of nearly isotropic turbulence using two oscillating grids. *Exp. Fluids* **20** (5), 395–397.

Thompson, S. & Turner, J. 1975 Mixing across an interface due to turbulence generated by an oscillating grid. *J. Fluid Mech.* **67** (2), 349–368.

Townsend, A. A. 1976 *Structure of Turbulent Shear Flow*. Cambridge Univ. Press., England.

Umlauf, L. 2001 Turbulence parameterisation in hydrobiological models for natural waters. Dissertation, Technische Universität Darmstadt.

Van Driest, E. R. 1956 On the turbulent flow near a wall. *J. Aero. Sci.* **23**, 1007–1011.

Wallin, S. & Johansson, A. 2000 An explicit algebraic Reynolds stress model for incompressible and compressible turbulent flows. *J. Fluid. mech.* **403**, 89–132.

Wallin, S. & Johansson, A. 2001 Modelling of streamline curvature effects on turbulence in explicit algebraic Reynolds stress models. In *Proceeding of Turbulence and Shear Flow Phenomena II*, , vol. II. Stockholm.

Wallin, S. & Johansson, A. 2002 Modelling streamline curvature effects in explicit algebraic Reynolds stress turbulence models. *Int. J. Heat Fluid Flow* **23**, 721–730.

Wallin, S. & Martensson, G. 2004 A general 1D-solver for partial differential equations. Internal report. Department of Mechanics, KTH, Stockholm, Sweden.

Wiegeland, R. & Nagib, H. 1978 Grid-generated turbulence with and without rotation about the streamwise direction. *Tech. Rep.* R 78-1. IIT Fluids and Heat Transfer Rep.

Wilcox, C. D. 1993 *Turbulence Modeling for CFD*. Griffin Printing, Glendale, California.

Yoshizawa, A. 1984 Statistical analysis of the derivation of the Reynolds stress from its eddy-viscosity representation. *Phys. Fluids* **27**, 1377–1387.

Zaets, P., Kurbatskii, A., Onufriev, A., Poroseva, S., Safarov, N., Safarov, R. & Yakovenko, S. 1998 Experimantal study and mathematical simulation of the characteristics of a turbulent flow in a straight circular pipe rotating about its longitudinal axis. *J. of Applied Mechanics and Technical Physics* **39**, 249–260.

Zaets, P., Safarov, N. & Safarov, R. 1985 Experimantal study of the turbulence characteristics behavior under rotating a pipe around its longitudinal axis (in russian). *Current Problems of Continuum Mechanics* pp. 136–142.

Zawistowski, Z. 2001 *Symmetries of Integro-Differential Equations*, *269*, vol. 48. Rep. Math. Phys.

Author index

A Navier-Stokes equations in a rotating frame

Since rotating flows play a very important role in engineering applications as e.g. turbomachinery or aeronautics and are thus frequently used as testcases for every kind of turbulence model, the Navier-Stokes equations in a rotating frame have been written down here Oberlack (2005).

Introduced variables:

$$\begin{aligned} x_k^* &= Q_{kl} x_l & &\Rightarrow x_k = Q_{kl}^T x_l^* \\ u_i^* &= Q_{ik} u_k + \dot{Q}_{in} x_u & &\Rightarrow u_i = Q_{ik}^T \left[u_k^* - e_{lkm} \Omega_l x_m^* \right] \end{aligned}$$

where

$$\begin{aligned} Q_{ik} Q_{kj}^T = Q_{ik}^T Q_{kj} &= \delta_{ij} & &\text{and } |Q| = 1 \\ \dot{Q}_{ik} Q_{jk} &= e_{kij} \Omega_k & &\Rightarrow \frac{d}{dt} \left(\dot{Q}_{ik} Q_{jk} \right) = e_{kij} \dot{\Omega}_k \end{aligned}$$

Derivatives:

$$\begin{aligned} \frac{\partial}{\partial x_k} &= Q_{kl}^T \frac{\partial}{\partial x_l^*} & &\Rightarrow \frac{\partial^2}{\partial x_k^2} = Q_{kl}^T Q_{km}^T \frac{\partial^2}{\partial x_k^2 \partial x_m^2} = \frac{\partial^2}{\partial x_k^{*}} \\ \frac{\partial}{\partial t} &= \frac{\partial}{\partial t} + \dot{Q}_{kl} Q_{lm}^T x_m^* \frac{\partial}{\partial x_k^*} = \frac{\partial}{\partial t} + e_{lKm} \Omega_l x_m^* \frac{\partial}{\partial x_k^*} \end{aligned}$$

Navier-Stokes in an initial frame:

$$\frac{\partial u_i}{\partial t} + u_k \frac{\partial u_i}{\partial x_k} = -\frac{\partial p}{\partial x_i} + \nu \frac{\partial^2 u_i}{\partial x_k^2}$$

Navier-Stokes in a rotating frame:

$$\begin{aligned} &\left[\frac{\partial}{\partial t} + e_{lkm} \Omega_l x_m^* \frac{\partial}{\partial x_k^*} \right] \left[Q_{ip}^T \left(u_p^* - e_{qpr} \Omega_q x_r^* \right) \right] \\ &+ \left[Q_{sp}^T \left(u_p^* - e_{qpr} \Omega_q x_r^* \right) \right] Q_{st}^T \frac{\partial}{\partial x_t^*} \left[Q_{ik}^T \left(u_k^* - e_{lkm} \Omega_l x_m^* \right) \right] \\ &= -Q_{ik}^T \frac{\partial p}{\partial x_k^*} + \nu \frac{\partial^2}{\partial x_k^{*2}} \left[Q_{ik}^T \left(u_k^* - e_{lkm} \Omega_l x_m^* \right) \right] \end{aligned}$$

$$
\begin{aligned}
&\Rightarrow \dot{Q}^T_{ip}\left(u^*_p - e_{qpr}\Omega_q x^*_r\right) + Q^T_{ip}\left(\frac{\partial u^*_p}{\partial t} - e_{qpr}\dot{\Omega}^*_q x^*_r\right)\\
&+ Q^T_{ip}e_{lkm}\Omega_l x^*_m\frac{\partial u^*_p}{\partial x^*_k} - Q^T_{ip}e_{lkm}\Omega_l x^*_m e_{qpr}\Omega_q\delta_{kr}\\
&+ Q^T_{ik}\left[u^*_p\frac{\partial u^2_k}{\partial x^*_p} - u^*_p e_{lkm}\Omega_l\delta_{pm} - e_{qpr}\Omega_q x^*_r\frac{\partial u^*_k}{\partial x^*_p} + e_{qpr}\Omega_q x^*_r e_{lkm}\Omega_l\delta_{pm}\right]\\
&= -Q^T_{ik}\frac{\partial p}{\partial x^*_k} + \nu Q^T_{ik}\frac{\partial^2 u^*_k}{\partial x^{*^2}_n}|Q_{ai}\\
&\Rightarrow \frac{\partial u^*_a}{\partial t} + u^*_p\frac{\partial u^*_a}{\partial x^*_p} = -\frac{\partial p}{\partial x^*_a} + \nu\frac{\partial^2 u^*_a}{\partial x^{*^2}_n}\\
&- e_{ipa}\Omega_i\left(u^*_p - e_{qpr}\Omega_q x^*_r\right) + e_{qar}\dot{\Omega}_q x^*_r + u^*_m e_{lam}\Omega_l\\
&+ e_{lkm}\Omega_l x^*_m e_{qak}\Omega_q - e_{qmr}\Omega_q x^*_r e_{lam}\Omega_l\\
&\Rightarrow \frac{\partial u^*_a}{\partial t} = -\frac{\partial p}{\partial x^*_a} + \nu\frac{\partial^2 u^*_a}{\partial x^{*^2}_k} - e_{kla}\dot{\Omega}_k x^*_l - 2e_{kla}\Omega_k u^*_l\\
&+ e_{kla}\Omega_k e_{plq}\Omega_p x^*_q + e_{kal}\Omega_k e_{plq}\Omega_p x^*_q - e_{kal}\Omega_k e_{plq}\Omega_p x^*_q\\
&\Rightarrow \boxed{\frac{\partial u^*_i}{\partial t} = -\frac{\partial p}{\partial x^*_i} + \nu\frac{\partial^2 u^*_i}{\partial x^{*^2}_k} - e_{kli}\dot{\Omega}_k x^*_l - 2e_{kli}\Omega_k u^*_l - e_{kli}\Omega_k e_{pql}\Omega_p x^*_q}
\end{aligned}
$$

with

$$
\begin{aligned}
&- e_{kli}\Omega_k e_{pql}\Omega_p x^*_q\\
&= -\left(\delta_{ip}\delta_{kq} - \delta_{iq}\delta_{kp}\right)\Omega_k\Omega_p x^*_q\\
&= -\left(\Omega_i\Omega_k x^*_k - x^*_i\Omega_k\Omega_k\right)
\end{aligned}
$$

2D Navier Stokes equation in a rotating frame about x_3: $\underline{u} = \underline{u}(x_1 x_2 \cdot t)$

$$\frac{\partial u^*}{\partial t} = -\frac{\partial p}{\partial x_i^*} + \nu \frac{\partial^2 u_i^*}{\partial x_k^{*^2}} - 2e_{3li}\Omega_3 u_l^* + \delta_{i1}\Omega_3^2 x_1^* + \delta_{i2}\Omega_3^2 x_2^*$$

Stream function:

$$\begin{aligned}
u_1^* =& \frac{\partial \Psi^*}{\partial x_2^*} \,; u_2^* = -\frac{\partial \Psi^2}{\partial x_1^*} \Rightarrow \Psi^* = \int_s (u_1^* dx_2^* - u_2^* dx_1^*) + \Psi_0 \\
\Rightarrow \frac{\partial u^*}{\partial t} =& -\frac{\partial p}{\partial x_i^*} + \nu \frac{\partial^2 u_i^*}{\partial x_k^{*^2}} + \delta_{i1}\left[2\Omega_3 u_2^* + \Omega_3^2 x_1^*\right] + \delta_{i2}\left[-2\Omega_3 u_1^* + \Omega_3^2 x_2^*\right] \\
=& \nu \frac{\partial^2 u_i^*}{\partial x_u^{*^2}} - \frac{\partial p}{\partial x_i^*} + \delta_{i1}\left[-\Omega_3 2\frac{\partial \Psi^*}{\partial x_1^*} + \Omega_3^2 \frac{\partial}{\partial x_1^*}\left(\frac{1}{2} x_1^{*^2}\right)\right] \\
& + \delta_{i2}\left[-\Omega_3 2\frac{\partial \Psi^*}{\partial x_2^*} + \Omega_3^2 \frac{\partial}{\partial x_2^*}\left(\frac{1}{2} x_2^{*^2}\right)\right] \\
=& \nu \frac{\partial^2 u_i^*}{\partial x_k^2} - \frac{\partial}{\partial x_i^*} \underbrace{\left[p + \Omega_3 2\Psi^* - \Omega_3^2 \frac{1}{2}\left(x_1^{*^2} + x_2^{*^2}\right)\right]}_{p^*} \\
p^* =& p + 2\Omega_3 \Psi^* - \Omega_3^* \frac{1}{2}\left(x_1^{*^2} + x_2^{*^2}\right) \\
\Rightarrow p^* =& p + 2\Omega_3 \Psi - \Omega_3^2 \frac{3}{2}\left(x_1^{*^2} + x_2^{*^2}\right) \quad \text{to be shown!}
\end{aligned}$$

Auxiliary calculation:

$$
\begin{aligned}
& 2\int u_1^* dx_2^* - 2\int u_2^* dx_1^* - \Omega\frac{1}{2}\left(x_1^{*^2} + x_2^{*^2}\right) \\
=& 2\int \left(Q_{11}u_1 + Q_{12}u_2 + \dot{Q}_{11}x_1 + \dot{Q}_{12}x_2\right) d\left(Q_{21}x_1 + Q_{22}x_2\right) \\
& - \int \left(Q_{21}u_1 + Q_{22}u_2 + \dot{Q}_{21}x_1 + \dot{Q}_{22}x_2\right) d\left(Q_{11}x_1 + Q_{12}x_2\right) \\
& - \frac{1}{2}\Omega\left(\left(Q_{11}x_1 + Q_{12}x_2\right)^2 + \left(Q_{21}x_1 + Q_{22}x_2\right)^2\right) \\
=& 2\int \left(\cos(\cdot)u_1 - \sin(\cdot)u_2 - \Omega\sin(\cdot)x_1 - \Omega\cos(\cdot)x_2\right) d\left(\sin(\cdot)x_1 + \cos(\cdot)x_2\right) \\
& - 2\int \left(\sin(\cdot)u_1 + \cos(\cdot)u_2 + \Omega\cos(\cdot)x_1 - \Omega\sin(\cdot)x_2\right) d\left(\cos(\cdot)x_1 - \sin(\cdot)x_2\right) \\
& - \frac{1}{2}\left[\left(\cos(\cdot)x_1 - \sin(\cdot)x_2\right)^2 + \left(\sin(\cdot)x_1 + \cos(\cdot)x_2\right)^2\right]\Omega \\
=& 2\int \Bigg[\underbrace{\left(\cos(\cdot)\sin(\cdot) - \sin(\cdot)\cos(\cdot)\right)}_{=0} u_1 + \left(-\sin^2(\cdot) - \cos^2(\cdot)\right) u_2 \\
& + \Omega\left(-\sin^2(\cdot) - \cos^2(\cdot)\right) x_1 + \Omega\left(\underbrace{-\cos(\cdot)\sin(\cdot) + \sin(\cdot)\cos(\cdot)}_{=0}\right) x_2\Bigg] dx_1 \\
& + 2\int \Big[\left(\cos^2(\cdot) + \sin^2(\cdot)\right) u_1 + \left(\underbrace{-\sin(\cdot)\cos(\cdot) + \cos(\cdot)\sin(\cdot)}_{=0}\right) u_2 \\
& + \Omega\left(-\sin(\cdot)\cos(\cdot) + \cos(\cdot)\sin(\cdot)\right) x_1 + \Omega\left(-\cos^2(\cdot) - \sin^2(\cdot)\right) x_2\Big] dx_2 \\
& - \frac{\Omega}{2}\left[\left(\cos^2(\cdot) + \sin^2(\cdot)\right) x_1^2 + (\ldots) x_2^2\right]
\end{aligned}
$$

$$
\begin{aligned}
&= -2\int \left[u_2 + \Omega x_1\right] dx_1 + 2\int \left[u_1 - \Omega x_2\right] dx_2 \\
&\quad - \frac{\Omega}{2}\left[x_1^2 + x_2^2\right] \\
&= 2\int u_1 x_2 - 2\int u_2 dx_1 - \frac{\Omega}{2}\left(x_1 + x_2^2\right) 3
\end{aligned}
$$

B Attempt to solve the linear Bragg-Hawthorne equation

In this appendix we try to determine the general analytical solution of the linear Bragg-Hawthorne equation

$$\psi_{zz} + \psi_{rr} - \frac{1}{r}\psi_r = r^2(\alpha\psi + \beta) + (\gamma\psi + \delta). \tag{B.1}$$

The general solution of this linear PDE can be split into a homogeneous and an inhomogeneous part

$$\psi(r, z) = \psi_{\mathrm{H}}(r, z) + \psi_{\mathrm{I}}(r, z). \tag{B.2}$$

The general solution of the homogeneous equation ($\beta = 0, \delta = 0$) is constructed by the method of separation of variables by writing

$$\psi_{\mathrm{H}}(r, z) = f(r) \cdot g(z), \tag{B.3}$$

where $g(z)$ can be easily determined as

$$g(z) = c_1 \sin\left(z\sqrt{\lambda - \gamma}\right) + c_2 \cos\left(z\sqrt{\lambda - \gamma}\right), \tag{B.4}$$

where λ is a real arbitrary constant. The function $f(r)$ obeys the following ordinary differential equation

$$f_{rr} - \frac{1}{r}f_r - (\lambda + \alpha r^2)f = 0. \tag{B.5}$$

Depending on the value of α we obtain the following set of solutions

- $\alpha = 0$: the substitution of the expression $f(r) = r \cdot F\left(r\sqrt{-\lambda}\right)$ turns equation (B.5) into Bessel's differential equation

  $$x^2F''(x) + xF'(x) + (x^2 - 1)F(x) = 0, \tag{B.6}$$

  with its general solution

  $$F(x) = c_3 \cdot J_1(x) + c_4 \cdot Y_1(x), \tag{B.7}$$

  where J and Y represent the linear independent Bessel functions of the first and second kind respectively (Abramowitz & Stegun, 1968), with $x = r\sqrt{-\lambda}$.

- $\alpha \neq 0$: the substitution of the expression $f(r) = r^2\sqrt{\alpha}e^{-\frac{1}{2}r^2\sqrt{\alpha}}F\left(r^2\sqrt{\alpha}\right)$ turns equation (B.5) into Kummer's differential equation

  $$xF''(x) + (2 - x)F'(x) - \left(1 + \frac{\lambda}{4\sqrt{\alpha}}\right)F(x) = 0, \tag{B.8}$$

with its general solution

$$F(x) = c_3 \cdot M_{1+\frac{\lambda}{4\sqrt{\alpha}},2}(x) + c_4 \cdot U_{1+\frac{\lambda}{4\sqrt{\alpha}},2}(x), \tag{B.9}$$

where M and U represent the linear independent confluent hypergeometric functions being at the origin regular and irregular respectively (Abramowitz & Stegun, 1968), with $x = r^2\sqrt{\alpha}$. The corresponding functions $f(r)$ as given above are called Whittaker functions (Abramowitz & Stegun, 1968).

This completes the general investigation of the homogeneous part of the linear Bragg-Hawthorne equation (B.1). Depending on whether α is zero or not, the homogeneous solutions are either proportional to Bessel functions or to Whittaker functions respectively.
The most difficult part of determining the general solution of (B.1) is now to construct a special solution of the inhomogeneous part. By taking care not to end up in a contradiction, we will look for a special solution which only depends on the radius $\psi_{\mathrm{I}}(r, z) = w(r)$, obeying

$$w_{rr} - \frac{1}{r}w_r - (\alpha r^2 + \gamma)w = \beta r^2 + \delta. \tag{B.10}$$

For this ordinary linear differential equation of second order for $w(r)$, it is everything but easy to find a special solution. A reasonable way is to split it up again into a homogeneous and a inhomogeneous part

$$w(r) = w_{\mathrm{H}}(r) + w_{\mathrm{I}}(r). \tag{B.11}$$

From the theory of ordinary linear differential equations of second order, it is always possible to construct the inhomogeneous solution out of the knowledge of the general homogeneous solution. If the homogeneous solution is given as

$$w_{\mathrm{H}}(r) = c_5 \cdot h_1(r) + c_6 \cdot h_2(r), \tag{B.12}$$

the inhomogeneous solution in our case takes on the structure (Bronstein & Semendjajew, 1981)

$$w_{\mathrm{I}}(r) = h_2(r) \int \frac{F(r)}{r} h_1(r) dr - h_1(r) \int \frac{F(r)}{r} h_2(r) dr, \tag{B.13}$$

with $F(r) = \beta r^2 + \delta$ being the inhomogeneous term of equation (B.10). Since its homogeneous part is the same as in equation (B.5), the functions $h_i(r)$ will be proportional either to Bessel or to Whittaker functions depending on whether α is zero or not, leading to solutions (B.13) of great complexity. Especially for integrals over Whittaker functions there exists no analytical nor a numerical theory to simplify or calculate a quantity like (B.13) properly. For achieving progress, the only reasonable way is to solve the differential equation (B.10) directly in the usual numerical fashion.

C The B-tensor model

The complete ansatz for the sixth rank B-tensor can be written

$$
\begin{aligned}
B_{ijpqrs} =& c_1 2K\delta_{ij}N_{pqrs} + c_2 2K\left[\delta_{ip}N_{jrsq} + \delta_{iq}N_{jprs} + \delta_{ir}N_{jpqs} + \delta_{is}N_{jpqr}\right] \\
&+ \left(c_3 R_{ij} + c_4 Y_{ij}\right) N_{pqrs} \\
&+ c_5\left(R_{mp}N_{nqrs} + R_{mq}N_{nprs} + R_{mr}N_{npqs} + R_{ms}N_{npqr}\right)\left(\delta_{im}\delta_{jn} + \delta_{in}\delta_{jm}\right) \\
&+ c_6\left(Y_{mp}N_{nqrs} + Y_{mq}N_{nprs} + Y_{mr}N_{npqs} + Y_{ms}N_{npqr}\right)\left(\delta_{im}\delta_{jn} + \delta_{in}\delta_{jm}\right) \\
&+ c_7\delta_{ij}\left(\delta_{pq}R_{rs} + \delta_{pr}R_{qs} + \delta_{qr}R_{ps} + \delta_{ps}R_{qr} + \delta_{qs}R_{pr} + \delta_{rs}R_{pq}\right) \\
&+ c_8\delta_{ij}\left(\delta_{pq}Y_{rs} + \delta_{pr}Y_{qs} + \delta_{qr}Y_{ps} + \delta_{ps}Y_{qr} + \delta_{qs}Y_{pr} + \delta_{rs}Y_{pq}\right) \\
&+ c_9\left(R_{pq}N_{ijrs} + R_{pr}N_{ijqs} + R_{ps}N_{ijqr} + R_{qr}N_{ijps} + R_{qs}N_{ijpr} + R_{rs}N_{ijpq}\right) \\
&+ c_{10}\left(Y_{pq}N_{ijrs} + Y_{pr}N_{ijqs} + Y_{ps}N_{ijqr} + Y_{qr}N_{ijps} + Y_{qs}N_{ijpr} + Y_{rs}N_{ijpq}\right) \\
&+ c_{11}\delta_{ij}\left(M_{rspq} + M_{psrq} + M_{qspr} + M_{pqsr} + M_{prsq} + M_{qrps}\right) \\
&+ c_{12}\left(\delta_{qr}M_{ijps} + \delta_{qs}M_{ijpr} + \delta_{rs}M_{ijpq} + \delta_{pr}M_{ijqs} + \delta_{ps}M_{ijqr} + \delta_{pq}M_{ijrs}\right) \\
&+ c_{13}\left(\delta_{qr}M_{psij} + \delta_{qs}M_{prij} + \delta_{rs}M_{pqij} + \delta_{pr}M_{psij} + \delta_{ps}M_{qrij} + \delta_{pq}M_{rsij}\right) \\
&+ c_{14}\left(\delta_{qr}M^{h1}_{ispj} + \delta_{qs}M^{h1}_{iprj} + \delta_{rs}M^{h1}_{ipqj} + \delta_{pr}M^{h1}_{iqsj} + \delta_{ps}M^{h1}_{iqrj} + \delta_{pq}M^{h1}_{irsj}\right) \\
&+ c_{15}\left(\delta_{ip}M^{h2}_{jqrs} + \delta_{jp}M^{h2}_{iqrs} + \delta_{iq}M^{h2}_{jprs} + \delta_{jq}M^{h2}_{iprs} + \delta_{ir}M^{h2}_{jpqs} + \delta_{jr}M^{h2}_{ipqs}\right. \\
&\left.+\delta_{is}M^{h2}_{jpqr} + \delta_{js}M^{h2}_{ipqr}\right) \\
&+ c_{16}\left(\delta_{ip}M^{h3}_{jqrs} + \delta_{jp}M^{h3}_{iqrs} + \delta_{iq}M^{h3}_{jprs} + \delta_{jq}M^{h3}_{iprs} + \delta_{ir}M^{h3}_{jpqs} + \delta_{jr}M^{h3}_{ipqs}\right. \\
&\left.+\delta_{is}M^{h3}_{jpqr} + \delta_{js}M^{h3}_{ipqr}\right),
\end{aligned}
$$

where, for brevity of notation

$$
\begin{aligned}
M^{h1}_{ipqj} &= M_{ipqj} + M_{jpqi} + M_{iqpj} + M_{jqpi}, \\
M^{h2}_{ipqr} &= M_{ipqr} + M_{irpq} + M_{iqrp}, \\
M^{h3}_{ipqr} &= M_{pqri} + M_{rpqi} + M_{qrpi}
\end{aligned}
$$

has been introduced.
The fourth rank isotropic tensor is defined as

$$
N_{ijpq} = \frac{1}{15}\left(\delta_{ij}\delta_{pq} + \delta_{ip}\delta_{jq} + \delta_{iq}\delta_{jp}\right),
$$

so that contraction of any index pair leaves one third times the Kronecker delta.
The coefficients above are related as (derived by use of MAPLE)

$c_1 = -650a - \frac{25}{49}$, $c_5 = -155a - \frac{3}{49}$, $c_9 = -70a - \frac{5}{42}$, $c_{13} = -28a - \frac{8}{315}$,

$c_2 = 160a + \frac{23}{196}$, $c_6 = -155a - \frac{13}{98}$, $c_{10} = -70a - \frac{1}{28}$, $c_{14} = 0$,

$c_3 = 600a - \frac{11}{147}$, $c_7 = 37a + \frac{61}{1470}$, $c_{11} = -259a - \frac{41}{315}$, $c_{15} = \frac{49}{3}a$,

$c_4 = 600a + \frac{22}{40}$, $c_8 = 37a + \frac{301}{2940}$, $c_{12} = -28a + \frac{41}{315}$, $c_{16} = \frac{49}{3}a + \frac{1}{45}$.

D Tensor basis and scalar invariants in cylindrical coordinates

Relevant tensors in cylindrical coordinates

The four tensors giving a non-zero contribution to non-linear eddy viscosity models for the fully developed rotating turbulent pipe flow are in cylindrical coordinates:

$$\boldsymbol{T}^1 = \begin{bmatrix} 0 & \frac{\frac{d\bar{u}_\phi}{dr}r - \bar{u}_\phi}{2r} & \frac{1}{2}\frac{d\bar{u}_z}{dr} \\ \frac{\frac{d\bar{u}_\phi}{dr}r - \bar{u}_\phi}{2r} & 0 & 0 \\ \frac{1}{2}\frac{d\bar{u}_z}{dr} & 0 & 0 \end{bmatrix},$$

$$\begin{aligned}
\boldsymbol{T}^5[1,1] &= 0, \\
\boldsymbol{T}^5[1,2] = \boldsymbol{T}^5[2,1] &= -\frac{\left(\frac{d\bar{u}_z}{dr}\right)^2}{8r}\left(\left(\frac{d\bar{u}_\phi}{dr}r - \bar{u}_\phi\right) + \left(\frac{d\bar{u}_\phi}{dr}r + \bar{u}_\phi\right)\right), \\
\boldsymbol{T}^5[1,3] = \boldsymbol{T}^5[3,1] &= -\frac{\left(\frac{d\bar{u}_z}{dr}\right)}{8r^2}\left(\left(\frac{d\bar{u}_\phi}{dr}r - \bar{u}_\phi\right)\left(\frac{d\bar{u}_\phi}{dr}r + \bar{u}_\phi\right) - \left(\frac{d\bar{u}_\phi}{dr}r - \bar{u}_\phi\right)^2\right), \\
\boldsymbol{T}^5[2,2] &= 0, \\
\boldsymbol{T}^5[2,3] = \boldsymbol{T}^5[3,2] &= 0, \\
\boldsymbol{T}^5[3,3] &= 0,
\end{aligned}$$

$$\begin{aligned}
\boldsymbol{T}^6[1,1] &= 0, \\
\boldsymbol{T}^6[1,2] = \boldsymbol{T}^6[2,1] &= -\frac{3\left(\frac{d\bar{u}_z}{dr}\right)^2}{8r}\left(\left(\frac{d\bar{u}_\phi}{dr}r - \bar{u}_\phi\right) + \left(\frac{d\bar{u}_\phi}{dr}r + \bar{u}_\phi\right)\right) - \frac{3}{4r^3}\left(\frac{d\bar{u}_\phi}{dr}r - \bar{u}_\phi\right)\left(\frac{d\bar{u}_\phi}{dr}r + \bar{u}_\phi\right)^2, \\
\boldsymbol{T}^6[1,3] = \boldsymbol{T}^6[3,1] &= -\frac{3\left(\frac{d\bar{u}_z}{dr}\right)}{8r^2}\left(\left(\frac{d\bar{u}_\phi}{dr}r - \bar{u}_\phi\right)\left(\frac{d\bar{u}_\phi}{dr}r + \bar{u}_\phi\right) + \left(\frac{d\bar{u}_\phi}{dr}r + \bar{u}_\phi\right)^2\right) - \frac{3}{4}\left(\frac{d\bar{u}_z}{dr}\right)^3, \\
\boldsymbol{T}^6[2,2] &= 0, \\
\boldsymbol{T}^6[2,3] = \boldsymbol{T}^6[3,2] &= 0, \\
\boldsymbol{T}^6[3,3] &= 0,
\end{aligned}$$

and

$$\begin{aligned}
\boldsymbol{T}^{10}[1,1] &= 0,\\
\boldsymbol{T}^{10}[1,2] = \boldsymbol{T}^{10}[2,1] &= -\frac{\left(\frac{d\bar{u}_z}{dr}\right)^2}{32r^3}\left(\left(\frac{d\bar{u}_\phi}{dr}r-\bar{u}_\phi\right)^2\left(\frac{d\bar{u}_\phi}{dr}r+\bar{u}_\phi\right)+\left(\frac{d\bar{u}_\phi}{dr}r+\bar{u}_\phi\right)^3\right.\\
&\quad \left.-2\left(\frac{d\bar{u}_\phi}{dr}r-\bar{u}_\phi\right)\left(\frac{d\bar{u}_\phi}{dr}r+\bar{u}_\phi\right)^2\right),\\
\boldsymbol{T}^{10}[1,3] = \boldsymbol{T}^{10}[3,1] &= -\frac{\left(\frac{d\bar{u}_z}{dr}\right)^3}{32r^2}\left(\left(\frac{d\bar{u}_\phi}{dr}r-\bar{u}_\phi\right)^2+\left(\frac{d\bar{u}_\phi}{dr}r+\bar{u}_\phi\right)^2\right.\\
&\quad \left.-2\left(\frac{d\bar{u}_\phi}{dr}r-\bar{u}_\phi\right)\left(\frac{d\bar{u}_\phi}{dr}r+\bar{u}_\phi\right)\right),\\
\boldsymbol{T}^{10}[2,2] &= 0,\\
\boldsymbol{T}^{10}[2,3] = \boldsymbol{T}^{6}[3,2] &= 0,\\
\boldsymbol{T}^{10}[3,3] &= 0.
\end{aligned}$$

Relevant scalar invariants in cylindrical coordinates

The five scalar invariants for the fully developed rotating pipe flow are in cylindrical coordinates:

$$I_1 = \frac{1}{2}\left(\frac{d\bar{u}_\phi}{dr}-\frac{\bar{u}_\phi}{r}\right)^2+\frac{1}{2}\left(\frac{d\bar{u}_z}{dr}\right)^2,$$

$$I_2 = \frac{1}{2}\left(\frac{d\bar{u}_\phi}{dr}+\frac{\bar{u}_\phi}{r}\right)^2+\frac{1}{2}\left(\frac{d\bar{u}_z}{dr}\right)^2,$$

$$I_3 = 0,$$

$$I_4 = 0,$$

and

$$I_5 = \frac{1}{8}\left[\left(\frac{d\bar{u}_\phi}{dr}-\frac{\bar{u}_\phi}{r}\right)^2+\left(\frac{d\bar{u}_z}{dr}\right)^2\right]^2 = \frac{1}{2}I_1^2.$$